The RNA-dependent RNA polymerase of the hepatitis A virus

Jamieson, Lauren Vilda

Award date:
1998

Awarding institution:
University of Bath

The RNA-dependent RNA polymerase of the hepatitis A virus

submitted by
Lauren Vilda Jamieson
for the
degree of Ph.D.
of the
University of Bath 1998

ProQuest LLC
789 East Eisenhower Parkway
P.O. Box 1346
Ann Arbor, MI 48106-1346

Acknowledgements

I would like to thank both my supervisor, Adrian Wolstenholme for his help and advice throughout my time in Bath and the BBSRC, SERC of old, for funding me throughout this project.

I am indebted to present and past members of 0.47, and past members of 3.44, who taught me all I needed to know with especial thanks owed to, in no particular order, Di Cope for protein 'stuff', Dave Laughton, for advice on everything, Momna Hejmadi for her 'scintillating' help and Tom Skinner for just being there, except when he let my column run dry!

Thanks are due also to the dim and distant Michelle McCormack (well maybe not so dim) for keeping me 'sane', making me laugh and shouting at me when motivation and progress were sorely lacking. I must thank also Ben and Dave, a.k.a Bert and Ernie who have given freely of their time, experience and computer expertise, not forgetting Lucy and Catherine who kept me abreast of the departmental gossip whilst I was writing-up.

I would also like to thank anyone and everyone who donated time, experience, apparatus, helpful hints, and, of course, money for UBSA when all else failed.

Finally I would like to thank my whole family for their love, financial backing and for putting up with me being a student all this time - hopefully now I can get you guys some decent Christmas presents!

Abstract

Hepatitis A virus (HAV) exhibits slow non-cytopathic replication in tissue culture. When adapted to growth in cell culture a change in phenotype to a more rapid and productive infection is observed which is associated with changes in the nucleotide sequence of the viral genome. Most of these changes are found in the regions of the genome encoding non-structural polypeptides. In order to determine the reason for this slow proliferation of HAV it is necessary to characterise the non-structural proteins of the virus. It has been postulated that slow growth of HAV in cell culture could be due to slow replication of viral RNA by an inefficient RNA polymerase and attempts were made here to characterise this enzyme.

Constructs which export the P3 HAV-specific sequences into the bacterial periplasmic space as a fusion protein with staphylococcal Protein A, with the aim of improving solubility, allowed the partial purification, using GTP-agarose affinity chromatography, of a 53kDa protein believed to be the HAV $3D^{pol}$. Unfortunately, the apparent copurification of Protein A with the 53kDa protein highlighted the inadequacies of Protein A as a fusion partner in this case. Problems of low yield and reproducibility also prompted consideration of other methods.

Individual P3 regions, 3AB, 3C, 3D, 3CD and P3 were amplified by PCR and cloned into pMAL™-c2, creating MBP gene fusions, directing expression products to the cytosol thereby improving the yield and hopefully solubility. Good yields were obtained for some of the fusion proteins expressed, however, the final yield of 'purified' 3D was very poor. Apparent autocatalysis of the processing intermediates suggested that the MBP-3C protease expressed was active. Expression of the MBP-3AB, both as the individual fusion protein, and resulting from cleavage of MBP-P3, was lethal, as indicated by the lysis of bacterial cultures upon induction. Only HAV 3C was purified, however the pMAL expression system did yield several useful products, free from bacterial contamination, which were assessed for poly(U) polymerase activity.

A degree of reproducible poly(U) polymerase 'activity' was observed when assaying both purified MBP-fusion protein and factor Xa-cleaved fusion protein expressed by 3D/pMAL, however this did not display true enzyme 'activity' with a reduction in incorporation of ^{3}H-UTP being observed upon increasing concentration of 'enzyme' which is not as one would expect.

Contents

Figures

Tables

Abbreviations

Standard abbreviations used in text are as defined in "Instructions to Authors" of the Biochemical Journal 1997.

%..... percent

°C..... degrees Celcius

μg..... micrograms

μl..... microlitre(s)

μm..... micrometre(s)

NANB..... non-A, non-B

μM..... micromolar

Å..... angstrom

A_b..... absorbance at wavelength *b*nm

Ab..... antibody

Ag..... antigen

Ala (A)..... alanine

APS..... ammonium persulphate

Arg (R)..... arginine

Asn (N)..... asparagine

Asp (D)..... aspartic acid

ATP..... adenosine triphosphate

bp..... base pairs

CDC..... Centres for Disease Control

cDNA..... complementary deoxyribonucleic acid

cm..... centimetre(s)

CPE..... cytopathic effect

CV..... Coxsackie virus

Cys (C)..... cysteine

d(d) ATP..... 2′(3′-di) deoxyadenosine 5′-phosphate

d(d) CTP..... 2′(3′-di) deoxycytidine 5′-phosphate

d(d) GTP..... 2′(3′-di) deoxyguanosine 5′-phosphate

d(d) NTP..... 2′(3′-di) deoxynucleotide 5′-phosphate

d(d) TTP..... 2′(3′-di) deoxythymidine 5′-phosphate

DI..... defective interfering particle

DNA..... deoxyribonucleic acid
ECL..... enhanced chemiluminescence
EDTA..... ethylenediaminotetra-acetic acid
eIF..... eukaryotic initiation factor
EMCV..... encephalomyocarditis virus
FMDV..... foot-and-mouth-disease virus
FPLC..... fast protein liquid chromatography
FRhK..... foetal Rhesus monkey kidney cells
g..... gram(s)
g..... gravitational force
Gln (Q) ..... glutamine
Glu (E)..... glutamic acid
Gly (G)..... glycine
h..... hour(s)
HAV..... hepatitis A virus
HAVcr-1..... HAV cellular receptor 1
HBV..... hepatitis B virus
HCl..... hydrochloric acid
HCV..... hepatitis C virus
HDV..... hepatitis Delta 'virus'
HEV..... hepatitis E virus
HGV..... hepatitis G virus
His (H)..... histidine
HRP..... horse-radish peroxidase
HRV..... human rhinovirus
Ig..... immunoglobulin
Ile (I)..... isoleucine
IPTG..... isopropylthio-β-galactoside
IRES..... internal ribosome entry site
ISG..... immune serum globulin
IU..... international unit(s)
kb..... kilobase(s)
kDa..... kilodalton(s)
kg..... kilogram(s)
L..... litre

Leu (L)..... leucine
Lys (K)..... lysine
M ..... molar
mA..... milliampere
Met (M)..... methionine
min ..... minute(s)
mg ..... milligrams
$MgCl_2$..... magnesium chloride
ml ..... millilitre
mm ..... millimetres
mM ..... millimolar
mRNA..... messenger ribonucleic acid
NBT ..... nitroblue tetrazolium
ng ..... nanograms
nm ..... nanometres
nM ..... nanomolar
nt..... nucleotide
NTR..... nontranslated region
OD..... optical density
ORF..... open reading frame
PAGE ..... polyacrylamide gel electrophoresis
PBS..... phosphate buffered saline
PCR..... polymerase chain reaction
pH ..... $-\log_{10}$ (hydrogen ion concentration)
Phe (F) ..... phenylalanine
Pol..... polymerase
Pro (P)..... proline
psi ..... pounds per square inch
PV ..... polio virus
PVR..... polio virus receptor
RC..... replication complex
RF ..... replicative form
RI..... replicative intermediate
RNA..... ribonucleic acid
RNase ..... ribonuclease

rpm ..... revolutions per minute
RR ..... rapid replication
RRL ..... rabbit reticulocyte lysate
rRNA ..... ribosomal RNA
s ..... second(s)
SDS ..... sodium dodecyl sulphate
Ser (S) ..... serine
spp ..... species
TBP ..... TATA-binding protein
TCA ..... tri-chloroacetic acid
TE ..... tris/Na_2EDTA buffer
TEMED ..... N,N,N′,N′-tetramethylethylenediamine
Thr (T) ..... threonine
TMEV ..... Theiler's murine encephalomyelitis virus
Tris ..... tris (hydroxymethyl) amino methane
tRNA ..... transfer RNA
Trp (W) ..... tryptophan
Tyr (Y) ..... tyrosine
U ..... unit(s)
UV ..... ultraviolet
V ..... volts
v/v ..... volume to volume
Val (V) ..... valine
VP ..... viral protein
W ..... watts
w/v ..... weight per unit volume
WHO ..... World Health Organisation
X-gal 5-bromo-4-chloro-3-indolyl-β-D-galactoside

1. Introduction

1.1 Viral hepatitis

Viral hepatitis was reviewed at a Hepatitis Challenge Workshop held in Vienna in 1996 by the Viral Hepatitis Prevention Board/International Commission on Occupational Health.

Six distinct viruses causing viral hepatitis have been identified, each differing in the severity of disease they cause, epidemiological characteristics, modes of transmission and recommendations for control. These six viruses are hepatitis A, B, C, D, E, and G (Table 1).

Hepatitis A virus (HAV) is characterised by low mortality, no chronic carrier state and lifelong immunity following infection. Modes of transmission include faecal-oral, person-to-person, and contaminated water and food.

Historically, infection with HAV was common in young children and not considered a public health problem. With improved hygiene and socio-economic conditions, however, the virus now often strikes at a later age and with more severe consequences.

The outcome of hepatitis B virus (HBV) infection is often severe, with acute HBV infection leading to chronic carrier state, cirrhosis, liver cancer and death. Six to 10 percent of infected adults will become chronic carriers; infection during infancy and childhood frequently progresses to the chronic carrier state, with 70-90 percent of neonates becoming chronic carriers. Hepatitis B is transmitted through infected blood and body fluids, perinatal transmission, horizontal transmisssion, sexual transmission and intravenous drug use. Both plasma derived and recombinant vaccines are approved for use in most parts of the world; even so, worldwide one million deaths per year are directly related to HBV infection. To control the disease, the WHO recommends that "the most effective strategy is incorporation of universal hepatitis B vaccination into the routine infant or adolescent immunisation schedules".

Discovered in 1989, the hepatitis C virus (HCV) is a small, single-stranded RNA virus. It is estimated that approximately 1% of the world's population have HCV. The virus is blood-borne, and the majority of those infected with HCV show no symptoms initially. Approximately 50% of people infected with HCV become chronic carriers; of these, half develop cirrhosis or liver cancer.

The hepatitis Delta 'virus' (HDV) is associated with hepatitis B. Too small to replicate itself, the Delta 'virus' lives as a parasite on the HBV, using the S antigen of HBV to multiply. The Delta 'virus' is relatively rare and is not present with every case of HBV infection. The progression to chronicity is not uncommon. If HBV infection does become chronic, however, the Delta 'virus' speeds the progression to chronic liver disease. Vaccination against HBV protects against Delta infection as well.

Formally known as enterically transmitted non-A, non-B (NANB) hepatitis, hepatitis E virus (HEV) has no chronic carrier state and does not cause chronic liver disease. Hepatitis E infection is highly dangerous, however, for pregnant women, causing up to 20% mortality in women in their third trimester of pregnancy. Largely transmitted through faecal-oral transmission, hepatitis E epidemics are usually waterborne epidemics. The disease can be controlled through the provision of safe water and food. There is no vaccine as yet, though recombinant vaccines are currently under investigation, with the focus now on immunogen, adjuvant and immunisation schedules.

"Hepatitis E looks like hepatitis A but it has the propensity for killing pregnant women" says Dr Mark Kane of the World Health Organisation (WHO). Even though prevalence rates of HEV are less than one percent in Western Europe and North America "it is a major pathogen around the world and we'll be hearing quite a bit about hepatitis E in the next few years".

Hepatitis F virus (HFV) has been described in only a handful of cases (from France) with subsequent experimental transmission to primates (Deka *et al.*, 1994). The virology, epidemiology, hepatotropicity and clinical importance of HFV are quite uncertain.

The hepatitis G virus (HGV; also called hepatitis GB virus C or HGBV-C), only recently identified in 1995 and fully characterised in early 1996 (Linnen *et al.*, 1996), is an RNA virus and as a member of the Flaviviridae family of viruses, is closely related to HCV. Associated with acute and chronic hepatitis, HGV is spread parenterally; the virus can cause persistent infection and is prevalent in volunteer blood donor populations. HGV and HCV infection can be simultaneously transmitted and result in persistent coinfection. It is presently unknown whether a normal carrier state exists for patients infected with HGV. The role of HGV in cirrhosis and hepatocellular carcinoma also remains to be investigated.

Table 1: Families of hepatitis viruses

VIRUS TYPE	FAMILY	NUCLEIC ACID GENOME	VIRION SIZE
A	Picornavirus	ssRNA	27nm
B	Hepadnavirus	dsDNA	42nm
C	Flavivirus	ssRNA	45nm
D	Viroid or satellite virus	ssRNA	36nm
E	Calicivirus	ssRNA	32nm
G	Flavivirus	ssRNA	40-60nm

1.2 Hepatitis A

1.2.1 History

Reported epidemics of human disease resembling acute hepatitis A extend back into antiquity, although the specific etiology of these outbreaks is, of course, unknown (Ross *et al.*, 1991; Lemon, 1994; Hollinger & Ticehurst, 1996). Acute infectious hepatitis was first recognised as a transmissable entity in the early twentieth century and was clearly separated from homologous serum hepatitis in 1947 when the terms *hepatitis A* and *hepatitis B* were introduced by MacCallum (MacCallum, 1947).

The virus responsible for hepatitis A was identified by immune electron microscopy in 1973 by Feinstone *et al.* Until recently, however, the only method available for the study of this disease consisted of experimental infection of primates, the marmoset *Sanguinus mystax* being the animal most extensively used (Ross *et al.*, 1991). More recently, the virus has been propagated in a permanent line (FRhK6) of foetal Rhesus monkey kidney cells (Provost & Hilleman, 1979). This and other cell culture systems (e.g. African green monkey kidney and human hepatoma cell lines) have proved useful for virus assay and production (Ross *et al.*, 1991). Lemon *et al.* (1983) described a modified plaque assay which has become the method of choice for quantitation of infectious hepatitis A virus (HAV) in many laboratories (Ross *et al.*, 1991).

Portions of the RNA genome of HAV were molecularly cloned by Ticehurst *et al.* in 1983 making possible the use of blot hybridisation as a diagnostic test, and the first full-length nucleotide sequences of HAV were reported by Cohen *et al.* (1987a). These studies revealed that the genomic organisation of HAV was similar to that of other picornaviruses, containing a single large open reading frame presumably encoding a

polyprotein which is co- and post-translationally processed during replication of the virus. The first infectious cDNA clone of HAV was reported by Cohen *et al.* in 1987(b).

In recent years, there has been a dramatic increase in research into the molecular basis of HAV replication and the function of the viral proteins and their effect on viral replication. The most recent findings are discussed later on in this chapter under the relevant headings.

1.2.2 Hepatitis A infection

1.2.2.1 Epidemiology

Hepatitis A is a widespread infectious disease that is endemic in developing countries, and that also may account for up to 25% of all cases of hepatitis in the developed world (Tedeschi *et al.*, 1993). In fact, nearly half of the documented cases of viral hepatitis in the United States are caused by HAV (Lemon & Thomas, 1997). HAV is excreted in the faeces of infected persons and spread via personal contact and ingestion of contaminated water or food (Ross *et al.*, 1991). Some outbreaks have been associated with ingestion of uncooked shellfish, as shellfish are capable of concentrating HAV from polluted waters (Le Guyader, 1993). In 1987/88 in Shanghai, some 292,301 individuals contracted hepatitis A from eating contaminated clams.

Transmission of the infection is almost always by the faecal-oral route. Virus shed in the faeces is largely or exclusively replicated within the liver, and gains access to the intestinal contents by passage through the biliary tract (Figure 1). There have been reports of extra-hepatic replication, suggested by the presence of HAV RNA found by dot-blot hybridisation in tissues such as the intestine, spleen and kidney, however the presence of viral antigens and nucleic acid at these sites may merely indicate immune complex deposition or contamination by faecal contents (Taylor *et al.*, 1992).

A significant viraemia (perhaps as high as 1×10^5 infectious particles per millilitre of serum) may be present for several weeks in individuals experiencing primary infection with HAV, and this may occasionally lead to blood-borne transmission of the virus (Lemon, 1994). The viraemia often precedes the development of clinical symptoms by 7-10 days and was thought to be short-lived (Hollinger & Ticehurst, 1996). A study by

Yotsuyanagi *et al.* (1993), however demonstrated that viraemia may exist as long as 7 days after clinical onset and also after ALT reached peak levels. Transmission by transfusion, or recently by contaminated factor VIII has been reported, but such blood-borne transmissions are rare (Purcell, 1994).

It is also possible that needle-borne transmission contributes to the spread of HAV among intra-venous drug abusers, although this is not known for certain. Virus has been found in saliva late in the course of infection, but the source of this virus (possibly blood) is not known. Sexual activity may also influence transmission of hepatitis A, especially among homosexual males (Ross *et al.*, 1991). This is probably due to enhanced faecal-oral transmission related to oral/anal contact. Heterosexual activity may similarly influence hepatitis A transmission, but the data are less convincing (Lemon, 1994).

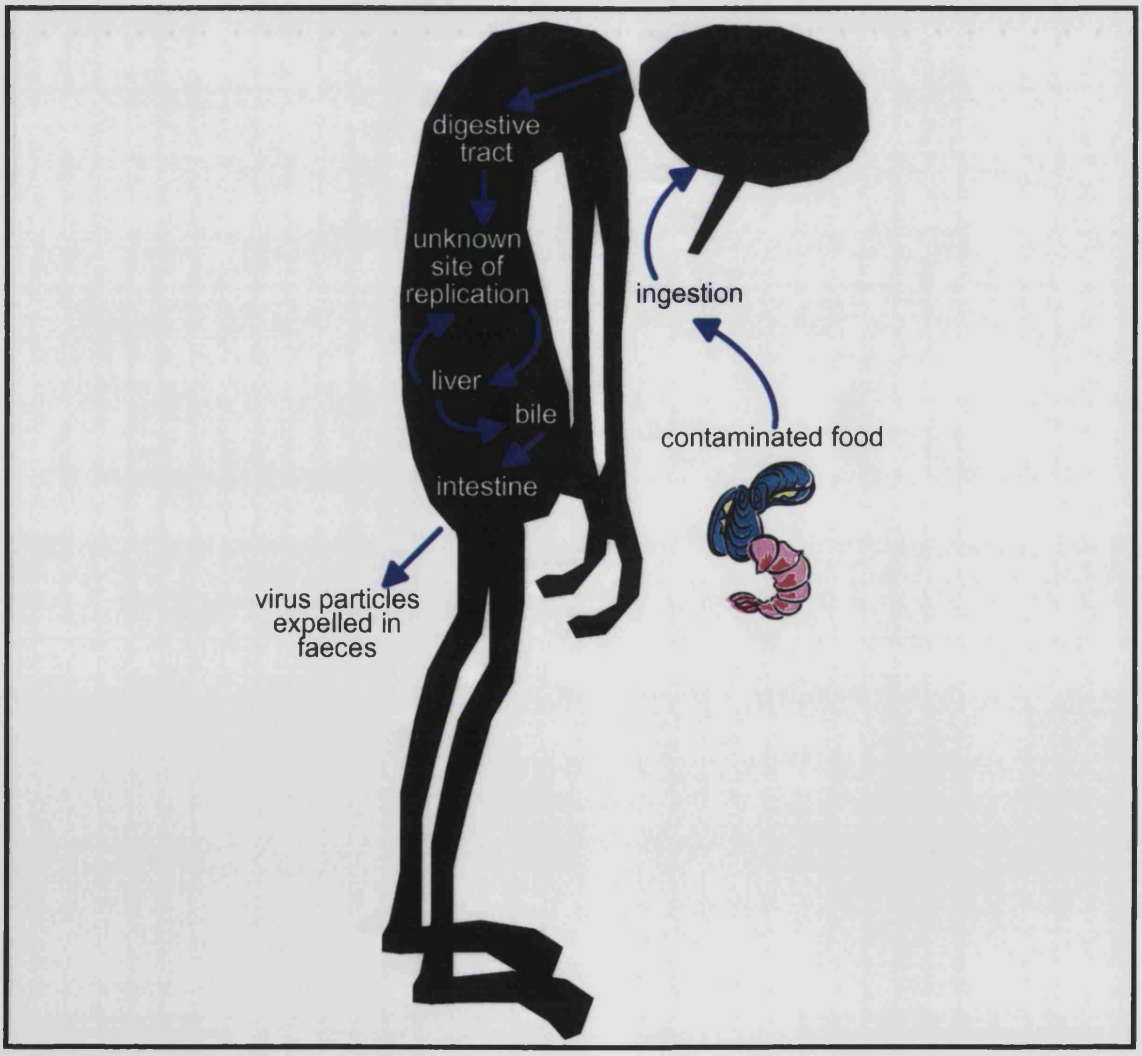

Figure 1: Pathway of hepatitis A infection

Although infection of young children is usually asymptomatic, infection of older individuals often results in clinical illness. In developing countries, rapid improvement in sanitation and hygiene can actually result in increased morbidity because infection with HAV is often delayed until adolescence or adulthood when the symptoms of infection are more severe (Ross *et al.*, 1991; Tedeschi *et al.*, 1993; Hollinger & Ticehurst, 1996). The changing epidemiology of hepatitis A is thought to be the result of better sanitation, principally in the form of improved treatment of water and sewage and improved personal hygiene. Consequently, the epidemiology of hepatitis A has changed from one of diffuse person-to-person spread to one of association with specific high risk groups (Figure 4) (Purcell, 1994). In countries of low endemicity, HAV infection usually occurs in cyclical outbreaks in the general population, according to studies conducted by the United States Centres for Disease Control (CDC). The virus circulates in the population, striking when large numbers of people become susceptible.

On the basis of cases of hepatitis A reported in 1992 to the CDC, the most frequently reported risk factor was household or sexual contact with a person with hepatitis, followed by day-care attendance or employment, recent international travel, and association with a suspected food- or water-borne outbreak (Shapiro, 1994) (Figure 2). Dr Mark Kane of the WHO reckons that hepatitis A is probably the most important travel-related, vaccine-preventable disease (see 1.2.2.4).

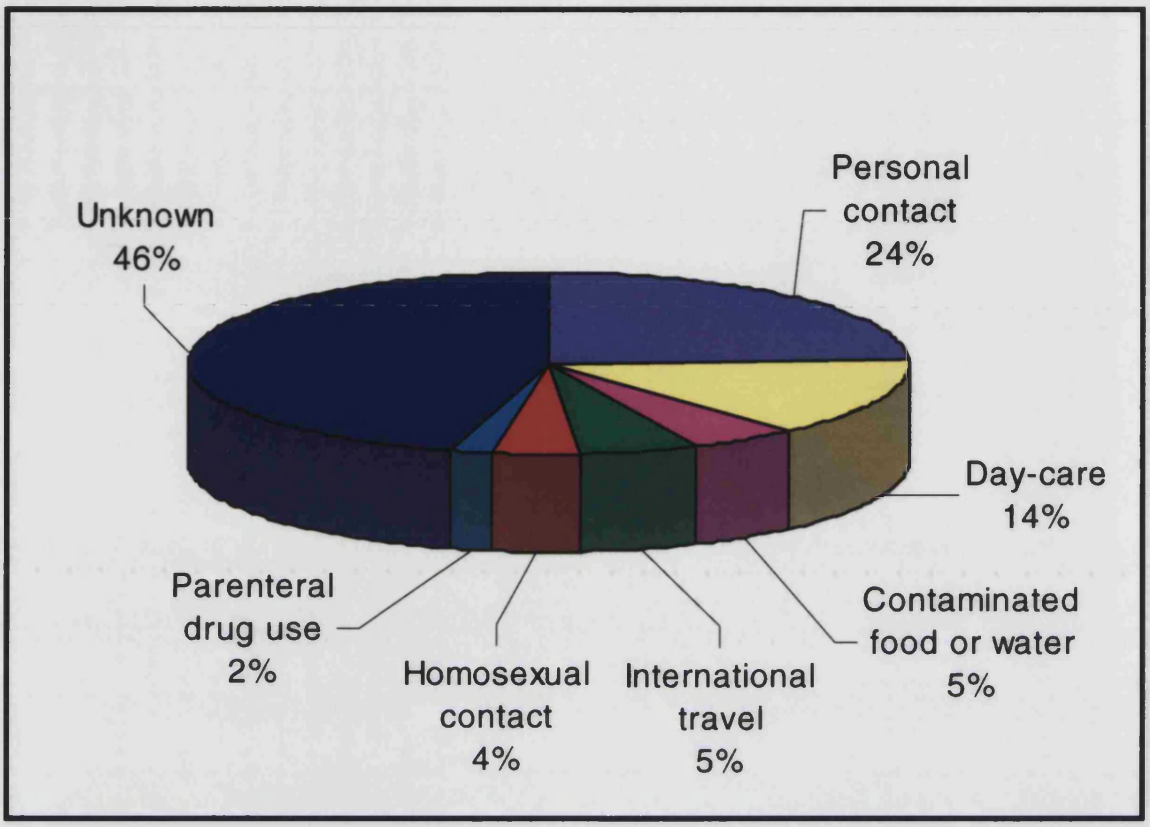

Figure 2: Risk factors associated with acquiring hepatitis A infection
Adapted from Shaw (1997).

1.2.2.2 Pathology

The incubation period of hepatitis A is approximately 4 weeks, averaging 25 days, with a range of perhaps 2-6 weeks (Figure 3). During the incubation period, the liver is infected with virus and copious amounts of virus may be shed in the faeces despite the absence of symptoms. This is particularly true near the end of the incubation period (Lemon, 1994). Yotsuyanagi and colleagues (1996) found that faecal shedding of HAV continued for up to 3 months after onset of illness, and even after the normalisation of the serum ALT levels, a marker of liver cell damage, using the two-stage reverse-transcription (RT)-PCR method. Such patients could be a source of further spreading of the virus in the community.

Disease is typically abrupt in onset and at times is associated with high fever (Hollinger & Ticehurst, 1996). More characteristically, the onset of hepatitis A is marked by

malaise, nausea, right upper quadrant tenderness, and eventually scleral icterus and jaundice, dark urine (at times the colour of Coca-Cola™ and quite frothy) and light clay-coloured stool. Diarrhoea is an uncommon manifestation of viral hepatitis A in adults but may be seen in children (Ross *et al.*, 1991; Lemon, 1994; Hollinger & Ticehurst, 1996). Confluent hepatic necrosis is potentially a progressive lesion that may lead to fulminant hepatitis and death (Hollinger & Ticehurst, 1996). Hepatitis A is generally mild to moderate in severity with a mortality rate of 0.2% or less, and never becomes chronic. However, inapparent infection with shedding of virus may persist for up to 6 months in neonates (Purcell, 1994).

1.2.2.3 Immune response and serological diagnosis

Virus-induced cytopathology may not be responsible for the pathologic changes seen in HAV infection and it has been suggested that host-mediated immunologic responses may contribute to the pathogenesis of hepatitis A (Hollinger & Ticehurst, 1996). The humoral immune response to hepatitis A is well characterized. IgM class antibodies to the native virion are present in almost all patients by the onset of symptoms, and persist for upto a year following infection. IgA and IgG antibodies to HAV also develop within a few days of the onset of symptoms. Both IgG and IgM antibodies have been shown to have virus-neutralising activity, and the efficacy of passively administered immunoglobulins in prevention of symptomatic hepatitis A suggests that IgG anti-HAV is protective against subsequent symptomatic re-infection. IgG antibody generally persists for the life of the individual. Current evidence suggests that secretory immunity plays little if any role in protection against hepatitis A (Lemon, 1994; Hollinger & Ticehurst, 1996).

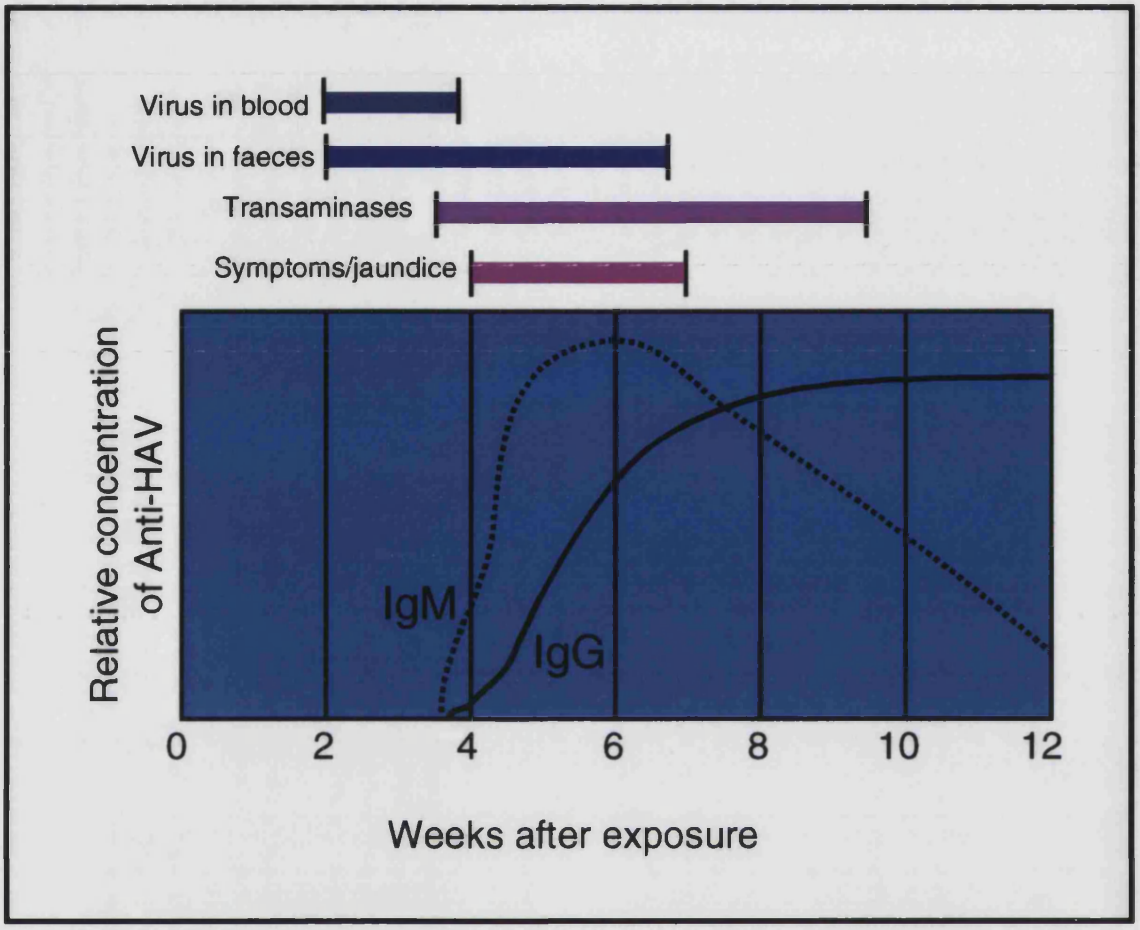

Figure 3: Immunologic and clinically relevant biologic events associated with HAV infection in humans

Adapted from Hollinger & Ticehurst (1996) and references therein.

1.2.2.4 Prevention and control

As almost all hepatitis A infections are, as previously mentioned, transmitted by the faecal-oral route the most effective means of prevention is an improvement in community public health measures. These include the provision of clean water, proper disposal of sewage and high standards of personal hygiene (Ross *et al.*, 1991).

Passive immunisation, by administering pooled immune serum globulin (ISG) from human beings, has had an efficacy as high as 87% in preventing symptomatic hepatitis when administered to household contacts within 2 weeks of exposure (Lemon, 1985).

Since only a single serotype of HAV has been identified and infection results in lifelong

immunity, a vaccine to prevent the disease is feasible. In recent years, several inactivated hepatitis A vaccines prepared from cell culture-grown virus have displayed a high level of immunogenicity in clinical trials, and one was licensed for human use in 1991 (Tedeschi *et al.*, 1993). Duff and Duff very recently (1998) reported that two new inactivated vaccines are available, Vaqta™ (Merck and Co., West Point, PA) and Havrix™ (Smithkline Beecham, Philadelphia, PA). However, inactivated vaccines are often more difficult than attenuated vaccines to administer to large populations and prove costly, given the relatively low yields of virus obtained in cell culture, and therefore development of an efficacious attenuated vaccine would be advantageous (Lemon, 1985).

Development of such vaccines is based on the host range change accompanying the adaptation and passage of HAV in cell cultures, usually monkey kidney cells. These variants appear incapable of initiating infection and also have a markedly reduced ability to replicate in the liver. These candidate attenuated vaccines, however, have been plagued with problems of poor immunogenicity and at times residual hepatovirulence (Lemon, 1994). For optimum safety and efficiency of production of an attenuated vaccine, it would be useful to understand the genetic basis of attenuation and virulence and how these relate to efficient growth of the virus in cell culture (Tedeschi *et al.*, 1993).

Other possible avenues for vaccine development, reviewed in André (1995), include the use of either conventional or recombinant DNA techniques to obtain subunit vaccines, empty capsids, live viral or bacterial vectors, genetic immunization, synthetic peptides and anti-idiotypes (Table 2) overleaf.

Table 2: Current options for development of an hepatitis A virus

LIVE VACCINE	NON-REPLICATING VACCINES
Attenuated HAV strain *Conventionally attenuated* (passaging in cell culture) by recombinant DNA techniques **Live attenuated vectors** Viruses (e.g. vaccinia, polio, canarypox) Bacteria (e.g. *S. Typhimurium*)	**Inactivated virions** *Empty capsid* (produced by recombinant DNA technology) *Subunit* Viral capsid polypeptides Recombinant DNA fusion proteins *Synthetic peptides* *Microencapsulated antigens* *"Naked DNA"* *Anti-idiotype*

As well as the groups featured in Figure 4, the individuals most likely to benefit from routine vaccination are children living in communities with a high prevalence of hepatitis A; persons with clotting-factor disorders, especially those receiving factor concentrates treated with solvent detergents; persons working in laboratories where HAV is handled; recipients of liver transplants and those awaiting one; and persons older than 30 years of age with chronic liver disease (Duff & Duff, 1998).

- Travellers from industrialised countries to regions of world where HAV is endemic
- Military personnel who regularly travel to endemic areas of the world
- American Indians; native Alaskans
- Preschool children attending day-care centres; staff, parents, and siblings
- Residents and staff of closed communities (institutions)
- Refugees residing in temporary camps following catastrophes
- Homosexually active males
- Parenteral illicit drug users
- Food handlers
- Persons residing in areas where extended community outbreaks exist

Figure 4: High risk groups potentially targeted for vaccination with hepatitis A vaccine

1.2.3 Taxonomy and classification

Despite early classification among the enteroviruses, HAV, provisionally classified in the early 1980s as enterovirus type 72 because its biophysical characteristics are like those of enteroviruses and cardioviruses, and its biochemical features resemble those of enteroviruses (Table 3), is now widely recognised to constitute a unique genus, hepatovirus, within the family *Picornaviridae*, a family of pathogens which includes poliovirus (PV), human rhinoviruses (HRVs), encephalomyocarditis virus (EMCV) and foot-and-mouth disease virus (FMDV) with which HAV shares many structural and biological attributes (Palmenberg, 1989; Stanway, 1990).

This classification is based on several unique features (Figure 5) of HAV including, amongst others: liver cell tropism, small and possibly absent VP4 protein, striking thermostability, relatively slow and usually noncytopathic replication cycle and a strong tendency to initiate persistent infections in cell culture (Lemon, 1994). The nucleotide sequence of HAV, while relatively well conserved among different isolates, is also widely divergent from those of other picornaviral genera.

- HAV nucleotide and amino acid sequences are dissimilar from those of other picornaviruses, as are the predicted sizes of several HAV proteins
- HAV is difficult to adapt to growth in cell culture and usually replicates very slowly without cytopathic effect
- HAV is resistant to temperatures and drugs that inactivate many picornaviruses
- HAV exhibits an outstanding stability at pH1, remaining infectious for up to 5 hours
- HAV has only one serotype and one neutralisation site is immunodominant
- An enteroviral-specific monoclonal antibody does not react with HAV

Figure 5: Characteristics distinguishing HAV from other picornaviruses

1.2.4 Physical properties

A striking property of the HAV particle which may well contribute to its potential for epidemic spread is its resistance to thermal denaturation. The HAV particle is stable when incubated at 60°C for 60 minutes and is only partially inactivated after 10-12 hours at 60°C. The temperature at which 50% of PV particles disintegrate and release their RNA in the absence of cations is 43°C after 10 minutes compared with 61°C for HAV (Siegl *et al.*, 1984). In the presence of 1M $MgCl_2$, this striking thermal stability is substantially enhanced, with the $T_{50,10}$ (temperature at which 50% of particles

disintegrate after 10 minutes of incubation) of PV and HAV shifting to 61°C and 81°C respectively, generating empty capsids that retain antigenicity (Hollinger & Ticehurst, 1996). The HAV particle is remarkably resistant to low pH conditions, with the loss of infectivity reported at pH 1.0 (Scholz *et al.*, 1989). The virus is also relatively resistant to detergent inactivation, easily surviving 37°C for 30 minutes in 1% sodium dodecyl sulphate. There is no information concerning the radiation sensitivity of HAV, although it has been suggested that infectivity may be reduced by microwaving HAV-contaminated food (Lemon, 1994). A summary of the biophysical characteristics of HAV compared with those of other members of the picornavirus family can be found in Table 3.

Table 3: Biophysical characteristics of HAV compared with other picornaviruses

	HAV	ENTERO	RHINO	CARDIO	APHTHO
Serotypes	1	>70	>130	2	7
Strains	13			6	53
1° Host	Humans, other primates	Humans, other mammals	Humans, other mammals	Mice, other mammals	Cloven-footed, other mammals
Tissue Tropism	Narrow	Narrow to wide	Narrow	Wide	Wide
Target Organ	Liver	Gut	Upper respiratory tract	CNS, heart	Generalised
Sensitivity					
Acid (pH3)	Stable	Stable	Labile	Stable	Labile
Heat (60°C)	Stable	Labile	Labile	Labile	Labile
Guanidine	Resistance	Sensitive	Sensitive	Resistance	Resistance
Disoxaril	Resistance	Sensitive	Sensitive	Resistance	Resistance
Biophysical					
Buoyancy density (g/cm^3 CsCl)	1.32-1.34	1.34	1.39-1.42	1.34	1.43-1.45
Sedimentation coefficient	156-160	156-160	149	156	142-146

1.3 Properties and replicative strategies of the picornaviruses

1.3.1 Picornavirus family

The Picornaviridae, among the smallest ribonucleic acid-containing viruses known, comprise one of the largest and most important families of human and agricultural pathogens. PV, human HAV, and FMDV virus are all members of the picornavirus family. So too are the HRVs, the single most important etiologic agents of the common cold. Because of the economic and medical importance of picornaviruses, it is not surprising that they have been prominently involved in the development of modern virology. Foot-and-mouth disease, the most important single pathogen of livestock, was in fact the first animal virus to be recognised when Loeffler and Frosch, in 1898, discovered that the causative agent passes through Berkfeld filters and was therefore much smaller than other microorganisms then known to transmit disease. That poliomyelitis was also caused by a virus was announced about a decade later by Landsteiner and Popper but it did not come to be called poliovirus until around 1955 (Rueckert, 1996).

Members of the picornavirus family share a number of structural and organisational features (discussed below); however, picornaviruses are diverse in terms of their host specificity and the symptoms they induce. The picornavirus family is currently divided into five genera: the enteroviruses, the cardioviruses, the rhinoviruses, the aphthoviruses and most recently hepatovirus.

PV is the prototypic member of the *Picornaviridae* family and is classified with the enteroviruses, named for their ability to infect the alimentary (enteric) tract. A high degree of sequence similarity exists between the enteroviruses and rhinoviruses. Rhinoviruses are so called because of their adapted growth in the nasopharyngeal tissue; infection of this tissue by rhinovirus is the major cause of the common cold (Rueckert, 1996; Stewart & Semler, 1997).

Strains of EMCV make up one of the two serotypes of the cardiovirus genera, which are generally murine viruses, although their host range also includes humans, pigs, elephants, and squirrels. The second serotype of cardioviruses is Theiler's murine encephalomyelitis viruses (TMEV), which as their name suggests, infect mice and result in neuronal degeneration. The *aphthoviridae* include the foot-and-mouth disease

viruses, which produce vesicular lesions in cloven-footed animals, especially in cattle, goats, pigs, and sheep. Formerly a member of the enteroviruses, HAV lacks a high degree of sequence homology with the enteroviruses and is now the sole member of the hepatovirus genus (Rueckert, 1996; Stewart & Semler, 1997).

As a basic pattern, the viruses divide into four main phylogenic branches, designated (arbitrarily) Groups I, II, III and IV. Group I viruses include the FMDV strains (aphthoviruses), Group II the murine cardioviruses (EMCV, Mengo, TMEV), Group III the hepatitis A isolates, and Group IV the rhino, polio, Coxsackie, and other enteroviruses. For convenience (and whimsy) the strains in the latter group are sometimes referred to as "renteroviruses" because they include isolates from the more traditional rhino and entero taxonomic designations (Palmenberg, 1990).

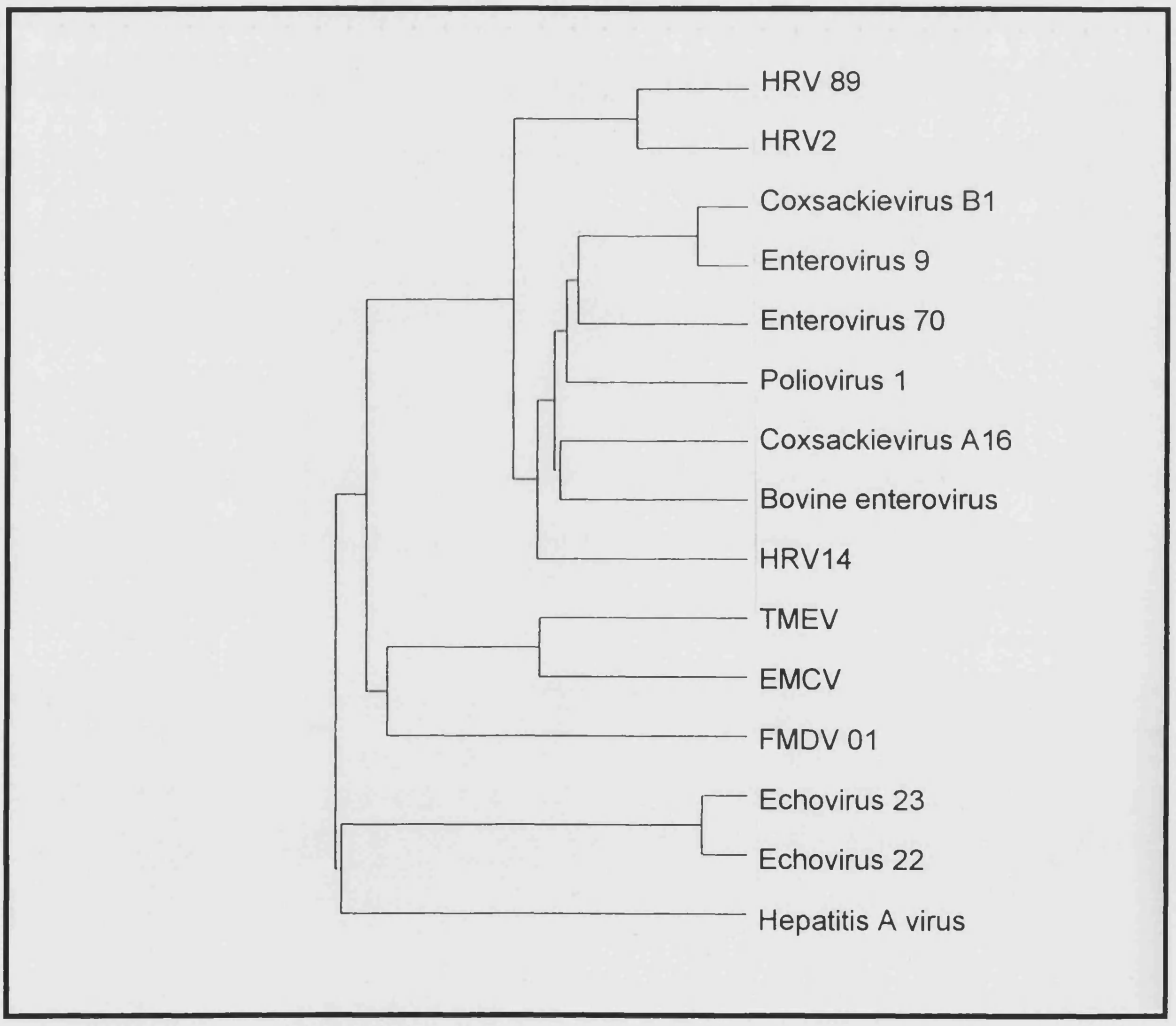

Figure 6: Dendrogram constructed by comparing alignments of amino acid sequences for 15 picornaviruses

Thus, for simplicity in the following sections, the 'renteroviruses' will be discussed primarily. Similarly the cardio- and aphtho-viruses will be covered together and finally the hepatovirus genus will be discussed.

1.3.1.1 General properties of virions

X-ray crystallographic structures have now been determined for at least one member of each picornavirus genus except HAV. All share similar features: a protein shell roughly 5nm thick and 30nm in diameter surrounding a single strand of mRNA. The RNA core, including VPg, is largely invisible to X-ray crystallographic analysis because, unlike the protein shell, the RNA has no symmetry and can occupy 60 different orientations in the crystal lattice. Therefore, its contribution to the crystallographic diffraction pattern is too smeared to be solved by current methods (Rueckert, 1996).

The capsids of all picornaviruses are composed of a 60-subunit protein shell (20-30nm diameter) having intrinsic 5:3:2 icosahedral symmetry. Each subunit contains four nonidentical polypeptide chains (virion proteins: VP1, VP2, VP3, and VP4) the largest three of which share, as a common structural motif, a wedge-shaped, eight stranded, antiparallel β barrel configuration (Hogle *et al.*, 1987; Luo *et al.*, 1987; Acharya *et al.*, 1989; Kim *et al.*, 1989). Sixty of these identical four-segmented subunits, now called protomers, are organised into pentameric units (dodecahedral model of shell structure). Of these subunits, 60-n are identical mature protomers (VP1, 2, 3, 4) and n are immature protomers (VP0, 1, 3). VP0 represents an uncleaved precursor of chains VP2 and VP4. Picornavirions rarely if ever contain fewer than two immature subunits. The protein shell encapsidates a single-copy of the positive-sense RNA genome, which is released into the cytoplasm of a target cell (Palmenberg, 1990).

The dissociation of the shell can be explained by the presence of just two kinds of bonding domains within each of the identical protein subunits. One domain holds pentamers together; the other binds monomers into pentamers. Assembly of the picornaviral shell can be understood by the operation of these domains in reverse order (Figure 7) (Rueckert, 1996).

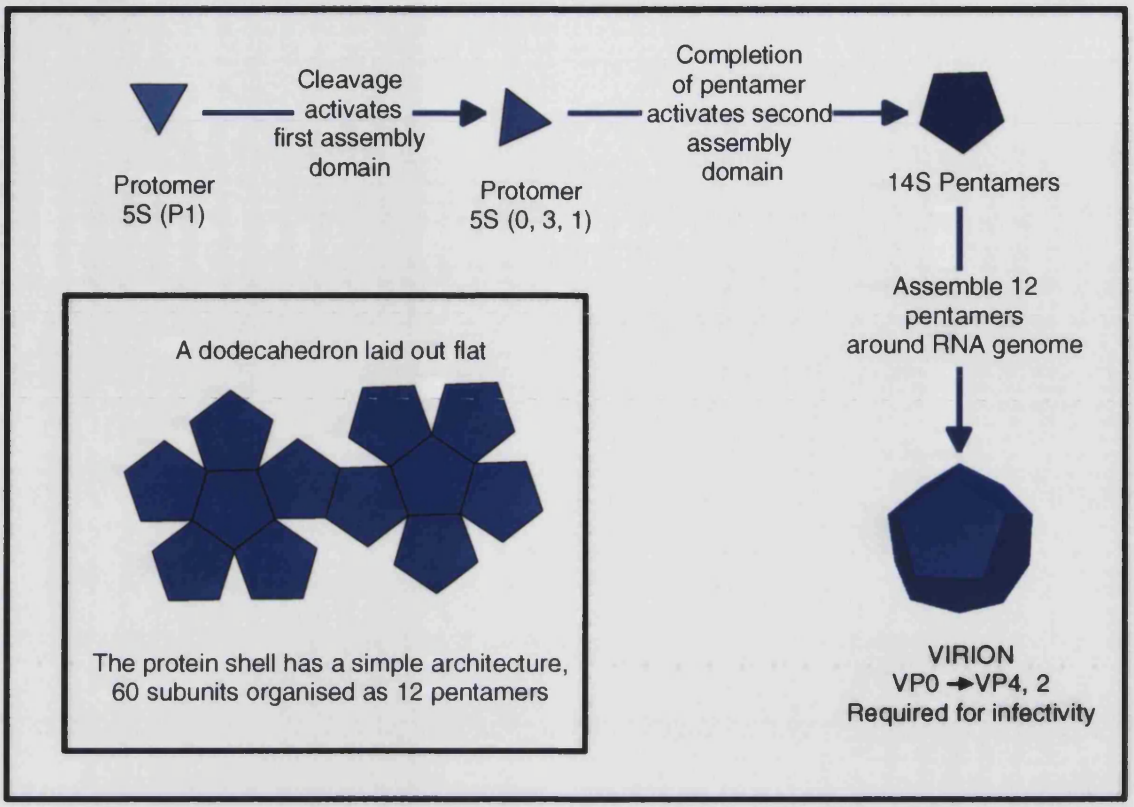

Figure 7: Dodecahedral model of picornavirus structure and assembly
Adapted from Rueckert *et al.*, 1969.

Coat proteins serve several key functions: (a) they protect the RNA genome from nucleases in the environment; (b) they recognise specific cell-coded receptors in the plasma membrane and is therefore one important determinant of host range and tissue tropism (disease pathology); (c) they determine antigenicity; (d) they carry directions for selecting and packaging the viral genome and provides a proteinase involved in maturation of the virion; and (e) they disgorge the RNA genome and deliver it through the cell membrane and into the cytosol of susceptible host cells. The atomic structure has provided significant insight into many of these functions (Rueckert, 1996).

The surface topography of each type of virus is as varied and characteristic as faces in the human race, hence the many serotypes listed in Figure 11, Figure 12, Figure 17, and Figure 18. Human rhinoviruses and enteroviruses, for example, feature prominent canyons, like ragged moats encircling a plateau at the centre of each pentameric unit in the shell; cardioviruses and aphthoviruses on the other hand, lack such canyons (Rueckert, 1996).

Myristic acid, also called *n*-tetradecanoic acid, is covalently linked to amino terminal glycine residues on VP4 and to its precursors VP0, and P1 of most picornaviruses (Chow *et al.*, 1987); HAV appears to be an exception (Tesar *et al.*, 1993). Cellular enzymes are known to recognise the signal for acylation myristate -Gly-X-X-X-Ser/Thr (X = any amino acid) (Rueckert, 1996). In entero- and rhinoviruses the N-terminal glycine requires removal of a methionine residue, whereas in the cardio- and aphtho-viruses myristylation of the N-terminal glycine requires proteolytic removal of a leader peptide (Rueckert, 1996). Myristylation is required for assembly of pentamers (Ansardi *et al.*, 1992; Moscufu & Chow, 1992) and may also play a role in early stages of infection e.g. reorientation of the pentamer and release of VP4 (Chow *et al.*, 1987).

1.3.1.2 General properties of picornaviral genome

The picornaviral genome consists of a single "plus" strand of messenger-active RNA that can be extracted out of virions by shaking aqueous suspensions of virus with an equal volume of buffer-saturated phenol. When the resulting emulsion is separated, proteins partition to the phenol-rich phase while RNA remains in the aqueous phase (Rueckert, 1996).

The specific infectivity of the naked RNA is about one millionth that of virions. That this infectivity is indeed due to free RNA and not to traces of surviving virions is shown by its extreme sensitivity to ribonuclease (<0.01μg/ml). With intact virions, by contrast, where the RNA resides in a protective protein shell, the infectivity is completely resistant to ribonuclease even at millionfold higher concentrations. A single break in the RNA, whether free or inside the virus, is sufficient to destroy infectivity (Rueckert, 1996).

The first picornaviral RNA to be completely sequenced and molecularly cloned into DNA was that of PV1 (Kitamura *et al.*, 1981; Racaniello & Baltimore, 1981). Since this landmark work, sequencing of many other picornaviral RNAs has shown a common organisational pattern (Figure 8).

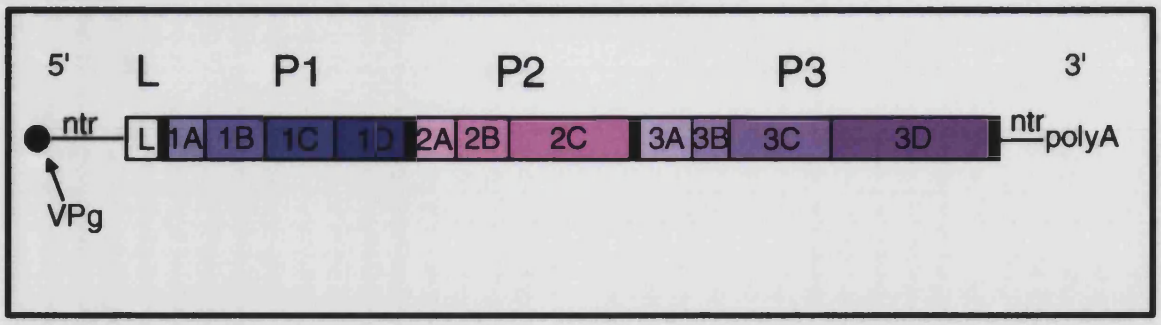

Figure 8: Structure of picornaviral RNA and genetic organisation of its polyprotein

The RNA is organised 5′-VPg-ntr-polyprotein-ntr-poly(A). ntr refers to nontranslated regions flanking the polyprotein. L434 is a mnemonic for recalling the polyprotein cleavage pattern; L specifies a leader protein found in cardioviruses, Theiler viruses, and aphthoviruses, but not in enteroviruses, HRVs, or human HAV. P1, P2, and P3 refer to precursor proteins cleaved by virus-coded proteinases into four, three, and four end products, respectively (Adapted from Palmenberg, 1990).

Sequence comparisons show significant variations in the size of picornaviral RNAs, which range in length from 7,209 to 8,450 bases. The 3′ ends of all picornaviral RNAs are polyadenylated, as is characteristic of most eukaryotic mRNAs (Ahlquist & Kaesberg, 1979). However, the 5′ ends are not capped in the usual manner with 5′-5′ triphosphate linkages. Instead, these viruses have small, viral-coded, genome-linked proteins (virion protein, genome; VPg) covalently attached by a tyrosine O^4-phosphodiester bond to the 5′ uridylyl nucleotide of the RNA (Nomoto *et al.*, 1976; Ambros & Baltimore, 1978; Rothberg *et al.*, 1978). VPg sequences are rich in basic, hydrophilic amino acids and have only one tyrosine residue (the attachment site) at position 3 from the amino end of the peptide (Nomoto *et al.*, 1976; Ambros *et al.*, 1978; Rothberg *et al.*, 1978; Ambros & Baltimore, 1980; Palmenberg, 1990).

Once released inside the cell, the single-stranded RNA genome must serve several distinct functions:

First, the genome serves as an unusual mRNA that successfully competes with cellular mRNAs for the cellular translation machinery. As mentioned, picornaviral genomic RNA is not capped but, instead linked to VPg. Interestingly, VPg is cleaved from all viral RNA molecules that serve as mRNA (VPg-pUUAAAACAG ...→ pUUAAAACAG ...), leaving a simple monophosphorylated pU terminus. The reason for removal of VPg, and the cellular enzyme catalysing it, is unknown. Initiation of translation is mediated by the IRES element, a peculiarly long (400nt) segment of the genomic RNA that directs

efficient cap-independent translation in all picornaviruses. It has been previously shown that the picornaviral IRESes can be classified into three distinct groups on the basis of primary sequence and secondary structure conservation and also on the basis of their requirements for efficient internal initiation of translation *in vitro* as discussed later.

Second, the viral genome must carry signals to warrant separation from the components of the translational machinery so that it can assume the role of template for RNA replication. This switch from translation is important only in the initial stage of replication as in later stages the abundantly synthesised plus-strand RNA can choose to become mRNA (after VPg cleavage), serve as template for minus-strand synthesis, or be encapsidated to form progeny virions. However, the mechanism by which the infecting virion RNA switches to transcription is unknown.

Third, the viral RNA must express specific signals for the recognition of the viral replication proteins. Finally, progeny RNA that will not engage in translation or RNA synthesis will be encapsidated. The packaging process, which may also involve a specific packaging signal, is still obscure (Xiang *et al.*, 1997).

1.3.1.3 General properties of picornaviral proteins

To complete a round of infection, a number of complex activities must be performed and coordinated. These include replication of the plus-strand RNA via minus-strand intermediates, translation, proteolytic processing, inhibition of host cell transcription/translation, virion assembly, and cell lysis. These activities must be directed by the 26 or more viral polypeptides detected in virus-infected cells, although most of these polypeptides are intermediates in the processing of the polyprotein precursor with no known function (Porter, 1993). Depending on the genus, about 11 to 13 fully processed viral polypeptides are produced in infected cells (Figure 9). Of these about seven to nine proteins are nonstructural (i.e. noncapsid) proteins and their multiple roles both in virus replication and in the associated inhibition of cellular functions are discussed, for the different genera, in the relevant sections below.

To simplify homologue identification, in 1983 the European Study Group on the Molecular Biology of Picornaviruses adopted a uniform nomenclature system, designated L-4-3-4, based upon an idealised map of the picornavirus polyprotein (Figure 9) (Rueckert & Wimmer, 1984).

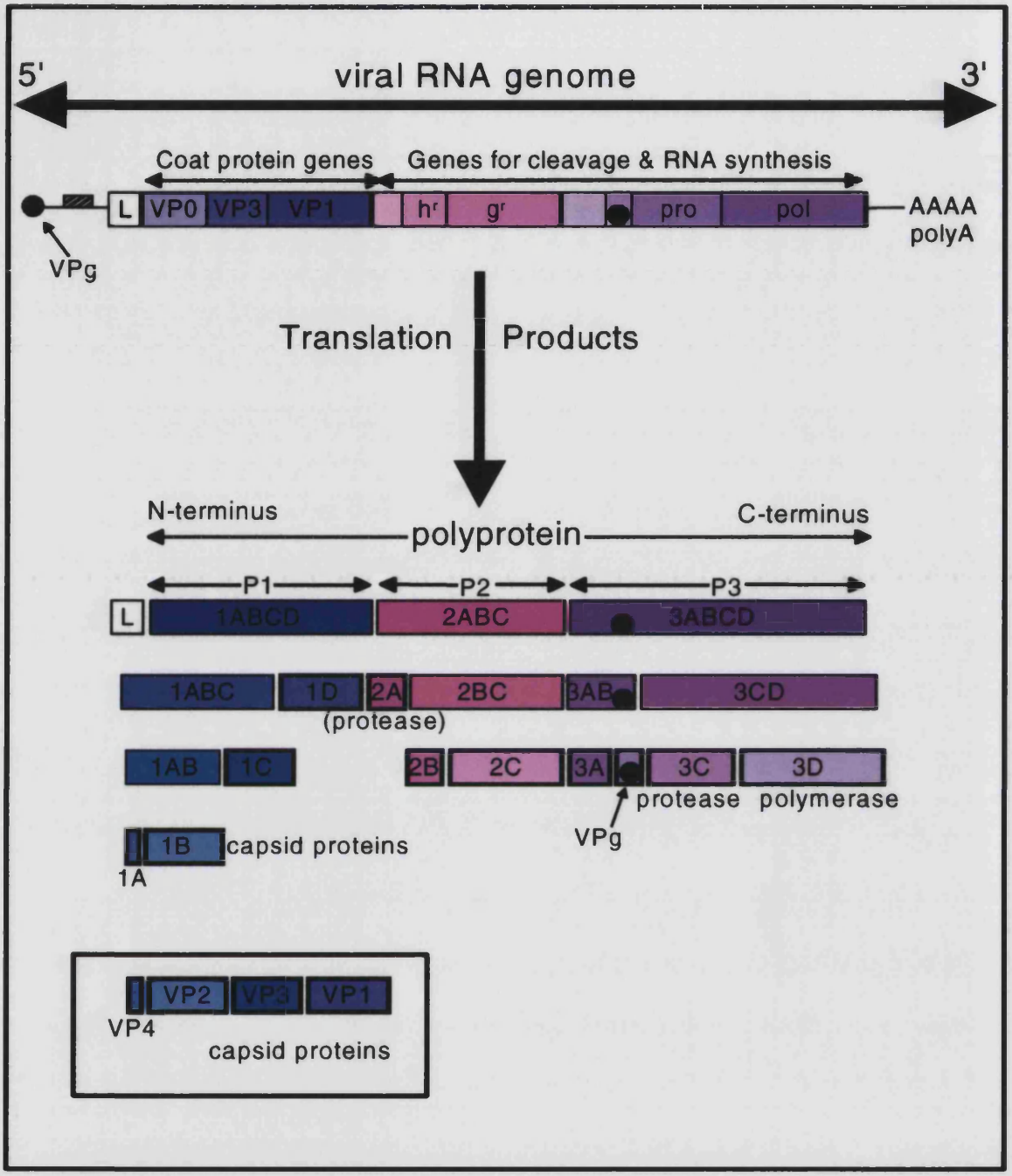

Figure 9: Picornavirus polyprotein and its processing

Processing map of a picornavirus genome. The striped bar over the 5′-nontranslated region indicates the presence of a polycytidylic acid tract found in EMC-like viruses and aphthoviruses. Synthesis of the protein is from left (N-terminus) to right (C-terminus). Growth functions, i.e., proteins needed for RNA synthesis and proteinases required to cleave the polyprotein, are encoded downstream from the capsid protein. g^r represents the guanidine-resistance marker, a genetic locus affecting the action of a drug thought to block initiation of RNA synthesis. The 2B gene, h^r, carries a host range determinant involved in RNA synthesis. The leader protein L is similarly only found in cardio- and aphthoviruses. The polyprotein of FMDV contains three 3B (VPg) segments, while all other viruses contain only one. Protein 2A has been identified only as a proteinase in the rhino- and enterovirus isolates (Adapted from Palmenberg, 1990).

Mature viral proteins are derived by progressive posttranslational cleavage of the polyprotein and this proteolytic processing is a distinguishing feature of the picornavirus life-cycle. Though the RNA genomes are effectively monocistronic, the three-tiered cascade of primary, secondary and maturation cleavage efficiently produces the spectrum of viral proteins necessary for a productive infection (Palmenberg, 1990).

This proteolytic cascade, common to all picornaviruses, is largely mediated by a virally encoded protease, $3C^{pro}$, the central enzyme in the cleavage cascade. An exception is the first polyprotein scission, a cotranslational (occurring as soon as the ribosome has reached the middle, or P2 region, of the genome), autoproteolytic cleavage referred to as the primary cleavage. The primary cleavage can occur in one of two places: between 1D and 2A in enteroviruses and rhinoviruses, or between 2A and 2B in cardio- and aphthoviruses. In entero- and rhinoviruses, the cleavage is mediated by a self-coded protease $2A^{pro}$, and does not require downstream viral proteins. In cardio- and aphthoviruses, the cleavage also occurs cotranslationally but the 2A protein is not a protease and the mechanism is less understood. Less still is known about this process in HAV.

Most subsequent or secondary cleavages are effected by viral protease $3C^{pro}$. The eventual result of the secondary cascade is release of all mature viral proteins necessary for establishment and completion of a successful infectious cycle as described in 1.3.1.4. The final cleavage within picornaviral polyproteins, maturation processing of the 1AB peptide (also called VP0), is, interestingly, not catalysed by any of the other identified viral proteases (Palmenberg, 1990).

Genetic and biochemical evidence have implicated all nonstructural PV polypeptides, including the proteinases, as being involved in genome replication (Wimmer *et al.*, 1993). It is important to realise that, in most cases, the virus utilises processing intermediates and processing end products for different functions, a strategy designed to expand the menu of useful polypeptides derived from a small genome. The best-studied example is the P3 region of the polyprotein that yields 3AB and $3CD^{pro}$. 3AB is a multifunctional RNA-binding protein, the precursor for 3A and 3B(=VPg), the terminal protein, which is an essential component in the initiation of RNA synthesis. $3CD^{pro}$ is a multifunctional proteinase, RNA-binding protein and the precursor of $3C^{pro}$ and $3D^{pol}$ (viral RNA polymerase). Equally important was the observation that many of the nonstructural proteins interact with each other to form homo- or heterodimers, or even oligomers (Lama *et al.*, 1994; Molla *et al.*, 1994; Paul *et al.*, 1994; Pata *et al.*, 1995; Xiang, 1995a).

The most important interactions that have been suggested to play a crucial role in genome replication, particularly in PV, are:

1. $3AB + 3CD^{pro} \rightarrow [3AB/3CD^{pro}] + cloverleaf \rightarrow [3AB/3CD^{pro}/cloverleaf]$
2. $3AB + 3CD^{pro} \rightarrow [3AB/3CD^{pro}] \rightarrow 3AB + 3C^{pro} + 3D^{pol}$
3. $3AB_{membrane\text{-}bound} + 3CD^{pro} \rightarrow 3A + VPg + 3CD^{pro}$
4. $VPg + 3D^{pol} + poly(A) + UTP \rightarrow VPgpU(pU) + 3D^{pol} + poly(A) + PP_i$
5. $3AB + 3D^{pol} \rightarrow [3AB/3D]^{super\text{-}pol}$
6. homointeractions of 2B, 3AB, and $3D^{pol}$

The AB/CD^{pro} complex, formed after cleavage between the two polypeptide chains, plays a central role in these interactions (Molla *et al.*, 1993, 1994). Depending on the environment, this complex can react in three different pathways depicted 1-3. 3AB stimulates proteolysis of proteinase $3CD^{pro}$ thereby yielding polymerase $3D^{pol}$ (2), while $3CD^{pro}$ cleaves membrane-associated 3AB to 3A and VPg (3). $3D^{pol}$ will uridylylate VPg to VPg-pU(pU) (4), the primer for initiation of RNA synthesis. 3AB and $3D^{pol}$ can also form a complex with significantly increased polymerase activity (5) (Paul, 1994; Plotch & Palant, 1995) and it is likely that this complex is important for the recognition of the 3′ end of the plus-strand template. At higher enzyme concentration, $3D^{pol}$ forms homooligomers with RNA binding and increased polymerase activity. Head-to-tail interactions between polymerase molecules along an extensive interface region have been observed in PV, leading to the suggestion that the enzyme complex funtioning in chain elongation may therefore be $[3AB_n/3D_m]^{superpol}$ (Xiang, 1997 and references within).

Of the proteins mapping to the P2 region of the polyprotein, only 2C has been shown to have RNA binding activity (Rodríguez & Carrasco, 1993; Rodríguez & Carrasco, 1995). 2A, a protease plays a role in host-cell shut-off, as well as effecting the primary cleavage in some picornaviruses. Protein 2B or 2BC is thought to participate in two of the major biochemical alterations that occur during PV infection: the inhibition of protein secretion (Doedens & Kirkegaard, 1995), in particular the disassembly of the Golgi complex (Sandoval & Carrasco, 1997) and the permeabilisation of the plasma membrane (Lama & Carrasco, 1992). These proteins will be discussed in the relevant sections below for the different genera.

Table 4: Structural characteristics of HAV compared with other picornaviruses

	HAV	ENTERO	RHINO	CARDIO	APHTHO
Virion Proteins (M_R) kDa					
VP1	<33.2	33.5	32.4	31.7	23.3
VP2	24.8	30	28.5	29	24.7
VP3	27.8	26.4	26.2	25.1	24.3
VP4	≤2.5	7.4	7.2	7.2	8.5
VPg	2.4	2.3	2.4	2.2	2.6-2.7
Genome					
Length (kb)	7.48	7.44	7.21	7.84	8.4
%(G+C)	38	47	40	50	43
Poly(C)′	-	-	-	+	+
Poly(C+T)′	+	-	-	-	-
Similarity	HAVs	Entero, Rhino	Rhino, Entero	Cardio	Aphthos

1.3.1.4 General replication strategy

Multiplication of picornaviruses occurs entirely in the cytoplasm. The initial event in infection is attachment of the virion to specific receptor units embedded in the plasma membrane (Figure 10, step 1). The function of receptors is twofold: to position the virion to within striking distance of the membrane (step 1), then to trigger a conformational change in the virion (step 2), which involves loss of an internally located protein and delivery of the viral RNA genome across the membrane and into the cytosol (step 3), where translation can begin (step 4) (Rueckert, 1996).

The successful completion of the picornaviral replicative cycle depends largely on the ability of the viral RNA species to compete with capped cellular RNAs for the host cell translation machinery. For all members of the picornavirus family except the cardioviruses, this goal is achieved through the inhibition of initiation of translation of capped cellular mRNAs.

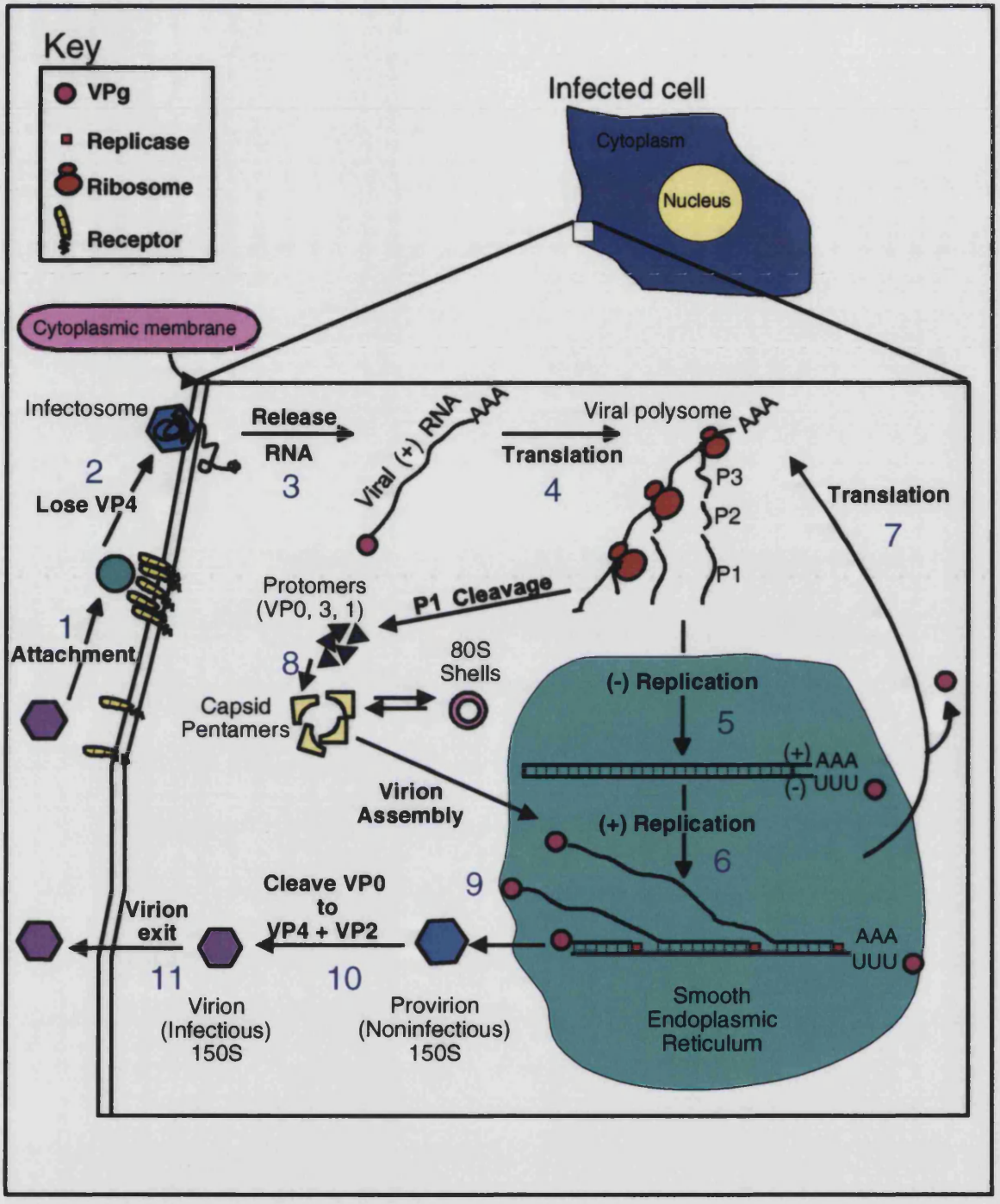

Figure 10: Overview of the picornaviral infection cycle

This inhibition of capped mRNA translation, known as host cell shut-off, is due, at least in part, to the proteolytic cleavage of the cellular translation initiation factor eIF-4γ (formerly known as p220), which is part of the eIF-4 cap-binding complex. The cleavage of eIF-4γ is carried out by the 2A proteinase during a rhinovirus, PV, and CV infection and by the leader (L) proteinase during FMDV infection. Cleavage leads to the inactivation of the

cap-binding complex, so that cellular capped mRNAs can no longer associate with the 40S ribosomal subunit. Picornavirus RNA translation can continue unabated in such conditions, as it is initiated in a cap-independent manner by ribosomes which have entered the RNA internally. Initiation of translation is mediated by the internal ribosome entry site (IRES) element, a peculiarly long higher order RNA structure of about 400 nt present in the picornaviral 5′ NTR. The different picornaviral IRESes can be separated into three distinct groups on the basis of sequence and structural considerations required for their optimal activity: type I entero-and rhinoviral IRESes (PV, HRV, ECHOvirus); type II cardio- and aphthoviral IRESes (FMDV, EMCV); type III IRESes, of which the HAV element is the only example to date (Borman and Kean, 1997). Translation is a crucial step because synthesis of new viral RNA cannot begin until the virus has successfully manufactured the virus-coded RNA-synthesising machinery.

By confiscating ribosomes and other protein-synthesising machinery of the host cell, the incoming RNA strand directs synthesis of a polyprotein, which is then cleaved into segments while still in the process of synthesis. Translation of a viral message is not restricted to a single ribosome; indeed, polysomes carrying up to 40 ribosomes have been reported in PV-infected cells. In PV, the first fragment released from the nascent polyprotein is a coat precursor protein (P1); the next released is a mid-piece precursor protein (P2); and the last segment released is P3. Each segment is released from the polyprotein by proteinases encoded in the polyprotein (Figure 10).

Protein P3 can be further cleaved by two separate mechanisms (Palmenberg & Rueckert, 1982). One mechanism is a monomolecular or *cis* cleavage, i.e. a concentration-independent self-cleavage that yields (a) a proteinase, 3C or 3CD; (b) a protein, 3AB, which is involved in initiating RNA synthesis; and (c) an RNA polymerase, 3D, which can elongate a primer RNA bound to a template RNA. The other mechanism is *trans* cleavage, i.e. bimolecular cleavage, involving one P3 molecule and the 3C proteinase generated by cleavage of another P3 precursor molecule. *Cis* cleavage of P3 presumably dominates the early stages of infection when the concentration of viral proteinases in the cytosol is low. Insights from the crystal structure of PV suggest that proteinase 3C cannot be active in the monomeric form (Chemaia *et al.*, 1993; Matthews *et al.*, 1994). *Cis* or intramolecular cleavage might therefore be accomplished by pairing of nascent P3 molecules on closely spaced ribosomes even before they have left the viral polysome.

The first step in synthesis of new viral RNA is to copy the incoming genomic RNA to form complementary minus-strand RNA (Figure 10, step 5), which then serves as a template for synthesis of new plus strands (step 6). Synthesis of plus-stranded RNA, which occurs on smooth endoplasmic reticulum, is initiated so rapidly (20- to 50-fold that of minus strands) that it generates multistranded replicative intermediates (RI) consisting of one minus-stranded template and many plus-stranded copies. During the early steps of replication, newly synthesised plus-strand RNA molecules are recycled to form additional replication centres (step 7 → step 5 → step 6) until, with an ever-expanding pool of plus-stranded RNA, a greater and greater fraction of the plus-stranded RNA in the RC is packaged into virions (Rueckert, 1996).

Virion assembly (steps 8 and 9) is controlled by a number of events. One is that, before assembly can begin, coat precursor protein P1 must be cleaved to form immature protomers composed of three tightly aggregated proteins (VP0, 3, 1). Early in the infection cycle this cleavage is likely very slow because the concentrations of P1 and the necessary proteinase (3C or 3CD) are low. Later, with increasing proteinase activity, the rising concentration of immature (5S) protomers triggers assembly into pentamers (step 8), which then package the plus-stranded VPg-RNA to form provirions (step 9). Infected cells often contain empty 80S protein shells that are reversibly dissociable into 15S subunits. Whether pentamers condense around RNA or RNA is threaded into 80S shells is still a subject of debate (Rueckert, 1996).

Provirions are not infectious. Formation of infective 150-160S particles (step 10) requires a "maturation cleavage" in which most of the VP0 chains are cleaved to form the mature four-chain subunits (VP4, 2, 3, 1) characteristic of picornavirions. Completed virus particles, which often form crystals in infected cells, are ultimately released by infection-mediated disintegration of the host cell (step 11) (Rueckert, 1996).

The time required for a complete multiplication cycle from infection to completion of virus assembly, generally ranges from 5 to 10 hours. The precise timing depends on variables such as pH, temperature, the virus, the host cell, the nutritional vigour of the cell, and the number of particles that infect the cell (Baltimore *et al.*, 1966). Some viruses such as hepatitis A, set up nonlytic infections that persist indefinitely (Provost & Hilleman, 1979). The precise characteristics must be established experimentally for each virus-cell system.

The available data on rearrangements (recombinations, deletions, and insertions) of picornavirus genomes fit the replicative template switch model postulating that an incomplete nascent minus RNA strand leaves the template and resumes its synthesis on another template (or another locus of the original template). The nascent strand dissociation is believed to be facilitated by the elongation pausing caused by secondary structure elements or nucleotide misincorporations. Rearrangements may involve (nearly) identical or completely dissimilar pairs of parting and anchoring sites (Agol, 1997). Such rearrangements contribute to both conservation and variation of the picornaviral genomes and observations for the individual genera will be discussed under the relevant headings.

1.3.2 Enterovirus and rhinovirus genera

The enteroviruses include not only the PVs but also the CVs, the ECHOviruses (Enteric Cytopathic Human Orphan), human enteroviruses (68-71) and a number of nonhuman enteric viruses.

ENTEROVIRUSES

Human polioviruses 1-3
Human Coxsackieviruses A1-22, 24
A23 is ECHOvirus 9
Human Coxsackieviruses B1-6
Human ECHOviruses 1-7, 9, 11-27, 29-34
ECHO 8 is ECHO 1
ECHO 10 is reovirus, type 1
ECHO 28 is human rhinovirus 1A
Human enteroviruses 68-71
Vilyuisk virus
Simian enteroviruses 1-18
Bovine enteroviruses 1 and 2
Porcine enteroviruses 1-8

Figure 11: Enterovirus serotypes

Infections with the enteroviruses - even the more virulent members of the genus - are characterised by a high proportion of subclinical manifestations. The clinical expressions of infection, when they do occur, range from severe and permanent paralysis, sometimes fatal, to minor undifferentiated febrile illnesses. Although certain enteroviruses have been more frequently responsible for epidemics involving a specific syndrome, at other times or in other places the same serotypes may be associated with sporadic or epidemic infections having different clinical manifestations or producing no symptoms. However, different enteroviruses may produce the same syndrome.

Enteroviruses multiply throughout the alimentary tract and cause a variety of infections. Because of their acid stability, enteroviruses that have undergone limited replication in the oropharynx survive transit through the stomach and become implanted in the lower intestinal tract, where they undergo more extensive multiplication. Rhinoviruses, which inhabit the upper respiratory tract, not only differ in that they are acid labile (they begin to lose infectivity at pH 6 and are completely unstable at pH 3), and this lability has become a defining characteristic of rhinoviruses, but are further distinguished from enteroviruses by their low optimal temperature of replication (33°C), reflecting their adaptation to the nasopharynx. Inactivation at low pH is associated with appearance of empty capsids and a loss of VP4 similar to receptor binding-induced uncoating, but possibly by a different mechanism. The buoyant density of enteroviruses in CsCl is 1.34g/ml, whereas rhinoviruses have a density of 1.4g/ml. Enteroviruses and some rhinoviruses can be stabilised by molar magnesium chloride against thermal inactivation (Melnick, 1996).

Rhinoviruses are the most commonly isolated viruses from persons experiencing mild upper respiratory illnesses (common colds). In contrast to the enteroviruses, rhinoviruses do not appear to replicate in the intestinal tract. They also differ from enteroviruses in their more extreme species specificity and more fastidious growth requirements (Rueckert, 1996). There are over 100 different serotypes of HRVs, which are divided into two groups based on their cellular receptors. The majority of HRVs (belonging to the "major receptor group") use ICAM-1 as their receptor. The remaining rhinoviruses (belonging to the "minor receptor group"), except for HRV87, utilise the low density lipoprotein receptor (Zhao *et al.*, 1997 and references therein).

RHINOVIRUSES	
Human rhinoviruses 1A-100, 1B, "Hanks"	Bovine rhinoviruses 1-3

Figure 12: Rhinovirus serotypes

PV is the prototype enterovirus that, in many ways, has spear-headed research not only on picornaviruses but on plus-strand RNA viruses in general and, along with rhinoviruses and CVs, will be the viruses which feature predominantly in the subsequent section.

1.3.2.1 Properties of virion

The diameter of the HRV is about 300Å and the molecular weight of the virus is approximately 8.16 x 10^6 Da, including RNA. The crystal structures of HRV14

(Rossmann *et al.*, 1985), HRV16 (Oliveira *et al.*, 1993), and HRV3 (Zhao *et al.*, 1996), all major receptor group viruses, have been determined, as well as the structure of HRV1A (Kim *et al.*, 1989), a minor receptor group virus.

The PV particle is approximately 28nm (310Å) in diameter with a molecular mass of 8.43 x 10^6 (Hogle *et al.*, 1985). The virion, composed of 60 copies of viral proteins VP1 to VP4 as previously described and illustrated in 1.3.1.1, contains an RNA core that when unravelled and fully extended for measurement in the electron microscope has a length of about 2,500nm. The tightly packed RNA resides in the central cavity of a thin protein shell.

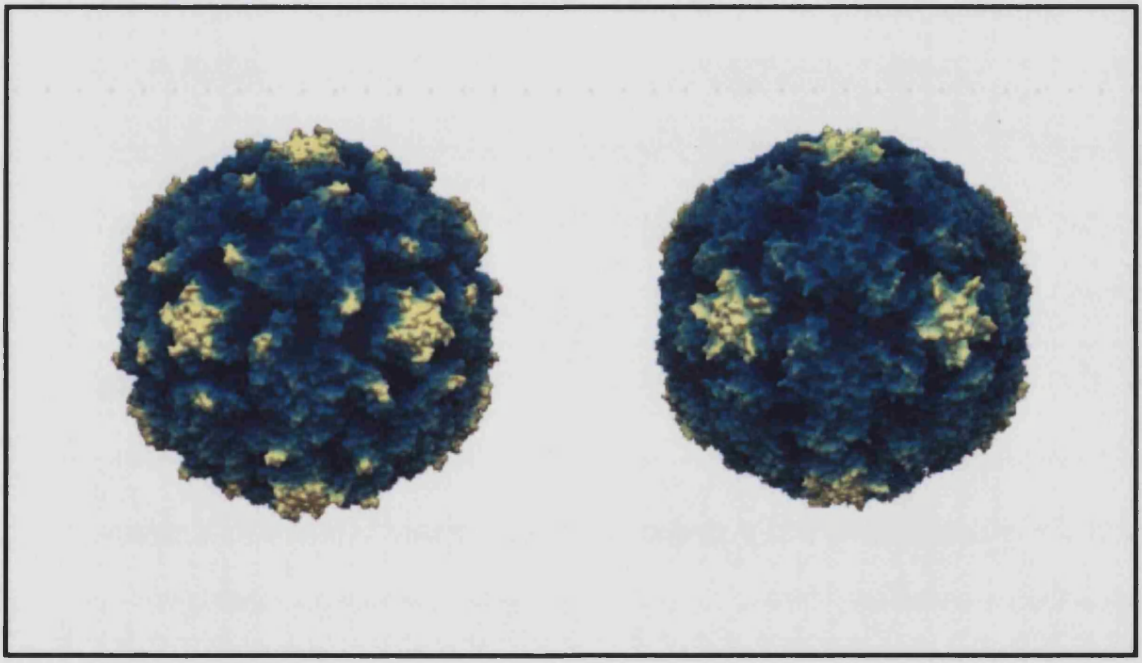

Figure 13: Molecular surface of poliovirus type 1 and rhinovirus 14

Molecular surface of PV type 1 Mahoney (left) and rhinovirus 14 (right), radially depth cued, as solved by X-ray crystallography by Hogle *et al.* (1985) and Rossmann *et al.* (1985) respectively. Images courtesy of J. -Y. Sgro on Silicon Graphics taken from http://www.bocklabs.wisc.edu/images/polio1.jpg and r14.jpg

With general acceptance of the 60-protomer model of capsid structure, attention focused on the structural organisation of the four-segmented protomer. The most prominent feature of the protomer, evident in HRV14, was the presence of a prominent cleft or "canyon" on its surface. This canyon was later shown to be the acceptor site for the receptor used by the virus to infect susceptible host cells. Of the four proteins, VP1 exhibits the greatest sequence variability and VP4 the least. VP1 is also the dominant

protein, playing key roles in surface topography and in several viral functions, including antigenicity, receptor attachment, and probably also viral uncoating (Rueckert, 1996). In PV and HRV the dominant neutralising immunogenic sites reside in the BC loop of VP1. Some ECHOviruses and CV As attach to a group of receptors called integrins, which have the ability to discriminate between different RGD-containing proteins (Rueckert, 1996).

In all of the rhinoviruses for which the structure is known, there is some density on the fivefold axes that cannot be interpreted as a part of the capsid protein and Zhao and colleagues (1997) have proposed that it is a Ca^{2+} ion. The putative Ca^{2+} ions in HRVs have been proposed to play a role in viral stability. When viruses enter the cell, the lower pH of the endosome and the lower Ca^{2+} concentration in cytoplasm may help to release the Ca^{2+} ion and facilitate virus uncoating.

Empty capsids lacking the viral RNA are generated during infection by most picornaviruses. Although such capsids have the same total protein content as do normal virions, they are noninfectious and are considered to be a by-product of infection or a storage form of capsid proteins. Since empty capsids lack viral RNA, maturation cleavage of VP0 does not usually occur.

1.3.2.2 Properties of genome

Enteroviruses contain a 7.5 kb single-stranded RNA molecule of positive polarity, which has a highly unusual structure that is, nevertheless, representative of many RNA viruses which is translated into a large polyprotein. This polyprotein is processed by virally encoded proteinases to the P1 region proteins, which form the viral capsid, and the P2 and P3 region proteins, most of which are required for viral RNA (vRNA) replication as previously mentioned.

Human rhinovirus (HRV) is a positive-stranded RNA virus, the genome being about 7.2 kb in length, with an ORF that encodes for a single polypeptide of about 3000 amino acids which is also proteolytically processed; eight of nine cleavages being catalysed by the 3C and/or the 3CD proteinases.

VPg is attached to the stem of a stable stem-loop "cloverleaf" structure, the first domain of the unusually long 5′NTR. Genetic analyses have shown that the integrity of the stem

regions in stem loops b and d, but not their sequence, is important for viral viability. On the other hand, the sequence of the loops in b and d appears to be very important as insertions or nucleotide changes lead to severe RNA replication phenotypes. The outstanding length of the 5´ NTR of the renteroviruses (610-747nt) and the high degree of homology within this region (64%-99%), which exceeds that of any coding region in the genome, suggest an important role. Additions to or deletions of part of the NTR of PV and HRV genomes resulted in transcripts that were not infectious, while transcripts containing completely intact NTRs were infectious. This 5'NTR harbours a second, very complex structure, the IRES that consists of domains II to VI. The IRES controls the translation of the polyprotein. Rivera *et al.* (1988) found that of the nine members of these genera they studied, conserved features in the 5´ NTR included long stretches of conserved sequence, pyrimidine-rich regions, and over 20 stem and loop structures. Pyrimidine-rich regions have been implicated as serving as recognition sites for 18S rRNA which contains a purine-rich region at its 3´-terminal end and may play an important role in initiation of translation, initiation of positive-strand replication, and packaging (Rivera *et al.*, 1988).

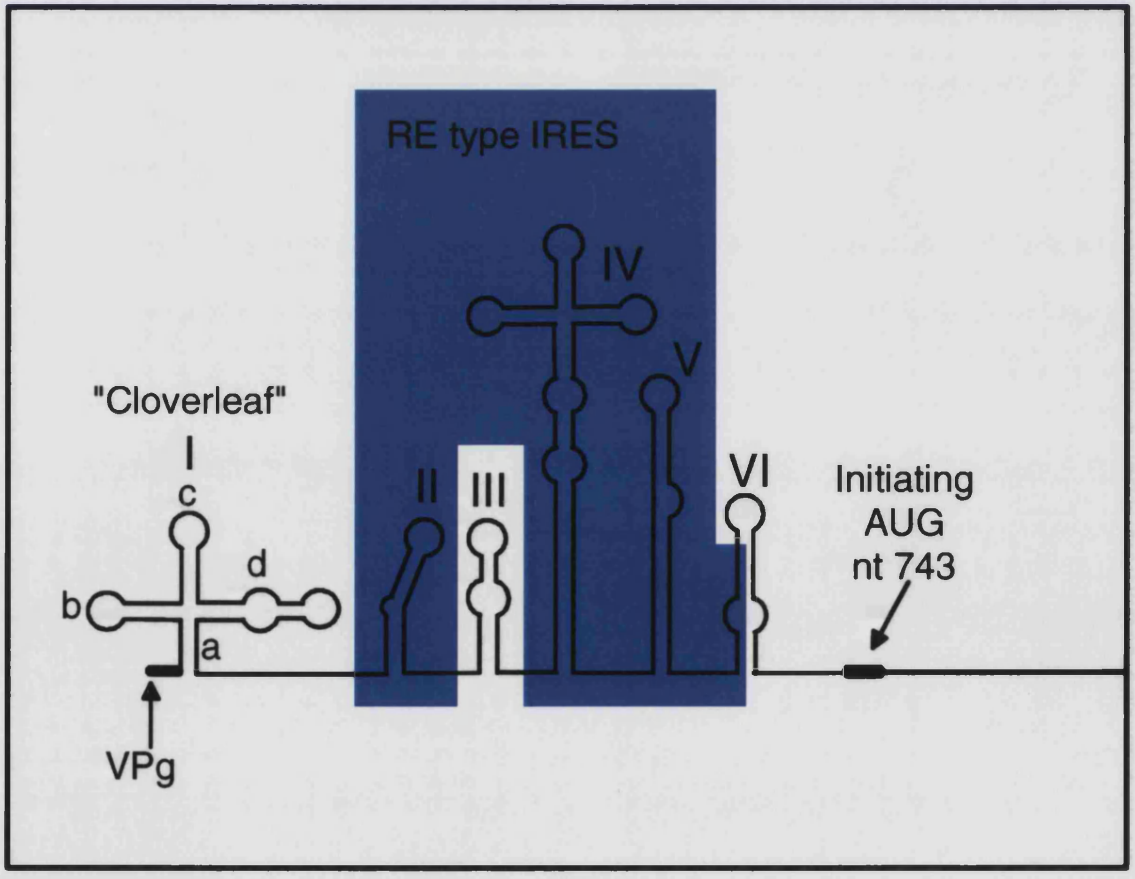

Figure 14: Poliovirus 5′ NTR with type I IRES

Following the 5′ NTR comes the ORF for the polyprotein that occupies nearly 90% of the viral genome. Finally the genome is terminated by the 3′ NTR consisting of two stem-loop structures and poly(A). The cloverleaf and entire 3′ NTR are involved in RNA synthesis. Pilipenko *et al.* (1992) compared the 3′ NTR sequences of entero- and rhinoviruses and proposed that they have highly organised secondary structures (stem loops or domains X, Y, Z) that can be grouped into three categories; (i) a single stem-loop structure (Y) in rhinoviruses (e.g. HRV14); (ii) two stem-loop strucutres (Y, X) in PVs; and (iii) three stem-loop strucutres (X, Y, Z) in some Coxsackieviruses and ECHOviruses (e.g. CV B3). Jacobson *et al.* (1993) proposed that a pseudoknot, formed between sequences in domain Y and upstream sequences may play an important role, however some sequences in loops Y and X of PV1 and CV B3 are complementary and could interact in a "kissing mode", and this model, which is supported by genetic analyses, is currently favoured. Interference with kissing resulted in an RNA replication phenotype whereas mutations interfering with the pseudoknot showed little or no effect of the growth properties of the corresponding viral variants. The heteropolymeric regions of the 3′ NTR of different picornavirus species is very diverse, even within a single genus. HRV14 has, in addition, evolved a third structural element essential for RNA synthesis that maps, surprisingly, to the coding region P1 of the capsid precursor.

1.3.2.3 Properties of viral proteins

Of the viral noncapsid proteins, 2A, 3C, and 3CD are viral proteinases involved in the processing specific to PV polyprotein. 2C has ATPase activity, 3B is VPg, 3D is a viral RNA-dependent RNA polymerase which has unwinding activity, 2B and 2C are considered to play important roles in viral RNA synthesis, and 3A could have an important role(s) in uridylylation of VPg in the process of initiating RNA synthesis (Shiroki *et al.*, 1995).

In the renteroviruses, the 2A region codes for a cysteine proteinase ($2A^{pro}$), which shares significant sequence homology to the trypsin-like small serine proteases (Sommergruber *et al.*, 1989; Lu *et al.*, 1995), cleaves only at tyrosine-glycine bonds in PV, and is autocatalytically released from the nascent polyprotein by rapid cotranslational cleavage in *cis* at its own amino terminus at (Y, T, H, F, A, or V)-G dipeptide pairs and studies by Wang *et al.* (1997) suggest that the eight residues upstream of the scissile bond are sufficient for the cleavage by HRV2 2A. Cleavage is a prerequisite for further proteolytic processing of the capsid precursor region.

The first cleavage of the HRV polyprotein is catalyzed by the 2A protease and has been found to be a co-translational event. This cleavage, occurring between the capsid protein VP1 and the N-terminus of 2A itself, separates the viral capsid from the nonstructural proteins.

A wealth of evidence, both genetic and biochemical, shows that a second function of $2A^{pro}$ is to initiate the cleavage of the large subunit eIF-4G (also known as p220) of the eukaryotic translational initiation factor 4 (eIF-4), thereby causing a shut-off of cap-dependent translation of cellular mRNAs (Wang *et al.*, 1997). The inactivation of the cellular cap-dependent translational machinery facilitates the IRES-driven translation of the viral open reading frame. However, recent studies showed that cap-dependent translation could still occur in the presence of cleaved p220. It is believed that PV $2A^{pro}$ does not directly cleave p220, rather it activates a quiescent cellular protease which then cleaves p220 (Wyckoff *et al.*, 1990). In contrast, rhinovirus or Coxsackievirus $2A^{pro}$ is capable of cleaving p220 directly. No cellular protein has been shown to be directly cleaved by PV $2A^{pro}$ to date (Yalamanchili *et al.*, 1997a).

In addition, recent studies from a number of groups suggest that the $2A^{pro}$ protein of PV is involved in viral RNA replication and in the *trans*-activation of IRES-driven translation (Molla *et al.*, 1993(b); Macadam *et al.*, 1994; Lu *et al.*, 1995). Interestingly, PV genomes containing heterologous 2A-encoding sequences displayed different translational activities *in* vitro, while the kinetics of proteolytic processing of their translation products were indistinguishable from those of wild-type PV (Lu *et al.*, 1995).

It has been shown that PV-encoded protease $3C^{pro}$ directly inhibits host cell transcription catalysed by RNA polymerase II (Pol II) and III both *in vivo* and *in vitro.* The TATA-binding protein (TBP), a component of transcription factor TFIID, is directly cleaved by $3C^{pro}$, which leads to Pol II transcription shut-off. The cleaved TBP is unable to form a complex with the TATA box. Likewise, the largest subunit of the Pol III DNA-binding transcription factor is cleaved by $3C^{pro}$, leading to shut-off of Pol III transcription. Apparently cleavage of TBP does not contribute to Pol III transcription shut-off, although the multicomplex Pol III transcription factor TFIIIB contains the TBP polypeptide. $3C^{pro}$ also catalyses shut-off of Pol I transcription. However, the precise nature of the Pol I transcription factor(s) inactivated by $3C^{pro}$ remains unknown (Yalamanchili *et al.*, 1997a and 1997b).

Davies *et al.* (1991) demonstrated that transient expression of $2A^{pro}$ in eukaryotic cells inhibited both cellular translation and transcription. The inhibition of transcription seen in cells expressing $2A^{pro}$ could be due to a primary effect or a secondary effect caused by inhibition of translation. TBP contains a cleavable tyrosine-glycine bond, and it was recently determined that $2A^{pro}$ directly cleaves the single tyrosine-glycine bond (at position 34) of TBP. This cleavage is also seen in virus-infected cells. Surprisingly, despite TBP cleavage at this bond, Yalamanchili *et al.* (1997a) found that $2A^{pro}$ was unable to inhibit RNA Pol II transcription *in vitro*.

Ziegler *et al.* (1995) have not only shown that the protein and RNA components involved in the stimulation of IRES-driven translation are interchangeable between rhino- and entero-viruses, but not the distantly related cardioviruses, but also that the HRV2 2A proteinase is more efficient at stimulating IRES-driven translation than any other protein identified to date and that the stimulation correlates with the enzymatic activity of the 2A proteinase, the proteolytic conversion of some cellular component(s) being involved in 2A proteinase-mediated translational transactivation. More recently, Haghighat *et al.* (1996) demonstrated that HRV2 $2A^{pro}$ cleaves purified recombinant eIF4G directly *in vitro*, although relatively poorly. In contrast, a complex of eIF4G with eIF4E is a preferable substrate for HRV2 $2A^{pro}$. It was therefore proposed that eIF4F, and not the eIF4G subunit alone, is the primary target for cleavage by HRV2 $2A^{pro}$. Consistent with these results, restoration of cap-dependent translation in $2A^{pro}$-treated extracts requires both the eIF4E and eIF4G subunits of the eIF4F complex.

Recently it was found that the expression of PV protein 2B or 2BC results in two of the major biochemical alterations that occur during enterovirus infection: the inhibition of protein secretion (Doedens & Kirkegaard, 1995), in particular the disassembly of the Golgi complex (Sandoval & Carrasco, 1997) and the permeabilisation of the plasma membrane (Lama & Carrasco, 1992). The relevance of these activities to the viral life-cycle remains to be elucidated (van Kuppeveld *et al.*, 1997). Both biochemical functions in CV B3 are dependent upon the integrity of one of two hydrophobic domains found within enterovirus 2B proteins, one, the more amino-terminal of which, a predicted cationic amphipathic α-helix, involved in both the inhibition of protein secretion and the permeabilising activity, whereas mutation of the second hydrophobic domain, near the C-terminus of 2B, has a greater effect on the secretion inhibition function (van Kuppeveld *et al.*, 1997). A moderate degree of hydrophobicity of this domain is essential for the function of 2B. In CV B3, mutations which caused a major increase or decrease in hydrophobicity as well as the introduction of negatively charged residues interfered with

virus growth by an effect on its interaction with the membrane (van Kuppeveld *et al.*, 1995). By interfering with the 2B/2C cleavage site, the importance of efficient processing at this site was identified and subsequently it was determined that a critical level of CV B3 protein 2B or 2BC, or both, may be required to alter membrane permeability (2C does not alter plasma membrane permeability) and, possibly as a consequence, to shut-off host cell translation (van Kuppeveld *et al.*, 1996). Sandoval & Carrasco recently (1997) demonstrated that transient expression of the PV protein 2B in COS-7 cells causes the disassembly of the Golgi complex by a process preceded by the accumulation of the protein in the Golgi area. Inhibition of protein secretion during enterovirus infection is not a direct result of increased membrane permeability, but is likely to result from alteration or sequestration of membranes or proteins required for secretory transport. This could simply be a consequence of RNA RC assembly, or it may play an additional role in viral amplification such as blocking host antiviral responses (Doedens & Kirkegaard, 1995).

Proteins 2C and 2BC, in the absence of other PV proteins, associate with membranes and induce formation of vesicles and therefore may be the viral protein(s) responsible for the generation of the small membrane vesicles on which vRNA replication takes place. In addition to inducing proliferation of membranous vesicles PV 2BC also alters cellular calcium homeostasis (Aldabe *et al.*, 1997). As well as vesicles, protein 2C induces formation of a tubular, myelin-like membrane structure which is not seen in PV-infected cells (Cho *et al.*, 1994). Although the 2C protein lacks a defined membrane binding domain, Echeverri & Dasgupta (1995) demonstrated that the N-terminal region, encompassing amino acids 21-54 and containing a putative amphipathic helix, plays an important role in membrane binding both *in vivo* and *in vitro*, whereas the C terminus half, includes the NTPase motifs (RNA binding is abolished when C terminal 74 amino acids are removed (Rodríguez & Carrasco, 1993)) and the other amphipathic helix, appears to be unecessary for membrane association. More recently however, Teterina *et al.* (1997b) showed that both the N- and C-terminal regions, but not the central region, of 2C interact with intracellular membranes and induce major changes in their morphology, leading to the prediction that the protein folds into a structure composed of three domains, connected by small conserved loops or disordered regions. Prior to this, the observation that 2C copurifies with 3AB, led to a speculation that 2C may be associated with membranes by virtue of its affinity to 3AB (Takegami *et al.*, 1983). Paul *et al.* (1994) believe it is likely that 2C associates with the membrane through a hydrophobic face formed on an alpha helix and/or β sheets. It has been seen since, however, that cells expressing plasmid-encoded PV 2C or 2BC protein, in the absence of other viral proteins, displayed extensive rearrangement of intracellular membranes, to

form vesicles as well as other organised membrane structures by virtue of an interaction of 2C and 2BC with intracellular membranes (Cho *et al.*, 1994; Aldabe & Carrasco, 1995).

Protein 2C is a small NTPase with RNA binding properties (Rodríguez & Carrasco, 1993; Mirzayan & Wimmer, 1994) located at the cytoplasmic surface of the virus-induced membrane vesicles where it may be involved in attaching the vRNA to the membranous RC, and is one of the most highly conserved viral proteins among all picornaviruses.

Identification of putative NTP binding motifs in the highly conserved region of the protein suggested that 2C may be involved in binding and/or hydrolysis of NTP and led to a speculation that 2C may function as an RNA helicase (Gorbalenya *et al.*, 1990), consistent with its proposed role in RNA replication. The NTP binding activity of the central domain of 2C is not required for vesicle induction, although, when fused to the N-terminal domain, profound changes in the specific membrane architecture, generating formation of numerous smooth vesicles, is seen (Teterina *et al.*, 1997b). Recently, PV 2C and 2BC were expressed in *E. coli* as MBP-fusion proteins and shown to have ATPase and GTPase activities (Rodríguez & Carrasco, 1993). A recombinant baculovirus expression system was used to produce PV 2C that also displayed ATPase activity (Mirzayan & Wimmer, 1994). However, no helicase activity was reported and it remains to be seen whether 2C possesses an RNA helicase activity which may perhaps function at the initiation step of RNA synthesis (Cho *et al.*, 1994).

Guanidine has been shown to inhibit viral RNA replication by affecting coupling between the NTP binding and/or splitting, on the one hand and the 2C function (related to conformational changes), on the other, thereby implying that oligomerisation of 2C is an essential step in the replication of viral genome (Tolskaya *et al.*, 1994). The data of Vance *et al.* (1997) support a role for 2C in the assembly of mature virions. Perhaps 2C affects the association of capsid precursors with each other or with the RNA to facilitate the encapsidation of the RNA.

Mutations in 2B and 2C have been shown to be important with respect to RNA synthesis and host range change that occurs during adaptation and passage of virus in cell culture and leads to attenuation of the virus (Emerson *et al.*, 1993; Graff *et al.*, 1994) and will be covered later.

3B is usually referred to as VPg, a small peptide of 22 amino acids in PV covalently linked via tyrosine to the 5′ termini of all full-length and nascent viral plus- and minus-strand RNAs. PV VPg is removed by a cellular unlinking enzyme (leaving 5′ pU) from those viral RNAs destined to become mRNAs. An attractive hypothesis is that 5′-linked VPg serves as an encapsidation signal, leaving the mRNAs free for translation without obstruction from the replication machinery (Porter, 1993).

The PV-encoded, membrane-associated VPg-precursor, 3AB, a 12kDa polypeptide abundantly found in PV-infected cells, has been implicated in the initiation of viral RNA synthesis and may be used for the delivery of VPg to the membrane-associated PV RC. RNA RCs form on membranous vesicles that contain viral proteins, newly synthesised viral RNA, and host proteins. Both RNA synthesis and RNA packaging occur in association with the membrane-associated RC (Hope *et al.*, 1997). It has been postulated that a uridylylated form of VPg (VPg-pU) or a precursor thereof (3AB-pU) may serve as primer for $3D^{pol}$, a mechanism by which the viral protein would be linked to the nascent strand. A second hypothesis proposes that hairpins, formed at the 3′ termini of the viral RNA, serve as primers. VPg supposedly functions subsequently as a highly specific nuclease that cleaves the hairpin structure thereby linking itself to newly generated 5′ termini of viral RNA (Tobin *et al.*, 1989). Available evidence favours the first of these models (Lama *et al.*, 1994).

Expression of PV 3AB and 3A is extremely toxic to bacteria and this toxicity correlates with the ability of these proteins to make *E. coli* cells permeable to different compounds. This suggests that the two PV polypeptides may act as pore-forming proteins when expressed in *E. coli* (Lama *et al.*, 1992; Lama & Carrasco, 1996). The C-terminal 22 amino acids of 3A constitute a hydrophobic domain through which 3AB is believed to be anchored onto cytoplasmic smooth membranes where active RNA replication occurs. Further evidence making 3AB, which associates with intracellular membranes in isolation (Datta & Dasgupta, 1994) and binds directly to polymerase 3D, a likely candidate for the membrane tether for 3D polymerase comes from Hope and colleagues (1997) who discovered that detergent-solubilised and purified 3AB can be co-immunoprecipitated with either 3D polymerase or 3CD protease, which contains all 3D sequences but does not exhibit polymerase activity. Detergent-solubilised 3AB has been shown to stimulate both the polymerase activity of purified 3D polymerase and the proteolytic activity of 3CD in cell extracts. However, detergent-solubilised 3AB is not a substrate for 3CD cleavage, whereas membrane-associated 3AB is.

PV protein 3AB has been shown to form a complex with and stimulate the activity of the viral RNA polymerase, $3D^{pol}$ (Plotch & Palant, 1995) which will be discussed later. More recently Hope *et al.* (1997) described the use of the yeast two-hybrid system to isolate and characterise mutations in the 3D polymerase that cause it to interact less efficiently with 3AB and concluded that interaction between 3AB and 3D or 3D-containing polypeptides plays a role in RNA synthesis during PV infection. Lama *et al.* (1994) have investigated the properties of purified recombinant PV 3AB and have suggested that it acts as substrate for viral proteinases and as cofactor for RNA $3D^{pol}$. Molla *et al.* (1994) have shown that addition of VPg or 3AB stimulated the appearance of the cleavage products of $3CD^{pro}$ by an effect on the 3C protease of PV.

The 3C regions of all picornaviruses code for a protease ($3C^{pro}$) with a critical function as the enzyme responsible for the majority of maturation cleavages in the precursor polyprotein (Figure 9). PV 3C proteinase proteolytically cleaves the translated polyprotein at 9 of 12 specific processing sites and is largely responsible for the liberation of the individual gene products. Proteolysis by $3C^{pro}$ occurs in a complex and incompletely understood cascade of *cis* and *trans* cleavages at mainly Q-G, Q-S, Q-A, and Q-N pairs (except in FMDV strains for which cleavage sites are more diverse, e.g., E-G, V-G, C-N, L-N, and Q-G). PV 3C also participates in the formation of the viral replicative initiation complex where it specifically recognises and binds the stem-loop structure in the 5′ NTR of its own genome (Andino *et al.*, 1990, 1993; Harris *et al.*, 1994). The recognition site of 3C is located on the opposite side of the molecule in relation to its proteolytic active site and is centred about the conserved KFRDIR sequence of the domain linker (Gorbalenya *et* al., 1989; Hämmerle *et al.*, 1992; Mossimann *et al.*, 1997). Mosimann *et al.* have recently (1997) published the refined X-ray crystallographic structure of the PV 3C gene product.

PV 3C is comprised of two six-stranded antiparallel β-barrel domains and is structurally similar to the chymotrypsin-like serine proteinases. The shallow active site cleft is located at the junction of the two β-barrel domains and contains a His40, Glu71, and a Cys147, equivalent to Cys146 in HRVs, as the active site nucleophile in the catalytic triad (Lawson & Semler, 1991; Leong *et al.*, 1993; Mosimann *et al.*, 1997). The polypeptide loop preceding Cys147 is flexible and likely undergoes a conformational change upon substrate binding (Mosimann *et al.*, 1997). Certain substitution mutations in the putative catalytic triad of PV $3C^{pro}$ had differential effects on cleavage at different $3C^{pro}$-sensitive sites, which complicated the task of identifying the members of the

catalytic triad (Hämmerle *et al.*, 1991; Kean *et al.*, 1991).

Severe inhibition of host cell RNA transcription by all three classes of host cell RNA polymerase (Pol I, Pol II, and Pol III) is observed in PV-infected cells, and known as host cell transcription shut-off, however, the RNA polymerases themselves are not affected by PV infection. There is persuasive evidence that PV $3C^{pro}$ specifically and directly cleaves the TATA-binding protein (TBP) subunit of transcription factor IID both *in vivo* and *in vitro*, leading to a loss of formation of of the TBP-TATA box complex *in vitro*, resulting in the inactivation of Pol II transcription (Yalamanchili *et al.*, 1996). More recently the cyclic AMP-responsive element binding protein (CREB) mediated activated Pol II transcription was shown to be inhibited by proteolytic cleavage of the phosphorylated, transcriptionally active form of the CREB protein by $3C^{pro}$ (Yalamanchili *et al.*, 1997b) and that cleavage mediated by $3C^{pro}$ both *in* vivo and *in vitro* of another transcription activator, Oct-1 occurs (Yalamanchili *et al.*, 1997c). Similarly, a RNA Pol III DNA-binding transcription factor, IIIC, the α subunit of which actually contacts the Pol III promoter and is the target of cleavage, is cleaved and inactivated by $3C^{pro}$ (Shen *et al.*, 1996) In addition, PV $3C^{pro}$ completes the proteolysis of an active form of transcription factor IIIC to an inactive form by about 5h post-infection, suggesting that this is an important mechanism for the shut-off of host transcription by Pol III. PV $3C^{pro}$ is further implicated in the destruction of a transcription factor complex essential for Pol I transcription. Thus, $3C^{pro}$ may be centrally involved in inhibiting transcription by the three major classes of RNA polymerase (Porter, 1993). In 1993 Leong and co-workers provided evidence that HRV14 $3C^{pro}$, which binds specifically to the 5′ NTR of the viral RNA, has different domains for this binding and its proteolytic activities. Joachims *et al.* (1995) have also described the cleavage of a cytoskeletal protein, microtubule-associated protein 4 (MAP-4) by $3C^{pro}$ and $3CD^{pro}$ in PV and HRV14 which correlated with a marked "collapse" of microtubules during late infection.

$3C^{pro}$ of the renteroviruses is unable to perform, however, the VP0-VP3 cleavage, which is carried out by 3CD (Ypma-Wong & Semler, 1987; Takahara *et al.*, 1989) and which in the case of purified PV $3CD^{pro}$ can accumulate due to the cleavage efficiency of 3C at its carboxy terminus being rather low (Gauss-Müller *et al.*, 1991). The 3CD precursor of the renteroviruses is, in fact, the catalytic unit vested with the cleavage of most capsid precursor locations. (Ypma-Wong *et al.*, 1988). Unlike $3C^{pro}$ cleavages, the 3CD cleavage at VP0-VP3 site in PV requires myristylation of the amino terminus of the polyprotein, and an unknown cellular cofactor facilitates efficient 3CD cleavage at the PV

VP0-VP3 site and, to a lesser extent, at the VP3-VP1 site. It should be kept in mind that 3CD may also play a role (with or without $3C^{pro}$) in the modification of transcription factor complexes associated with the inhibition of cellular Pol I, Pol II, and Pol III transcription by PV (Porter, 1993). Genetic evidence has revealed that, surprisingly, $3CD^{pro}$ has the propensity to bind the 5′-terminal cloverleaf of PV RNA, but this occurs only in the presence of a 36kDa host factor, one of two proteins (p50 and p36) that interact with this cloverleaf structure. Host protein p50 is the eukaryotic elongation factor EF-1α, and p36 an N-terminal fragment thereof (Harris *et al.*, 1994). Mutations in stem-loop structures within the first ~100 nt of the PV 5′ NTR and mutations in the 3C domain of protein 3CD affect *in* vitro binding of 3CD to viral RNA and plus-stranded RNA synthesis in infected or transfected cells (Andino *et al.*, 1990, 1993). The $3AB\text{-}3CD^{pro}$ complex, however, interacts with cloverleaf RNA and binds to 3′ RNA fragments of the PV genome in the absence of host factor (Harris *et al.*, 1994). Very recently, Roehl *et al.* (1997) demonstrated that the activity of the 3CD/3C proteinase results in the modification of a cellular precursor protein, yielding a 38kDa protein which binds to PV negative-strand RNA and is thought to be used for assembling a ribonucleoprotein complex at the 3′ end of PV negative-strand RNA. Hope *et al.* (1992) concluded from their work that $3CD^{proM}$ (M designates the cleavage site mutant $3CD^{pro}$ T181K) can process both structural and nonstructural precursors of the PV polyprotein and moreover, that cleavage of 3CD, inactive as a RNA polymerase (Harris *et al.*, 1992), to $3D^{pol}$ is needed to activate the 3D RNA polymerase (Gauss-Müller *et al.*, 1991). Blair *et al.* (1996) described mutations in the 3C residues (Thr-142 and Ala-172) of 3CD which may exert their effects on RNA binding through formation of an RNA binding domain rather than via direct interaction with RNA, as might be expected of properly positioned basic amino acid residues. Davis *et al.* (1997) have shown that the 3D domain of 3CD proteinase had some influence on substrate recognition, but did not have dramatic impact on its interaction with inhibitors, and thus suggest that the active site of 3CD has a similar conformation to that of the 3C proteinase.

The 3D regions of all picornaviruses code for a polymerase ($3D^{pol}$) which exhibits a RNA chain elongation activity that is dependent upon an RNA template and a DNA or RNA primer. The enzyme has been extensively purified from PV-infected cells, and its cDNA has been cloned and expressed in bacterial and insect cells (Richards *et al.*, 1987; Plotch *et al.*, 1989; Neufeld *et al.*, 1991). Neufeld *et* al. demonstrated in 1991 that PV RNA polymerase from native and recombinant sources, when purified exhibit identical properties validating the use of these recombinant proteins for further studies.

Several amino acid sequences are conserved among all RNA-templated polymerases, most likely reflecting their shared catalytic functions and serving as a signature to identify RNA-dependent polymerase function. In PV $3D^{pol}$, a 52kDa protein, these conserved residues include a YGDD sequence (residues 326 to 329), D-233, and G-289. Three-dimensional structural analysis of several polynucleotide polymerases reveal striking core structures, which are designated fingers, palm, and thumb domains, referring to the resemblance of the core structure to a right hand. The conserved residues in PV $3D^{pol}$ appear to reside in the palm domain and are thought to contribute to the catalytic pocket of the polymerase. D-328 and D-329 are residues which are probably involved in metal ion coordination. The roles of the other conserved residues are unknown. These enzymes, however, all share properties of template and nucleotide binding, as well as catalysis of phosphodiester bond formation. The PV $3D^{pol}$ contains two peptide segments previously shown to cross-link to nucleotide substrates via lysine residues (Richards *et al.*, 1995) and in fact, a lysine residue at position 61 of $3D^{pol}$ has been shown to be essential for polymerase catalytic function and that a basic (lysine or arginine) residue at position 276 is required for some other function of 3D important for virus growth but not for RNA chain elongation or polyprotein processing (Richards *et al.*, 1996). Data produced by Richards *et al.* in 1992 suggested that nucleotide binding causes conformational alteration of the polymerase enzyme's structure.

Together with 2C and the cellular protein actin, 3CD, 3C, and 3D are present in highly purified preparations of FMDV and PV. They remain bound in variable amounts to the RNAs when they are extracted with phenol. As described before RNA prepared by these methods is rapidly degraded, but hydrolysis can be prevented by antibody against *E. coli*-expressed 3D, indicating that it is the RNA polymerase that has nuclease activity (Newman & Brown, 1997).

In the studies by Richards *et al.* in 1987, it was shown that PV polymerase was produced (a) by intermolecular cleavage of a fusion protein by another protein with protease 3C activity and (b) by cleavage of a fusion protein containing 3C and 3D sequences in the same polyprotein. Cho and colleagues (1993) reported that highly purified recombinant PV $3D^{pol}$ can *in vitro* unwind a long stretch of RNA duplex so as to displace strands for continued polymerisation of nascent chains and that the unwinding reaction proceeds in an elongation-dependent, ATP-independent manner requiring no additional proteins. It was determined also that PV $3D^{pol}$ was able to add multiple adenylate (A) residues to the 3′ terminus of RNA in a nontemplated manner which was classified by Neufeld *et al.* in 1994 as a terminal adenylyl transferase (TATase) activity and proposed to effect the

initiation of plus-strand synthesis. PV $3D^{pol}$ is, in fact, the only protein required for elongation of RNA chains *in vitro*, however current models propose that *in vivo* $3D^{pol}$ must function in concert with other viral and/or cellular proteins (Cho *et al.*, 1993) as discussed later.

1.3.2.4 Replication

The replication of rhinoviruses is similar to that of enteroviruses except that time to completion is more variable and tends to be longer. In one-cycle growth experiments, new virus is frequently detectable in 5 to 7 hours, and a cycle is complete in 10 to 12 hours, whereas first appearance may be as late as 9 hours and completion as late as 15 to 17 hours. Yields vary from 10 to 200 plaque-forming units (PFU) per cell.

Molecules belonging to the immunoglobulin (Ig) superfamily serve as receptors for the major-group HRVs (intercellular cell adhesion molecule 1) and for PV (unknown cellular function) (Bibb *et al.*, 1994). Interestingly, Zhang & Racaniello (1997) have shown that expression of the PV receptor is not sufficient to permit replication in the mouse gut indicating that other factors are involved in determining the ability of PV to replicate in this tissue. ECHOviruses 1 and 8 attach to integrin VLA-2 and $\alpha v\beta 3$ integrin is reported to be the receptor for CV A9 and ECHOvirus 22. Minor-group HRVs, except HRV87 (Uncapher *et al.*, 1991), bind to cells via members of the low-density lipoprotein receptor family (Zhao *et al.*, 1997). Decay-accelerating factor (DAF, CD55) is recognised as the cellular receptor for at least six ECHOvirus serotypes and as a receptor for CVs B1, B3, and B5, and is the HeLa cell receptor for enterovirus 70 (Karnauchow *et al.*, 1996). Interaction of group B CVs with permissive cells may also involve a nucleolin-like membrane protein.

PV enters susceptible cells via the PVR as mentioned above, however the mechanism of uptake and uncoating are still unknown (Xiang *et al.*, 1997). PV and HRVs have been shown to attach to their receptor molecules on the cell membrane and enter the host cell or deliver its RNA by a poorly understood process involving the loss of VP4 and the formation of 135S "A" ("Altered") particles. After the "A" particles, found to be infectious in the case of PV (Curry *et al.*, 1996), have released their RNA, they form empty 80S particles. In PV, the N-terminus of VP1 is externalised and is available for proteolytic cleavage (De Sena and Mandel, 1977) and is thought to be deployed optimally for entry of the RNA genome (Curry *et al.*, 1996). While uncoating of major-group viruses results

in lysis of the endosomal membrane or release of subviral 135S and 80S particles into the cytoplasm, as described above, it appears that minor-group rhinoviruses transfer their genomic RNA to the cytoplasm through a pore in the endosomal membrane (Schober *et al.*, 1998).

Some picornaviruses inhibit cellular protein synthesis soon after infection. In the case of PV-infected HeLa cells, shut-off occurs quickly within the half hour or so required for attachment, penetration, and uncoating of the RNA genome. Host-cell shut-off and the proteins involved have been discussed previously.

Upon entry into the cell, the infecting RNA genome serves as messenger to direct the synthesis of virus-specific proteins which are required for RNA replication. The viral proteins are synthesised by translating a single large coding region on the genome, and the protein products are then produced by cleavage of the nascent polyprotein by the mechanisms discussed in 1.3.1.3. The time required for a ribosome to translate the RNA genome of PV from one end to the other is about 10 to 15 minutes. Because replication cannot begin until the polymerase gene has been completed, this probably represents the minimum time between the time of uncoating and the moment when synthesis of viral RNA can begin. Elongation of the RNA molecule is performed by $3D^{pol}$, some of which is found in the cytoplasm of infected cells tightly associated with its RNA template and with cellular membranes. Most $3D^{pol}$ is found in soluble form. It is not likely engaged in RNA synthesis but may simply result from the excess produced by the polyprotein strategy of expression.

Because ribosomes are known to bind and initiate translation internally on the PV genome, it is perhaps not surprising that eIF-2α is found in complexes that map to regions (nt 97-182 and nt 510-629) within the 5′ NTR. del Angel *et al.* (1989) speculate that the interactions between the complexes and eIF-2α may represent an early step in virus replication that precedes ribosome binding to PV mRNA.

It is unclear which translation features are required for IRES-driven translation initiation; however, it has only recently been shown that cellular proteins other than the generally recognised translation initiation factors are necessary. A 50kDa protein has been shown to interact with the RNA stem-loop structure located between nt 186 and 221 in PV type 1 RNA (Najita & Sarnow, 1990). Another protein present in abundance in HeLa cells compared with RRLs, called p52, found to be identical to the previously identified La

autoantigen, involved in host cells in the termination and reinitiation of RNA polymerase III transcription, has been shown to interact with PV RNA consisting of the polypyrimidine-rich region and stem loop VI and without which translation of PV in RRLs produced aberrantly initiated polypeptides. Das *et al.* (1994) discovered a small yeast RNA called I-RNA which competes with virus RNA structures within the 5′ NTR which bind the cellular p52 protein. It is reported elsewhere that the addition of at least two HeLa cell proteins to RRLs is required for efficient initiation of translation from the PV or HRV IRES. One of these, a 57kDa factor has been shown to interact with HRV and PV IRESs, as well as EMCV, HAV and FMDV. The physical, biochemical, and antigenic properties of p57 were found to be identical to the previously identified polypyrimidine tract-binding protein, PTB, which binds to pyrimidine-rich sequences in mammalian introns and is involved in pre-mRNA splicing. The second protein, of 97kDa, which apparently acts in concert with PTB, remains to be identified. Hellen *et al.* (1993) showed that immunodepletion of HeLa extracts using PTB antibodies nearly abolished both PV and EMCV translation; however, addition of purified PTB to these extracts did not restore translation, indicating that additional required factors may interact with PTB. Blyn and co-workers in 1996 isolated specific host cell proteins that bind to stem-loop IV of the PV 5′ NTR and identified one of these as poly (rC)-binding protein 2 (PCBP2) and in 1997 Blyn *et al.* demonstrated that PCBP2 is an essential factor required for efficient translation of PV RNA in HeLa cells.

In addition to the requirement for noncanonical cellular translation initiation factors, IRES-driven translation can be stimulated by viral components. Ziegler *et al.* (1995) demonstrated that the HRV2 2A proteinase is more efficient at stimulating IRES-driven translation than any other protein identified to date and that the stimulation correlates with the enzymatic activity of the 2A proteinase, the proteolytic conversion of some cellular component(s) being involved in 2A proteinase-mediated translational transactivation. Hence, 2A is important not only as a downregulator of cellular translation, but also as an enhancer of IRES-driven virus-specific translation (Macadam *et al.*, 1994).

Efficient functioning of the IRES itself involves two smaller elements in PV: UUUCC, considered to be an analogue of the Shine-Dalgarno sequence because of its complementarity to a segment at the 3′ end of the 18S rRNA, whose position, about 100nt upstream from the initiating AUG, in the PV system must be strictly fixed, relative to upstream *cis*-acting elements, and an AUG, which may not necessarily serve as an

initiation codon (Pilipenko *et al.*, 1992).

One of the major determinants for picornaviral species and tissue tropism is the presence or absence of the viral receptor on the cell surface. However, several results suggest that the IRES may also represent a determinant of viral tropism. *In vitro* studies have identified different cell factors that bind to the different IRESes and that may be required for translation initiation (del Angel *et al.*, 1989). Shiroki *et al.* suggested in 1997 that host factor(s) affecting IRES-dependent translation of PV differ between human and mouse and that the mutant IRES constructs they created detect species differences in such host factor(s), and the interaction between IRES and host factors is an important determinant of host specificity of PV replication.

Similarly, RNA sequences in the 5′ NTR of CV B1 and CV B3 are involved in virulence, however the sequences involved in the cardiovirulent phenotype are not within the boundaries of the predicted IRES. Thus, the interactions between IRESs and cellular cofactors involved in translation may only be involved in the cell-type tropism of some picornaviruses (Borman *et al.*, 1997; Stewart & Semler, 1997). Johnson and Semler (1988) suggest that sequences involved in "replicative fitness" are located in the 5′ NTRs of picornavirus genomic RNAs.

Further to their investigations into the poor translation efficiency of genome-length HRV RNA *in vitro* using HeLa cell-extract supplemented RRL compared with PV, Todd *et al.* (1997a) suggested that the rate-limiting step for rhinovirus assembly during an infection occurs at a step other than translation and the primary impediment for rhinovirus production is likely in packaging or capsid assembly discussed later.

One would envisage that the polymerase released from the polyprotein might first bind to a specific site near the 3′ end and then translocate to the end of the poly(A) tract to initiate negative strand RNA synthesis (Oberste & Flanegan, 1988). Flanegan and Baltimore (1977) isolated a template-dependent RNA polymerase from PV-infected cells, capable of copying poly(A) complexed to an oligo(U) primer, which may be important in initiating minus-strand synthesis by making poly(U), and which, by being unable to copy poly(A)-deficient RNA, supports the observation that poly(A) is required for infectivity.

The genomic RNA 3′ NTR is believed to be a major *cis*-acting molecular genetic determinant for regulating picornavirus negative-strand RNA synthesis by promoting RC

recognition, however it has been shown that while intact RNA 3′ NTRs may be required for efficient viral replication, they are not essential and they may have evolved to promote or regulate negative-strand synthesis, but the basic mechanism of replication initiation is not strictly template specific and may rely primarily upon the proximity of newly translated viral replication proteins to the 3′ terminus of template RNAs within tight membranous RCs (Todd *et al.*, 1997b).

Higher-order RNA structures in the 3′ NTR, however, are thought to play a pivotal role in the initiation of negative-strand RNA synthesis. The secondary structures predicted for the enterovirus 3′ NTR all seem to point to a conformation consisting of two (X and Y) to three (X, Y, and Z) hairpin structures, in which the poly(A) tract is partly included. It has been suggested that interactions occur either between the two predominant loops (X and Y) within the 3′ NTR or between one hairpin loop (Y) and the flanking coding sequences of the 3D RNA polymerase (Jacobson *et al.*, 1993), forming two higher-order tertiary RNA structures. The higher-order RNA structure of the 3′ NTR appears to be maintained by an intramolecular kissing interaction between the loops of the two predominant hairpin structures (X and Y) within the 3′ NTR, and this kissing interaction has been shown by Melchers *et al.* (1997) to be the essential structural feature of the origin of replication required for its functional competence in virus negative-strand RNA synthesis.

The presence of such a tertiary structure in the 3′ NTRs of both the CV B- and PV-like viruses allows the exchange of the 3′ NTR between these viruses without affecting subsequent replication since the binding sites are identical (Rohll *et al.*, 1995). On the other hand, the rhinovirus genus 3′ NTR, consisting of a single stem-loop structure cannot form a kissing interaction, and a PV chimera containing the HRV14 3′ NTR is, interestingly, still capable of initiating PV negative-strand synthesis (Rohll *et al.*, 1995). One explanation might be that this occurs because ribonucleoprotein (RNP) complex formation occurs differently in the rhinovirus 3′ NTR, although formation of the complex as such is sufficient to initiate replication.

As in the case of other complex higher-order RNA structures like pseudoknots, it is reasonable to assume that the kissing interaction in the 3′ NTR acts as a specific binding site for viral and/or cellular proteins involved in the initiation of negative-strand synthesis. Indeed, Harris *et al.* (1994) have described the formation of a 3′-terminal RNP complex composed of a 3AB-3CD interaction with the 3′ NTR. The subsequent proteolysis of

$3CD^{pro}$ releases the 3D polymerase. Protein 3AB then forms a complex with protein 3D to stimulate the activity of the virus polymerase (Harris *et al.*, 1994; Lama *et al.*, 1995; Plotch & Palant, 1995) which may use the uridylated VPg to initiate negative-strand RNA synthesis. A similar protein 3D interaction with tertiary (pseudoknot) structure in the 3′ NTR of EMCV has been proposed. Although Harris *et al.* (1994) did not consider other proteins to contribute to the complex formation, Todd *et al.* recently (1995) provided evidence for an interaction of the 3′ NTR with certain unidentified cellular proteins as well and more recently, (1997b) Todd *et al.* suggested that, while specific 3′-terminal RNA sequences and/or secondary structures may have evolved to promote or regulate negative-strand synthesis, the basic mechanism of replication initiation is not strictly template specific and may rely primarily upon the proximity of newly translated viral replication proteins to the 3′ terminus of template RNAs within tight membranous RCs.

The importance of RNA structures in RNA-protein interactions is generally known, and the tertiary RNA structure can be essential for stabilising the structure for the subsequent interaction with proteins (Frankel *et al.*, 1991).

Studies on cell-free synthesis of minus strands from the plus template indicate that at least three proteins are required: virus protein $3D^{pol}$, a VPg donor, and one or more host factor proteins [a terminal uridylyl transferase (TUT), and perhaps a protein kinase]. Two models have been proposed to explain the initiation of viral RNA synthesis on the poly(A) tail by $3D^{pol}$:

In one model, oligo(U) is added enzymatically to the 3′ terminus of the poly(A) by the host factor, TUTase, and the oligo(U) hybridises to the poly(A) to initiate RNA chains. Subsequently , the genome-linked peptide, VPg, cleaves the hairpin and is linked to the 5′-end of the oligo(U). In the second model, a uridylylated derivative of VPg is the primer, although the evidence suggests that it is mainly plus-strands that are synthesised by this mechanism (Takegami *et al.*, 1983). The cellular kinase and uridylylate transferase are however no longer under consideration and it has very recently come to light that synthetic VPg can be uridylylated with $3D^{pol}$ in a reaction requiring only poly(A) template UTP and magnesium. If uridylylation, however depends on a poly(A) template, how does $3D^{pol}$ select the 3′ end of PV RNA over the sea of polyadenylated mRNAs? Currently, available evidence suggests that the heteropolymeric 3′ NTR preceding the poly(A) serves as a recognition signal for RNA selection (Xiang *et al.*, 1997).

Synthesis of the negative-strand RNA yields a double-stranded intermediate, the RF which separates. The role of the RF in replication is not clear, but some of the RF in infected cells is in fact hair-pinned, i.e., contains a covalented attached plus and minus strand (Wimmer *et al.*, 1993). The involvement of RF as intermediate has not been generally accepted but is almost a necessity in view of the role of the cloverleaf. Xiang *et al.* (1997) speculate that the left end of RF may serve as a (double stranded) recognition signal for plus-strand RNA synthesis. The negative-strand therefore acts as a template for amplification of positive-sense genome. The RNA duplex unwinding activity of $3D^{pol}$ demonstrated by Cho *et al.* (1993) may be responsible for the separation of the two RNA strands of the RF at the replication fork.

Initiation of plus strands in a defined *in vitro* system by PV $3D^{pol}$ either does not occur or is extremely inefficient. One reason is likely to be that PV plus-strand initiation depends on the formation of a RNP complex on the plus strand, comprising 3CD, $3C^{pro}$, $3D^{pol}$ (?), and a ribosome-associated cellular protein (p36) bound to the proximal 88 nucleotides of the 5′ end folded into a cloverleaf-like structure. This structure is dispensable for the initiation of PV minus strands, suggesting that the complex is essential only for plus-strand initiation (Plotch *et al.*, 1989; Andino *et al.*, 1990, 1993). Indeed Borman *et al.* (1994) have shown that essential viral RNA replication signals are located in the 3′ region of the PV IRES, some 500 nt downstream from the 5′ end of the RNA and that a second element is located within the IRES whose disruption only minimally affects translation efficiency while greatly impairing RNA synthesis.

Shiroki and co-workers (1995) revealed that a host cellular factor(s) interacts with a RNA segment around nt 133 of the plus-strand RNA or the corresponding region of the minus-strand, contributing to efficiency of plus-strand RNA synthesis.

It is unclear whether PV 3CD, $3C^{pro}$, and $3D^{pol}$ all participate in complex formation, although it has been demonstrated that purified, recombinant HRV14 $3C^{pro}$ binds *in vitro* specifically to the 5′ terminal 126 nt of the 5′ NTR of the viral RNA in the absence of 3CD and $3D^{pol}$. Overall, the results support an intriguing speculative model of membrane-bound plus-strand initiation in *trans* involving the following steps (i) $3D^{pol}$ (and an associated protein(s))?, having just completed the synthesis of a minus strand, provides the signal for assembly of the RNP complex on the 5′ end of the neighbouring plus strand. (ii) The complex catalyses the formation of VPg-pU(-pU) via 3AB. The presence of a template RNA molecule in the complex triggers the uridylylation reaction

(Takeda *et al.*, 1987) (iii) The complex then catalyses the initiation of a new plus strand in *trans*, using the RNA template and the newly formed VPg-pU(-pU) as primer for the $3D^{pol}$ (Takeda *et al.*, 1987), at the 3´ end of the neighbouring minus strand newly exposed by the formation of the complex (Takegami *et al.*, 1983). The source of $3D^{pol}$ for plus-strand synthesis could be either $3D^{pol}$ or 3CD already present in the RNP complex (Porter, 1993). McBride *et al.* (1996) have identified cDNAs for several host proteins that interact with 3D polymerase, most notably a 68kDa protein that associates with Src during mitosis, Sam 68. Sam 68 coimmunoprecipitates with 3D polymerase from infected cells, is found on PV-induced membranes, and relocalises drammatically during PV infection which makes it a strong candidate for a host protein with a functional role in PV replication. Banerjee *et al.* (1997) have demonstrated that 2C specifically binds to the 3′ cloverleaf structure of the negative-strand RNA but not to the 5′-end cloverleaf of the positive-strand and as we have seen already, is important in initiation of positive-strand RNA synthesis (see Figure 15).

Replication takes place via a replicative intermediate (RI) which consists of a full-length template strand with some six to eight nascent daughter strands. (Figure 10, step 6). The time required for synthesis of each RNA molecule has been estimated at about 45 seconds. The RI-dependent plus-strand RNA synthesis proceeds in a viral complex, proposed by Plotch and Palant in 1995 to contain PV protein 3AB, which forms a complex with and stimulates the activity of the viral RNA polymerase and 3AB, $3D^{pol}$ (or its precursor 3CD) and viral RNA are brought together in host cell vesicles in which all viral RNA synthesis occurs.

Schlegel *et al.* (1996) revealed that the intracellular rearrangements that accompany PV infection result in the formation of double-membrane structures, containing replication protein 2C, that contain markers from the ER, the *trans* Golgi stacks and TGN, and lysosomes. The double-membrane structure implies that the membranes do not form by a simple budding mechanism from a discrete compartment in the cell but instead must form either by a double-budding mechanism or, more likely, by wrapping of cytosol by membranous compartments.

Likely candidates for the protein or activity that causes accumulation of these double-membrane structures and rearrangement of the intracellular secretory apparatus include PV 2A, 2C, 2BC, which have been found to induce, in various expression systems, the formation of large electron-dense cytoplasmic structures, vesicle formation, and membrane rearrangements respectively (Cho *et al.*, 1994; Aldabe & Carrasco, 1995).

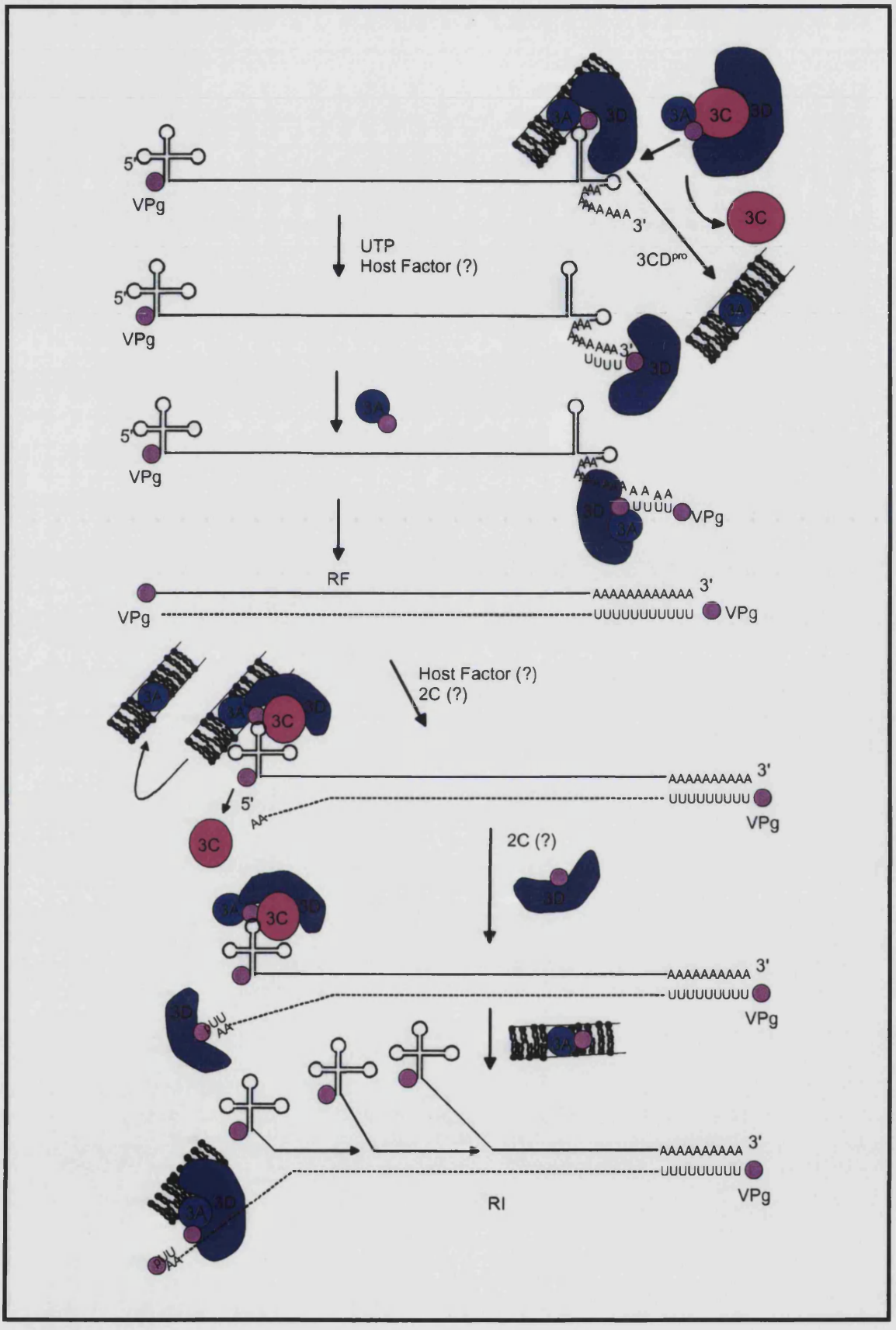

Figure 15: Models of PV minus and plus-strand RNA synthesis

Direct transfection of plasmids encoding 2B or 3A cause the inhibition of protein traffic between the ER and the Golgi apparatus and the expression alone of 3A, found to localise to intracellular membranes (Datta & Dasgupta, 1994), causes a normally secreted protein to colocalise with an ER luminal protein and which were subsequently found redistributed throughout the cytoplasm (Doedens & Kirkegaard, 1995).

Upon isolation from infected cells, the virus-induced vesicles were found to form rosettes which surround the RC, can be isolated in a functional state, and continue to initiate, elongate and release progeny plus-strand RNA in an *in vitro* transcription system (Takeda *et al.*, 1986). It was later found (Egger *et al.*, 1996) that these rosettes could reversibly dissociate into virus-induced vesicles and reassociate into rosettes. These vesicles carry a set of viral structural and nonstructural proteins as well as RI RNA and Egger *et al.* (1996) showed that the initiation and elongation of plus strands on individual vesicles are comparable to those in rosettes and also, by use of detergent treatment, that initiation, but not elongation, is dependent on vesicular membranes.

To form a rosette could be advantageous for virus replication because it could greatly increase the effectiveness and speed of plus-strand RNA synthesis. There are two main reasons for this: first, macromolecular crowding, exerted by the mass of vesicles, leading to an enhanced concentration of factors necessary for RNA synthesis; and second, the providing of more membrane-bound initiation sites (Harris *et al.*, 1994) for the RI. This allows the RI, or rather its minus-strand template RNA, to easily move on within the rosette and to combine with its 3′ end with the next initiation site on the same or the next vesicle. This would make the rosette, as such, a higher-order structure with functional subunits (vesicles), although in the infected cell the rosette could well be a short-lived, transient structure, changing its framework of individual vesicles continuously as the 3′ end of the minus strand moves on (Egger *et al.*, 1996).

A terminal adenylyl transferase (TATase) activity has been identified in preparations of purified PV $3D^{pol}$, which is able to add nontemplated A residues by virtue of this activity. The implication of the results of Neufeld *et al.* (1994) is that *in vitro*, $3D^{pol}$ can synthesise minus-strand RNA in a primer- and template-dependent manner and that once that has occurred, the minus-strand RNA can fold back to prime elongation of a plus-strand of RNA, and this model is compatible with data presented by Andino *et al.* (1990 and 1993).

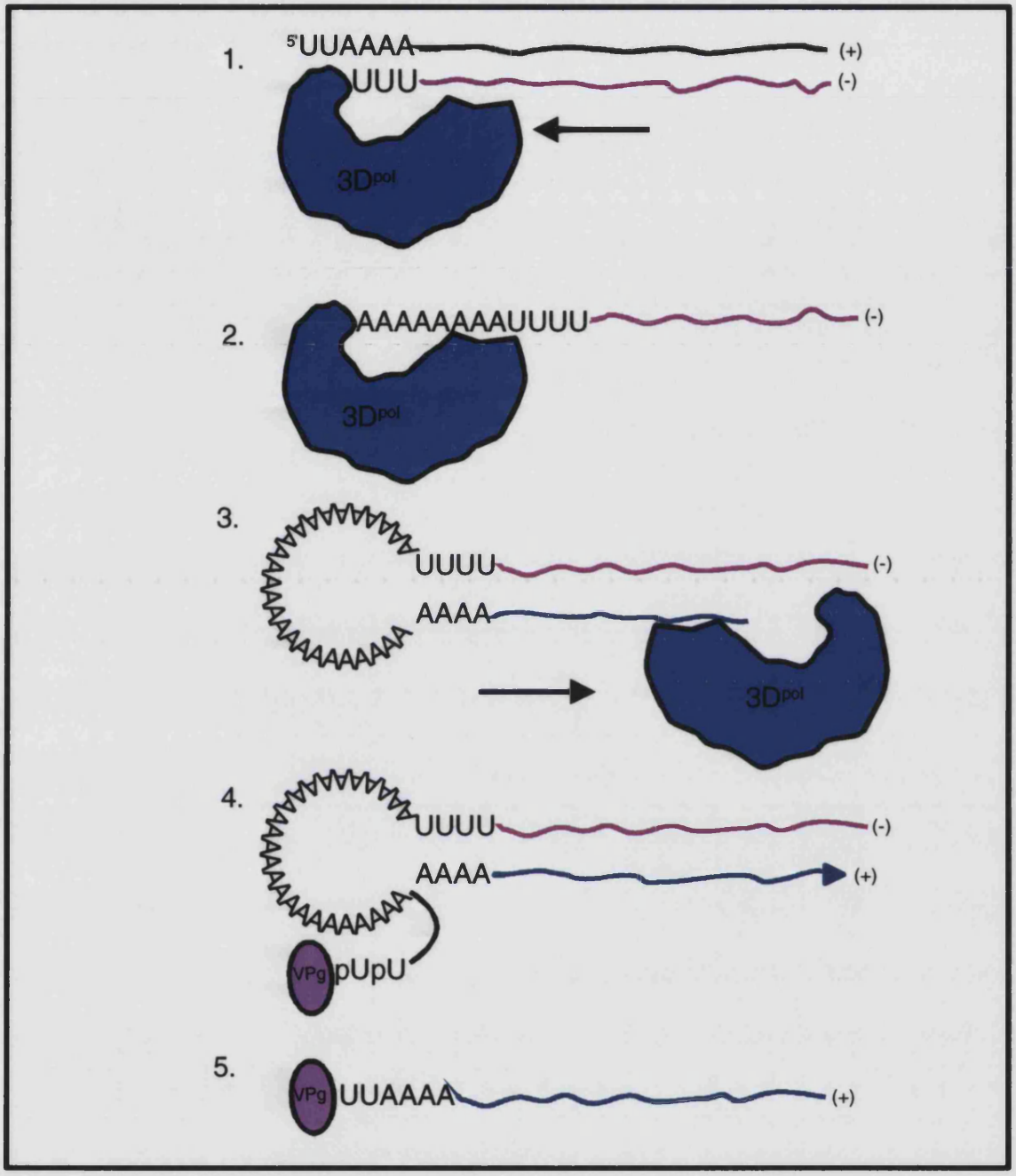

Figure 16: A possible role for TATase activity during poliovirus plus-strand RNA initiation and synthesis

(1) Poliovirus $3D^{pol}$ completes synthesis of minus-strand RNA in a template-dependent manner. (2) Following addition of the last templated nucleotide, $3D^{pol}$ adds three to six extra A residues by virtue of its TATase activity. (3) The 3′-terminal A residues fold back and pair with the U residues in the minus-strand RNA, priming synthesis of plus-strand RNA by $3D^{pol}$. (4) Uridylylated VPg is transferred to the plus-strand RNA between the extra A residues on the template and the base-paired product strand. (5) Following transesterification, the protein VPg is linked to the nascent plus-strand RNA (Modified from Neufeld *et al.*, 1994).

Once initiated, PV RNA synthesis proceeds exponentially, producing new templates and thus continually increasing the rate of synthesis. During this early stage of synthesis the rate doubles every 15 minutes until about 10% of the final yield has been produced. At this point the rate of synthesis becomes constant, accumulating linearly for an additional hour until the number of RNA molecules reaches about $4x10^5$ per cell. Some 2-5% of the total viral RNA in infected cells consists of minus strands. The mechanism controlling this differential synthesis is not clear. A substantial fraction of the RNA synthesised during the exponential phase of synthesis is destined to become mRNA, whereas about 50% of that made during the linear phase is packaged into virions. The switch from exponential to linear synthetic rate may reflect siphoning of the RNA pool into virions. Troxler *et al.* (1992) found that PV plus-strand RNA was found accumulated in the close surroundings of the membrane-bound complex and that riboprobes from two different regions of the viral genome hybridised with the same frequency, suggesting that the accumulation of hybridisation signal in the vicinity of the RC represents completed rather than RI-RNA. They proposed that newly made viral plus-strand RNA is set free from the core RC but remains associated with it, thereby forming a steady-state pool. This pool might be the site where the viral progeny RNA proceeds to encapsidation, thus linking RNA synthesis and virion formation. Specific interactions between the 2A-encoding sequence and the capsid proteins exist and a modification of these interactions by point mutations destabilises the virus, thereby contributing to the mouse neurovirulence of PV1 (LS-a). If this is the case, it is possible that sequences mapping to the coding region of $2A^{pro}$ function as an encapsidation signal (Lu *et al.*, 1994).

The type of subviral particle that associates with progeny RNA and proceeds to RNA encapsidation has not yet been identified, although some investigators have proposed that 14S pentamers, rather than empty capsids, may be involved in encapsidation of progeny plus-strand RNA and in fact Pfister *et al.* (1995) have shown that encapsidation of PV RNA starts in the RC and is initiated by 14S pentamers. RNase digestion experiments with isolated RNA-synthesising RC have shown, that upon completion, virtually all 36S RNA (in contrast to RI RNA) becomes RNase accessible, presumably after changing its location in the RC. The altered RNase accessibility seems to be coupled to or closely following the release of 36S RNA from the RI, since no RNase-protected 36S RNA can be found in an actively RNA-synthesising RC. Concomitantly or following the completion of 36S RNA, its association with 14S pentamers occurs.

1.3.2.4.1 Adaptation to cell culture and attenuation of virulence

Among the enteroviruses that are cytopathogenic - which include PVs, ECHOviruses, many of the CVs, and the enterovirus type 68-71 - growth can usually be obtained readily in primary cultures of human and monkey kidney cells and in some cell lines [such as HeLa, Vero, buffalo green monkey (BGM), or, for some serotypes, WI-38]. Until recently, primates were the only animal host susceptible to all three PV types (Wood & Macadam, 1997). The host restriction is due to the absence of a cellular receptor found on human and primate cells, the genes of which have been identified and isolated which has allowed the establishment of transgenic mouse lines that express the human receptor (TgPVR mice). A significant finding concerning PV host range is that variants of PV1 that carry the VP1 B-C loop (exposed loop formed by amino acids 95-105), which contributes substantially to neutralisation antigenic site I, of PV2 are neurovirulent in mice (Murray *et al.*, 1988). Furthermore, Moss and Racaniello (1991) identified second site suppressors, which restore virulence to viruses attenuated by changes in the B-C loop and suppressor mutations were located in the N-terminal extension of VP1 on the interior surface of the virus particle. The B-C loop and the internal suppressors are therefore host range determinants. Because the internal host range determinants are in a structure known to be important in conformational transitions of the virion, the host range of PV may be determined by the ability of virions to undergo transitions catalysed by cell receptors.

In contrast, most rhinoviruses of humans, grow efficiently only in human and some primate tissues; the presence of receptors on cell surfaces again influences this tissue specificity. Initial isolations were accomplished with rhesus monkey kidney tissue cultures, but a clear superiority of human tissues for isolation and growth was shown later. The increased frequency of isolations with human tissue cultures led to the commonly used designation of M- and H-strain rhinoviruses. The M strains grew in both monkey and human tissues, whereas the H strains grew only in human tissues; this separation is no longer used because it was shown that many H strains could be adapted to grow in monkey tissues. Persistent infection of HeLa M cells with type 2 has been described, but the basis for persistence was not identified (Couch, 1996).

Continued passage of viruses *in vitro* leads to incorporation of mutations into its genome as the virus adapts to growth in cell culture. The Sabin vaccine strains of the three serotypes of PV have played a large part in the effective control of poliomyelitis in developed countries and the molecular basis of attenuation of these live viral vaccines

has been extensively studied. A striking feature has been the discovery of attenuating determinants in the 5′ NTR of all three vaccine strains. Point mutations in the 5′ NTRs of PVs, known to be involved in attenuation of neurovirulence (Skinner *et al.*, 1989), have been shown to affect the ability of viruses to grow at elevated temperatures (Macadam *et al.*, 1991, 1992). This temperature sensitivity is almost certainly a measure of the ability of part of the 5′ NTR to form a specific secondary structure capable of interacting with cellular and/or viral factors and the ultimate effect of secondary structure perturbation by attenuating nucleotides may be on translation, mediated by factor-binding deficiencies. PVs containining a mutation at amino acid 424 of the $3D^{pol}$ displayed a temperature sensitive phenotype (Burns *et al.*, 1992). The genetic basis of the attenuated phenotype of the type 3 vaccine strain (Sabin 3) has been shown to be almost entirely explicable by just two point mutations (Westrop *et al.*, 1989). One of these, at nt 472 in the 5′ NTR, reverts rapidly when the virus replicates in the human gut and other changes including intertypic recombination occur frequently in vaccinees and recent evidence suggests that, although apparently not encountering factors that favour rapid reversion toward high neurovirulence (Georgescu *et al.*, 1997), this attenuation determinant might disrupt the interaction of the PV 5′ NTR with PTB in the CNS, reducing viral translation, replication and neurovirulence (Gutiérrez *et al.*, 1997). The other attenuating mutation, which involves a substitution at amino acid 91 of the capsid protein VP3, renders the virus temperature-sensitive (ts). Similarly a mutation in the puff region of VP2 attenuates the myocarditic phenotype of an infectious cDNA of the Woodruff variant of CV B3 (Knowlton *et al.*, 1996). Determinants of attenuation in the Sabin type 1 strain of PV are located in the 5′ NTR, the capsid coding region and the viral $3D^{pol}$ coding region. These mutations also contribute to a temperature sensitive phenotype of replication. The contribution of Sabin $3D^{pol}$ sequences to the inability of the virus to grow at elevated temperatures must, Baker *et al.* (1995) have shown, lie in a function or activity of the enzyme other than RNA polymerisation, most likely the initiation step of RNA synthesis.

A live-attenuated strain of rhinovirus type 15 was developed, and differing plaquing properties of the wild parent and the attenuated progeny were described. Use of attenuated viruses for immunisation would require use of multivalent live preparations; dual infection with two serotypes was induced experimentally and has been identified naturally. Despite some promise, the live virus vaccine approach has not been pursued. Problems for all rhinovirus immunisation approaches are the multiplicity of serotypes and the suggestion that most have epidemiological significance (Couch, 1996).

Recombination is a valuable strategy by which a virus strain can enhance its virulence and promote its growth and may be a more efficient means for evolution of a viral genome than mutation alone. In the case of two strains of CV B1, one, CV B1N, being less virulent than the other myotropic strain (CV B1T), sequencing of the 5′ NTR of CV B1T demonstrated areas with a greater similarity to particular ECHOviruses than to CV B1N (the less virulent strain), suggesting that recombination events might have occurred, perhaps influencing the virulence phenotype (Rinehart *et al.*, 1997). Amazingly, there is a report detailing the discovery of a nonhomologous recombination event which occurred in tissue culture between an engineered PV genomic RNA containing a lethal lesion and the human host cell RNA (Charini *et al.*, 1994).

1.3.3 Cardiovirus and aphthovirus genera

The cardioviruses all belong to a single serotype and are here all considered to be strains of EMCV. They are generally regarded as murine viruses although their host range includes humans, pigs, elephants, and squirrels among others.

CARDIOVIRUSES	
Encephalomyocarditis virus	Columbia SK
Mengovirus	Maus Elberfeld (ME) virus
Theiler's murine encephalomyelitis virus (TO, GDVII)	MM Virus

Figure 17: Cardiovirus serotypes

Aphthoviruses (foot-and-mouth disease viruses) infect cloven-footed animals, especially cattle, goats, pigs, sheep, and, rarely, even humans. Seven immunotypes have been identified: these include types A, C, O, Asia-1, and the South African Territory types, SAT-1, SAT-2, and SAT-3. Within these seven types, at least 53 subtypes have been designated by complement-fixation tests. The serological characteristics of the subtypes are sufficiently different to cause difficulty in classification and immunization. The aphthoviruses are highly labile, being rapidly inactivated at pH less than 7.

APHTHOVIRUSES
Foot-and-mouth disease virus 1-7 (serotypes A, C, O, SAT-1, 2, 3, Asia-1)

Figure 18: Aphthovirus serotypes

FMDV infection results in a severe disease that develops rapidly, with symptoms that are often apparent within 24 hours following exposure to the virus. Thus effective vaccines need to stimulate a strong immune response prior to infection since postexposure boosting of vaccine-induced responses cannot compete with the rapid onset of disease.

Foot-and-mouth disease, an economically important viral disease of livestock, is a problem in many developing countries and poses a continuous threat to FMD-free nations of North America and Europe as its remarkable antigenic variability complicates the development of new effective vaccines.

1.3.3.1 Properties of virion

Aphthoviruses, cardioviruses and TMEV are all plus-strand viruses with a molecular weight of between 2.70 x 10^6 and 2.93 x 10^6. Again, the virus capsid of the aphtho- and cardioviruses is made up from 60 copies each of four virus-encoded proteins, VP1 to VP4; VP1 to VP3 form most of the capsid shell, with VP4 lining the interior surface.

Figure 19: Molecular surface of foot-and-mouth-disease virus and mengo virus

Molecular surface of FMDV (left) and mengo virus (right), radially depth cued, as solved by X-ray crystallography determined by Logan *et al.* (1993) and Luo *et al.* (1987) respectively. Images courtesy of J. -Y. Sgro on Silicon Graphics taken from http://www.bocklabs.wisc.edu/images/fmdv.jpg and mengo.jpg.

The three major capsid proteins of all picornaviruses, VP1, VP2 and VP3, are structurally similar to each other and consist of an eight-stranded β-barrel with a jelly-roll topology. The surface exposed loops joining the strands of the jelly rolls differ radically between the genera, and to a lesser extent between serotypes. These exposed loops define much of the antigenic character of each virus. FMDV differs from the other picornaviruses in having a relatively smooth surface with one exceptionally long exposed loop, the GH-loop of VP1 (residues 134-160), which not only constitutes most of a major antigenic site but also contains a conserved RGD (Arg-Gly-Asp) sequence which has been demonstrated to be essential for attachment of the virus to cells. This loop is highly disordered in the native virus structure of all serotypes examined to date and Hewat *et al.* (1997) have published information on the structure of this receptor-binding loop in relation to the rest of the virus capsid and further reinforces the picture of the GH-loop acting as a mobile structural module.

Analysis of the structural tendencies of a synthetic peptide corresponding to the GH loop from the serotype 01 FMDV was undertaken by de Prat-Gay (1997). The observation that a synthetic peptide, corresponding to the GH loop, is largely disordered in aqueous solution has implications on the ability of GH loop peptides to elicit humoral protection in animals and therefore, on its effectiveness as a vaccine. The loop must be continuously subjected to a conflict between sequence conservation to function as receptor recognition signal and variation to escape from antibody neutralisation (Mateu, 1995). Recently the structure of a complex between the Fab fragment of a neutralising monoclonal elicited against FMDV and its 15 amino acid peptide antigen was reported (Verdaguer *et al.*, 1996). This type of structural information may eventually allow modelling of antibody-entire complex formation, an important event in neutralisation of viral infectivity.

There are two subgroups of Theiler's virus, a murine cardiovirus, which are closely related, serologically and at the genome level, but which differ in their phenotypes. Following intracranial inoculation either an acute encephailitis (strain GDVII) or a chronic demyelinating disease (strain DA) ensues. Studies indicate that the viral capsid contains determinants for persistence and demyelination (Fu *et al.*, 1990). Jarousse *et al.* (1996) have found that amino acid VP2-141, as well as rendering chimeric virus persistent, can modulate the tropism of Theiler's virus and their data indicates that the mechanism by which this region affects persistence may involve tropism.

The acid-labile aphthoviruses inhabit the nasal and oropharyngeal regions with no apparent need for acid stability. Indeed it may be that the structure conferring acid stability to the virion conveys some still inapparent counteradvantage because the highly labile aphthoviruses are among the most contagious viruses known (Rueckert *et al.*, 1996).

Empty capsids of FMDV, purified by Curry *et al.* (1997), were unusual among picornaviruses in that most of the capsid precursor VP0 had been cleaved into VP2 and VP4. Both the N terminus of VP1 and the C terminus of VP4, which pack together close to the icosahedral threefold symmetry axis where three pentamers associate, are more disordered than they are in the RNA-containing virus. The ordering of these termini in the presence of RNA strengthens interactions within a single protomer or between protomers belonging to different pentamers. The disorder in the FMDV empty capsid forms a subset of that seen in the PV empty capsid, which has VP0 intact. Thus, VP0 cleavage confers stability on the picornavirus capsid over and above that attributable to RNA encapsidation.

By contrast to other picornaviruses, the truncation of VP1 in FMDV exposes the five-stranded β annulus formed by the N termini of VP3 packing around the icosahedral five-fold axes. This forms a tube with an average diameter of 11Å. Although VP4 lies below this tube, no well-ordered residues obtrude close to the symmetry axis (in PV the N-terminal residues and myristic acid form an additional inner layer of structure, resulting in a hydrophobic hole (Acharya *et al.*, 1989).

1.3.3.2 Properties of genome

Aphthoviruses possess an RNA genome of approximately 8,400 nucleotides and cardioviruses possess an RNA genome of between 7,840 nt (EMCV) and 8,098 nt (TMEV).

Again, the protein coding region is flanked on each end by NTRs whose sequences tend to be highly conserved and carry signals initiating translation near the 5′ end and for initiation of RNA synthesis at the 3′ ends of the plus and minus strands, respectively.

The 5′ NTRs of aphtho- and cardioviruses (with the exception of TMEV) are unique in that they contain long homopolymeric polycytidylate (polyC) tracts, between VPg and the

beginning of the protein coding region, whose length (50-200 bases) and exact location relative to the 5′ end of the genome (150-330 bases) vary with different isolates of virus. Shortening of the long polyC regions markedly reduced the virulence of mengovirus (Duke *et al.*, 1990) but not of aphthovirus.

Statistical analyses of RNA folding in 5′ NTRs of EMCV, TMEV and FMDV indicate that two highly significant folding regions occur in the 5′ and 3′ portions of the 5′ NTR. The theoretical, common structural elements predicted in the 3′ parts of the 5′ NTR occur in a *cis*-acting element that is critical for internal ribosome binding. Nucleotides in the conserved single-stranded polypyrimidine tract for these RNAs are involved in a distinctly tertiary interaction that is located about 15nt prior to the initiator AUG. Intriguingly, the proposed common tertiary structure in this study shares a similar structural feature to that evident in the human enteroviruses and HRVs (Le *et al.*, 1993).

In contrast to the first class of picornavirus IRES elements, representative of the entero-/rhinovirus genera which function rather poorly in RRL translation system unless supplemented with additional cellular proteins, the second class, found in the cardio- and aphthoviruses, also displaying a complex secondary structure though quite distinct, from the first class IRES, functions very efficiently in the RRL system. Although often regarded as a *cis*-acting element, evidence exists that internal initiation of translation by severely defective IRES elements can be greatly enhanced by the coexpression (in *trans*) of the parental wt IRES within cells. Moreover, Roberts & Belsham (1997) have provided evidence that severely truncated EMCV IRES elements, insufficient to direct internal initiation themselves, can complement defective IRES elements.

The AC-folds of aphthoviruses and cardioviruses resemble that of EMCV as shown in Figure 20. Interestingly, the IRES of EMCV is now widely used in high-level protein expression systems because it is one of the most active translational initiation sites known (Elroy-Stein *et al.*, 1989; Elroy-Stein & Moss, 1990; Kaufman *et al.*, 1991; Rueckert, 1996).

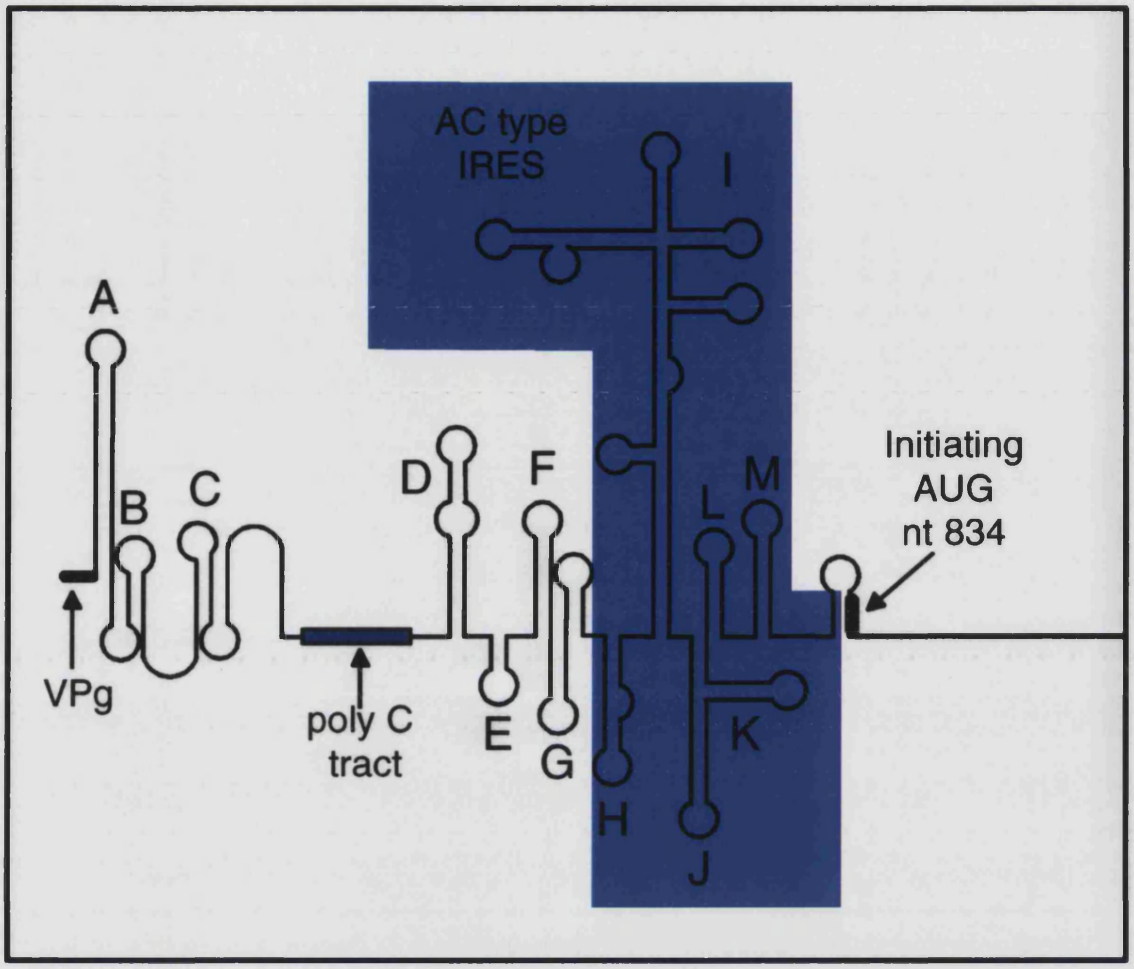

Figure 20: Encephalomyocarditis virus 5' NTR with type 2 IRES

The FMDV encodes three VPg genes in tandem, each with 23 or 24 amino acids, whereas the other picornaviruses encode one. The length of the poly(A) tract varies in size, being shortest in cardioviruses and longest in aphthoviruses.

Initiation of protein synthesis, normally proceeds from a unique start site on each RNA, however, in FMDV, two in-phase AUG codons (separated by 84 bases) initiate synthesis with equal frequency. Interestingly, molecules complementary to the translational start sites, and both sense and antisense molecules covering the 3′ end of the FMDV RNA, confer resistance to FMDV infection and it is thought that hybridisation of short sequences of both sense and antisense transcripts from the 3′ end induces distortion of predicted highly ordered structural motifs, which could be required for the synthesis of negative-stranded viral RNA, and correlates with inhibition of viral propagation (Gutiérrez *et al.*, 1994).

Bae *et al.* (1989) performed a genomic comparison between the diabetogenic EMCV-D and nondiabetogenic EMCV-B and have shown that EMCV-D differs from EMCV-B by only 14 nucleotides, consisting of two deletions, one insertion, and eight point mutations.

1.3.3.3 Properties of viral proteins

In the aphtho- and cardioviruses, the leader or L region maps in front of the capsid precursor region, 1A to 1D (L is absent in renteroviruses). The L protein of FMDV occurs in two distinct forms, termed Lab (23kDa) and Lb (16kDa), which are the result of ribosomes initiating translation at the two AUG codons 84 bases apart. Both Lab and Lb of FMDV are (thiol?) proteases with multiple activities; they cleave themselves (in *cis* or in *trans*) from the amino terminus of the capsid protein precursor P1 (Strebel & Beck, 1986) between a K-G dipeptide, thereby initiating the maturation of the adjacent capsid proteins. The two forms of L also initiate the cleavage of the p220 subunit of the ribosomal initiation factor eIF-4F protein complex, which appears to be partly responsible for the inhibition of cellular 5′ cap-dependent translation without affecting translation of the uncapped viral mRNA. The leader proteins of cardioviruses show no similarity to that of FMDV. They contain a zinc-binding motif, however their role in replication and pathogenesis is unknown and in fact, deletion of the leader region in the genome of TMEV had no effect on the replication and spread of the mutant virus in BHK-21 cells (Michiels *et al.*, 1997). In cardiovirus-infected cells p220 is not cleaved and shut-off is accomplished by an exceptionally active IRES, which enables the viral RNA to out-compete host messages (Rueckert, 1996).

Curiously, the $2A^{pro}$ region of FMDV is only 16 amino acids in length, and is totally conserved amongst all aphthovirus genomic RNAs sequenced to date, yet primary scission still occurs at the carboxy terminus at the 2A-2B junction (Ryan *et al.*, 1991). No host or viral protease has been implicated in this scission, and the balance of evidence favours the astonishing possibility that the sequence at the 2A-2B junction (consensus Asn-Pro-Gly-Pro - NPGP) is inherently unstable and literally breaks itself without being enzymatically cleaved. Synthetic tetrapeptides containing this sequence were spontaneously cleaved to Asn-Pro and Gly-Pro when incubated only in buffer (Palmenberg, 1990; Ryan & Drew, 1994). Interestingly, FMDV 2A is able also to generate cleavage in attenuated Sabin 3 PV vectors engineered for delivery of foreign antigens (Mattion *et al.*, 1996). In the cardioviruses, primary cleavage similarly occurs at the 2A-2B junction, and microsequencing revealed that scission occurs, as was

measured for FMDV A12, at the Gly-Pro pair within the NPGP sequence (Porter, 1993). The conserved sequence is extremely rare within current databases - the only examples are from cardio-, aphtho- and group C porcine rotaviruses - and is always associated with a proteolytic cleavage activity.

The 2A protein of cardioviruses, about 140 amino acids long and lacking sequence homology with the 2A of renteroviruses, has a C terminus similar to the 16-amino-acid 2A protein of aphthoviruses and is also involved in the primary cleavage event. The larger part of protein 2A, does not resemble any identified protein sequence, and has been shown to be dispensable for RNA replication of the viral genome, although spread efficiency was restricted in viruses with large deletions in the 2A region (Michiels *et al.*, 1997).

Lack of data on proteins 2B, 2C, and their precursor 2BC, for these genera leads me to surmise they perform functions similar to those of their counterparts in the renteroviruses, generally involving membrane proliferation and an involvement in the RC.

In FMDV, all cleavages, other than the autocatalytic cleavage of L from P1 and the primary 2A cleavage between 2A and 2B, are catalysed by 3C or a 3C containing precursor, except for the maturation cleavage of VP0 in the provirion to generate the capsid proteins VP4 and VP2 (Grubman *et al.*, 1995).

FMDV 3C residues His-46 and Cys-163 (equivalent to PV 3C His-40 and Cys-147), respectively) are implicated as part of the catalytic triad and His-181 (equivalent to PV His-161) as part of the binding pocket. The data of Grubman *et al.* (1995) support the prediction of Gorbalenya *et al.* (1989) in that the third member of the triad is Asp-84 and not Asp-98. It is interesting to note, however, that while the scissile bond cleaved by other picornavirus 3C enzymes is relatively conserved that for FMDV is highly variable.

In FMDV, $3C^{pro}$ also induces the specific cleavage of histone H3, *in vivo*. Because the deleted part of histone H3 is in the amino-terminal region corresponding to the presumed regulatory domain of transcriptionally active chromatin, it seems likely that this specific cleavage is related to the severe inhibition of host cell RNA transcription observed in FMDV-infected cells. It is unclear whether histone H3 cleavage is direct or mediated by a host protease.

For EMCV, the capsid region cleavages, except 1A-1B, are generally carried out by released 3C, although 3ABC, 3CD, and 3ABCD precursors also have demonstrable *trans* activity with these same substrates and it is assumed that these precursors play additional catalytic roles in the replication cycle, as they do for the enteroviruses and rhinoviruses. Engineered mutations preventing 3C-dependent cleavage at the 2C/3A, 3A/3B, 3B/3C, and 3C/3D processing sites were created and tested *in vitro* for their consequent blocks in the processing cascade and effects on polymerase activity. The mutations were also characterized *in vivo* within the context of full-length genomic sequences for defects in RNA synthesis, genetic stability, and subsequent infectivity. The data confirm the essential indispensability and preferred order of the natural processing cascade and point to a fine balance between 3C protein precursors and polyprotein products in establishment of an infectious cycle (Hall & Palmenberg, 1996).

Hahn & Palmenberg (1996) suggest that primary cleavage itself, though necessary, is not sufficient to ensure $3C^{pro}$ mediated P1 reactivity and that other functional requirements highly sensitive to changes, exist within the DIETNPGP sequence of EMCV 2A that they studied. Perhaps primary cleavage, occurring where and when it does, may ensure proper folding of the L-P1-2A precursor, making it a suitable substrate for $3C^{pro}$-mediated processing, or perhaps the order of cleavage events is critical in L-P1-2A processing. The preferred cleavage progression being 2A/2B, then L/1A, 1D/2A, 1C/1D, and 1AB/1C. A failed or sequence-defective primary reaction may, through steric hindrance or improper product release, prevent sequential exposure of the other four internal sites in their usual turns.

Evidence that FMDV particles contains replicase protein 3D was provided by Newman *et al.* in 1994, who showed that, in the presence of ammonium ions, the expressed polymerase degrades the RNA of the virus indicating that it can act as a hydrolytic as well as polymerising enzyme. Sankar & Porter (1991) expressed and purified the polymerase of EMCV and found it to exhibit poly(A)-dependent poly(U) polymerase activity and RNA polymerase activity, which are both oligo(U) dependent. Interestingly, further work on this enzyme revealed that point mutations which drastically affected the polymerisation activity corresponded to the active site of *E. coli* DNA polymerase I, suggesting that a basic structural and functional framework is conserved in the most distantly related classes of nucleic acid polymerases which supports the validity of modelling the active sites of RNA-dependent RNA polymerases on the known structure of a DNA polymerase (Sankar & Porter, 1992).

Cui *et al.* (1993) demonstrated binding of EMCV $3D^{pol}$ to the 3′ NTR(A) but not to globin mRNA, yeast tRNA or the 3′ NTR lacking the poly(A) tail. In contrast PV $3D^{pol}$ bound to PV RNA and virtually all RNAs tested including poly(U), poly(C), and poly(G), although a different assay, using partially purified $3D^{pol}$ was employed (Oberste & Flanegan, 1988). This suggests, as before, that the 3′ NTR and poly(A) together play an important role in viral template selection by $3D^{pol}$, and may explain why cDNA clones of EMCV lacking 3′ poly(A) are noninfectious.

1.3.3.4 Replication and adaptation to cell culture

FMDV enters the cells via a mechanism of receptor-mediated endocytosis in which the low pH of the endosomal compartment triggers uncoating of the viral genome. For FMDV A_{12} the receptor has been identified as the Arg-Gly-Asp (RGD)-binding integrin. The RGD to which the integrin binds is located on the G-H loop of VP1 and is highly conserved among all seven serotypes. Such conservation in a region that otherwise varies considerably in length and sequence suggests that all FMDV serotypes use RGD-binding integrins, including $\alpha v\beta 3$, as receptors for virus internalisation (Jackson *et al.*, 1996). They have also shown that type O FMDV has a specific affinity for heparan sulphate, an extracellular matrix component, and that this binding most likely is the initial event in cellular entry and is required to establish an efficient infection in cells grown in culture. It appears therefore, that FMDV attaches to the cell surface via interactions with a nonintegrin component of the plasma membrane or extracellular matrix before integrin-dependent internalisation.

Jin *et al.* (1994) recently indicated that EMCV attachment to permissive human cells is mediated by a cell surface sialoglycoprotein(S) with a molecular mass of 70kDa, but not by glycophorin A, which is the attachment molecule for EMCV on human erythrocytes with sialic acid being the residue involved in the virus binding. Human erythrocytes, however, do not support EMCV growth, in contrast to a number of nucleated cells in which the virus readily replicates.

As before, these viruses must also translate their genome into proteins required for replication and again this is achieved through the use of an IRES. Strong experimental evidence exists for the requirement of widely conserved motifs in IRES activity in FMDV and other picornaviruses and de Quinto & Martínez-Salas (1997) have shown that the

aphthovirus IRES loops located at the most distal part of domain 3, which carries GNRA and RAAA motifs, are essential for IRES function.

The p52 protein, a nuclear protein that binds to the 3′ terminus of nascent RNA polymerase III transcripts, La, mentioned previously binds to the IRES of EMCV as well as PV. Studies with EMCV and FMDV RNA established that a p57 protein also cross-linked to their IRES elements. As with studies on the renterovirus IRES, the p57 species has been identified as the PTB. Two binding sites were identified on the FMDV IRES, one close to the 5′ end (stem loop H [Figure 20]) and a second around the polypyrimidine tract at the 5′ terminus of the IRES. The major site of association between p57 and the EMCV IRES is in stem-loop H, although evidence for a second site in a region further upstream in the 5′ NTR was also obtained (Belsham & Sonenberg, 1996). Two additional proteins, p70 and p100 (p97), observed to cross-link fragments of various IRES elements, have been shown to bind specifically to multiple fragments of the EMCV IRES. It is suggested that each of these proteins recognises primarily, like those mentioned in the renterovirus section, a structural feature of the RNA rather than a specific sequence (Witherell & Wimmer, 1994).

Recently reported was the observation that the translational activities of the renterovirus IRES elements (but not the EMCV or FMDV IRES elements) appear to have been stimulated by the FMDV L protease. (Ziegler *et al.*, 1995).

EMCV RNA template specificity has been shown to depend only upon $3D^{pol}$, the 3′ NTR and the poly(A) tail, suggesting the poly(A) tail plays an essential role in viral RNA template selection by the polymerase. The fact that EMCV cDNA clones lacking the 15-20 3′ terminal A residues are non-infectious may be explained by the failure of $3D^{pol}$ to bind to the 3′-terminus of the viral RNA template and initiate negative-strand synthesis (Cui *et al.*, 1993).

Newman & Brown (1997) have shown consistently that nonstructural proteins 2C, 3C, 3CD, and 3D, components of the RC, and the cell protein actin are present in highly purified preparations of both FMDV and PV (Newman *et al.*, 1994; Newman & Brown, 1997) and it is thought FMDV replicates in a similar manner to that described previously for PV. If 2C has a role in virus structure, it may function by facilitating assembly around newly synthesised RNA, moreover the RC proteins, with an affinity for the 5′ end of the newly synthesised sense RNA and membranes, may be necessary for assembly (Andino

et al., 1993). In addition, a small protruberance, found on some FMDV complexed with antibody against 3D, could be the site from which the RNA is released particularly since the 3D is attached to the RNA (Newman & Brown, 1997).

To produce a new generation of safer FMDV vaccines, genetic engineering has been used to develop attenuated virions. In one case, attenuation has been achieved by removing the coding region for the viral leader proteinase, responsible for inhibition of translation of host-cell mRNAs during infection. In another case, the virus has been attenuated by deletion of the RGD sequences, that comprise the cell binding site. Ward *et al.* (1997) have most recently shown that a DNA vaccine based on a genome-length FMDV nucleic acid that undergoes genomic amplification in inoculated animals can immunise swine against foot-and-mouth disease.

1.3.4 Hepatovirus genus

1.3.4.1 Properties of the virion

The HAV particle is approximately 27nm in diameter and appears roughly spherical by electron microscopy (Feinstone *et al*, 1973) (Figure 21). HAV possesses a non-enveloped capsid structure (Lemon *et al.*, 1992). Based on the structure of picornaviruses generally, the HAV capsid is thought to have icosahedral symmetry and to contain 60 copies of each of three major polypeptides, VP1, VP2 and VP3 (Wheeler *et al.*, 1986b; Lemon & Robertson, 1993). It is not known whether HAV contains a fourth, smaller capsid protein (VP4) which is present in other picornaviruses. The genome of HAV potentially encodes a VP4 protein of 21-23 residues (Baroudy *et al.*, 1985; Cohen *et al.*, 1987a; Hollinger & Ticehurst, 1996). This putative VP4 sequence contains an internal consensus myristylation site (Gly-X-X-X-Ser/Thr, where X is any amino acid) starting at residue 5 from the preferred AUG codon (Palmenberg, 1989; Tesar *et al.*, 1993), which suggests that if VP4 is actually present in the virion and myristylated like the VP4 of other picornaviruses, it may be only 17 amino acids in length (2.5kDa) (Chow *et al.*, 1987; Palmenberg, 1989; Ross *et al.*, 1991). Myristylation occurs after the removal of an initial methionine residue or a leader peptide, resulting in the exposure of an N-terminal eight amino acid myristylation signal. Analysis of culture-adapted HAV and engineered mutants demonstrated that myristate was not incorporated, nor was a 5-residue leader peptide cleaved from 1A or VP0. Thus, VP4 has not been conclusively demonstrated in HAV particles; and if it exists, it is much smaller than other picornaviral VP4 molecules and not myristylated. Furthermore, data from Tesar *et al.* (1993)

indicates that HAV does not require leader cleavage and myristylation of VP4 for growth in cultured cells. Ross & Anderson (1991) estimated VP4 to have a relative molecular mass of less than 1kDa, which is substantially lower than the 2.5kDa predicted from the nucleotide sequence.

Preparations of HAV made from infected cell cultures typically contain large quantities of empty capsids. These capsids are composed of three polypeptides VP0 (VP2+VP4), VP3 and VP1. Mature capsids contain approximately 2 molecules of VP0 (Bishop & Anderson, 1993). Studies have shown that VP0 of the empty capsid is larger than the VP2 present in the complete virion, indicating that maturation cleavage of VP0 occurs in HAV, as in other picornaviruses (Updike *et al.*, 1991). Bishop & Anderson (1993) presented results which clearly show that the provirion is a true intermediate in the morphogenesis of HAV, with VP0 cleavage being dependent on the presence of encapasidated viral RNA. What remains unknown, however, is whether the N-terminal cleavage product of VP0 (that is, the VP4 moiety) is actually incorporated into the virion.

Recent evidence suggests that HAV may differ from other picornaviruses in that a large carboxy-terminal extension of VP1 is present in some virions. The function of this protein (termed 'pX') is unknown (Anderson & Ross, 1990) but is thought to represent a VP1-2A precursor that is cleaved by $3C^{pro}$ at a Glu-Ser linkage at amino acid position 273/274 (Probst *et al.*, 1997), 27 amino acids upstream of the predicted C-terminus of VP1, resulting in 1-273/VP1 as opposed to the 1-300/VP1 proposed. This cleavage site could represent the authentic carboxy terminus of VP1 generated by $3C^{pro}$ from the 40kDa (42kDa) protein (pX) and accounts for the difference between the 37kDa protein, which results from the translation of the proposed ORF for VP1, and the 33kDa protein, which is the mature VP1 observed in HAV-infected cells and HAV virions. The release of VP1 from its 40kDa precursor through cleavage between the Glu-Ser proposed (amino acids 764 and 765 of HAV polyprotein), may imply that $3C^{pro}$ alone is sufficient to perform release of VP1 and that the low specificity of protease 3C for this junction sequence is responsible for the relative stability of the VP1 precursor, as in the case of 3A/3B, which is separated by the amino acid pair Glu-Gly (Dotzauer *et al.*, 1995).

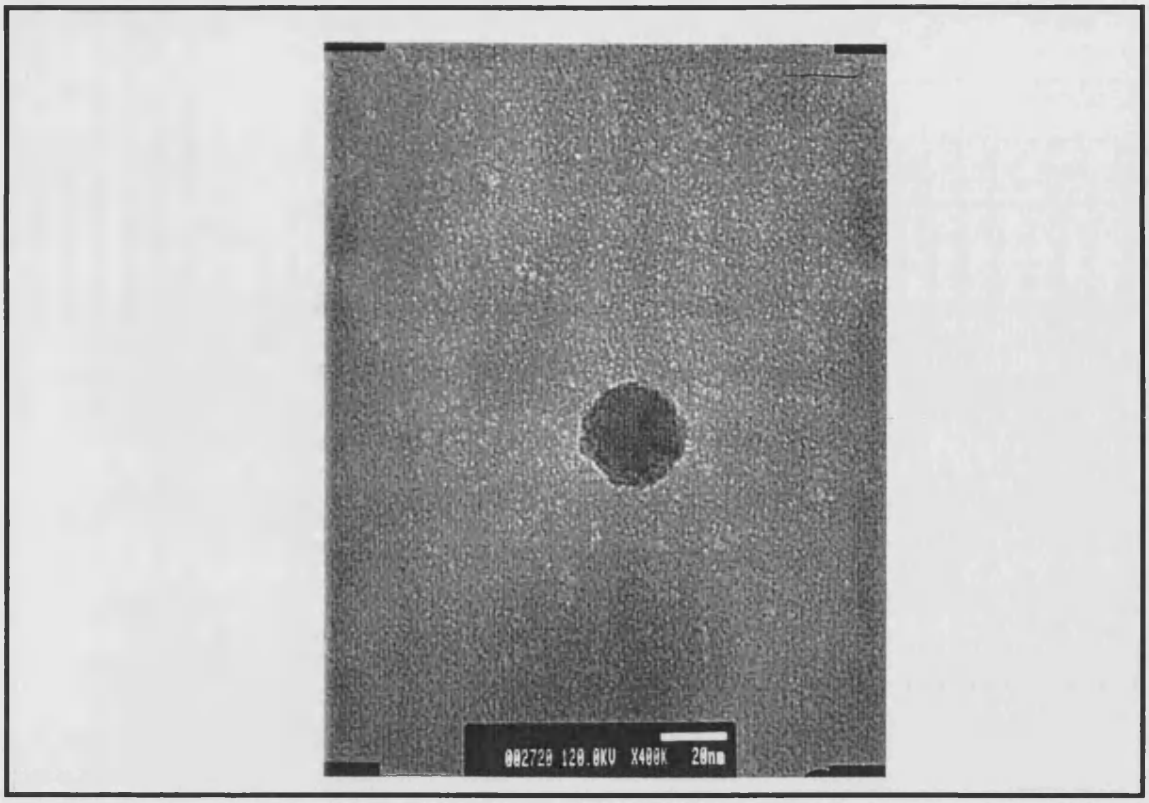

Figure 21: Electronmicrograph of a hepatitis A virus particle fixed and stained in phosphotungstic acid (x400,000)

The conformationally defined immunodominant antigenic site of HAV includes Asp-70 of VP3, but amino acid residues in VP1 also contribute to this site, as well as to at least one other functionally independent antigenic site (Stapleton & Lemon, 1987; Ping *et al.*, 1988; Gauss-Müller *et al.*, 1990; Nainan *et al.*, 1992). Interestingly, Emini *et al.* (1985) demonstrated that an anti-HAV antibody response could be primed by PV-specific synthetic peptides, suggesting the existence of a degree of higher-order homology between the poliovirion and the hepatitis A virion. HAV, however, shows the greatest overall homology to EMCV (Diamond *et al.*, 1986). Synthetic peptides derived from the capsid proteins of HAV used to search for B-epitopes, revealed that of the three regions used (VP1 (amino acids 115-139), VP2 (amino acids 69-99) and VP3 (amino acids 137-150)), only free peptide 69-99 from the VP2 protein caused formation of HAV binding antibodies. The dominant antigenic site of HAV is highly conserved among all human strains, and reversion of neutralisation escape mutants to the wild-type antigenic phenotype has been noted when escape mutants have been tested for virulence in owl monkeys (Lemon, 1994). Presumably, neutralisation-resistant HAV mutants arise during natural infections but do not replicate to significant levels *in vivo*. It is intriguing to consider therefore, that the immunodominant neutralisation epitopes of HAV may have a vital functional role in the replication of the virus *in vivo* and if this is true, then

neutralisation escape mutants may have lost a function necessary for *in vivo* replication and may be partially or completely attenuated (Stapleton & Lemon, 1987). Extensive digestion with high concentrations of trypsin and chymotrypsin result in cleavage primarily of VP2, but do not alter the antigenic characteristics, infectivity or exceptional thermostability of the virion (Lemon, 1994; Hollinger & Ticehurst, 1996). Domingo and colleagues (1993) suggest that there might be a natural restriction of substitutions at some antigenic sites due to their possible involvement in virus attachment and entry.

1.3.4.2 Properties of the genome

The genome of HAV is a single-stranded, positive-sense RNA (Coulepis *et al.*, 1981), approximately 7500 bases long. A short genome-linked protein (VPg) of 23 amino acids is present at the 5′-end (Weitz *et al.*, 1986) followed by a nontranslated region (NTR) of approximately 735 bases. This region contains extensive secondary structure, including a 5′-terminal hairpin, and as many as 10 AUG codons, scattered about in all three reading frames preceding the AUG which initiates the large open reading frame (ORF) encoding the polyprotein of HAV (Najarian *et al.*, 1985; Cohen *et al.*, 1987(a); Paul *et al.*, 1987). Recent data suggest that the 5′ NTR contains a *cis*-acting element which has been variably termed an IRES or 'ribosomal landing pad' (nt 154-735) (Brown *et al.*, 1991; Glass *et al.*, 1993; Whetter *et al.*, 1994), and that its structure and organisation are remarkably similar to that of the 5′ NTR of EMCV of mice (Glass *et al.*, 1993; Le *et al.*, 1993). The 5′ NTR is capable of forming two or more pseudoknots in the noncoding region upstream from the IRES. Also present in this region is a pyrimidine tract (pY1 domain (Id)) between nt 99 to 138 downstream of the putative 5′ pseudoknots, unique to HAV but which may be structurally analogous to the poly(C) tract of cardio- and aphthoviruses (Figure 23), which is not required for growth in cell culture as long as the sequence between nt 140 and nt 144 is present (Shaffer *et al.*, 1994). There are other pyrimidine-rich tracts within the 5′ NTR of HAV, but the pY1 domain is the lengthiest and most prominent of these regions. Large deletion mutations involving the first pyrimidine-rich tract of the 5′ NTR of human HAV define two adjacent domains associated with distinct replication phenotypes. The HAV IRES has only a very low level of functional activity in infected cells, which may contribute to the slow replication cycle of the virus (Whetter *et al.*, 1994). The 5′ NTR is extensively conserved among HAV strains (generally >92% nucleotide identity) and is very important for replication (Tesar *et al.*, 1992; Borman *et al.*, 1994). Harmon and co-workers (1991) observed that deletion of HAV nt 1 and 2 (both U residues) or nt 2 and 3 (a C residue), which are thought to form

part of a stem-and-loop, abolishes the infectivity of the RNA. PV lacking the first terminal uridylate residues is, on the contrary, infectious. The IRES itself contains sequences necessary for viral RNA synthesis *per se* (Borman *et al.*, 1994).

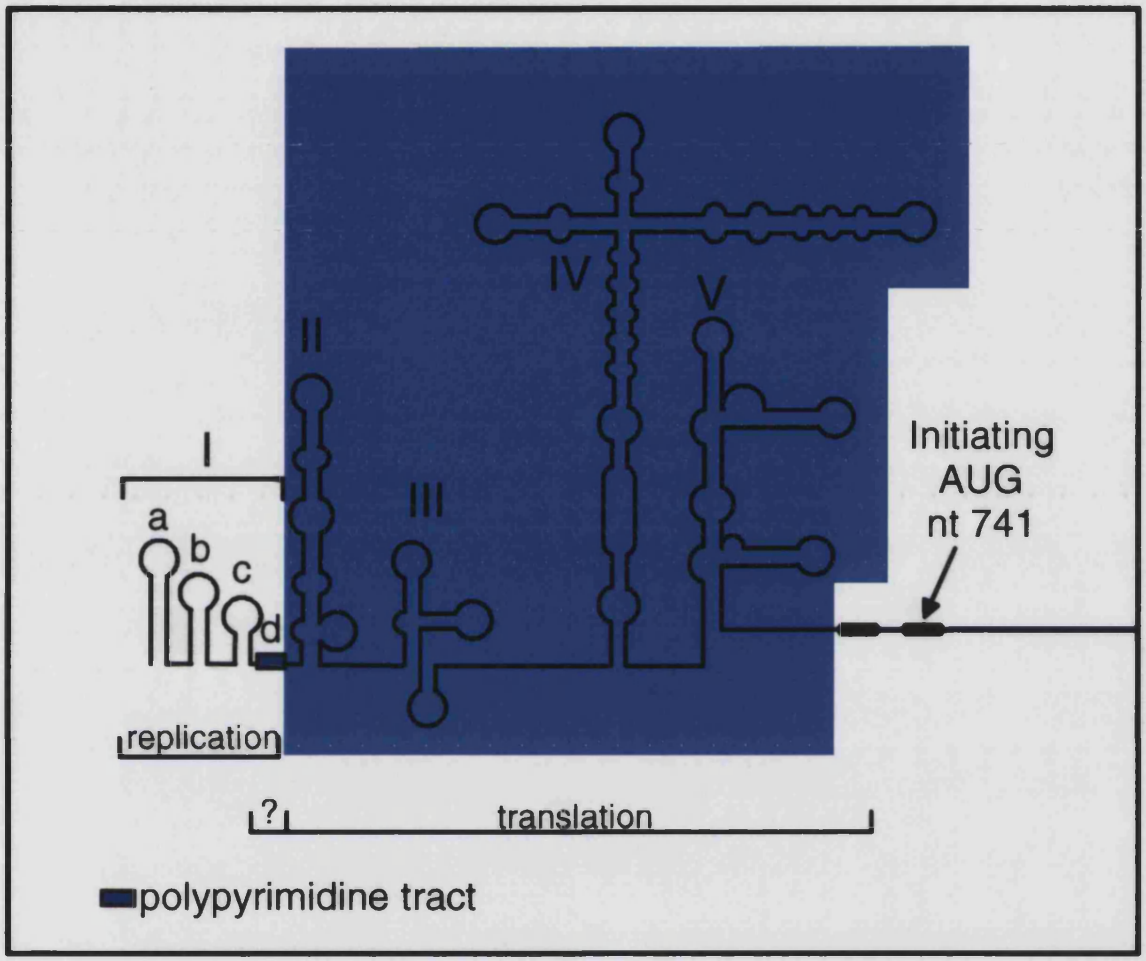

Figure 22: Hepatitis A virus 5' NTR with type III IRES

Mutations within the 5′ NTR have been shown to be involved in cell culture adaptation as discussed later (Brown *et al.*, 1991; Emerson *et al.*, 1993). Considerably greater sequence variation is evident within the large ORF, and several distinct genotypes of HAV have been described based upon the existence of >15% nonidentity within the VP1/2A (or pX) coding region (Lemon, 1994). The 3′ end of the genome includes a shorter NTR which may also display secondary structure similar to the PV ORF (Jacobson *et al.*, 1993) and a polyadenylated tail (Coulepis *et al.*, 1981). A 22S, double-stranded RNA form, closely resembling the RI of other picornaviruses, also has been detected. The general organisation of the genome is shown in Figure 23.

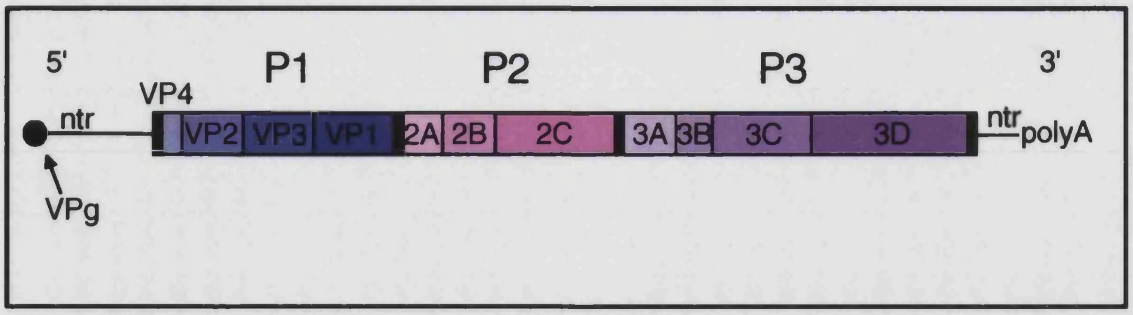

Figure 23: Organisation of the positive-stranded genome of hepatitis A virus

There is a small protein (VPg) attached at the 5′-terminus, followed by a nontranslated region of approximately 735 bases. A large open reading frame encodes a polyprotein of approximately 2235 amino acids which may be divided into three major domains: P1 (capsid proteins), P2 and P3 (non-structural proteins). The existence of VP4 (1A) remains uncertain, as does the possibility of a short leader protein (L, not shown) which would precede it within the polyprotein. pX extends into the 2A region shown in this figure, making 2A significantly smaller than depicted. The other capsid proteins VP2, VP3 and VP1 are also known as 1B, 1C and 1D. The large open reading frame is followed by a short 3′-NTR of approximately 64 bases, followed by a 3′-terminal poly(A) track.

1.3.4.3 Properties of the viral proteins

In accordance with other picornaviruses, it is presumed that the genetic information of HAV is expressed as a single polyprotein which is co- and post-translationally cleaved into proteins, named according to the L434 nomenclature of Rueckert and Wimmer (1984), involved in genome replication and virion formation (Jürgensen *et al.*, 1993) as shown in Figure 24.

HAV protein processing has been difficult to study due to the slow asynchronous, and low yielding replication of the virus and its failure to inhibit host-cell protein synthesis, although predictions can be made on the basis of sequence homology with other members of the *Picornaviridae*. Relatively little is also known about the specific function of the nonstructural proteins of HAV because they do not accumulate in infected cells to levels comparable to the capsid proteins (Updike *et al.*, 1991). Anderson & Ross (1990), as already mentioned, detected a 42kDa protein, designated 'pX', associated with some virion preparations which has been suggested to represent VP1 fused to a large (approximately 8kD) carboxy-terminal extension i.e. VP1-2A. Jia and co-workers (1993) identified a primary cleavage reaction which would generate a capsid protein precursor with a C-terminal extension of about one-third of what had been proposed to be the 2A sequence. This cleavage was mediated by the 3C protease in *trans*. If these observations are correct, the processing of the HAV polyprotein may differ significantly

from other picornaviruses (Jia *et al.*, 1993; Jürgensen *et al.*, 1993; Porter, 1993; Lu *et al.*, 1994).

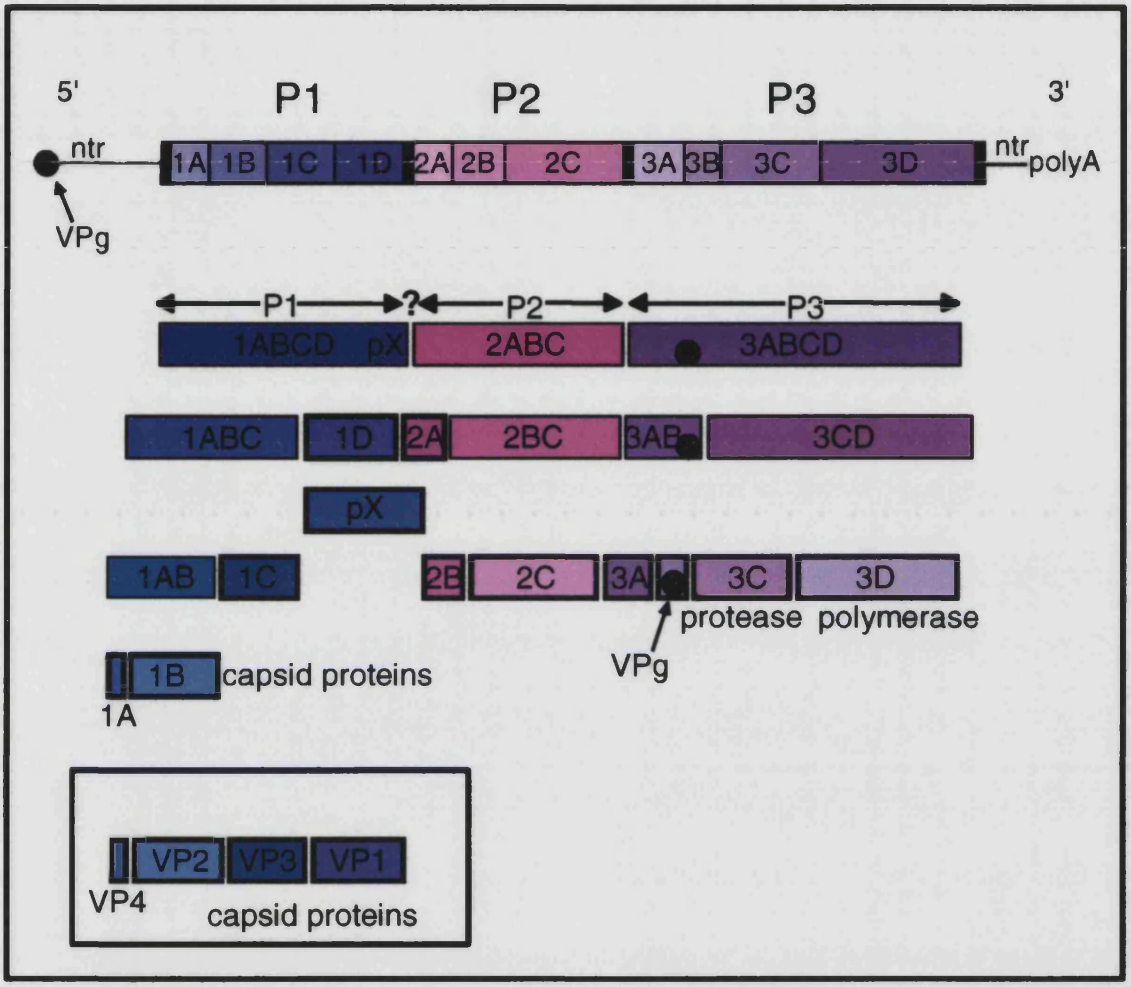

Figure 24: Proposed proteolytic cascade for hepatitis A virus

Top, HAV genomic RNA, with its 5′ VPg linked protein. 5′ nontranslated region, long single open reading frame, 3′ nontranslated region, and polyadenylated 3′ end. Open reading frame is cleaved into structural proteins (1AB, 1C and 1D [VP0, VP3, and VP1]) and nonstructural proteins. Nonstructural proteins with identified functions are below (protease, polymerase, VPg) (Adapted from Palmenberg, 1990).

The 2A protein of HAV, a polypeptide thought to be approximately 10KDa, does not contain a consensus protease active site, such as found in the 2A protein of PV, and has been found to be liberated by proteinase 3C from its precursors P1-2A and VP1-2A (pX) (Sculthеiß *et al.*, 1994). The truncated viral protein 2A, as implied above may not be functional in HAV or may have acquired a different and as yet unidentified role (Sculthеiß

et al., 1994), but 2A is nonetheless relatively large and well conserved (Jürgensen *et al.*, 1993). The protein pX could contain a 2A fragment produced by cleavage within the predicted 2A or it could contain an authentic 2A the size of which had been predicted on false positioning of the 2A-2B junction. With this in mind studies have very recently shown that the originally predicted Gln-Gly dipeptide cleavage site at position 980-981 of the HAV polyprotein (Najairian *et al.*, 1985; Cohen *et al.*, 1987a) has to be relocated to position 836-837 and that 2B is significantly larger than previously assumed (27.5kDa) (Martin *et al.*, 1995; Gosert *et al.*, 1996). These results not only redefined peptide 2B but also showed that 2A of HAV is much smaller than the 10kDa predicted by Schultheiß *et al.* (1994) and would be expected to have a molecular mass of 5.3kDa. 2A of HAV has features distinct from that of PV 2A and rhino- and enteroviruses - lack of protease activity and lack of p220 inactivation by HAV and thus failure of host-cell shut-off - which implies that it is unlikely that 2A of HAV functions in the same manner as the 2A of other picornaviruses, and its function remains unknown (Gosert *et al.*, 1996).

Proteins 2B and 2C are also of unknown function, although 2C contains an RNA helicase consensus sequence (Porter, 1993; Harris *et al.*, 1994) and in PV is needed continually for viral RNA synthesis in the formation and maintenance of RC-associated membranous structures as well as in anchoring RCs to these structures.(Cho *et al.*, 1993) and its function can be provided in *trans.* HAV 2C protein, like its PV counterpart, is thought to be an NTPase and may be involved with sensitivity to guanidine, and which in PV has been shown to inhibit viral RNA replication by affecting coupling between the NTP binding and/or splitting, on the one hand and the 2C function (related to conformational changes), on the other, thereby implying that oligomerisation of 2C is an essential step in the replication of viral genome (Tolskaya *et al.*, 1994; Hollinger & Ticehurst, 1996). The HAV 2C and 2BC proteins demonstrate efficient membrane association properties and causes major rearrangement of the ER and probably Golgi and perhaps other intracellular membrane compartments. Its slow growth phenotype is therefore not likely due to the inability of 2C to induce membrane changes *per se*, but the absence of such detectable membrane alterations and structural rearrangements into viral RCs in HAV-infected cells could be due to production of very low amounts of these and other viral proteins in the infected cells (Teterina *et al.*, 1997a).

2B or 2BC is another viral protein of PV required for RNA replication (Datta & Dasgupta, 1994). Mutations in 2B and 2C of HAV have been shown to be important with respect to RNA synthesis and host range change that occurs during adaptation and passage of virus in cell culture and leads to attenuation of the virus (Emerson *et al.*, 1993; Graff *et*

al., 1994; Gosert *et al.*, 1996). The analysis by Teterina *et al.* (1997a) of the effect of 2C (2BC) sequences from either a wild-type strain or a faster replicating cytopathic strain demonstrated that mutations acquired in wild-type virus during adaptation to cell culture do not change dramatically either the ability of these proteins to associate with membranes and induce membrane alterations or the specific architecture of the induced membrane structures. Protein 2C, but not 2BC, from the cytopathic strain of HAV induced different membrane structures.

Protein 3B has been shown to be the 5′ genome-linked viral protein (VPg) of HAV (Weitz *et al.*, 1986), initially present in its precursor form 3AB. VPg is required for viral RNA replication, and it is believed that the membrane-associated VPg-precursor protein, 3AB, may be used for the delivery of VPg into the 5′ ends of plus- and minus-strand RNAs during replication, as 3AB and 3A are capable of localizing in the endoplasmic reticulum and golgi apparatus in transfected HeLa cells in the absence of any other PV protein (Datta & Dasgupta, 1994). PV protein 3AB has been shown to form a complex with and stimulate the activity of the viral RNA polymerase, $3D^{pol}$ (Plotch & Palant, 1995) as discussed earlier. Amino acid sequence alignments suggest that membrane binding might be due to a hydrophobic stretch near the C-terminus of 3A found in all picornaviruses whereas the ability to induce permeability of *E. coli* membranes is determined by an amphipathic helix formed at the N-terminus of 3A of a cytopathogenic HAV strain (Pisani *et al.*, 1995). Beneduce and co-workers (1995), expressed protein 3A in *E. coli* and showed that an N-terminal deletion rendered this protein toxic to bacteria. Furthermore, Beneduce *et al.* (1997) have demonstrated that changes in the primary sequence involving charged amino acids at the N- and C- termini critically influenced the ability of the protein 3A of a cytopathic strain of HAV to change bacterial membrane permeability, demonstrating the strict correlation between the structure and pore-forming potential of HAV protein 3A. Hypothetical pore-formation into the nuclear membrane induced by the protein 3A of a cytopathic strain could account for the accelerated growth by promoting a more efficient relocalisation of nuclear proteins to the cytoplasm with respect to other strains, thereby possibly leading to a depletion of nuclear proteins needed for host cell replication and to cell death (cytopathic effect) (Beneduce *et al.*, 1997).

All picornaviruses process their polyproteins via a series of *cis* and *trans* cleavages, catalyzed primarily by the 3C gene product (Harmon *et al.*, 1992). In general, picornaviral 3C proteinases adopt a chymotrypsin-like fold and display an active site

configuration like those of the serine proteinases (Malcolm *et al.*, 1995).

The recently obtained crystal structure for HAV proteinase 3C reveals it is a cysteine-containing chymotrypsin-like serine proteinase (Allaire *et al.*, 1994) which seems to be the only virus-encoded proteinase which can catalyse cleavage at all sites in the HAV polyprotein including the primary cleavage, which separates the precursor of the structural from that of the nonstructural proteins (Jia *et al.*, 1991a; Harmon *et al.*, 1992; Sculthеiß *et al.*, 1994).

Harris and coworkers (1992) have shown that HAV 3C mediates cleavage at its own N- and C-termini and at the proposed junction between 2C and 3A (Jia *et al.*, 1991a), however cleavage at its C-terminus is less efficient than at its N-terminus (Harmon *et al.*, 1992). Comparisons of the HAV $3C^{pro}$ with those of other picornaviruses suggested that the catalytic triad may be composed of residues His-44, Asp-98 and Cys-172, however crystallographic have been interpreted as suggesting that the catalytic site consists only of a dyad, including Cys-172 as nucleophile and His-44 as general base, with His-191 defining the 3C cleavage specificity for glutamine residues (Allaire *et al.*, 1994; Gosert *et al.*, 1997; Hollinger & Ticehurst, 1996). Moreover Gosert *et al.* recently (1997) suggested that His-44 and Cys-172 are essential for polyprotein processing, whereas Asp-98 is not. Kusov & Gauss-Müller (1997) have shown that HAV $3C^{pro}$ is an RNA-binding protein with specificity for the most 5′-terminal RNA structures of the HAV genome, and further suggest that the RNA-binding region is located in an area distinct from the catalytic triad and that HAV 3C might serve multiple, yet unknown, functions during the life cycle. Purified PV $3CD^{pro}$, a proteinase thought to be essential for processing of the P1 capsid precursor, expresses no RNA polymerase activity (Harris *et al.*, 1992) and can accumulate due to the cleavage efficiency of 3C at its carboxy terminus being rather low (reference within Gauss-Müller *et al.*, 1991). $3CD^{pro}$ has the propensity to bind the 5′-terminal cloverleaf of PV RNA but this occurs only in the presence of a 36kDa host factor of uninfected HeLa cells, however the 3AB-$3CD^{pro}$ complex interacts with cloverleaf RNA and binds to 3′ RNA fragments of the PV genome in the absence of host factor (Harris *et al.*, 1994). In contrast to PV, Kusov & Gauss-Müller (1997) found that binding of HAV RNA of the 5′ NTR was not improved when similar concentrations of 3CD were used instead of 3C, suggesting that the 3D moiety does not affect the RNA binding specificity of HAV 3C. Furthermore, Jürgensen *et al.* (1993) revealed that for cleavages at 2C/3A and 3C/3D, the complete 3D moiety was not required. Kusov & Gauss-Müller (1997) found that HAV 3CD, unlike PV 3CD, was not

detected as a predominant product of polyprotein processing. Instead, HAV 3ABC, whose specific role is unknown, was found to be a relatively stable intermediate when the HAV polyprotein was translated *in vitro* or expressed in bacteria and mammalian cells (Harmon *et al.*, 1992; Schultheiß *et al.*, 1994). Kusov *et al.* (1997) showed that recombinant HAV 3ABC specifically interacts *in vitro* with secondary structures formed at both the 5′ and 3′ terminus of the viral genome. Similar to protein 3AB, HAV 3ABC bound to the 3′ terminal RNA structure which did not interact with the mature proteinase 3C. In contrast to 3AB, 3ABC interacted with RNA stem-loop Ib and combinations of individual secondary structure elements of the 5′ NTR. RNA binding of this precursor 3ABC was 50 times stronger than that of 3AB and 3C, implicating a specific role of this stable processing intermediate in viral genome replication. Cleavage of $3CD^{pro}$ to $3D^{pol}$ is needed to activate the 3D RNA polymerase (Gauss-Müller *et al.*, 1991). It has been shown that 3D is formed by cleavage at the Glu-Arg pair at position 1738 and 1739 of the HAV polyprotein (Tesar *et al.*, 1994). The HAV 3D protein produced by autocatalytic cleavage of P3 precursor proteins in BS-C-1 cells, however, was found to be virtually completely insoluble, unlike its PV counterpart which displayed an extent of solubility.

By analogy with other picornaviruses, HAV 3D is a RNA-dependent RNA polymerase. The amino acid homology of HAV 3D with other picornavirus polymerases is low (27-33%), but it shares several amino acid motifs with all sequenced RNA-dependent polymerases. Updike *et al.* (1991) have shown that HAV 3D does not accumulate in infected BS-C-1 cells. Moreover, 3D was not immunoprecipitated despite labelling periods as short as 10 minutes and immediate harvest, suggesting that 3D may have a short half-life in infected BS-C-1 cells. It is proposed that the active site of this enzyme consists of Tyr343-Gly344-Asp345-Asp346 (Hollinger & Ticehurst, 1996 and references therein)

In order for an RNA strand to serve as template for multiple rounds of product RNA synthesis, the RNA replicative machinery should either prevent formation of extensive base pairing between the template RNA and the complementary strand or contain a helicase activity which is able to unwind RNA duplex subsequent to its formation (Cho *et al.*, 1993). In addition to RNA-dependent RNA polymerase activity, $3D^{pol}$ protein sequences contribute to 3CD protease activity. Other suggested activities of $3D^{pol}$ include RNA unwinding, uridylylation of VPg, interaction with cellular proteins and PV RNA near the 5′ terminus of the positive strand, and association with membrane structures. It was recently determined that $3D^{pol}$ was able to add multiple adenylate (A)

residues to the 3′ terminus of PV RNA in a nontemplated manner and effect the initiation of plus-strand synthesis (Neufeld *et al.*, 1994).

1.3.4.4 Replication and adaptation to cell culture

Relatively few studies have addressed the replication of HAV in cell culture. Although HAV demonstrates some unique features, such as a very protracted replication cycle, it has generally been considered to replicate by a scheme similar to that of other picornaviruses (Figure 10).

Ashida and colleagues (1989) investigated propagation of HAV in hybrid cell lines in order to facilitate *in vitro* propagation. Virus grown *in vitro* is associated with host-cell derived material and has been shown to interact with the serum protein fibronectin. Dotzauer *et al.* (1994) recently investigated the replication of HAV in nonprimate cells and found that the cell surface receptor(s) and other host factor(s) required for HAV replication are present in nonprimate as well as primate cells. Purified HAV will attach to a wide range of cultured cells and attachment is affected by the cell type, the presence of calcium, temperature and the presence of serum. Results of investigations by Bishop and Anderson (1997) suggest that the major effect of calcium in promoting HAV-receptor interactions is through a direct effect on the conformation of the viral capsid. The enhancing effects of calcium ions and low pH on HAV, they observed, attachment are not additive. It is possible that virion-bound host components play a role in virus attachment and dissemination (Zajac *et al.* 1991). Investigation of HAV antigenic variant strains (neutralisation escape mutants) demonstrated identical attachment properties with neutralisation-susceptible strains, suggesting that the immunodominant antigenic site of HAV is not directly involved in cell attachment. Unlike FMDV, RGD peptides were also shown to be unable to interfere with HAV attachment, suggesting that the HAV binding region does not involve an RGD sequence or the immunodominant neutralisation site (Stapleton *et al.*, 1991). The HAV cellular receptor 1 (HAVcr-1) cDNA codes for a novel mucin-like class I integral membrane glycoprotein of unknown natural function (Cowan & Anderson, 1997; Locarnini, 1997), contains four putative N-glycosylation sites and two distinctive regions: an N-terminal Cys-rich region that displays homology to sequences of members of the immunoglobulin superfamily, and a mucin-like C-terminal region containing 27 repeats of the consensus PTTTTL (Thompson *et al.*, 1998), and serves as an African green monkey kidney (AGMK) cell receptor for HAV (Kaplan *et al.*, 1996). Further investigation revealed that the Cys-rich region of HAVcr-1 and its first

glycosylation site are required for binding of protective monoclonal antibody 190/4 and HAV receptor function (Thompson *et al.*, 1998).

Following uncoating in the cytoplasm releasing the RNA genome, which alone may take up to 12 hours in HAV (Updike *et al.*, 1991), and translation of genomic RNA the viral RNA polymerase $3D^{pol}$ is released, in PV, from the C-terminus of the large polyprotein precursor by protease-catalyzed autocatalytic cleavage that generates the mature viral proteins (Plotch *et al.*, 1989), and presumably replication in HAV is carried out by its viral RNA-dependent RNA polymerase, $3D^{pol}$. This enzyme has been well characterised in PV but HAV $3D^{pol}$ is proving to be more elusive.

The replication of HAV is not associated with shutdown of host-cell macromolecular synthetic processes, and usually does not lead to demonstrable cytopathic effects. However, rapidly replicating, cytopathic (RR/CPE+) strains of HAV, recovered from cells which had been persistently infected with virus for a period of many months, do induce a cytopathic effect characterised by vacuolation and cellular degeneration, but not associated with specific host cell metabolic shutdown (Lemon, 1994). Cytopathic variants of HAV have been shown to arise by a combination of genetic recombination and point mutations in both the 5′ and 3′ NTRs and the capsid region VP2, as well as in the nonstructural proteins 2A, 2B, 2C, 3A, VPg and $3D^{pol}$ (Jansen *et al.*, 1988; Lemon *et al.*, 1991; Zhang *et al.*, 1995). The results of Zhang *et al.* (1995) suggest novel interactions between the 5′ NTR and P2 proteins during HAV replication. Very recently a RR/CPE+ strain was isolated from persistently infected BS-C-1 cells by serial passages, sequencing of the the NTRs and coding regions for 2ABC and 3AB of which, revealed that mutations are distributed all over these regions and that certain mutated sites correspond to those in other cytopathogenic HAV variants, and on investigating the mechanisms causing the CPE in cells infected with this variant, Brack *et al.* (1998) found that an apoptotic reaction takes place. Beneduce *et al.* (1995) suggested that a deletion in 3A might be involved in the induction of a CPE, expression of which induces modifications of cell membrane permeability which lead to cell death.

Viral translation appears to proceed following internal entry of the 40S ribosomal subunit particle within the 3′ half of the 5′ NTR, just upstream of the AUG initiating the large ORF (Le *et al.*, 1993). Recent studies by Tesar *et al.* (1992) have shown that HAV RNA has two potential translation initiation sites, located at 735-737nt and 741-743nt, and that the preferred translational start site, however, is the second AUG within the ORF and not the

first AUG triplet. *In vitro* translation of HAV in RRLs is thought to be quite inefficient, and apparently plagued by both inappropriate termination and aberrant initiation (Glass *et al.*, 1993). Aberrant initiation is particularly prominent in the P3 region of the genome (Lemon, 1994). In addition, internal initiation of HAV translation appears to proceed only at a very low level of efficiency even within permissive cells (Whetter *et al.*, 1994). Jia *et al.* (1991b) demonstrated that translation of HAV RNA in RRLs initiates predominantly at a large number of internal AUG codons, especially those in the P3 coding region, however, replacement of the HAV 5′ NTR with EMCV 5′ end sequences increased initiation at the correct polyprotein start site and both reduced and altered the products generated by internal initiation. Since the EMCV RNA 5′ end functions quite well in RRLs to direct ribosomes to the appropriate AUG, it is likely that successive loading of ribosomes at the 5′ end, followed by ribosome translocation due to polypeptide chain elongation, makes internal RNA regions unavailable for aberrant initiation events. If ribosome entry at HAV 5′ end RNA sequences requires factors not adequately present in RRLs (as appears to be the case for PV RNA), then the failure to load ribosomes at the 5′ end would leave internal sites exposed and available for aberrant initiation. Chimeric RNAs containing the EMCV IRES and various lengths of the 5′-terminal HAV sequence were analysed and revealed that more than 151 nt from the 5′ terminus of HAV were found to be required to support virus replication, indicating either, that the signals governing RNA replication are localised to the 5′-terminal portion of the HAV 5′ NTR or that any replication signals that extend within the HAV IRES can be functionally provided by the EMCV IRES sequence-structure indicating that the inherent translation efficiency of the HAV IRES may not be the major limiting determinant of the slow-growth phenotype of HAV (Jia *et al.*, 1996). Similar experiments using constructs retaining the HAV 5′ NTR extending into various lengths of HAV coding sequences, using PV coding sequences as reporter, demonstrates that sequences downstream of the translation initiation AUG codon of the HAV IRES provided a four-fold increase of HAV IRES-driven translation *in vitro* over a construct without HAV downstream capsid coding sequences. More than 66nt of the HAV capsid coding sequence are necessary to support this stimulation (Graff & Ehrenfeld, 1998). Using dicistronic mRNAs translated *in vitro*, Borman & Kean (1997) have shown that the HAV IRES is inhibited by FMDV Lb proteinase, as well as by HRV 2A proteinase and, furthermore, have determined that HAV IRES requires intact eIF4G for activity which is unique among the picornavirus IRESes studied to date and may help explain why HAV does not inhibit host cell translation during viral infection (Borman & Kean, 1997). It is likely that cell-specific translation initiation factors also play a prominent role in this process, although there is a

need for further work in this area (Whetter *et al.*, 1994). Internal ribosome binding likely requires the interaction of *trans*-acting factors that recognise both the mRNA and the ribosomal complex (Witherell & Wimmer, 1994). Glass & Summers (1993) have identified a *trans*-acting activity from liver that stimulates HAV translation *in vitro* and from their data surmised that the absence of factors necessary for HAV translation could play a role in the nonlytic slow growth properties exhibited by HAV in tissue culture systems. This idea is supported by reports that have suggested the need for accumulation of a cellular component(s) for the HAV life cycle to progress in BS-C-1 cells (Cho & Ehrenfeld, 1991). This could also suggest that the hepatotrophism of HAV may be based in part on intracellular tissue-specific factors required for HAV translation and not solely rely on cellular receptors for HAV, therefore lack of factors could result in an aborted replication of HAV in tissues other than the liver.

Processing of the polyprotein is probably mediated largely or entirely by the 3C protein, as described earlier. Borovec & Anderson (1993) suggest that cleavage of the HAV polyprotein to produce pentamers is protracted (though not rate limiting) early in infection, while the assembly of pentamers into higher structures is a rapid process once sufficient viral RNA is produced for encapsidation.

Initially, a negative RNA strand, present in very small quantities in infected cells, is synthesised from the plus-strand template. It is reasonable to suppose that the initiation of minus-strand synthesis depends on $3D^{pol}$ first recognizing and binding to certain viral RNA sequences, including the 3′ terminus region and it has been observed in purified recombinant PV and ECMV that $3D^{pol}$ absolutely requires the 3′ poly(A) tail of the viral RNA in order to bind the 3′ NTR and initiate replication (Cui *et al.*, 1993). More recently it has been discovered that the 3′ NTR is a binding site for 3AB and 3CD of PV and for $3D^{pol}$ of ECMV (Rohll *et al.*, 1995). A pseudoknot structure has been proposed within the 3′ NTR of PV RNA which may participate in secondary interactions. As yet there is no information regarding the relevance of these 3′ interactions to HAV, although Nüesch and colleagues reported in 1993 that a signal sequence is present in the 3′ NTR of the HAV genome which is thought to be involved in regulation of viral RNA replication. Involvement of various host-cell proteins in the replication of picornaviruses has been reported and is discussed in the previous sections. A higher-order structure formed at the junction of the $3D^{pol}$-coding sequence and the 3′ NTR of the HAV genome (putative RNA pseudoknot) significantly improves binding of host proteins and thus suggests that this structure might be essential for the formation of the RC initiating minus-strand

synthesis (Kusov *et al.*, 1996). Like the other picornaviruses, synthesis of the negative RNA strand yields a double-stranded intermediate which separates, the negative strand acting subsequently as a template for amplification of positive-sense genome. The results of Anderson *et al.* (1988) indicate that while the very small amount of negative-strand HAV RNA is used efficiently as a template for RNA synthesis, HAV positive-strand RNA is preferentially encapsidated and only poorly utilised as a template for RNA synthesis. The means by which HAV exits the cell is not known, although HAV has been found within cytoplasmic vesicles in infected cells in the liver (Hollinger & Ticehurst, 1996).

Following infection of permissive cell cultures with cell culture-adapted virus, replication of the viral RNA has been shown to proceed in an increasing fashion for several days, but then becomes reduced in magnitude as persistent infection becomes established. The factors responsible for this downregulation in viral RNA replication remain unknown, although it has been shown that, at the critical time during virus replication, proteins accumulate which interact specifically with a distinct nucleotide sequence within the 3′ non-coding region of the HAV genome and/or within the 5′ terminal region of the HAV antigenome (Nüesch *et al.*, 1993) and may have a regulatory action on viral RNA synthesis. De Chastonay & Siegl (1987) have also observed a down-regulation of viral RNA synthesis following the initial period of replicative activity, perhaps related to the generation of defective interfering particles containing RNA with large deletions putatively extending from the P1 (capsid-encoding domain) into the nonstructural region of the genome. Viral antigen may continue to accumulate after maximal infectivity has been reached in infections carried out at low multiplicity of infection. The reasons for this are not clear, although empty capsids at times represent the dominant form of antigenic material harvested from infected cells (Lemon, 1994).

Although the apparent synchronisation of HAV replication in BS-C-1 cells following removal of guanidine inhibition shortens the infection cycle about three- to five-fold (from 14 days to 4 days), this replication cycle is still 10-fold longer than that of most picornaviruses whose cycles are complete within 6-8 hr (Cho & Ehrenfeld, 1991). Hypotheses advanced to explain the slow growth of HAV in cultured cells include a delay in uncoating of the virus upon entry, asynchronous uncoating, rapid encapsidation of plus-strand RNA (Anderson *et al.*, 1988), production of defective genomes, an inefficient viral polymerase and rapid degradation of the viral polymerase (Updike *et al.*, 1991 and references therein).

The selective forces influencing the spread of HAV within human populations have forced the virus to evolve toward such a poor replicative posture. Infection of the liver with a virus having the replication properties displayed by PV or EMCV in cell cultures would probably result in rapid, overwhelming hepatic failure and death. However, HAV depends upon its secretion into bile by a relatively normal functioning liver in order to be shed in faeces and transmitted to other individuals. The inefficient translational activity of the HAV IRES, and possibly other HAV replicative functions, detailed above, may reflect the adaptation of this RNA virus to a relatively unique epidemiologic niche (Lemon *et al.*, 1992).

Continued passage of HAV through cells *in vitro* leads to incorporation of mutations into its genome as the virus adapts to growth in cell culture. These mutants have a shorter life-cycle and some display an attenuation in their infectivity which could increase their potential in vaccine production (Lemon, 1994). Previous studies have shown that mutations which occur during adaptation of HAV to cell culture have been found over the entire genome (Graff *et al.*, 1994). Mutations present in the 2B/2C genome region, however, are common in different HAV strains and are shown to be essential for an enhanced viral growth (Emerson *et al.*, 1993; Tedeschi *et al.*, 1993). Prior to this, Robertson *et al.* (1987) found that, of the capsid regions of attenuated HAV isolates studies, only limited amino acid changes were observed in VP4, VP2, and VP3, whereas amino acid variability was found within VP1 when they were compared with each other. It was recently reported that enhanced viral growth required mutations in both 2B and 2C proteins, suggesting that these proteins remain closely associated during HAV replication. Mutations in the 5′ NTR or P3 proteins had no independent effect, but acted cooperatively with mutations in P2 proteins to enhance replication and render the virus capable of conventional plaque formation (Zhang *et al.*, 1995). Mutations within the 5′ NTR have a dramatic effect in effect in enhancing growth in certain cell lines and may be of relevance to viral attenuation because the change in host range that accompanies adaptation of HAV to growth in monkey kidney cells has been associated with reduced hepatovirulence in susceptible primates (Brown *et al.*, 1991). Mutations which alter the secondary structure of the 5′ NTR may lead to a more effective binding pattern for the ribosome in the internal segment and possibly enhance the process of viral translation in cell culture (Graff *et al.*, 1994). In addition, mutations in the 5′ NTR of a cell-culture adapted HAV have been shown to enhance viral replication by facilitating cap-independent translation in a cell-type-specific fashion, supporting the concept that picornaviral host range is determined in part by differences in cellular translation initiation

factors (Schultz *et al.*, 1996). Mutations, however, in the 5′-most pyrimidine rich tract of HAV have been found to reduce its ability to direct internal initiation of translation (Carneiro *et al.*, 1995).

The slow growth of HAV in cell culture has hampered the production of sufficient quantities of an attenuated vaccine, however recent research into cell culture adaptation and attenuation of virulence looks promising in the search for a more practically and economically viable vaccine against hepatitis A. Recently Funkhouser *et al.* (1996) have reported progress towards the development of a genetically engineered HAV vaccine.

1.4 Study of the hepatitis A virus 3D^{pol}

In order to determine the reason for slow proliferation of HAV it is necessary to characterise the non-structural proteins of the virus. It has been postulated that slow growth of HAV in cell culture may be due to inefficient replication of viral RNA but this could also be explained by an inefficient RNA polymerase and attempts have been made to characterise this enzyme by cloning the P3 region of the genome and expressing in *E. coli*.

Recently a plasmid (pRITPOL) was designed to export HAV-specific P3 sequences into the periplasmic space of *E. coli* as a fusion protein with staphylococcal Protein A. It was hoped that this procedure would increase the solubility of the 3D^{pol} protein which had previously accumulated in *E. coli* as an insoluble, inactive product. In *E. coli* transformed with pRITPOL a weak poly(U) polymerase activity was detected which demonstrated Mg^{2+} dependence, inhibition by Mn^{2+} and a temperature optimum of approximately 32°C, but no protein of the predicted size of 53kDa was detected with human convalescent serum by Western blotting.

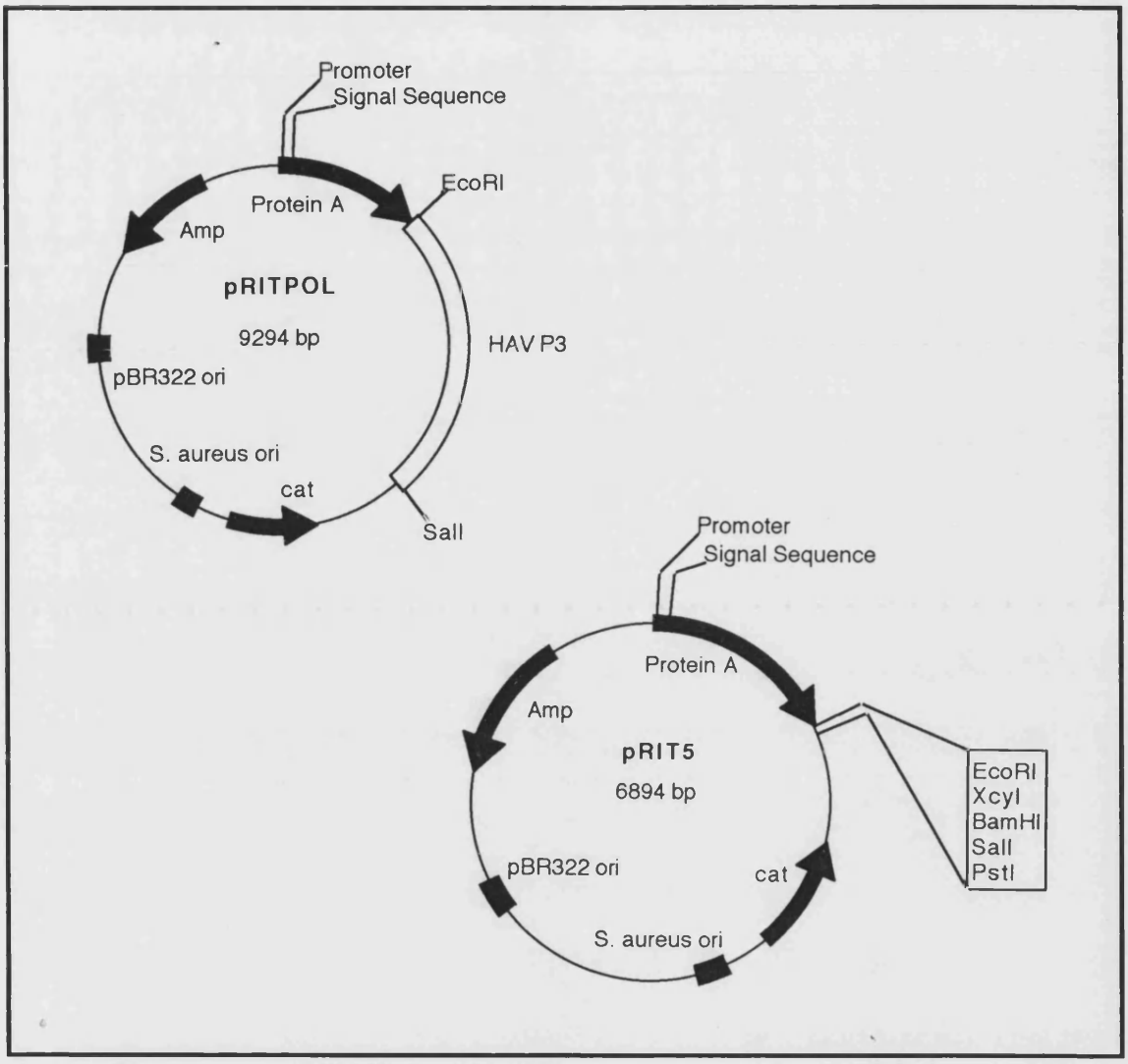

Figure 25: Plasmid construction pRITPOL and its parent vector pRIT5

An attempt was therefore made to improve expression levels and enzymic activity by making two new constructs based on the plasmid pMEX8, a strong, inducible expression vector (Figure 26). The first construct, HAV P3/pMEX8 contains most of the P3 regions with the exception of what was thought to be the first 11 amino acids of 3A under the control of a *tac* promoter. The corresponding proteins should be expressed in high levels in the cytoplasm. The second construct, Protein A/HAV P3/pMEX8, contains the P3 region as above, fused to selected staphylococcal Protein A sequences which direct the expression products to the periplasmic space. All three constructs including pRITPOL were transformed into *E. coli* strain JRR-600, a strain deficient in RNase I which contains episomal *lac* Iq, displaying tetracycline-retention of the episome (Wolstenholme *et al.*, 1993).

Purification of a protein believed to be the HAV RNA-dependent RNA polymerase from the periplasmic space of *E. coli* transformed with Protein A/HAV P3/pMEX8 has been achieved using affinity chromatography (Palmer, 1994).

A synthetic peptide corresponding to the N-terminus of the 3D region has been used to raise antisera in rabbit and this has been used to detect the HAV $3D^{pol}$ in cells expressing the P3 region (Nutter, 1992).

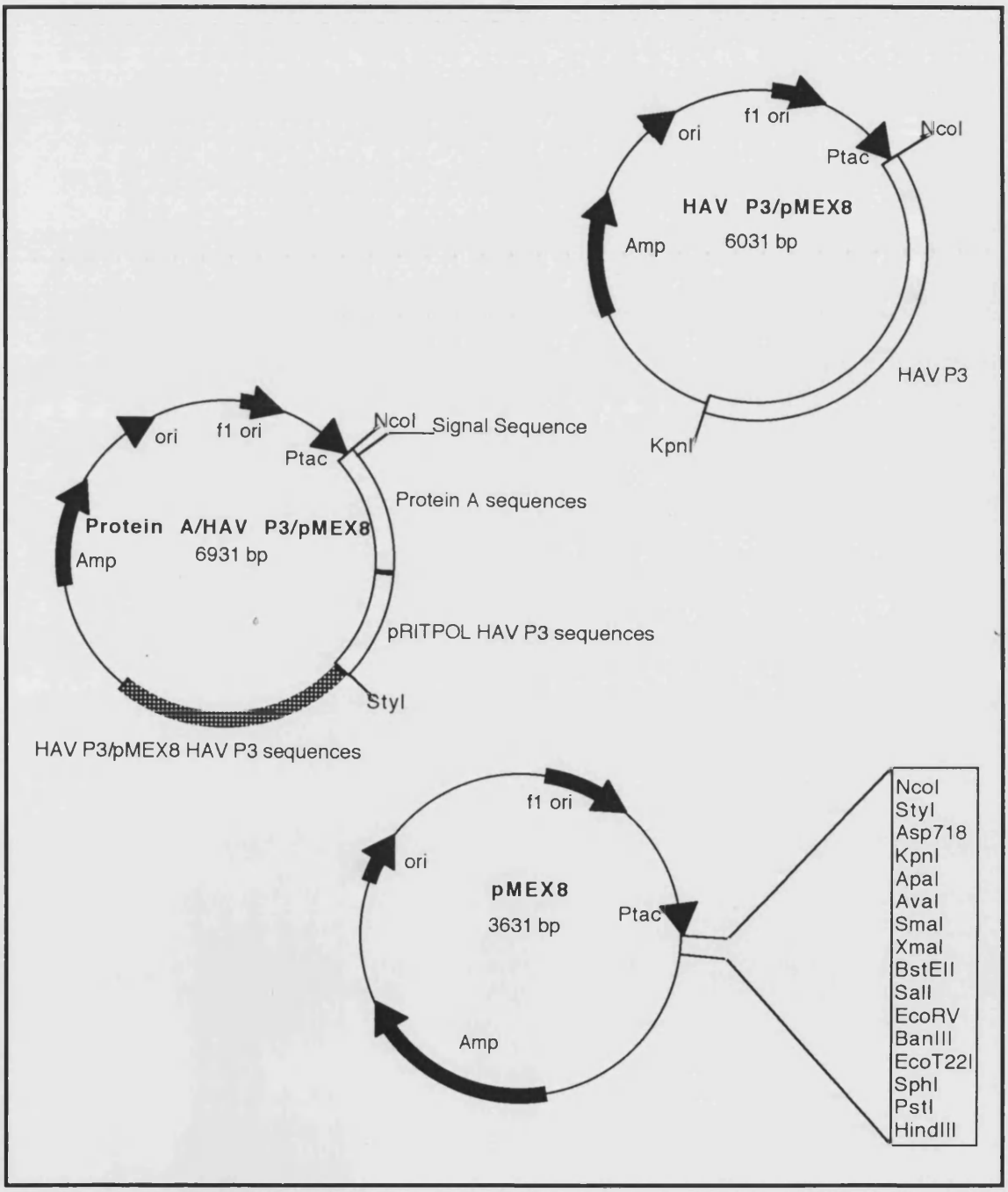

Figure 26: Plasmid constructions HAV P3/pMEX8 and Protein A/HAV P3/pMEX8 and their parent pMEX8 vector

1.5 Aims

To summarise, HAV shares many structural and biological attributes with other picornaviruses such as PV or EMCV. These include at least a superficially similar, non-enveloped capsid structure, and a positive-sense RNA genome of approximately 7.5kb which contains a single large ORF encoding a polyprotein which is post-translationally processed by virally encoded proteases into both structural and nonstructural proteins required for viral replication. Although the host range of PV is more restricted than EMCV, both of these viruses replicate rapidly in cultured cells. Following attachment, penetration, and uncoating there is a rapid shut-down of host-cell macromolecular synthesis and initiation of viral replication. Maximum titres of replicated virus are generally present within 6 hours or less. In contrast , one-step growth studies with HAV show that uncoating alone may take up to 12 hours, and that replication even of virus which has been substantially adapted to growth in cell cultures takes many hours more. Unlike PV and EMCV which generally cause rapid cytolytic infection, infection of cell cultures with HAV typically results in viral persistence, with little or no apparent impact on cellular growth.

What accounts for this marked difference in these picornaviruses? The virus appears to do poorly almost everything it must do to replicate and increase in number. One of several hypotheses advanced to explain this slow growth is the possibility that the polymerase enzyme is inefficient or rapidly degraded. The purpose of this investigation is to characterise the RNA polymerase activity encoded by the HAV. This is a key enzyme in viral replication, but the inefficiency of this process has made it impossible to study *in vivo*. The HAV RNA polymerase has previously been expressed in *Escherichia coli* systems and other vector/expression systems and I now propose to study the biochemical properties of the bacterially-expressed enzyme.

The polypeptides previously produced by Wolstenholme and colleagues (1993), however showed little or no polymerising activity. In this project, I hoped to improve the current expression system to maximise the enzyme yield and investigate the effects of viral and cellular cofactors on the *in vitro* activity of HAV RNA polymerase. This involved the cloning, expression and purification of other viral polypeptides e.g. 3AB, and the addition of the purified polypeptide to standard *in vitro* RNA polymerase assays. In this way the contribution of the RNA polymerase to the distinctive biological properties of HAV - slow, non-cytolytic growth in tissue culture and extremely conserved RNA genome sequence, can be assessed.

Essentially though, at commencement, this investigation had several specific aims.

1. Purification of the poly (U) polymerase, identification of the polypeptide responsible for this activity and determination of the N-terminal sequence which was incidently discovered in 1994 by Tesar and colleagues.
2. Biochemical characterisation of the poly (U) and RNA polymerase activities of the HAV $3D^{pol}$ expressed in *E. coli.*
3. Expression and purification of other viral polypeptides and their effects upon addition to standard *in vitro* RNA polymerase activity assays.
4. Development of a more efficient expression system for the HAV $3D^{pol}$. Expression levels obtained with the protein A fusion system described in Wolstenholme *et al.* (1993) were rather low, and higher levels of expression was expected to make the work described considerably easier.

The cost of an outbreak to society (individual patient, NHS and third parties combined) of hepatitis A, in Puglia, Italy, was recently calculated to be L37.406 billion ($US24.45 million) (Lucioni *et al.*, 1998). The overall aim of this project is the biochemical characterisation and reconstitution *in vitro* of the virus enzyme and it is hoped that in the long term, knowledge concerning the replication of viral RNA may permit the development of faster-growing 'high-yield' strains of virus that could reduce the cost of vaccine production.

2. Materials and methods

2.1 Materials

2.1.1 Escherichia coli strains

STRAIN	GENOTYPE (see Appendix 3)	SUPPLIER
XL1-Blue	*RecA1 endA1 gyrA96 thi-1 hsdR17*($r_K^- m_K^+$) *supE44 relA1 lac* [F′ *proAB lacI*^{q}*ZΔM15* Tn*10* (Tet^r)]	Stratagene Ltd., Cambridge, U.K.
XL2-Blue	*RecA1 endA1 gyrA96 thi-1 hsdR17* ($r_K^- m_K^+$) *supE44 relA1 lac* [F′ *proAB lacI*^{q}*ZΔM15* Tn*10* (Tet^r) Amy Cam^r]	Ultracompetent Epicurian® XL-2s purchased from Stratagene Ltd., Cambridge, U.K.
TB1	F$^-$ *ara Δ(lac-proAB) rpsL* (Str^r)[*ϕ80dlacΔ (lacZ)M15*]*thi hsdR* ($r_K^- m_K^+$)	New England Biolabs, Hitchin, U.K.
TG1	F′ *traD36 laqI*^{q} *Δ(laqZ)M15 proA*$^+$*B*$^+$*/ supE (hsdM-mcrB)5*($r_K^- m_K^-$McrB$^-$) *thi Δ(lac-proAB)*	Amersham International Plc, Little Chalfont, U.K.
JRR-600	*Produced by conjugation of MRE-600 cells with XL1-Blue cells*	Courtesy of Janet Rider, University of Bath, U.K.

2.1.2 Escherichia coli plasmids

PLASMID	GENOTYPE AND SIZE	SUPPLIER
pBluescript™	Amp^r, 2.96kb	Stratagene Ltd., Cambridge, U.K.
pMEX8	Amp^r, 3.63kb	United States Biochemical, Cleveland, OH, U.S.A.
pRIT5	Amp^r, 6.9kb	Pharmacia, St. Albans, U.K.
pMAL-c2	Amp^r, 6.7kb	New England Biolabs, Hitchin, U.K.

2.1.3 Enzymes

Restriction endonucleases and DNA modifying enzymes with associated buffers were purchased from New England Biolabs, Hitchin, U.K. or from the Promega Corporation, Southampton, U.K. with the exception of T4 DNA Ligase which was purchased from Gibco BRL, Paisley, U.K. and Expand™ Long Template PCR System, Expand™ High Fidelity PCR System and RNAse A which were from Boehringer Mannheim, Lewes, U.K. Sequenase™ sequencing kits were obtained from United States Biochemicals, Cleveland, OH, U.S.A.

2.1.4 Antibodies

Antibodies directed against a synthetic 3D peptide were courtesy of Miss E. Nutter. The synthetic peptide amino acid sequence is:-

M I E Y R L K S Y D W W R M F Y D Q C

This corresponds to the C-terminus of the predicted sequence of HAV 3D (nucleotides 7339 through to 7398 (Appendix 2 (7.2.3). By coupling this to thyroglobulin and forming an emulsion with the TiterMax™ Research Adjuvant (Sigma-Aldrich Chemical Company Ltd., Poole, U.K.) the serum collected from animals injected contained antibodies against the $3D^{pol}$. The titre of this antibody was found by Miss E. Nutter to be >1004.

Human convalescent serum was kindly supplied by the PHLS Laboratories, Royal United Hospital, Bath, U.K.

Anti-MBP antiserum was from New England Biolabs for use in pMAL expression analysis.

2.1.5 General laboratory reagents

Molecular biology grade chemicals were obtained from Fisons, Loughborough, U.K. Bacteriological culture media and Tris-saturated phenol:chloroform:isoamyl alcohol were obtained from the Sigma-Aldrich Chemical Company Ltd., Poole, U.K. Water-saturated phenol was from Rathbum, Walkerburn, U.K. Absolute ethanol was obtained from Hayman Ltd., Witham, U.K. Ultrapure Sequagel™ Sequencing Systems and Protogel™ acrylamide solutions were obtained from National Diagnostics, Hull, U.K. Falcon plasticware was supplied by Becton Dickinson and Company, Plymouth, U.K. and Nunc plasticware by Life Technologies, Glasgow, U.K. Whatman 3MM Chromatography Paper was from Whatman International Ltd., Maidstone, U.K. Trans-Blot® Transfer Medium (Pure Nitrocellulose Membrane) was from Bio-Rad Ltd., Hemel Hempstead, U.K.

Ultrapure dNTP sets were obtained from Pharmacia Biotech, St. Albans, U.K. Wizard™ Minipreps DNA Purification System kits were purchased from Promega and Sequenase™ Version 2.0 DNA Sequencing kits (United States Biochemical) from Amersham International Plc., Little Chalfont, U.K. The ECL kits and all radiochemicals were also purchased from Amersham International Plc. GENECLEAN *II*® kits (Bio101 Inc.) were from Anachem, Luton, U.K. and QIAquick PCR Purification kits and QIAfilter

Midi kits from QIAGEN Ltd., Dorking, U.K. Blue sensitive X-ray film was obtained from Genetic Research Instrumentation, Dunmow, U.K.

Oligonucleotides were synthesised either by R&D Systems Europe Ltd., Abingdon, U.K. or by Perkin Elmer - Applied Biosystems, Warrington, U.K.

2.1.6 Media and solutions

The composition of media and solutions used in the Methods section are given below. Solutions were sterilised either by autoclaving at 120°C, 1.41KPa for 20 minutes, or by filtering using Millipore 0.22μM syringe filters. All solutions were stored at room temperature in colourless glass or plastic bottles, unless otherwise stated.

2.1.6.1 Enzyme buffers

2.1.6.1.1 Polymerases and modifying enzymes and their buffers

ENZYME	REACTION BUFFER (1x)
Taq DNA polymerase	50mM KCl 10mM Tris-HCl (pH9.0) 0.1% (v/v) Triton X-100
Vent® DNA Polymerase	10mM KCl 20mM Tris-HCl (pH8.8 @24°C) 10mM $(NH_4)_2SO_4$ 2mM $MgSO_4$ 0.1% (v/v) Triton X-100
Expand Polymerase Enzyme Mix	50 mM Tris-HCl (pH 9.2) 16mM $(NH_4)_2SO_4$ 2.25 mM $MgCl_2$
Polynucleotide Kinase (PNK)	70mM Tris-HCl (pH7.6) 10mM $MgCl_2$ 5mM DTT
Calf Intestinal Alkaline Phosphatase (CIAP)	50mM NaCl 10mM Tris-HCl 10mM $MgCl_2$ 1mM DTT, pH7.9 @ 25°C
T4 DNA Ligase	50mM Tris-HCl (pH7.6) 10mM $MgCl_2$ 1mM ATP 1mM DTT 5% (w/v) PEG8000

Enzymes and buffers were stored at -20°C or as per manufacturer's recommendations.

2.1.6.1.2 Restriction endonucleases, their buffers and reaction conditions used

RESTRICTION ENDONUCLEASE	CONDITIONS	REACTION BUFFER (1x)	HEAT INACTIVATE?
Sac I *Kpn* I	Buffer 1 BSA (100μg/ml) 37°C	1mM Bis Tris Propane-HCl 1mM $MgCl_2$ 0.1mM DTT (pH7.0 @25°C)	YES NO
Xmn I	Buffer 2 BSA (100μg/ml) 37°C	5mM NaCl 1mM Tris-HCl 1mM $MgCl_2$ 0.1mM DTT (pH7.9 @ 25°C)	YES
*Cac*8 I	Buffer 3 37°C	10mM NaCl 5mM Tris-HCl 1mM $MgCl_2$ 0.1mM DTT (pH7.9 @ 25°C)	YES
*Bam*H I	Unique Buffer BSA (100μg/ml) 37°C	15mM NaCl 1mM Tris-HCl 1mM $MgCl_2$ 0.1mM DTT (pH7.9 @ 25°C)	NO
Sal I	Unique Buffer BSA (100μg/ml) 37°C	15mM NaCl 1mM Tris-HCl 1mM $MgCl_2$ 0.1mM DTT (pH7.9 @ 25°C)	YES

All enzymes and buffers stored at -20°C as per manufacturer's recommendations.

Double digests were conducted using the buffer directed by the manufacturer as detailed in section 2.2.4.1.

2.1.6.2 Media

MEDIUM	COMPONENTS
Luria-Bertani (LB) Broth	1% (w/v) bacto-tryptone 1% (w/v) NaCl 0.5% (w/v) yeast extract
LB-Agar	LB Broth 1.5% (w/v) agar
DYT	1.6% (w/v) bacto-tryptone 0.5% (w/v) NaCl 1% (w/v) yeast extract
LB-Glucose	LB Broth 0.02% (w/v) glucose (added post autoclaving as filter-sterilised stock solution)
LB-Expression	LB Broth 1mM IPTG (added post autoclaving)
Rich Broth (pMAL)	1% (w/v) bacto-tryptone 0.5% (w/v) NaCl 0.5% (w/v) yeast extract 0.2% (w/v) glucose

2.1.6.3 General solutions

BUFFER	COMPONENTS
Chloroform	24:1 (v/v) Chloroform:isoamyl alcohol
Phenol	Obtained distilled and stored at 4°C, equilibrated with 2 volumes 50mM Tris-HCl (pH8.0) (stored in the dark at -20°C)
Phenol/chloroform	50% (v/v) Phenol equilibrated with 10mM Tris-HCl, pH7.6 49% (v/v) chloroform 1% (v/v) isoamyl alcohol (stored in the dark at 4°C)
Ethidium Bromide	10mg/ml stock, stored in the dark at 4°C
RNAse A (DNAse free)	10mg/ml stock in TE Buffer, incubated at 95°C for 30 minutes and stored at -20°C.
PBS	0.14M NaCl 2.7mM KCl 10mM Na_2HPO_4 1.76mM KH_2PO_4, pH7.4

2.1.6.4 Buffers used in plasmid DNA preparation and analysis

BUFFER	COMPOSITION
GTE Buffer	25mM Tris-HCl (pH8.0) 10mM EDTA 50mM glucose
Standard Lysis Buffer (made up just prior to use)	0.2M NaOH 1% (w/v) SDS
Potassium Acetate Solution	3M potassium acetate 11.5% (v/v) glacial acetic acid, pH4.6
TE	10mM Tris-HCl 1mM EDTA, pH7.6
10x TBE	0.89M Tris-HCl 0.89M H_3BO_3 20mM EDTA, pH8.0
6x Loading Buffer	0.25% (w/v) bromophenol blue 0.25% (w/v) xylene cyanol FF 15% (w/v) Ficoll

2.1.6.5 Buffers used in protein analysis techniques

2.1.6.5.1 SDS-PAGE gel electrophoresis solutions

BUFFERS	COMPOSITION
30% (w/v) Acrylamide (stored at 4°C)	28.4% (w/v) acrylamide 1.6% (w/v) bis-acrylamide Deionised by stirring with dextran beads for 2 hours and filtered.
Solution A (Protogel) (stored in dark at 4°C)	29.2% (w/v) acrylamide 0.8% (w/v) N,N'-methylenebisacrylamide
Solution B/Resolving Gel Buffer (stored in dark at 4°C)	18.2% (w/v) Tris-HCl 0.4% (w/v) SDS, pH8.8
Solution C/Stacking Gel Buffer (stored in dark at 4°C)	6.1% (w/v) Tris-HCl 0.4% (w/v) SDS, pH6.8
Solution D/10% APS (made up just prior to use)	10% (w/v) ammonium persulphate
SDS-PAGE Sample Buffer (stored at 4°C)	50mM Tris-HCl (pH6.8) 0.1M dithiothreitol (DTT) 2% (w/v) SDS 0.1% (w/v) bromophenol blue 10% (v/v) glycerol
Tank Buffer	25mM Tris-HCl 0.25M glycine 0.1% (w/v) SDS, pH8.3
Fix	45% (v/v) methanol 10% (v/v) acetic acid
Coomassie Blue Stain	Fix 0.25% (w/v) Coomassie Brilliant Blue R-250

2.1.6.5.2 Western blotting and immunodetection buffers

BUFFER	COMPOSITION
Transfer Buffer	39mM glycine 48mM Tris base 0.037% (w/v) SDS 20% (v/v) methanol, pH8.3
10x Ponceau-S	2% (w/v) Ponceau-S 30% (w/v) trichloroacetic acid 30% (w/v) sulfosalicylic acid
Blocking Buffer	5% (w/v) Marvel™ non-fat dried milk 0.02% (w/v) NaN_3 in PBS
Phosphate-free, Azide-free Blocking Buffer	5% (w/v) Marvel™ non-fat dried milk 0.15M NaCl 50mM Tris-Cl
Washing Buffer	0.15M NaCl 50mM Tris-Cl

2.1.6.6 Buffers used in protein techniques

2.1.6.6.1 Buffers used in protein isolation

BUFFER	COMPOSITION
IC Resuspension Buffer	50mM Tris-HCl (pH8.1) 0.15M NaCl 0.25mM EDTA
PS Resuspension Buffer	0.3M Tris-Cl (pH8.1) 1mM EDTA 0.5mM $MgCl_2$ 20% (w/v) sucrose (sucrose added post autoclaving as filter sterilised stock)

2.1.6.6.2 GTP-Agarose affinity chromatography buffers

BUFFERS	COMPOSITION
Equilibration Buffer (stored at 4°C)	50mM KCl 10μM NaF
Elution Buffer (stored at 4°C)	Equilibration Buffer 5mM ATP

2.1.6.6.3 FPLC buffers

BUFFER	COMPOSITION
Column Equilibration Buffer	10mM Tris-Cl 25mM NaCl, pH8.0
Buffer A	20mM Tris-Cl 25mM NaCl, pH8.0
Buffer B	20mM Tris-Cl 0.5M NaCl, pH8.0

2.2 Methods

2.2.1 Techniques used in DNA preparation and synthesis

2.2.1.1 Calcium chloride competent cells

Competent cells were made using the calcium chloride method (adapted from Mandel and Higa, 1970). A 5µl culture of the desired cell strain, generally *E. coli* TG1 cells, in LB was incubated with shaking at 37°C overnight. An aliquot (200µl) of overnight culture was added to 50ml DYT and incubated with shaking at 37°C until an A_{550} of 0.3 was reached. The cells were placed on ice for 5 minutes, centrifuged at 1,090*g*, 4°C for 5 minutes and the pellet resuspended in 20ml 0.1M $CaCl_2$. After a further 20 minutes on ice, the cells were centrifuged as above and the pellet resuspended in 2ml 0.1M $CaCl_2$. Competent TG1s were used within 24 hours. Ultracompetent Epicurian® XL2s were used as directed by manufacturer.

2.2.1.2 Transformation and culture of clones

DNA (50-100ng) was added to 200µl competent cells and incubated on ice for 40 minutes. The cells were heat shocked at 42°C for 90 seconds, 1ml DYT was added and the cells incubated at 37°C for 40 minutes before being plated onto LB agar plates containing ampicillin at 100µg/ml for transformant selection. Plates were then incubated at 37°C overnight. Individual colonies were lifted and transferred aseptically to 10ml of LB containing 100µg/ml ampicillin. The cultures were incubated overnight at 37°C with shaking.

2.2.1.3 α-Complementation

Transformed competent cells which utilised the replacement of the lacZ gene with foreign DNA were selected for on LB ampicillin plates supplemented with the chromogenic substrate X-gal and the inducer IPTG as described in Sambrook *et al.*, (1989).

2.2.1.4 Storage of bacterial cultures

Bacterial cultures were stored indefinitely at -20°C with the addition of 15% (v/v) sterile glycerol, as described in Sambrook *et al.*, (1989).

2.2.1.5 Plasmid DNA preparations

2.2.1.5.1 'Mini'-scale

2.2.1.5.1.1 Standard alkaline lysis method

Small amounts (~10μg) of plasmid DNA were isolated from cultures using a modified alkaline lysis method (Birnboim and Doly, 1979). 1.5ml of an overnight culture was centrifuged for 1 minute, and the supernatant removed. The pellet was resuspended, with mixing, in 100μl of ice-cold GTE and then 200μl of freshly prepared Standard Lysis Buffer was mixed in by repeatedly inverting the tube. The tube was incubated on ice for 5 minutes, before 150μl of chilled Potassium Acetate Solution was added and the tube vortexed. After a further 5 minutes on ice the tube was centrifuged at 12,000*g* for 5 minutes at 4°C and the supernatant preserved. The DNA was then extracted once with phenol:chloroform and precipitated for 15 minutes at -20°C with 2 volumes of ethanol. After a 10 minute centrifugation the pellet was washed with 70% (v/v) ethanol and dried under vacuum. The pellet was then resuspended in TE containing 10μg/ml RNAse A.

2.2.1.5.1.2 Promega "Wizard"™ miniprep method

3ml of an overnight culture were centrifuged in a benchtop microcentrifuge in two microcentrifuge tubes at 10,000*g* for 90 seconds. Each of the pellets was resuspended by vortexing in 100μl of Cell Resuspension Solution (50mM Tris-HCl (pH7.5), 10mM EDTA, 100μg/ml RNAse A) and the two aliquots combined. 200μl of Cell Lysis Solution (0.2M NaOH, 1% (w/v) SDS) were added and the tube's contents mixed by inverting several times. After the addition of 200μl of Neutralisation Solution (1.32M potassium acetate) the tube was again inverted several times and spun at top speed (10,000*g*) in a microcentrifuge for 5 minutes. The clear supernatant was retained and the pellet of bacterial debris discarded.

A Wizard™ Minicolumn was prepared by attaching the barrel of a 3ml syringe to the Minicolumn and 1ml of resuspended Wizard™ Minipreps DNA Purification Resin was added to the Minicolumn/syringe assembly. The clear supernatant was transferred to the barrel of the Minicolumn/syringe assembly and the plunger pushed home gently, after which the syringe was removed from the column and the plunger withdrawn. The syringe barrel was then reattached and 2ml of Column Wash Solution (80mM potassium acetate, 8.3mM Tris-HCl (pH7.5), 40μM EDTA and 55% (v/v) ethanol) was passed through the Minicolumn. The syringe was again removed and the Minicolumn transferred to a clean 1.5ml microcentrifuge tube. The Minicolumn was centrifuged at 10,000*g* in a microcentrifuge for 2 minutes to dry the resin. Plasmid DNA was eluted by adding 50μl of water, waiting 1 minute and then centrifuging at 10,000*g* for 30 seconds.

2.2.1.5.2 'Midi'-scale

2.2.1.5.2.1 Alkaline lysis method

50ml of DYT media containing ampicillin at 100μg/ml was inoculated with 200μl of glycerol stock and incubated with shaking at 37°C overnight. Cells were harvested by centrifugation in a Sorvall SS34 rotor at 3,000*g* for 5 minutes. The pellet was resuspended in 4ml of GTE and the cells lysed with 4ml of fresh Standard Lysis Buffer. The alkali was neutralised by the addition of 4ml of neutralising solution (3M sodium acetate, pH4.8) and the mixture centrifuged in a Sorvall SS34 rotor at 17,400*g* for 5 minutes.

The supernatant was mixed with an equal volume of isopropanol and centrifuged at 17400*g* for 5 minutes. The pellet was resuspended in 500μl of sterile water in a microcentrifuge tube and the alkaline lysis and neutralisation steps repeated using 250μl volumes in order to eliminate any remaining cellular DNA. The pellet obtained after a second isopropanol precipitation was resuspended in 500μl of sterile water and incubated for 5 minutes with an equal volume of 6M LiCl in order to precipitate RNA. After centrifuging at high speed for 2 minutes the DNA in the supernatant was ethanol precipitated (as described in 2.2.2.2) and the subsequent pellet resuspended in 400μl of TE (pH7.8). RNA was digested by the addition of DNAse-free RNAse to a concentration of 100μg/ml and incubation at 37°C for 30 minutes. The reaction was stopped by the addition of 20μl 10% (w/v) SDS and incubation at room temperature with 6M LiCl for 15 minutes and pelleted by centrifugation at high speed. DNA in the supernatant was

ethanol precipitated and the subsequent pellet resuspended in sterile water before extraction of protein once with phenol:chloroform:isoamyl alcohol (25:24:1) and twice with chloroform:isoamyl alcohol (24:1). After a final ethanol precipitation, the DNA pellet was resuspended in 100µl sterile water.

2.2.1.5.2.2 QIAGEN "QIAfilter"™ Midi method

LB containing chloramphenicol (180mg/l) improves yield of low-copy-number plasmids containing the ColE1 origin of replication, such as pMAL-c2, and they can then be treated as high-copy-number plasmids and as such the following procedure was adhered to:

The bacterial pellet was resuspended in 4ml of Resuspension Buffer (50mM Tris-HCl (pH8.0), 10mM EDTA, 100µg/ml RNAse A). 4ml of Lysis Buffer (0.2M NaOH, 1% SDS) was added, the solution was mixed gently and then 4ml of chilled Neutralisation Buffer (3M potassium acetate (pH5.5)) was added. Immediately the tube was mixed gently and the lysate transferred to the barrel of the QIAfilter Midi cartridge where it was incubated at room temperature for 10 minutes. Meanwhile, a QIAGEN-tip 100 was equilibrated by applying 4ml of Equilibration Buffer (0.75M NaCl, 50mM MOPS (pH7.0), 15% (v/v) ethanol, 0.15% (v/v) Triton X-100) and allowing the column to empty by gravity flow. The plunger was inserted into the QIAfilter Midi cartridge and the cell lysate filtered while holding it over the previously equilibrated QIAGEN-tip. The cleared lysate enters the resin by gravitational flow and the QIAGEN-tip washed twice with 10ml Wash Buffer (1M NaCl, 50mM MOPS (pH7.0), 15% (v/v) ethanol). The DNA was eluted with 5ml Elution Buffer (1.25M NaCl, 50mM Tris-HCl (pH8.5), 15% (v/v) ethanol), precipitated with 3.5ml room-temperature isopropanol and centrifuged at 15,000*g* for 30 minutes at 4°C. The supernatant was carefully removed and the DNA was washed with 2ml of 70% (v/v) ethanol, centrifuged at 15,000*g* for 10 minutes and the supernatant again carefully removed. The pellet was air-dried for approximately 5 minutes and then dissolved in a suitable volume of sterile distilled water or TE Buffer.

2.2.1.5.3 'Maxi'-scale

2.2.1.5.3.1 Alkaline lysis method using CsCl and EtBr

This method is a modification of the method of Birnboim and Doly (1979) and is

designed to be used in conjunction with a subsequent purification step such as equilibrium centrifugation in CsCl-ethidium bromide gradients.

From the cells stored at 4°C, 500µl was used to inoculate 500ml LB broth with ampicillin (100µg/ml). The cells were grown overnight, then pelleted by centrifugation at 3,000*g* for 20 minutes at 4°C. The pellet was resuspended in 8ml of GTE. The cells were lysed by adding 16ml Standard Lysis Buffer and then incubated on ice for 10 minutes. The cell debris was precipitated with 5ml Potassium Acetate Solution and then pelleted by centrifuging at 10,000*g* for 30 minutes at 4°C. The supernatant was decanted and kept. Nucleic acids were precipitated from the supernatant with 0.6 volumes of propan-2-ol at room temperature for 10 minutes, then pelleted by centrifugation at 10,000*g* for 10 minutes at room temperature. The vacuum dried pellet was resuspended in 10ml of sterile distilled water and the volume accurately noted. Exactly 1g of CsCl for every 1ml (or part thereof) of DNA solution was added, with 300µl of 10mg/ml Ethidium Bromide (EtBr) and this solution transferred to Beckman heat-sealable tubes. The tubes were balanced to within 10mg, sealed and centrifuged at 340,000*g* for 18 hours.

The lower, supercoiled plasmid band was taken and solvent extracted with amyl-alcohol to remove the EtBr. The aqueous phase was diluted with 1ml sterile distilled water and then the DNA precipitated with 3 volumes ice cold absolute ethanol. The vacuum dried pellet was resuspended in 1ml sterile distilled water, then precipitated with 2ml absolute ethanol plus 100µl 3M sodium acetate (pH5.2). The vacuum dried pellet was resuspended in 1ml sterile distilled water and precipitated as before. This pellet was resuspended in 200µl sterile distilled water.

2.2.1.5.3.2 Alkaline lysis method using LiCl

From the cells at 4°C, 100ml LB broth was inoculated, cells pelleted and resuspended in 4ml GTE as before. The cells were lysed with 8ml Standard Lysis Buffer and incubated on ice for 10 minutes. Cell debris from the lysate was precipitated with 15ml ice-cold Potassium Acetate Solution and the suspension incubated on ice for 15-30 minutes. The suspension was centrifuged at 1,000*g* for 15 minutes at room temperature. The supernatant was filtered through muslin into another tube. Nucleic acids were precipitated by adding 18ml propan-2-ol and incubating on ice for 30 minutes. The nucleic acids were pelleted by centrifugation for 30 minutes as before and the air dried

pellet resuspended in 1ml TE Buffer. The suspension was split between two tubes, 500µl 6M LiCl added to each tube and incubated on ice for 15 minutes. The RNA/protein/salt complex was pelleted at 20,000*g* for 10 minutes at room temperature. The supernatants were split between two tubes and 1ml of -20°C absolute ethanol added to each tube and incubated at -20°C for 30 minutes. The nucleic acids were pelleted by centrifuging for 10 minutes at 20,000*g* at room temperature. The pellets were then washed in 500µl 70% (v/v) ethanol and repelleted by centrifugation as before. The pellets were vacuum dried and combined by resuspension in 400µl TE Buffer. RNA was removed by the addition of 4µl (10mg/ml) RNAse A and incubation at 37°C for 30 minutes. The sample was further incubated with 20µl 10% (w/v) SDS at 75°C for 10 minutes. 420µl 6M LiCl was added and incubated for 15 minutes at room temperature before centrifugation as before. The supernatant was split between two tubes, 1ml absolute ethanol was added to each tube and the tubes incubated on ice for 30 minutes. The DNA was pelleted by centrifugation at 20,000*g* for 30 minutes at room temperature. The pellets were washed in 500µl 70% (v/v) ethanol, then repelleted by centrifugation for 10 minutes at 20,000*g* at room temperature. The pellets were resuspended in 400µl sterile distilled water, then solvent extracted with an equal volume of phenol/chloroform (1:1). This was followed by 2 further equal volume chloroform extractions, then an absolute ethanol precipitation. The pelleted DNA was resuspended in 100µl sterile distilled water and could be used in further procedures.

2.2.2 Techniques used in the purification of DNA

2.2.2.1 Extraction of DNA with phenol:chloroform

Purification of DNA by phenol:chloroform extraction was routinely performed as described in Sambrook *et al.* (1989).

2.2.2.2 Concentration of DNA by ethanol precipitation

DNA was concentrated by precipitation with 0.1 volumes 3M sodium acetate (pH5.2) and 2.5 volumes absolute ethanol at -70°C for 20 minutes or -20°C overnight, centrifuged at high speed for 20 minutes, washed in 70% (v/v) ethanol and resuspended in sterile water.

2.2.2.3 Purification of DNA from agarose gels

Bands of DNA were excised from agarose gels and purified using a GENECLEAN *II*® Kit (Bio101, Inc.) or a Sephaglas BandPrep™ Kit (Pharmacia) as described below.

With Sephaglas, the band of interest was cut out with a clean razor blade and any excess agarose trimmed away. The gel slice was weighed and 250µl (or 1µl for each mg of agarose, whichever is the greater) of gel solubiliser (buffered NaI) added. The agarose was dissolved by incubating the tube at 60°C for 10 minutes. 5µl of Sephaglas BP (20% (w/v) Sephaglas in aqueous solution) was added (or 5µl per estimated µg of DNA present) the contents of the tube mixed by vortexing and incubation continued on the bench for a further 5 minutes with additional periodic vortexing. The Sephaglas was spun down at top speed in a microcentrifuge for 1 minute and the supernatant aspirated. 40µl (or 8x the volume of Sephaglas used) of wash buffer (60% (v/v) ethanol, 20mM Tris-HCl (pH 8.0), 1mM EDTA, 0.1mM NaCl) was added and the pellet resuspended by vortexing. The Sephaglas was again spun down and the supernatant aspirated. This step was repeated twice and the pellet was air dried for 10 minutes.

DNA was eluted by adding a suitable volume of elution buffer (10mM Tris-HCl, 1mM EDTA), not less than half the volume of Sephaglas used, vortexing briefly to resuspend the pellet and incubating at room temperature for 5 minutes. The Sephaglas was spun down again for 1 minute at top speed and the supernatant carefully removed and retained.

With the GENECLEAN *II*® Kit, 0.5 volume of TBE Modifier™ and 4.5 volumes of NaI stock solution were added to a given volume of agarose, excised from a gel, and the tube incubated at 45-55°C until the agarose completely dissolved. To solutions containing 5µg or less of DNA, 5µl of GLASSMILK® suspension were added with an additional 1µl GLASSMILK® being added for each 0.5µg of DNA above 5µg. After addition of the GLASSMILK® suspension to the solution, the tube was mixed and placed on ice for 5 minutes to allow binding of the DNA to the silica matrix, mixing every 1-2 minutes to ensure that the GLASSMILK® stayed suspended. The silica matrix with the bound DNA was next pelleted by centrifugation. The NaI supernatant was removed and discarded and the white pellet washed 3 times with NEW WASH by adding approximately 10-50 volumes of ice-cold NEW WASH to the pellet. Elution of the DNA was achieved by resuspending the washed, white pellet in water and heating to 45-55°C for 2 or 3 minutes. The tube was next centrifuged for about 30 seconds and the

supernatant containing the DNA removed and placed in a new tube.

2.2.2.4 Removal of short fragments of DNA

Fragments of DNA less than 100bp in size, contaminating fragments, glycerol, salts, or enzymes were removed after enzymatic reactions, if necessary, using the QIAGEN QIAquick PCR Purification Kit. 5 volumes of buffer PB were added to the DNA solution and the mixture loaded onto a QIAquick spin column. The column was centrifuged for 2 minutes at 10,000*g* and the eluate discarded. 750µl of buffer PE was loaded onto the column which was centrifuged as before and the eluate again discarded. The last traces of wash buffer were removed by a final spin for 1 minute at 10,000*g*. The purified DNA was eluted from the column by the addition of 30µl of water and incubation for 2 minutes prior to a final spin at 10,000*g* for 2 minutes.

2.2.3 Techniques used in the analysis of DNA

2.2.3.1 Estimation of concentration of DNA

The concentration of nucleic acid was calculated from readings of the absorbance at 260nm on a Perkin Elmer UV/VIS Lambda 11 Spectrometer. For double-stranded DNA, at 260nm, 1OD = 50µg/ml and for single stranded oligonucleotides, at 260nm, 1OD = 20µg/ml (Sambrook *et al.*, 1989). Contamination with protein was calculated using the ratio: absorbance at 260nm / absorbance at 280nm. A ratio of $\geq$ 1.8 was taken to indicate purity.

2.2.3.2 Agarose gel electrophoresis of DNA

Agarose gel electrophoresis was performed as described in Sambrook *et al.* (1989). DNA samples for agarose contained 0.16 volumes of 6x loading buffer. These were loaded onto 1x TBE gels of varying percentage agarose, containing 50ng/ml ethidium bromide. Gels were typically run at $6Vcm^{-1}$ for an hour prior to visualisation under UV illumination. Phage λ DNA cut with the restriction enzyme *Pst* I was used as a size marker. Gels were photographed under UV light using a Polaroid camera with yellow filter and Polaroid 667 black and white ISO 3000/36° film.

2.2.3.3 Sequencing of cloned PCR products

DNA was sequenced using the dideoxynucleotide chain termination method of Sanger *et al.* (1977), using T7 DNA polymerase in a Sequenase™ Version 2.0 DNA Sequencing Kit (United States Biochemical/Amersham). Samples were electrophoresed on a 6% (w/v) acrylamide sequencing gel, for 2-4h at 30mA, 40W. Gels were fixed in 10% (v/v) methanol, 10% (v/v) acetic acid, dried, and exposed to Kodak X-Omat LS™ film at room temperature overnight. A number of clones were sequenced directly on an automated Perkin Elmer ABI PRISM™ 377 DNA Sequencer.

2.2.3.3.1 Preparation of polyacrylamide gels for sequencing

The gels were cast in rigs supplied by Flowgen. Both glass plates were washed in water and polished with 95% (v/v) ethanol. The back plate was laid flat and coated in a mixture of 200µl silane, 25ml absolute ethanol and 1.2ml 10% (v/v) acetic acid. After 5 minutes the plate was rinsed first with water then with ethanol and polished. The front plate was similarly coated in 1% (v/v) dichlorodimethylsilane in 1,1,1, trichloroethane, left for 5 minutes, washed with water and polished with 95% (v/v) ethanol. The gel rig was assembled with 0.2mm spacers and a gel mixture of the required acrylamide concentration was made up, adding 300µl of fresh 16% (w/v) ammonium persulphate (APS) and 30µl of TEMED just before pouring. The gel was poured in a horizontal position and the reverse (flat) face of a 0.2mm thick shark's tooth sequencing comb inserted into the upper edge of the gel. The acrylamide was allowed to set for an hour before the comb was removed and reversed so that the teeth impinged about 1.5mm into the surface of the gel.

The gel rig was mounted vertically in the equipment supplied and the reservoirs filled with 1xTBE. The wells were washed clear of urea and any loose polyacrylamide fragments with a pasteur pipette to prevent interference with the DNA samples. 3µl of each sample was loaded onto the gel which was run at a limiting 45W. The run was terminated after approximately 45 minutes when the first blue dye had reached the bottom of the gel. After the run, the two plates were separated and the back plate with attached gel was fixed with 10% (v/v) methanol, 10% (v/v) acetic acid for 10 minutes then rinsed under a gentle flow of water for a further 10 minutes. After drying in an oven at 90°C the gel was autoradiographed.

2.2.3.3.2 Searching of sequence databases

The databases were searched using the specified sequence and GCG Tfasta program (Devereux *et. al.* 1984). The Tfasta method compares the specified amino acid sequence with the products of all six reading frames of the query nucleic acid sequence, using the method of Pearson and Lipman (1988).

2.2.4 Techniques used in the manipulation of DNA

2.2.4.1 Restriction digests of plasmid DNA

The restriction digest was performed generally in a total volume of not greater than 50µl. Plasmid DNA (up to 1µg) in sterile water, 0.1 volumes of the appropriate 10x reaction buffer and 1Unit/(µg DNA) of the relevant restriction enzyme were mixed gently and incubated under optimal conditions of time and temperature (generally 37°C overnight). If necessary, 0.01 volumes of 100x BSA (10mg/ml) were also added to the digest. The digest was stopped by the addition of EDTA to 5mM and/or heat inactivation of the restriction enzyme (generally 75°C for 20 minutes). When using thermostable enzymes an additional QIAquick purification step was used instead.

DNA needing double digestion under incompatible conditions was digested with one restriction enzyme, the restriction enzyme inactivated, the DNA ethanol precipitated and then re-digested with the second restriction enzyme. In some cases, usually where an enzyme was thermostable, a QIAquick purification step was used after the first digest and the purified DNA digested with the second restriction enzyme.

2.2.4.2 Ligations

Ligations were performed with varying vector:insert ratios (generally a 3-fold molar excess of vector, a 3-fold molar excess of insert and equal amounts of vector and insert). Two vector only controls were included, one without ligase. An optimal amount of vector (250ng), the corresponding amount of insert, 0.2 volumes 5x T4 DNA Ligase buffer and 5Units T4 DNA Ligase were mixed in a minimal volume, generally 20µl.

Blunt end ligations were incubated at room temperature overnight whereas sticky end ligations were incubated at 16°C overnight. Ligations were diluted 5-fold in sterile water

before adding to competent cells.

2.2.4.3 The polymerase chain reaction (PCR)

PCR amplification of DNA fragments was performed using oligonucleotide primers designed to specific sequences within the desired regions. Four different PCR methods were employed: Promega *Taq* polymerase, Vent DNA Polymerase and Expand Long Template and Expand High Fidelity as detailed below.

PCR was performed in a 100µl total volume, containing 0.1 volumes 10x *Taq* DNA Polymerase buffer, 1.5-4mM $MgCl_2$, 0.2mM dNTPs, 1µM each primer and approximately 100ng DNA template. If necessary, magnesium titrations were performed, in which the concentration of Mg^{2+} was varied from 1 to 4mM, in order to achieve the optimal amount of specific product. The reaction mix was overlaid with sterile mineral oil in a 0.5ml microcentrifuge tube.

Using a PTC-100™ from MJ Research, Inc., the template was fully denatured at 95-96°C for 5 minutes (a hotstart reaction). 2.5Units *Taq* DNA Polymerase (Promega) was added and generally 30-40 cycles of denaturation at 95°C for 1 minute, annealing at 37-65°C for 1 minute, and extension at 72°C for 1 minute commenced. The cycles were followed by a final extension of 72°C for 5 minutes. Exact conditions were dependent on the annealing temperature and GC content of the primer pairs (see calculation of annealing temperature in Appendix 2, part d) and the length of the template, and are given in figure legends.

In some cases, the proof reading enzyme, $Vent_R$® DNA Polymerase (New England Biolabs) was used. Conditions were similar but used a different 10x reaction buffer. Again exact conditions are listed in figure legends.

PCR amplifications using Expand™ Long Template and Expand™ High Fidelity PCR kits (Boehringer Mannheim) were also undertaken.

Template DNA (250ng), 0.1 volumes of 10x reaction buffer (0.5M Tris-HCl (pH9.2 @ 25°C), 0.16M $(NH_4)_2SO_4$, 17.5mM $MgCl_2$), 0.35mM dNTPs, 0.3µM sense primer and 0.3µM antisense primer and 2.5Units Expand™ Long Template were incubated at 94°C

for 2 minutes and then subjected to 30 cycles of 94°C for 30 seconds, 50-65°C for 30 seconds and 68°C for 2 minutes. Any PCR products were subjected to an extension of 68°C for 5 minutes.

In preliminary experiments with the Expand High Fidelity PCR kit, reactions involved mixing 0.1 volumes of 10x buffer (0.5M Tris-HCl (pH9.2 @ 25°C), 0.16M $(NH_4)_2SO_4$, 15mM $MgCl_2$), 0.2mM dNTPs, 0.3μM sense primer, 0.3μM antisense primer, 2.6Units Expand High Fidelity PCR System enzyme mix, and template DNA (100ng) in a thin-walled tube and subjecting it to the following cycles: denaturation at 94°C for 2 minutes, 10 cycles of denaturation at 94°C for 30 seconds, annealing at 55°C for 30 seconds and elongation at 72°C for 2 minutes, followed by 20 cycles of the same conditions but with an extra 20 seconds for each elongation step of each cycle. Any PCR products were subjected to a final extension of 72°C for 5 minutes. Exact optimal conditions, however, for each primer pair are listed in figure legends.

2.2.4.4 Subcloning PCR products

PCR products were analysed on 1-3% agarose gels and bands of the predicted size were excised and purified with Sephaglas or GENECLEAN. Primers incorporating unique restriction sites resulted in PCR products that were digested with the appropriate restriction enzyme, re-purified and ligated into a suitable digested vector, either pMAL-c2, pBluescript™ or pMEX8.

PCR primers that did not incorporate restriction sites resulted in PCR products that were phosphorylated and ligated into a blunt ended, dephosphorylated vector as products generated using *Taq* DNA polymerase have a 5' A overhang due to the terminal transferase activity of this enzyme. The purified, amplified DNA was simultaneously blunt-ended and phosphorylated with the addition of 0.1 volumes of Pharmacia's 10x One-Phor-All buffer PLUS (0.1M Tris-acetate (pH7.5), 0.1M magnesium acetate, 0.5M potassium acetate), DNA Polymerase I (5Units), T4 Polynucleotide Kinase (10Units) and 0.5mM ATP and incubated for 3 minutes at room temperature before 0.2mM dNTPs were introduced. The reaction mixture was incubated at 37°C for 30 minutes, after which time the reaction was terminated by the addition of EDTA to a final concentration of 50mM. The DNA was extracted once with an equal volume of phenol:chloroform:isoamyl alcohol (25:24:1) and once with an equal volume of

chloroform:isoamyl alcohol (24:1). The DNA was ethanol precipitated and resuspended in sterile water.

1-5μg vector (pBluescript) was digested with EcoRV at 37°C for 2 hours. Following heat inactivation of the enzyme at 75°C for 20 minutes, the linearised vector was dephosphorylated with 6μl CIAP (10Unit/μl) in CIAP buffer with incubation at 37°C for 1 hour. The enzyme was inactivated with EDTA to 5mM and heat to 75°C for 10 minutes. The DNA was extracted once with an equal volume of phenol:chloroform:isoamyl alcohol (25:24:1) and once with an equal volume of chloroform:isoamyl alcohol (24:1), ethanol precipitated and resuspended in sterile water.

Both insert and vector were run out on a 1% agarose gel, and the quantity of each estimated before ligation. Vector and insert were mixed in varying ratios as described under Ligations (2.2.4.2).

2.2.5 Techniques used in protein analysis

2.2.5.1 Estimation of protein concentration

Protein concentration was estimated by the method of Bradford (1976) using a kit from Bio-Rad and a standard curve prepared from dilutions of bovine serum albumin.

Alternatively 0.2ml of dye reagent (a solution of 0.06% (w/v) Coomassie Brilliant Blue G250 in 0.3M perchloric acid, filtered through Whatman No1) was added to 0.8ml of samples containing 1-20μg protein. Samples were left to stand for 5-30 minutes then absorbance at 595nm was measured against a blank prepared from 0.8ml of sample buffer and 0.2ml dye reagent.

2.2.5.2 Sodium dodecyl sulphate polyacrylamide gel electrophoresis

2.2.5.2.1 Preparation of samples

Protein samples were mixed with Sodium Dodecyl Sulphate Polyacrylamide Gel Electrophoresis (SDS-PAGE) Sample Buffer, boiled for 5 minutes and allowed to cool before analysis by SDS-PAGE and Western blotting.

The concentrated GTP-affinity column eluate and crude sample were diluted 1:1 in SDS-PAGE Sample Buffer.

2.2.5.2.2 Preparation and running of polyacrylamide gels

This method of analysis was performed initially using the discontinuous buffer system of Laemmli (1970):

Samples were electrophoresed through a large polyacrylamide gel consisting of a 12% (w/v) resolving gel and a 6% (w/v) stacking gel comprised of the components listed in Table 5, using Tank Buffer, at a current of 40-65mA/gel using a Protean II (Bio-Rad) gel-rig. In both cases polymerisation was achieved by the use of ammonium persulphate (APS) and N,N,N′,N-tetramethylethylenediamene (TEMED).

Table 5: Composition of 12% SDS-PAGE gels

	RESOLVING GEL (ml)	STACKING GEL (ml)
30% (w/v) Acrylamide	20	1.8
Resolving Gel Buffer	12	-
Stacking Gel Buffer	-	7.2
ddH_2O	16	7.2
10% (w/v) APS	0.2	0.1
TEMED	0.05	0.01

(volumes shown are sufficient for one large gel)

Molecular weight markers, sometimes pre-stained (Bio-Rad) were used according to the manufacturer's instructions.

Small 1mm thick 12% SDS-PAGE mini-gels (Gradipore) were used for the non-discontinuous, rapid analysis of partially-purified protein eluted from the GTP-agarose affinity column. 20µl of sample prepared using the method described were loaded onto the mini-gel and electrophoresed at 20-40mA for approximately 1¼ hours. The production of these gels was later discontinued.

Later SDS-PAGE analysis employed the Atto™ Mini gel system and a series of buffers A-D. The gels in this system proved more manageable than the larger gels.

Similarly, resolving gels for this mini system were made by mixing the components listed

in Table 6 and they were poured into an "Atto™" minigel rig. Gels were overlaid with water-saturated butan-1-ol and allowed to set for 20 minutes. The butan-1-ol layer was discarded and the comb inserted between the gel plates. 5% stacking gels were made by combining the necessary components, again listed in Table 6. This was poured onto the resolving gel and allowed to set for a further 40 minutes. 10µl of sample was loaded into each well and gels were run in tank buffer at 175V for 90 minutes.

Table 6: Composition of 10% SDS-PAGE gel

	RESOLVING GEL (ml)	STACKING GEL (ml)
Solution A	6	0.9
Solution B	4.5	-
Solution C	-	1.5
Solution D	0.08	0.01
TEMED	0.01	0.01
Water	7.5	3.6

(volumes shown are sufficient for two mini-gels)

2.2.5.3 Coomassie stain of polyacrylamide gels

Following electrophoresis the gel was stained for 1 hour at room temperature in Coomassie Blue Stain and then destained in several changes of fix until the background colour was removed.

2.2.5.4 Western transfer to nitrocellulose membranes

The method used for Western blotting has been adapted from the method used by Towbin *et al.* (1979). Protein samples were subjected to SDS-PAGE as described, using pre-stained molecular weight markers.

The graphite plates of a Pharmacia LKB NovaBlot Multiphor II electroblotter were rinsed in water. Six gel-sized pieces of Whatmann 3MM filter paper were soaked in Transfer Buffer and individually stacked onto the bottom plate, carefully eliminating any air bubbles formed, using a glass rod. Nitrocellulose paper presoaked in transfer buffer was placed on top of this and then the SDS gel was added to the stack. The sandwich was completed with a further six pieces of pre-soaked filter paper and the electroblotter was then run with the cathode at the base at $0.8mA.cm^{-1}$ for 1¼ hours. Transfer efficiency was assessed by staining the gel with Coomassie Blue Stain at room temperature overnight followed by 8 hours in destain solution.

2.2.5.5 Immunodetection of bound HAV proteins

Protein bands on the nitrocellulose were visualised by staining with Ponceau-S, marked with pencil or waterproof ink, and destained by washing with distilled water prior to probing with antibodies.

Detection was performed using the horseradish peroxidase chemiluminescent detection method which exploits indirect immunodetection with a peroxidase conjugated secondary serum. Detection relies on the oxidative action of peroxide on luminol, a cyclic diacylhydrazide, the activated oxidised form of luminol decays back to its ground state with the concomitant emission of light. The ECL kit was used which also contains enhancers such as phenols, in the presence of which, both the intensity and duration of the chemiluminescent reaction are enhanced.

Western blots were incubated in Blocking Buffer at room temperature on a shaking table for 1-2 hours, frequently overnight. The blots were incubated with shaking for 2 hours at 4°C in primary antiserum diluted 1:1000 in Blocking Buffer. All subsequent steps were carried out at room temperature on a shaking table unless stated otherwise. The membranes were washed three times in 100ml PBS for 10 minutes each and then transferred to a tray containing Washing Buffer and incubated for 10 minutes. The membranes were incubated for 1 hour with the enzyme-coupled secondary reagent diluted 1:2000 in Phosphate-Free, Azide-Free Blocking Buffer. Unbound secondary serum was removed by washing 3 times with 10 minute washes in Washing Buffer as before.

3ml of each of the detection reagents were combined and poured onto the drained membranes. The luminescence reaction was allowed to proceed for 1 minute, before draining off excess solution, wrapping the filter in Saranwrap™ and autoradiography. A series of exposures were taken, starting with 1 minute and increasing or decreasing this time as required.

2.2.6 Techniques used in protein expression

2.2.6.1 Expression of 3D polypeptide in JRR constructs

10µl aliquots of glycerol stock cultures were used to inoculate 10ml LB containing the appropriate antibiotics. The overnight cultures were incubated with shaking at approximately 32°C. 1ml of overnight culture was used to inoculate 10ml LB-Glucose

and incubated overnight at 32°C. 1ml of overnight LB-Glucose culture was used to inoculate 50ml LB-Glucose and incubation was continued for a further 4 hours. Aliquots for analysis were removed at this stage. Cells were pelleted and washed twice with 50ml of 50mM NaCl solution before being resuspended in LB-Expression. The cultures were incubated at 32°C overnight for 15 hours. Aliquots were removed 2 hours after induction and after overnight induction for analysis.

2.2.6.2 Intracellular extraction of the 3D polypeptide

1ml aliquots removed from the expression medium were pelleted in a microcentrifuge. The supernatant was removed by aspiration and the cells resuspended in IC Resuspension Buffer. These samples were lysed by sonication (4x 30 seconds) and were observed to clarify. The lysate was spun in a microcentrifuge to sediment insoluble material and the supernatants predicted to contain the RNA-dependent RNA polymerase were removed for analysis.

2.2.6.3 Periplasmic space extraction of the 3D protein

10ml samples were removed from the overnight cultures and the cells pelleted by centrifugation in a Sorvall SS-34 rotor at 2,500*g* at 4°C for 10 minutes. The pellet was resuspended in 2.5ml of PS Resuspension Buffer, allowed to stand at room temperature for 10 minutes and re-pelleted. Periplasmic extracts were prepared by osmotic shock in 2.5ml of ice-cold 0.5mM $MgCl_2$, allowing to stand on ice for a further 10 minutes. Finally the extract was centrifuged at 12,000*g* for 10 minutes and the supernatants removed for analysis.

2.2.6.4 Expression of HAV proteins from pMAL constructs

Pilot experiments to identify the optimal conditions for expression of each protein were undertaken by inoculating 80ml of Rich Broth (containing 100μg/ml ampicillin) with 0.8ml of an overnight culture of XL2s transformed with pMAL/3AB, pMAL/3C, pMAL/3CD, pMAL/3D or pMAL/P3. The culture was incubated at between 30 and 37°C, depending on the construct, with shaking to an A_{600} of ~0.5 (approximately 3½ hours). 1ml of culture was taken and centrifuged at maximum speed in a microcentrifuge tube for 2

minutes. The supernatant was discarded and the pellet resuspended in 100µl of SDS-PAGE sample buffer prior to storage at -20°C.

IPTG was added to the remainder of the culture to a final concentration of 0.3mM and the culture incubated for between 2 and 15 hours depending on the individual construct. A 0.5ml sample of induced culture was taken at various time points and processed as above.

Large-scale expression experiments were set up by inoculating 1L cultures of Rich Medium, containing ampicillin at 100µg/ml, with 10ml of overnight culture of the required plasmid construct.

2.2.7 Techniques used in protein purification

2.2.7.1 GTP-Agarose affinity chromatography

The following procedure was carried out at 4°C using a method based on that of Richards *et al.* (1992) in the purification of poliovirus RNA polymerase.

A 1ml GTP-agarose column was packed and washed thoroughly in equilibration buffer to remove all traces of glycerol. A 10ml sample of periplasmic space extract was dialysed overnight against equilibration buffer and filtered prior to loading the column. 5ml of the solution was loaded onto the column at a rate of 0.1-0.2ml/min and the column was washed with 2ml equilibration buffer. Bound protein was eluted with 2ml elution buffer and fractions of 0.5ml were collected. The column was re-equilibrated with 2ml equilibration buffer.

The procedure was scaled-up by packing a 5ml GTP-agarose column and purifying the protein from approximately 25ml of dialysed, filtered periplasmic space extract.

Protein-containing fractions eluted from the affinity column were concentrated approximately 20 times on Filtron 10 centrifugation filter units and analysed as described above.

2.2.7.2 Amylose affinity chromatography

1L of culture, containing the desired construct, induced for the appropriate time was harvested by centrifugation at 4,000*g* for 20 minutes and the supernatant discarded. The pellet of cells was resuspended in 50ml column buffer. This suspension was frozen overnight at -20°C and then thawed in cold water. The sample was placed in an ice-water bath and sonicated in short pulses of 15 seconds or less. The release of protein was monitored using the Bradford assay, by adding 10µl of the sonicate to 1.5ml Bradford reagent and mixing. Absorbance at 595nm was measured. Sonication was continued until the released protein reached a maximum (usually about 2 minutes sonication time). The suspension was then centrifuged at 9,000*g* for 30 minutes. The supernatant (crude extract) was saved and diluted if necessary to 2.5mg/ml with column buffer. 15ml of amylose resin (New England Biolabs) was poured in a 2.5x10cm column. The column was washed with 8 column volumes of Column Buffer. The diluted crude extract was loaded at a flow rate of [10x (diameter of column in cm)^2]ml/h. This is about 1ml/min for a 2.5cm column. The column was washed with 10-12 column volumes of Column Buffer. The fusion protein bound to the amylose was eluted with Column Buffer +10mM maltose. 10-20 fractions of 0.2 column volumes were collected. The protein-containing fractions were identified by Bradford assay and pooled and, if necessary, concentrated to about 1mg/ml in a Centriprep™ concentrator (Amicon).

2.2.7.3 Cleavage of fusion proteins with Factor Xa

Factor Xa cleavage was carried out at a w/w ratio of 1% the amount of fusion protein (e.g., 1mg factor Xa for a reaction containing 100mg fusion protein). A factor Xa cleavage pilot experiment was set up by mixing 20µl fusion protein (1mg/ml) with 0.2µg factor Xa and incubated at room temperature. 5µl samples taken at 2, 4, 8, and 24 hour intervals were mixed with 5µl 2x SDS-PAGE sample buffer and stored at 4°C. A mock fusion control and an uncut fusion control were included. The samples were boiled for 5 minutes and run on an SDS-PAGE gel. The pilot experiment was scaled up for the portion of fusion protein to be cleaved. Complete cleavage was ascertained by SDS-PAGE analysis.

2.2.7.4 Q-sepharose ion-exchange chromatography

Ion exchange chromatography was performed on a fast protein liquid chromatography

(F.P.L.C.) system (Pharmacia LKB, Sweden).

A 1ml Mono-Q (anionic exchange) column was equilibrated with Column Equilibration Buffer and left running until a level baseline was obtained. The fusion protein cleavage mixture, dialysed against Buffer A overnight, was loaded onto the equilibrated column at a flow rate of 0.5ml/min. After unbound material had washed through the column (4-10 volumes of Buffer A), bound material was eluted with a linear NaCl gradient, 20mM-0.5M (Buffer A-Buffer B) over 40ml, at a flow rate of 0.5ml/min. Fractions of 1ml were collected. Any A_{280} peaks were concentrated using Centricon concentrators, checked by SDS-PAGE analysis, and the desired protein frozen by beading in liquid nitrogen and stored subsequently at -70°C.

2.2.8 Assay for poly(A):poly(U)-dependent poly(U) polymerase activity

The assay was carried out essentially as described by Flanegan & Baltimore (1977) except for the removal of phospho*enol*pyruvic acid and pyruvate kinase from the reaction mixture and replacement of actinomycin D with rifampicin to inhibit *E. coli* RNA polymerase.

50µl (the amount assayed depended on the concentration of protein in the preparation, generally between 5 and 50µl) of cell lysate supernatant, MBP-fusion protein, fusion protein cleavage mixture or purified protein were assayed in a total volume of 125µl containing 50mM Hepes buffer (N-2-hydroxyethylpiperazine-N'-ethanesulphonic acid) (ph7.4), 8mM $Mg(CH_3COO)_2$, 1.7µM [5,6-^{3}H] UTP (10µCi per reaction), 20µg/ml poly(A):poly(U) template, 74Units RNA-guard, 4mM DTT, 20µg/ml rifampicin and RNAse-free ddH_2O.

Assays were carried out at 31°C. 20µl aliquots were removed from the reaction mixture at various time intervals and precipitated for 10 minutes in 60µl ice-cold 8% (w/v)TCA to which had been added 400µg yeast carrier tRNA. The acid-insoluble material was collected on GF/C filters (Whatman) by filtration and the radioactivity solubilised in 5ml "Optiphase" scintillation fluid before being counted on a Packard Tricarb 1500 liquid scintillation counter.

Aliquots were precipitated at 0, ½, 2, 5, 10 and 15 minute intervals and incorporated radioactivity assessed as above.

2.2.9 Oligonucleotides

2.2.9.1 In house synthesis and deprotection of oligonucleotides

Oligonucleotides were synthesised in house, using the phosphoramidite method, on an Applied Biosystems 381A DNA Synthesiser using chemicals supplied by Cruachem, Glasgow, UK. Oligonucleotides were deprotected with ammonia solution of Analar grade at 55°C for 6 hours. The ammonia was neutralised with glacial acetic acid and the oligonucleotide precipitated with absolute ethanol. The precipitated oligonucleotide was spun, washed, dried and resuspended in 1ml sterile water. The absorbance at 260nm was taken and the oligonucleotide diluted to a working stock solution of 20μM.

Other oligonucleotides, purchased from Perkin-Elmer, were used with the Expand™ kits at the required concentration.

2.2.9.2 Radiolabelling of oligonucleotides

Oligonucleotides at 2μM were radiolabelled with 5μCi [γ-^{32}P]ATP (specific activity 3000Ci/mmol; 10mCi/ml) and 10Units T4 Polynucleotide Kinase in 0.1 volumes of 10x buffer at 37°C for 30 minutes. The enzyme was inactivated with EDTA (pH8.0) to 5mM and 1 volume of sequencing stop dye (95% (v/v) formamide, 20mM EDTA, 0.05% (w/v) xylene cyanol FF) was added. The radiolabelled oligonucleotide was heated at 80°C for 3 minutes and electrophoresed on a 12% (w/v) acrylamide sequencing gel for 1 hour at 30mA, 40W. The gel was immediately exposed to Kodak X-Omat LS™ film at room temperature for 15-30 minutes.

3. Detection and purification of HAV $3D^{pol}$ in Protein A/HAV P3/pMEX8 and pRITPOL constructs

3.1 Introduction

The first report of an HAV specific polymerase activity was by Wolstenholme *et al.* (1993) where the HAV $3D^{pol}$ was expressed in an *E. coli* vector carrying the protein A gene fused to most of the P3 region of the genome. The purpose of the Staphylococcal protein A was to maintain soluble viral proteins which would be correctly post-translationally cleaved and hence, conserve enzyme activity. *E. coli* transformed with this plasmid exhibited poly (U) polymerase activity in the periplasmic space. This was found to be similar to that of other picornaviruses in that it was primer-dependent, with a requirement for magnesium, inhibition with manganese and an optimum temperature of 30°C. However, the activity measured was much lower than reported for other picornavirus enzymes and attempts by other workers to express this enzyme in bacteria, or anywhere else for that matter, have been unsuccessful (Gauss-Müller *et al.*, 1991; Jia *et al.*, 1991a; Updike *et al.*, 1991; Harmon *et al.*, 1992; Tesar *et al.*, 1994). Prior attempts at expressing this enzyme in the baculovirus expression system in this laboratory proved unsuccessful (Nutter, 1992).

With the ultimate aim of this project being the biochemical characterisation of the HAV polymerase, a necessary first step was the production of highly purified protein. This would also allow the identification of the protein species that is responsible for the poly(U) polymerase activity detected previously in the periplasmic space of bacteria transformed with pRITPOL and Protein A/HAV P3/pMEX8. A number of strategies have been described for the purification of picornaviral polymerases, but the most rapid approach is based on affinity chromatography using GTP-agarose, poly(A)-Sepharose or a similar matrix. By applying a suitable ammonium sulphate cut to such a matrix and eluting with increasing concentrations of ATP the eluted fractions can be monitored for poly(U) polymerase activity. Previously, preliminary experiments (Palmer, 1994) indicated that HAV-specific polypeptides from the periplasmic space of *E. coli* transformed with pRITPOL or Protein A/HAV P3/pMEX8 will bind to GTP-agarose and can be eluted with ATP, but at the commencement of this project it was uncertain whether these polypeptides were responsible for the poly(U)-polymerase activity detected.

3.1.1 Protein purification

Before embarking on the purification of a protein, however, a few key questions must

first be addressed. Thus: what is the protein required for? Which would be the most suitable source? What is known about the protein? How should the protein be assayed? By answering these questions the aims of the purification and criteria for success were defined, and the background knowledge required to plan a suitable strategy was acquired.

3.1.1.1 What is the protein required for?

The purification of a protein is frequently not the end point itself, but is the means to obtain a pure protein for further studies. These studies may be on the activity of the protein, on its structure, or on its structure-function relationships. The requirements of these studies will define how much of the purified protein is required, whether loss of activity can be tolerated, how pure it should be, and the time and cost of purifying it. Thus, for studies on enzyme activity relatively small amounts of active protein will be required. High purity will probably not be essential provided any interfering activities are removed. Cost will probably not be very important, but speed will be important to minimize activity losses. In contrast, structural studies require larger amounts of highly pure protein. Cost and time will be of secondary importance, except for structure-function studies where activity is required and therefore speed will probably be important. Here, the protein was required eventually for activity assays and as such only small amounts of relatively pure protein were required.

3.1.1.2 What source should be used?

With the advent of gene cloning techniques proteins can now be expressed in high amounts in cells which can be grown in culture. In addition to the above-mentioned advantages the percentage of the protein of interest is usually higher than in its native source, thus making purification easier. The host cell should be chosen with care since each has its advantages and disadvantages. *E. coli* is the most commonly used host due to ease of handling, however, proteins are often not secreted, and in addition are often produced in an insoluble form (known as inclusion bodies). Secreted proteins are usually easier to purify since there are fewer contaminating proteins present. Inclusion bodies can be relatively easily purified and consist mainly of expressed protein, however the protein must be denatured and refolded to obtain a soluble, active form. With this information in mind, the constructs directing expressed proteins to the periplasmic space were employed in the first instance especially with regard to the affinity chromatography

steps.

Cloned proteins can also be modified to ease purification. Thus, a basic tail may be added to aid purification by ion-exchange chromatography, or part of another protein may be added and exploited for affinity purification. After purification, the foreign part of the protein is removed by chemical or enzymatic cleavage. The pMAL protein purification system, discussed fully in Chapter 4, is an example of this, where fusion proteins bound to maltose-binding protein (MBP) are produced.

3.1.1.3 What do we know about the protein?

The RNA polymerase activity encoded by the hepatitis A virus is crucial for replication but so far, it has not been identified *in vitro* for HAV due to the inefficiency of this process. Previously the 3D region from several picornaviruses have been expressed in *E. coli* and the RNA-dependent RNA polymerase activity has been shown to be contained within the 3D protein sequence (Flanegan & Baltimore, 1977; Lowe & Brown, 1981; Morrow *et al.*, 1987; Plotch *et al.*, 1989; Sankar & Porter, 1991; Newman *et al.*, 1994). Of some concern was whether enzyme produced by expression of cDNAs in bacterial cells would be structurally and functionally identical to enzyme synthesized in the natural mammalian host cell. Neufeld *et al.* (1991) have shown that PV enzyme preparations from bacteria, insect, or mammalian cells are indistinguishable by all measured criteria, and this research validates the use of these proteins for additional mechanism and structure studies. It was therefore reasonable to assume that the same would be true of the HAV enzyme.

3.1.1.4 How can the protein be assayed?

Assays devised for the investigation of polymerase activity in other picornaviruses (Flanegan & Baltimore, 1977; Sankar & Porter, 1991) were used as the basis for an assay developed by Palmer (1994) which was used in this research and is discussed further in Chapter 5.

3.2 Results

3.2.1 Expression of P3 proteins in E. coli

Proteins expressed by the following constructs were extracted from the cytosol or periplasmic space as described in Chapter 2. Presence of protein was assessed using method 2.2.5.1 in order to ensure the extraction process was correct and/or complete, prior to SDS-PAGE. Controls, JRR-600, pMEX8 and pRIT5 were run at the same time. Generally two gels were run simultaneously. One was stained with Coomassie Blue; the other Western blotted, probed with an anti-3D peptide antibody and visualised using an ECL kit. Once transferred the nitrocellulose was stained with Ponceau-S and the location of lanes and any visible bands was marked before destaining and probing with antibody.

Table 7: Expression plasmids

PLASMID CONSTRUCT	PROTEINS EXPRESSED WHERE?
Protein A/HAV P3/pMEX8 in JRR-600	Periplasmic expression
HAV P3/pMEX8 in JRR-600	Intracellular expression
PMEX8 in JRR-600 (control)	Intracellular expression
pRITPOL in JRR-600	Periplasmic expression
pRIT5 in JRR-600 (control)	Periplasmic expression

Induction of *E. coli* cultures transformed with the recombinant plasmids produced a number of novel, HAV-specific proteins which were visualised by Western blotting using the polyclonal rabbit α-3D peptide antibody. These proteins had apparent molecular weights of 36kDa, 53kDa, 77kDa, and 117kDa. The Western blot is shown in Figure 27, however the corresponding Coomassie-stained gel is not shown. Predicted sizes for the P3 proteins are 36kDa (Protein A-3A), 2.5kDa (3B), 24kDa (3C) and 53kDa (3D), as shown in Table 8, along with simplified tabulated results of initial expression studies.

Table 8: Summary of results observed for initial expression experiment

HAV P3 PROTEINS EXPECTED	PREDICTED SIZE (kDa)	PROTEIN A/ HAV P3/ pMEX8	HAVP3/pMEX8	pMEX8	pRITPOL
Protein A-3ABCD	117	✓	✓?	✗	✗
3CD	77	✓	✓	✗	✓
3D	53	✓	✓	✗	✓
Protein A-3A	36	✓	✗	✗	✓

A clear band of approximately 117kDa, likely to correspond to Protein A-3ABCD can be seen in the lane containing Protein A/HAV P3/pMEX8 induced overnight, as would be expected, however, no such band is observed with pRITPOL, lanes 5 and 6, as we would expect. Surprisingly lane 2, containing HAV P3/pMEX8, displays a band of ~117kDa however, with the absence of Protein A sequences in this construct, this band cannot correspond to Protein A-3ABCD, in this case anyway.

The next band of interest is ~77kDa, thought to correspond to 3CD, and appears in the lanes containing HAV P3/pMEX8 and Protein A/ HAV P3/pMEX8. No distinct band can be seen at this molecular weight in the lanes containing pRITPOL but a darker smear possibly indicates its presence.

Bands of 53kDa can be observed in lanes containing each of the three constructs with Protein A/HAV P3/pMEX8 and HAV P3/pMEX8 appearing as the more successful constructs. Lanes containing pRITPOL show the presence of a 53kDa protein but the banding is not so well defined. Finally, a 36kDa protein, thought to be Protein A-3A, can be seen in lanes 3 and 6, as would be expected of the constructs pRITPOL and Protein A/HAV P3/pMEX8 containing protein A sequences. This polypeptide is not observed in the lane containing HAV P3/pMEX8 nor in the pMEX8 control lane.

Interestingly, a large amount of protein expresses at about 32kDa in lanes containing induced Protein A/HAV P3/pMEX8 and pRITPOL and could correspond to protein ABC, a remarkably stable processing intermediate whose specific role is unknown (Schultheiß *et al.*, 1994), however such a cleavage, between Protein A sequences and 3A is unlikely in these constructs nor is it likely that an antibody raised against the C-terminus of 3D would react with this polypeptide. It is possible that the protein A sequences or some

part thereof, in these constructs, could be responsible for this observation.

As well as the proteins of interest a great number of other bands can be seen in Figure 27, demonstrating the need for further purification.

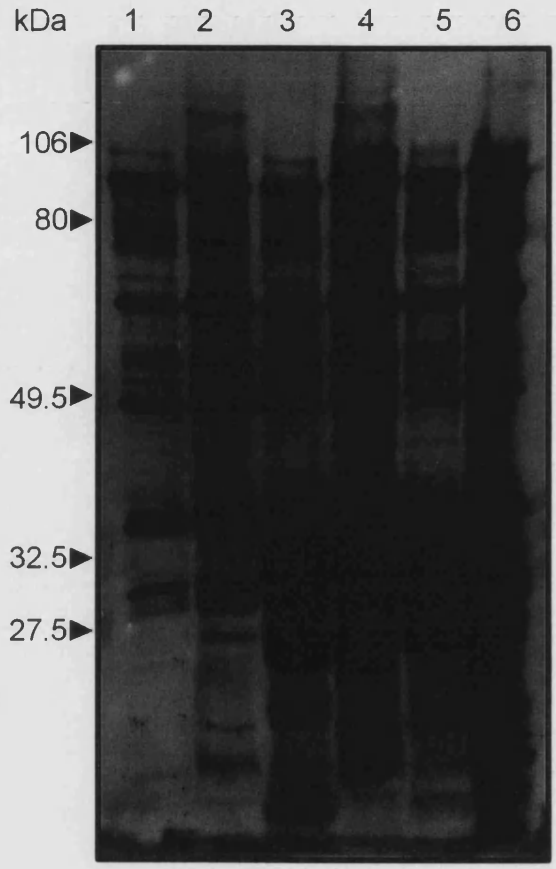

Figure 27: Initial expression studies of P3 proteins in *E. coli*

This figure shows a Western blot of a 12% SDS-PAGE gel (Coomassie-stained - not shown) probed with polyclonal rabbit peptide anti-HAV $3D^{pol}$ antibody and visualised using a light reaction - exposed for 15 seconds.

Lane 1: pMEX8 induced for 2h (control)
Lane 2: HAV P3/pMEX8 incduced overnight
Lane 3: Protein A/HAV P3/pMEX8 induced 2h
Lane 4: Protein A/HAV P3/pMEX8 induced overnight
Lane 5: pRITPOL expressed 2h
Lane 6: pRITPOL expressed overnight

3.2.2 Initial GTP-agarose affinity studies

Attempts were subsequently made to purify 3D RNA polymerase from *E. coli* transformed with the plasmid constructs detailed in Table 7, using its nucleotide binding properties with the help of GTP-agarose. Pilot experiments were first carried out, which coincidentally allowed better visualisation of the proteins present in whole cell extracts and allowed further investigation into the suitability of GTP-agarose affinity chromatography as a method for purification of the $3D^{pol}$ (Palmer, 1994). Initial gels of whole-cell lysate samples appeared smeared and, hence, a series of gels were subsequently run with whole cell, crude extract, and insoluble extract samples, as well as crude extract and insoluble extract bound batch-wise to GTP-agarose samples, in an attempt to clarify the protein bands present from induction of the available constructs, prior to GTP-agarose affinity column chromatography. Western blots probed with anti 3D-peptide antibody, yielded clearer results than their corresponding Coomassie-stained gels and hence more attention is paid to these results.

Table 9: Summary of proteins induced by pMEX8 constructs

HAV P3 PROTEINS EXPECTED	PREDICTED SIZE (kDa)	HAV P3/pMEX8			PROTEIN A/ HAV P3/pMEX8			pMEX8		
		PROTEINS	IMMUNOREACTIVE PROTEINS	SOLUBLE GTP-BINDING PROTEINS	PROTEINS	IMMUNOREACTIVE PROTEINS	SOLUBLE GTP-BINDING PROTEINS	PROTEINS	IMMUNOREACTIVE PROTEINS	SOLUBLE GTP-BINDING PROTEINS
Protein A-3ABCD	117	✓?	×?	×?	?	✓	×	×	×	×
3CD	77	✓	✓	✓	✓	✓	✓	✓?	×	×
3D	53	✓	✓	✓	✓	✓	✓	✓?	✓?	×
Protein A-3A	36	✓	✓	✓	✓?	✓	×?	✓?	×	×

With Protein A/HAV P3/pMEX8, a number of novel bands were observed by Coomassie-staining of the SDS-PAGE gel (Figure 30), including bands of 53kDa and 77kDa, and possibly one of 36kDa and one of 117kDa. Furthermore, clear immunoreactive bands were observed at 36kDa, 45kDa, 53kDa, 77kDa and 117kDa (Figure 31), as well as numerous bands between 28kDa and 62kDa. The major band of approximately 32kDa

could correspond to 3ABC, a stable intermediate whose specific role is unknown (Schultheiß *et al.*, 1994), although, again one would not expect cleavage between Protein A and the truncated 3A to occur nor would one expect binding to the anti-3D antibody. As before, the 36kDa protein could be Protein A-3A, that of 53kDa could be 3D, the 77kDa protein could represent the 3CD protein, and the 117kDA protein could be Protein A-3ABCD.

Soluble proteins binding to the GTP-agarose have molecular weights of, 32kDa (3ABC?), 77kDa (3CD?) and 53kDa (3D?). Proteins of between 32 and 36kDa are also observed to bind to GTP-agarose possibly representing Protein A-3A or parts thereof. Furthermore, faint bands of between 42 and 48kDa are observed which could represent bacterial proteins. No protein of 24kDa, corresponding to 3C, was observed which is as expected as anti-3D would not react with this protein.

The lane showing insoluble extract was essentially disregarded as the process of spinning the insoluble matter down with GTP-agarose, served only to concentrate it and not to 'select' those proteins specifically binding to the GTP.

Expression of the P3 proteins in HAV P3/pMEX8 and analysis by SDS-PAGE (Figure 28) revealed numerous novel proteins - 36kDa, 53kDa, 77kDa and again possibly 117kDa. As previously mentioned the latter band cannot represent Protein A-3ABCD as this construct is deficient in Protein A sequences.

Bands of ~28kDa, ~32kDa, 47kDa, ~53kDa, and 77kDa appear on the Western blot (Figure 29) and of these it appears that three are soluble and bind to GTP-agarose which are the 53kDa, 77kDa and 32kDa proteins. It is not known what the proteins of ~28, ~32 and 47kDa correspond to and perhaps are evidence of bacterial contamination.

Little can be deduced from the control gel (Figure 32) showing proteins expressed upon induction of the pMEX8 vector alone, however immunoreactive proteins of ~79kDa and a faint band of ~53kDa can be seen on the Western blot (Figure 33), the latter of which interestingly does not bind to GTP-agarose. In addition to these, numerous bands of between ~25 and 32kDa can be seen, of which only a protein of ~31kDa binds to GTP-agarose.

Samples of pRIT5 and pRITPOL used in pilot experiments were grown in LB-glucose throughout induction as pRIT5 is constitutive. In initial assessment of these constructs however, IPTG was added to all cultures as it may cause changes in bacterial protein expression even if it is not inducing gene expression from a plasmid.

Three dominant bands with an apparent molecular weight of, 53kDa, 77kDa, and 117kDa, are visible on the Coomassie-stained gel (Figure 34) of pRITPOL. More can be gleaned from the Western blot (Figure 35) which shows that proteins of between ~26 and 31kDa, ~32kDa (3ABC?), 36kDa (Protein A-3A?), 45kDa, 50kDa, 53kDa (3D?) and 77kDa (3CD?) are present and react with the anti-3D antibody. Of these proteins, it appears that a protein of ~31kDa, as well as those of ~32kDa, 36kDa, 53kDa, and 77kDa are soluble and bind to the GTP-agarose.

In the pRIT5 control experiment various bands were observed (Figure 36 and Figure 37), although bands of the sizes predicted to correspond to HAV P3 proteins were not apparent. As well as bands of ~85kDa, 65kDa, and ~33kDa, faint immunoreactive bands of between 32 and 65kDa were also observed in whole cell lysate samples. The proteins present which bound GTP-agarose included the 33kDa protein, possibly corresponding to a Protein A polypeptide, and two others of approximately 65 and 85kDa in weight of unknown identity.

A summary of these results can be found in Table 10.

Table 10: Summary of proteins expressed in pRIT5 constructs

HAV P3 PROTEINS	PREDICTED SIZE (kDa)	pRITPOL			pRIT5		
		PROTEINS	IMMUNOREACTIVE PROTEINS	SOLUBLE GTP-BINDING PROTEINS	PROTEINS	IMMUNOREACTIVE PROTEINS	SOLUBLE GTP-BINDING PROTEINS
Protein A-3ABCD	117	✓?	✗	✗	✓?	✗	✗
3CD	77	✓?	✓	✓	✗?	✗	✗
3D	53	✓?	✓	✓	✓?	✗	✗
Protein A-3A	36	✓?	✓	✓	✓?	✓?	✗

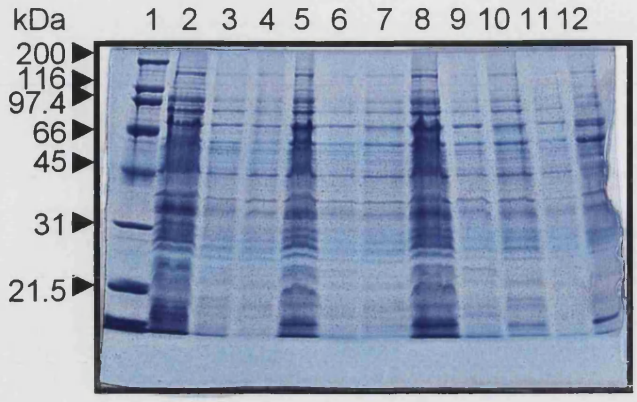

Figure 28: Expression of P3 proteins in *E. coli* transformed with HAV P3/pMEX8 (Coomassie-stained 10% SDS-PAGE gel)

Lane 1:	markers	
Lane 2:	whole cell lysate	uninduced
Lane 3:	crude extract	
Lane 4:	insoluble extract	
Lane 5:	whole cell lysate	induced 2h
Lane 6:	crude extract	
Lane 7:	insoluble extract	
Lane 8:	whole cell lysate	induced 5h
Lane 9:	crude extract	
Lane 10:	insoluble extract	
Lane 11:	crude extract induced 5h	GTP-agarose binding
Lane 12:	insoluble extract induced 5h	

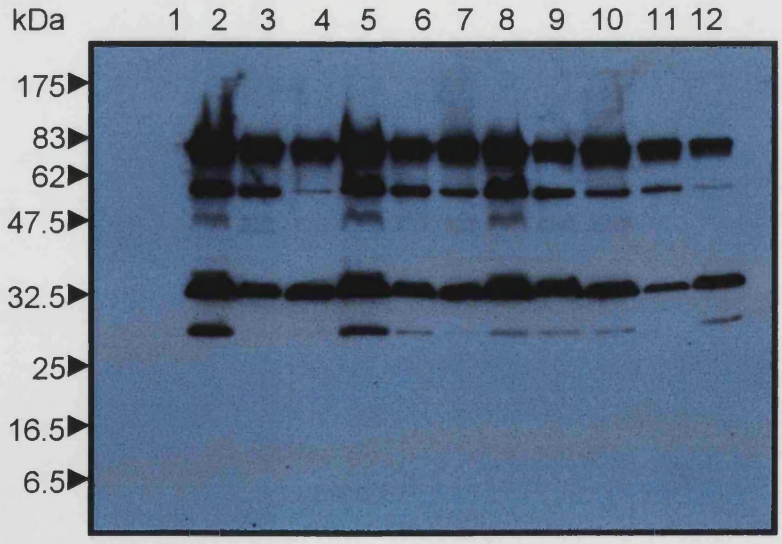

Figure 29: Expression of P3 proteins in *E. coli* transformed with HAV P3/pMEX8 (Western blot of SDS-PAGE gel shown above)

This figure shows a Western blot probed with polyclonal rabbit peptide anti-HAV $3D^{pol}$ antibody and visualised using a light reaction - exposed 15 seconds. Lane order as above.

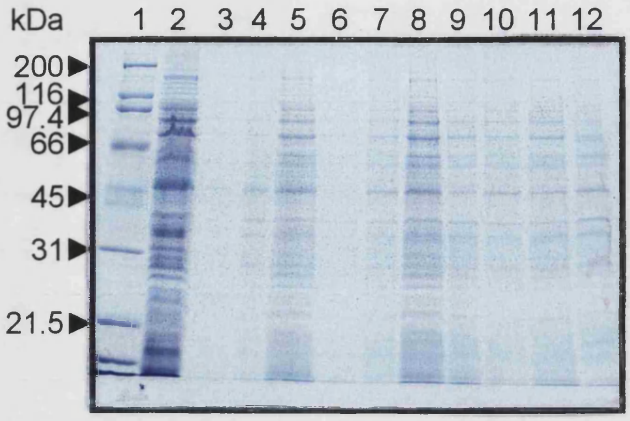

Figure 30: Expression of P3 proteins in *E. coli* transformed with Protein A/HAV P3/pMEX8 (Coomassie-stained 10% SDS-PAGE gel)

Lane 1:	markers	
Lane 2:	whole cell lysate	uninduced
Lane 3:	crude extract	
Lane 4:	insoluble extract	
Lane 5:	whole cell lysate	induced 2h
Lane 6:	crude extract	
Lane 7:	insoluble extract	
Lane 8:	whole cell lysate	induced 5h
Lane 9:	crude extract	
Lane 10:	insoluble extract	
Lane 11:	crude extract induced 5h	GTP-agarose binding
Lane 12:	insoluble extract induced 5h	

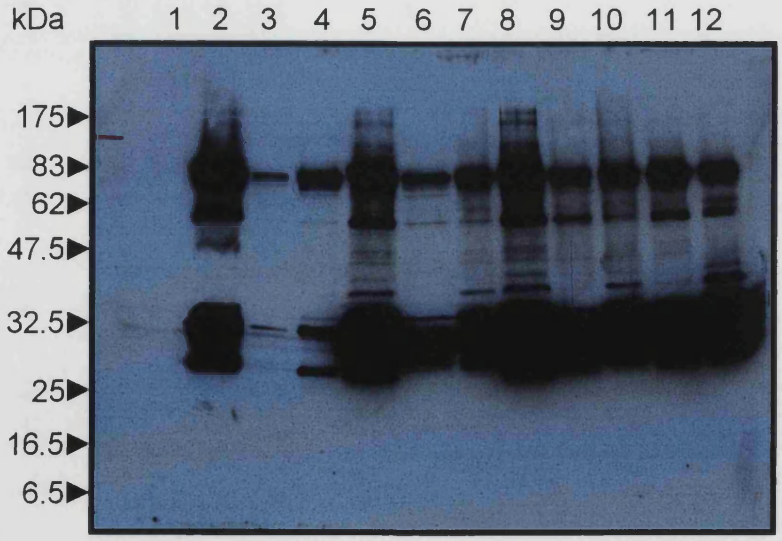

Figure 31: Expression of P3 proteins in *E. coli* transformed with Protein A/HAV P3/pMEX8 (Western blot of SDS-PAGE gel shown above)

This figure shows a Western blot probed with polyclonal rabbit peptide anti-HAV $3D^{pol}$ antibody and visualised using a light reaction - exposed 15 seconds. Lane order as above.

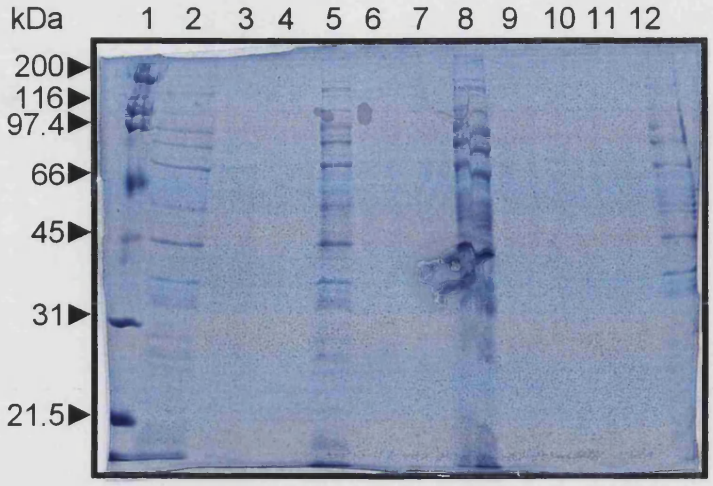

Figure 32: Expression of proteins in *E. coli* transformed with pMEX8 - control (Coomassie-stained 10% SDS-PAGE gel)

Lane 1:	markers	
Lane 2:	whole cell lysate	uninduced
Lane 3:	crude extract	
Lane 4:	insoluble extract	
Lane 5:	whole cell lysate	induced 2h
Lane 6:	crude extract	
Lane 7:	insoluble extract	
Lane 8:	whole cell lysate	induced 5h
Lane 9:	crude extract	
Lane 10:	insoluble extract	
Lane 11:	crude extract induced 5h	GTP-agarose binding
Lane 12:	insoluble extract induced 5h	

Figure 33: Expression of proteins in *E. coli* transformed with pMEX8 - control (Western blot of SDS-PAGE gel above)

This figure shows a Western blot probed with polyclonal rabbit peptide anti-HAV $3D^{pol}$ antibody and visualised using a light reaction - exposed 15s. Lane order as above.

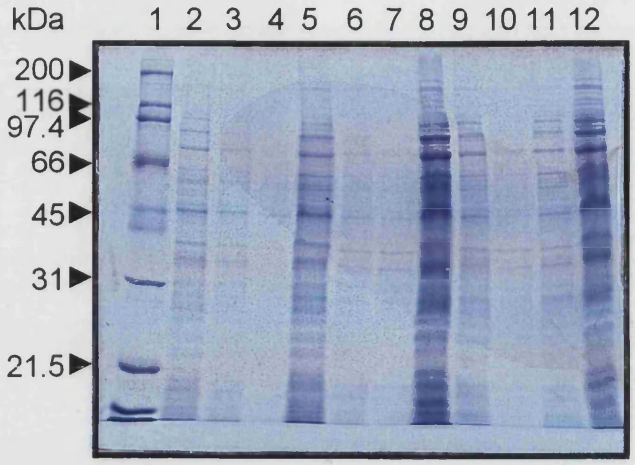

Figure 34: Expression of P3 proteins in *E. coli* transformed with pRITPOL (Coomassie-stained 10% SDS-PAGE gel)

Lane 1:	markers	
Lane 2:	whole cell lysate	uninduced
Lane 3:	crude extract	
Lane 4:	insoluble extract	
Lane 5:	whole cell lysate	induced 2h
Lane 6:	crude extract	
Lane 7:	insoluble extract	
Lane 8:	whole cell lysate	induced 5h
Lane 9:	crude extract	
Lane 10:	insoluble extract	
Lane 11:	crude extract induced 5h	GTP-agarose binding
Lane 12:	insoluble extract induced 5h	

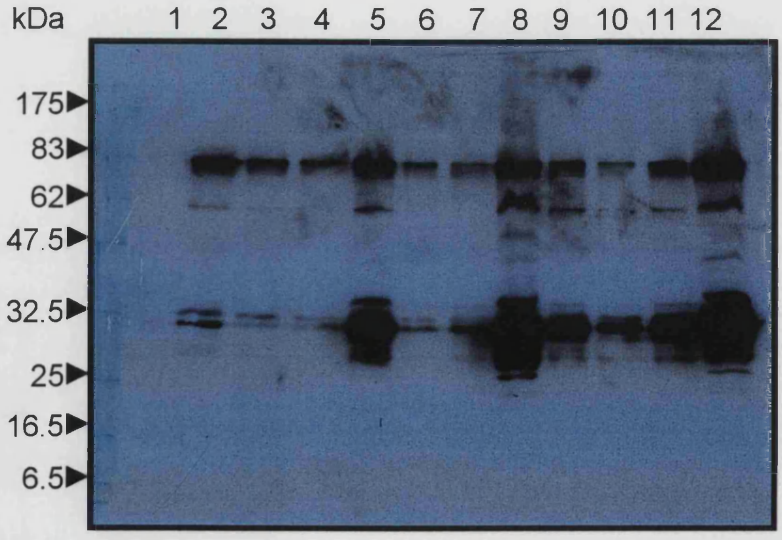

Figure 35: Expression of P3 proteins in *E. coli* transformed with pRITPOL (Western blot of SDS-PAGE gel above)

This figure shows a Western blot probed with polyclonal rabbit peptide anti-HAV $3D^{pol}$ antibody and visualised using a light reaction - exposed 15 seconds. Lane order as above.

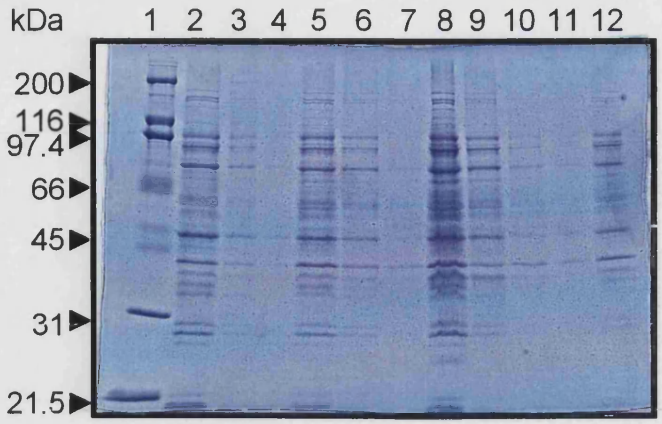

Figure 36: Expression of proteins in *E. coli* transformed with pRIT5 - control (Coomassie-stained 10% SDS-PAGE gel)

Lane 1:	markers	
Lane 2:	whole cell lysate	uninduced
Lane 3:	crude extract	
Lane 4:	insoluble extract	
Lane 5:	whole cell lysate	induced 2h
Lane 6:	crude extract	
Lane 7:	insoluble extract	
Lane 8:	whole cell lysate	induced 5h
Lane 9:	crude extract	
Lane 10:	insoluble extract	
Lane 11:	crude extract induced 5h	GTP-agarose binding
Lane 12:	insoluble extract induced 5h	

Figure 37: Expression of proteins in *E. coli* transformed with pRIT5 - control (Western blot of SDS-PAGE gel above)

This figure shows a Western blot probed with polyclonal rabbit peptide anti-HAV $3D^{pol}$ antibody and visualised using a light reaction - exposed 15 seconds. Lane order as above.

Batch-wise GTP-agarose affinity appeared successful at purifying the cell lysates to a certain degree, however it was assumed proper column chromatography was required for improved purification as no 'elution' step was employed during this assessment.

3.2.3 GTP-agarose affinity chromatography

On the basis of both previous studies in this laboratory and the pilot results, an attempt was made to purify 3D RNA polymerase from the periplasmic space of *E. coli* in order to obtain a pure sample of enzyme, free from contamination with bacterial proteins, for use in assay and possibly sequencing procedures.

Promising initial results were obtained from a 1ml affinity column (results not shown) but an increase in the amount of eluted protein was required to improve visibility of protein bands on SDS-PAGE gels and Western blots. The purification process was scaled up to a 5ml column, allowing a reduction in pressure in the column and an increase in flow rate. A number of bands were seen on the gel stained with Coomassie Blue, demonstrating that many different proteins in the periplasmic space have an affinity for GTP (not shown).

Results of Western blotting using the polyclonal rabbit peptide antibody showed a couple of HAV-specific bands which had been purified from the periplasmic space. These bands had apparent molecular weights of 36kDa and 53kDa; the protein of 36 kDa probably corresponds to Protein A-3A and the other is thought to be the $3D^{pol}$ enzyme (Figure 38). Other proteins visualised in pilot gels and by Western blotting which did not bind to the GTP-agarose affinity column had molecular weights of 32kDa (3ABC?), 77kDa (3CD) and 117kDa (Protein A-3ABCD). Western blots probed with human convalescent serum (Public Health Laboratories Service Laboratories, Royal United Hospital, Bath, U.K.) were unsuccessful in visualising these proteins, probably due to the inability of the antibodies to bind to denatured proteins. In addition, it is uncertain whether the convalescent serum contains antibodies raised against non-structural HAV proteins, although anti-3D reactivity in sera from acute and convalescent HAV patients has previously been demonstrated by Jia *et al.* (1992), however, reactivity was demonstrable only with antigen that had not been denatured with SDS, suggesting that the antibodies were primarily directed against conformation-specific epitopes. In some cases a gel of JRR-600 extract was run and blotted. This blot was exposed to the antibody in the hope that the non-specific binding observed previously would be

minimised. The pre-adsorbed diluted antibody was then added directly to blots where a degree of improvement in clarity of results was observed but did not warrant the extra labour involved.

It should be noted that the eluted fractions were concentrated approximately 20-fold before analysis by SDS-PAGE. A gel with *E. coli* transformed with the plasmid controls, pRIT5 and pMEX8, was run and yielded a blot (Figure 39) with no obvious immunoreactive bands when probed with antibody and subjected to ECL analysis.

Shortly thereafter, however, this result was not reproducible and other methods were investigated as described in 3.3.

To summarise, however, this result indicates that it is possible to isolate an HAV-specific 53kDa protein from the periplasmic space of *E. coli* transformed with Protein A/HAV P3/pMEX8 and to a lesser extent pRITPOL, supporting the decision made to persevere with bacterial expression systems. Unfortunately, the samples used here were concentrated to minute amounts for SDS-PAGE analysis and as difficulties were encountered in reproducing this result, samples were not available for activity assay analysis nor protein sequencing.

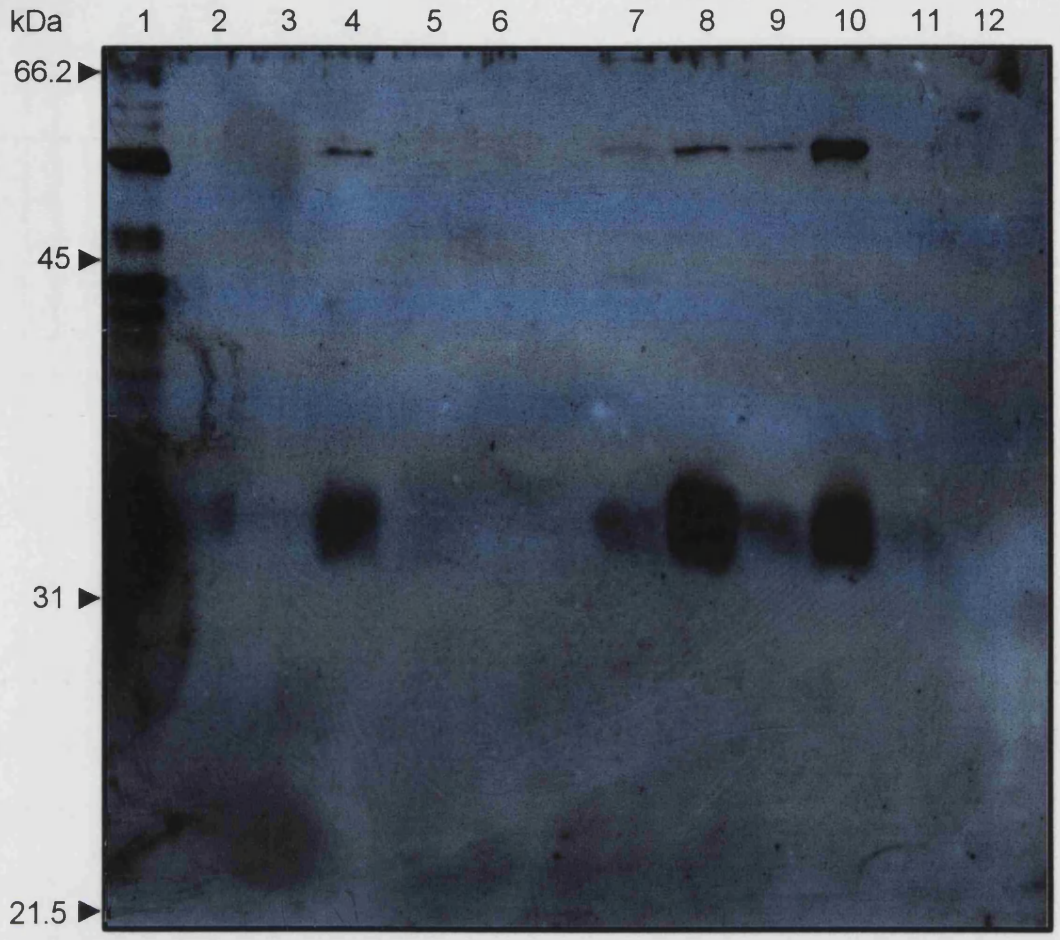

Figure 38: Proteins eluted from the GTP-agarose affinity column

This figure shows a Western blot probed with polyclonal anti-HAV $3D^{pol}$ antibody and visualised using a light reaction - exposed 15 seconds.

Lane 1: crude sample of pRITPOL
Lane 2: fraction 1
Lane 3: fraction 2
Lane 4: fraction 3
Lane 5: fraction 4
Lane 6: fraction 5
} pRITPOL eluted from column

Lane 7: crude sample of Protein A/HAV P3/pMEX8
Lane 8: fraction 1
Lane 9: fraction 2
Lane 10: fraction 3
Lane 11: fraction 4
Lane 12: fraction 5
} Protein A/HAV P3/pMEX8 eluted from column

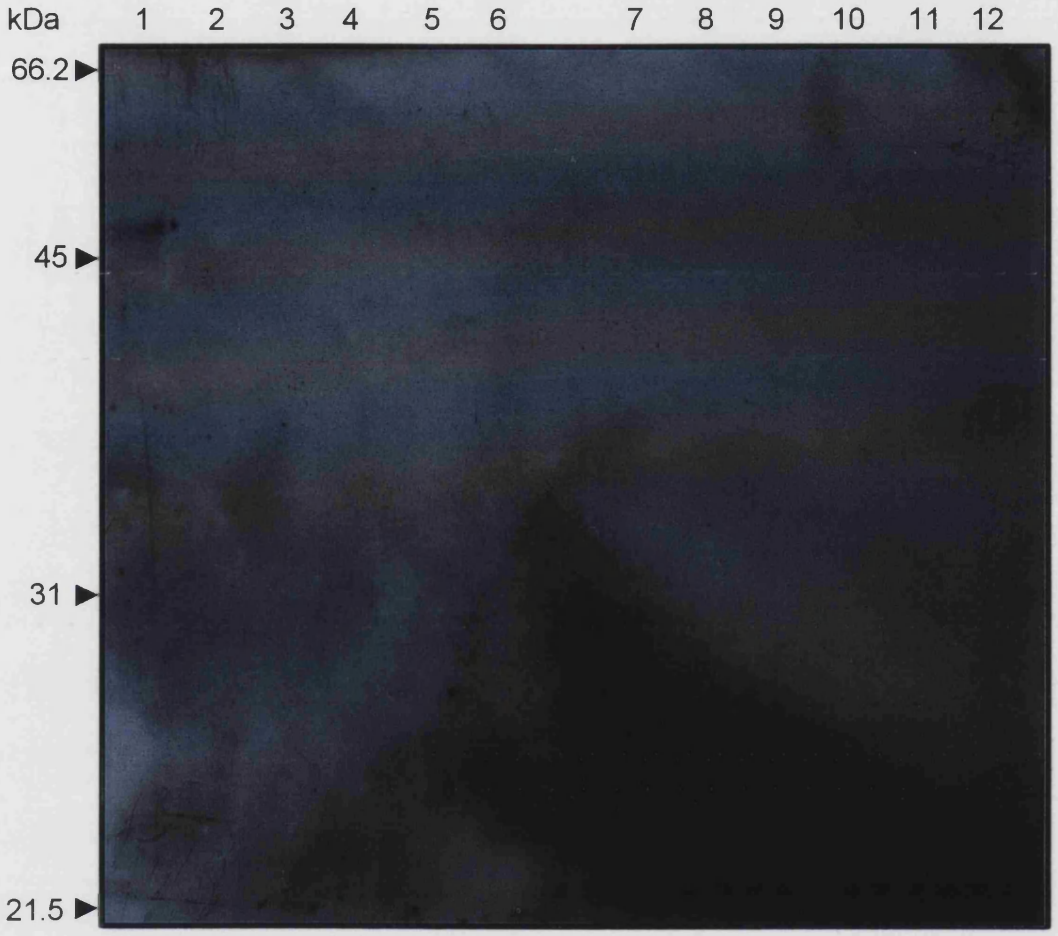

Figure 39: Proteins eluted from the GTP-agarose affinity column (control)

This figure shows a Western blot probed with polyclonal anti-HAV $3D^{pol}$ antibody and visualised using a light reaction. Exposed 15 seconds.

Lane 1: crude sample of pRIT5
Lane 2: fraction 1
Lane 3: fraction 2
Lane 4: fraction 3
Lane 5: fraction 4
Lane 6: fraction 5
} pRIT5 eluted from column

Lane 7: crude sample of pMEX8
Lane 8: fraction 1
Lane 9: fraction 2
Lane 10: fraction 3
Lane 11: fraction 4
Lane 12: fraction 5
} pMEX8 eluted from column

3.3 Discussion

As a first step in the characterisation of the polymerase enzyme, I required a purified preparation of HAV $3D^{pol}$. Initially, expression was achieved by using the available plasmid constructs, pRITPOL, Protein A/HAVP3/pMEX 8 and HAVP3/pMEX8 which contained the P3 region from a truncated 3A to 3D. This allowed expression of all of the P3 products and therefore allowed normal post-translational processing of the polyprotein to yield mature $3D^{pol}$. This was initially important since no information on the actual site of cleavage in this region was available at that time, and the exact N-terminus of the 3D protein could not be definitely ascertained.

Proper post-translational processing appears to have been both possible and present with bands corresponding to both processing intermediates and mature products being observed - the 33kDa protein, possibly of 3ABC (more likely to be Protein A), the 53kDa protein of 3D, and the 77kDa protein of 3CD, as well as a band of 117kDa proposed to correspond to protein A-3ABCD - in various permutations in *E. coli* carrying the different constructs.

The pilot experiment gels gave a clearer indication of the immunoreactive species present upon induction of the constructs and revealed some interesting results with regard to GTP-agarose-binding of some of these species. The 53kDa protein was observed to bind consistently to the GTP-agarose, as was the 36kDa protein proposed to be Protein A-3A which is as expected. The 77kDa protein, although observed to bind to GTP-agarose in pilot experiments, was later absent from GTP-agarose column fractions eluted, which is probably due to the batch-wise pilot method being unsuitable for this purification purpose with the column chromatography method yielding much clearer results as discussed below. So, all in all, the 3CD is either more sporadic in its binding to GTP-agarose or else the pilot binding is an artefact. Evidence supports the latter hypothesis, that 3CD fails to bind to GTP, confirming the observation that the precursor of $3D^{pol}$, $3CD^{pro}$, displays no RNA polymerase activity (Harris *et al.*, 1992).

A 33kDa protein, the size predicted for 3ABC, was observed to bind GTP in pRITPOL and Protein A/HAV P3/pMEX8. Previously during this study this band was assumed to have something to do with the 36kDa protein corresponding to Protein A-3A or perhaps could be Protein A alone although cleavage between Protien A and 3A was deemed unlikely. Interestingly though, RNA binding of the stable precursor polypeptide 3ABC has recently been shown to be 50 times stronger than that of 3AB and 3C, implicating a

specific role of this stable processing intermediate in viral genome replication which would possibly account for its presence here (Kusov *et al.*, 1997). As we would neither expect this protein to cleave itself from Protein A nor expect it to react with the anti-3D antibody however, a Protein A component, probably the IgG domain accounts for the presence of the large immunoreactive band observed at ~33kDa present in recombinant samples, the soluble protein of which binds GTP in Protein A/HAV P3/pMEX8 and pRITPOL, but, as expected, not in HAV P3/pMEX8 which lacks the Protein A sequences.

The presence of a major immunoreactive species of ~53kDa in samples eluted from a GTP-agarose affinity column was a real boost, however all of the concentrated fraction was loaded for analysis and as such, activity assays could not be undertaken. After these initially encouraging results, however, the reproducibility of the detection of the polymerase remained disappointingly uncertain and yields were frequently low, with fractions from the GTP-agarose affinity column often containing more than one protein. Here, inconsistent results for expression of 3D from both periplasmic and cytosolic preparations prompted the use of a different approach as these problems were expected to cause problems in further purification steps and it was anticipated that by making a fusion plasmid using pMAL™-c2, one could, with the resulting MBP-fusion protein, achieve better yields and purification. The cloning of genes into this plasmid, initial expression assessment of the fusion plasmids, large-scale expression and attempts at purification of the $3D^{pol}$ and other P3 nonstructural proteins will be covered in Chapter 4. Chapter 5 is devoted to $3D^{pol}$ enzyme activity and the effects, on this activity, of addition of the P3 nonstructural proteins I was able to 'purify'.

In conclusion though, this affinity chromatography protocol has been successful in initiating the purification of a protein from the periplasmic space of *E. coli* transformed with either Protein A/HAV P3/pMEX8 and pRITPOL, moreover the immunoreactive and GTP-binding 53kDa protein observed is the predicted size of the polymerase $3D^{pol}$; however its activity as a polymerase enzyme was not confirmed by enzyme assays. The aim of obtaining a sample of enzyme free from contamination with bacterial proteins was not realised, even though the Western blots appeared very encouraging. It is likely that a number of the proteins observed on Coomassie-stained gels would not react with the HAV-specific antibody, yet would bind and elute with the desired protein, therefore this affinity chromatography method can really only be regarded as a semi-purification step and further purification steps would be required. The results herein also indicate that Protein A is perhaps not the fusion partner of choice for subsequent attempts.

4. Amplification of P3, 3AB, 3C, 3CD and 3D from HAV P3/pMEX8 and their expression and purification using the pMAL™ system

4.1 Introduction

Although the $3D^{pol}$ has been successfully expressed in the periplasmic space of *E. coli* using the available constructs, the amount of protein produced is low, making some of the experiments described above difficult and time-consuming. Tesar *et al.* (1994), who enjoyed good expression levels in a bacterial system and were surprised by the lack of measurable RNA polymerase activity, later observed that the HAV 3D proteins sedimented after low-speed centrifugation, suggesting that the protein was insoluble or somehow associated with large subcellular components, this is in contrast with observations made for PV.

A number of proteins have been expressed in *E. coli* in the Department of Biochemistry at Bath University using vectors based on the strong, inducible tac promoter, and gene fusions. Although not essential for the assay experiments described, high-level expression of the $3D^{pol}$ would make it easier to detect low-activity enzyme, and may permit the purification of sufficient protein to allow biophysical characterisation. In this case it was decided to, as well as continuing attempts with the available constructs, create a fusion protein which, once purified, is separated into fusion partner and target protein, by chemical or enzymatic cleavage. By cloning the gene of interest into the pMAL vector, a gene fusion was created with the MBP-encoding *malE* gene, which, it was hoped, would ease purification of the desired protein and that the MBP-fusion partner would help keep the protein soluble. Transformed *E. coli* are grown and the culture induced to produce MBP-fusion protein constituting up to 30% of the cellular protein. Fusion protein expressed form pMAL™-c2 constitutes 20-40% of the total cellular protein, while fusion protein expressed from pMAL™-p2, directing fusion protein to the periplasmic space constitutes 5-10% of the total cellular protein. So, whilst enjoying limited success with periplasmically expressed protein, the greater yields of fusion protein likely with pMAL™-c2 swung the balance in its favour.

4.1.1 The pMAL™-c2 expression system

The *E. coli* plasmid expression vector pMAL-c2 is a fusion protein vector (Figure 40); the peptide encoded by the cloned sequence is expressed as a fusion protein linked by its N-terminus to a 40.6kDa MBP. Expression of the fusion protein is under the control of the high activity inducible Ptac promoter. Under normal growth conditions the promoter is silent due to binding of the Ptac inhibitor, encoded by the LacIq gene. Addition of IPTG disrupts this interaction resulting in high-level transcription of the Ptac gene product. The *malE* gene encoding the MBP (Duplay *et al.*, 1984) lies downstream of this promoter, followed by a

sequence which codes for a factor Xa cleavage site. The multiple cloning site is located immediately 3′ to this recognition sequence permitting the insertion of a chosen coding sequence in the correct reading frame and subsequent recovery of the protein of study by factor Xa cleavage. Growth of transformed cells in the presence of IPTG induces high-level expression of the MBP fusion product. pMAL-c2 also includes the LacZ gene to allow blue/white selection of plasmids containing inserts, and the β-lactamase gene (Ap) which confers ampicillin resistance for the selection of transformants.

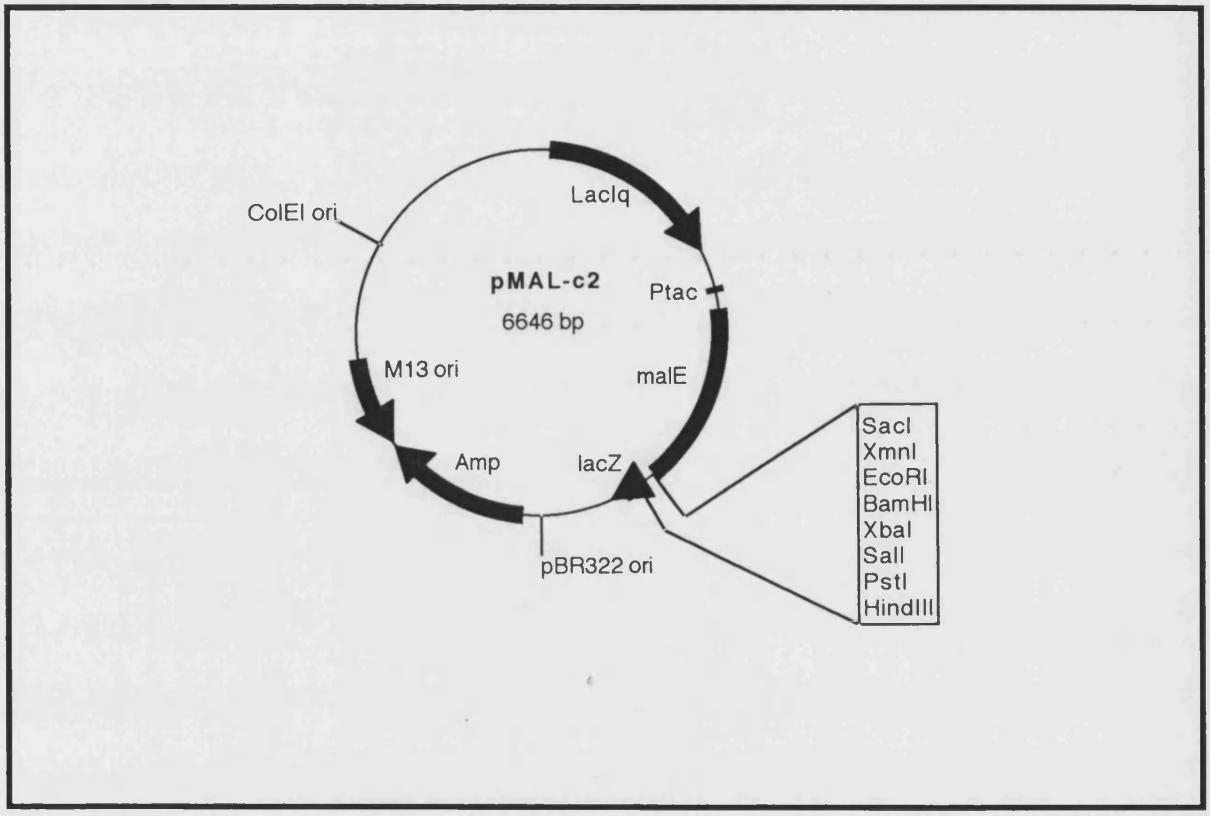

Figure 40: Map of the prokaryotic expression vector pMAL™-c2

Although it was possible that the lack of detectable HAV RNA polymerase activity, encountered by Tesar and colleagues (1994), was due to the absence of soluble protein in their preparations, an alternative explanation is that the poly(U) polymerase assay or the assay conditions are inappropriate for the HAV enzyme. The assay was optimised for the poliovirus 3D protein (Flanegan & Baltimore, 1977) and works well for the EMCV enzyme as well (Sankar & Porter, 1991). With HAV, only very low levels of activity have been unreliably detected which could imply that the RNA polymerase may require certain factors for activity not present in the reaction mixture used previously (Palmer, 1994).

Knowledge of the amino-acid sequence of the N-terminus of the 3D protein allowed attempts to express this molecule in bacterial cells, without the rest of the P3 region of the HAV genome. Furthermore, it has been established that levels of polymerase activity observed for PV are greatly enhanced by addition of purified 3AB which may be a co-factor for $3D^{pol}$ in viral transcription (Lama *et al.*, 1994). This led us to surmise that perhaps the same could be true of HAV and addition of purified 3AB to the reaction mixture could be the missing piece to the puzzle.

Undoubtedly 3CD plays an important role and, with its interaction with both 3AB and the 5'-terminal cloverleaf, is essential for RNA replication (Xiang *et al.*, 1995b). Harris *et al.* (1992) have suggested that PV $3CD^{pro}$ has no polymerase activity. The same could be true of HAV, however one cannot eliminate the possibility that the HAV 3CD may be a component of the RNA polymerase. It was therefore decided to clone certain individual genes into the pMAL™-c2 expression vector and the polyproteins expressed would be used in assays for polymerase activity as well as providing information on the effect, on this activity, of the individual polyproteins. Interestingly, expression of protein 3A in *E. coli* with an N-terminal deletion rendered this protein toxic to bacteria (Beneduce *et al.*, 1995). Moreover, the toxic potential to bacteria of protein 3AB of a cytopathic strain of HAV has been demonstrated, and found to be similar to that observed in PV (Pisani *et al.*, 1995; Beneduce *et al.*, 1997). The P3 region amplified here, and the constituent 3AB, were lacking the first 14 amino acids, and expression of the truncated 3AB region in this system could result in bacterial cell lysis if recombinant 3AB is active, thereby performing as a 'positive control'. With HAV 3C known to be expressable as a soluble and active enzyme in bacterial expression systems (Gauss-Müller *et al.*, 1991; Malcolm *et al.*, 1992), it became feasible to use this protein as a 'positive control' for the expression system used here as well.

Amplification of the required regions, however, was first of all necessary. As detailed in Chapter 1, the HAV P3/pMEX8 construct contains the HAV gene sequence stretching from a truncated 3A to 3D. In utilising this HAV sequence in HAV P3/pMEX8, endeavors to amplify the specific P3, 3AB, 3C, 3CD and 3D regions for subsequent subcloning were made (Figure 41).

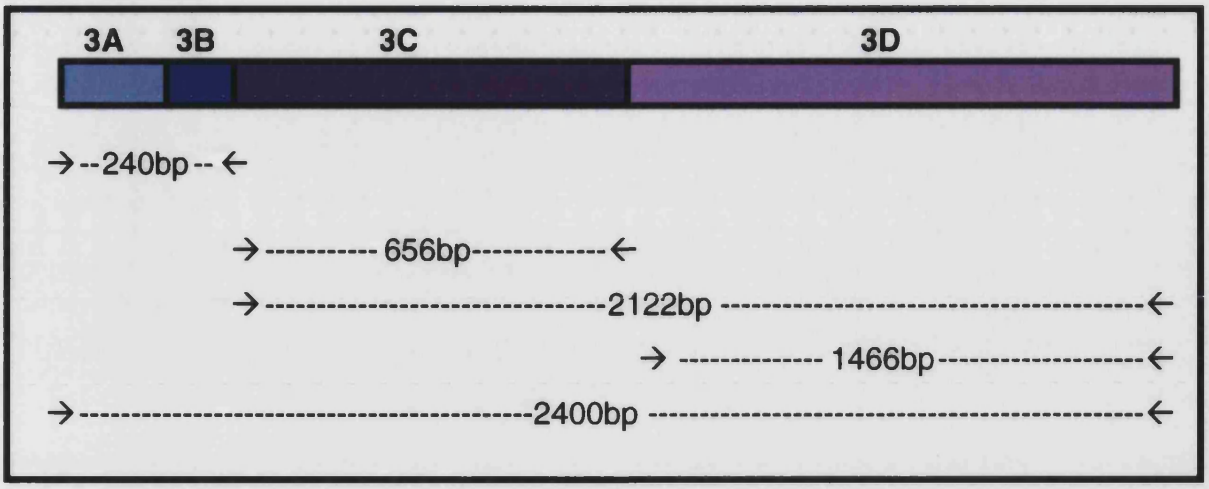

Figure 41: Diagram of the desired amplification products

The five regions pictured above were successfully amplified and cloned into pMAL-c2™, and have undergone sequence analysis. Preliminary expression studies using these constructs, proved successful for some of the aforementioned regions, and the purified polyproteins produced from overexpression of some of these fusion proteins have been used in enzyme assays in an attempt to determine the activity, and requirements for such activity, of the HAV RNA polymerase. This approach to amplification and cloning of the desired genes/regions and the subsequent expression and purification of the related gene products and their results are discussed below, with the enzyme activity information covered in Chapter 6.

The objective of the work included in this chapter, therefore, was three-fold:

1. Development of a more efficient expression system
2. Purification of the polymerase enzyme
3. Purification of other P3 nonstructural proteins

4.2 Results

4.2.1 Construct verification of HAV P3/pMEX8 by DNA analysis

DNA extracted, using a standard mini-prep (2.2.1), from harvested cultures grown from glycerol stocks (courtesy of Dr. J. Rider) was checked for the presence of the HAV P3 insert by digesting a small volume with suitable restriction enzymes and analysing the results on a 1% (w/v) agarose gel.

The sizes of the bands appearing on the gel corresponded with the expected fragment sizes as detailed below:

Table 11: Restriction products of HAV P3/pMEX8

RESTRICTION ENZYME	FRAGMENT SIZES (kb)
*Eco*RI	4.2 1.8
*Hin*dIII	4.7 1.3
*Pst*I	3.7 1.4 0.9

4.2.2 Amplification by the PCR, using HAV primers

Following the protocol outlined in 2.2.4.3, a number of PCRs, using primers HAV4 and HAV7-9 (Appendix 1), were carried out. Samples were then analysed on 1% (w/v) agarose gels as in 2.2.3.2, visualised under UV light and on completion of a successful PCR, purification of the amplified DNA was achieved using the Sephaglas BandPrep Kit from Pharmacia, as detailed in 2.2.5.

Attempts at amplifying the 3AB, 3C, 3CD, 3D and P3 regions from HAV P3/pMEX8 proved difficult. The PCR products were run on a 1% (w/v) agarose gel, but no bands corresponding to the 3AB at 0.24kb, 3C at 0.6kb, 3CD at 2.1kb, 3D at 1.4kb or P3 at 2.4Kb were seen. Whenever PCR products were viewed in an agarose gel under UV light, there were always products of a very low molecular weight, which, it was concluded, were possibly the primers annealing together to form 'primer-dimers'.

4.2.2.1 Radiolabelling of HAV primers

End-labelling of the HAV primers and running with a primer of known size on a polyacrylamide gel (result not shown) revealed that they were all of approximately the correct size and no real degradation was seen. Continued attempts at amplification of these products, however, remained unsuccessful.

4.2.2.2 Sequencing of HAV P3/pMEX8

The plasmid construct HAV P3/pMEX8 was subsequently manually sequenced in order to identify the reason behind this continuing problem with amplifcation. Sequencing of the construct HAV P3/pMEX8 showed that the 5′-terminal nucleotides of the 3A region were missing thought to have been 'nibbled away', revealing that the primers constructed for amplification of 3AB and P3 had nothing to bind to apart from each other (Figure 42) and that the problem lay with the template and not the primers.

The sequence of HAV P3/pMEX8 should read:

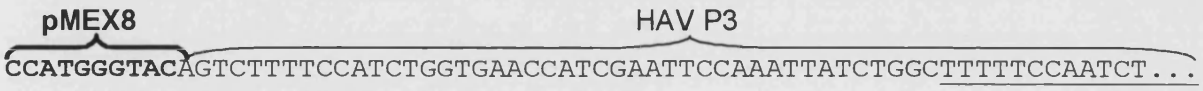

Manual sequencing however yielded the following results and from the bottom of the gel the sequence actually read:

This revealed that much of the 3A region was missing and new primers were required which encompassed this missing region, or at least the most part of it.

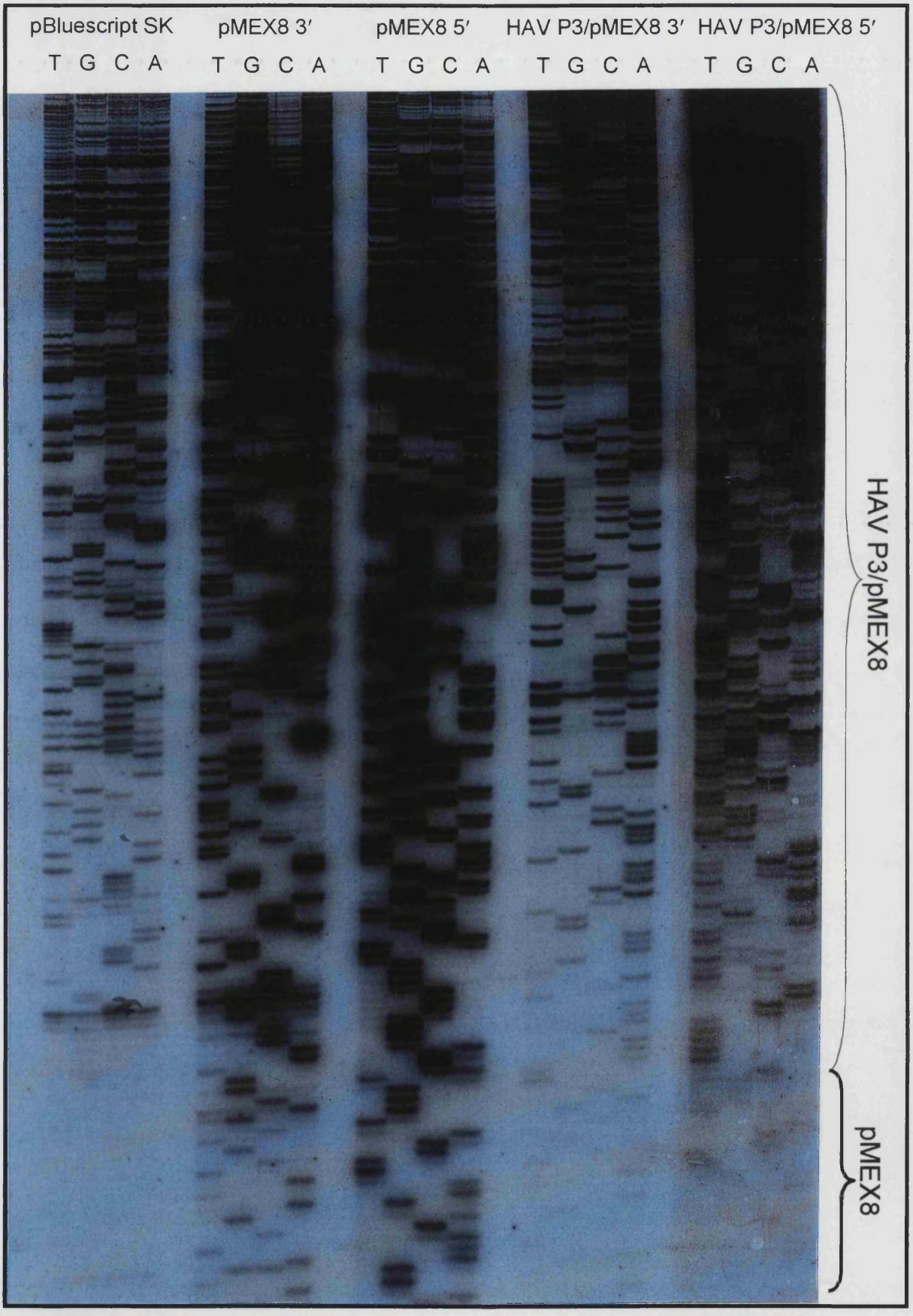

Figure 42: Manual sequencing of HAV P3/pMEX8 and pBluescript and pMEX8 (controls)

A new oligonucleotide primer synthesised (HAV9) encompassed the missing region and further attempts at amplifying these regions yielded bands at 0.24kb and 2.4kb using forward primer HAV9 and reverse primers HAV8 and HAV4 respectively (Appendix). These bands correspond to the 3AB region and P3 region of HAV (Figure 43). Bands were excised from the gel and purified using the Sephaglas BandPrep kit as previously described for subsequent cloning.

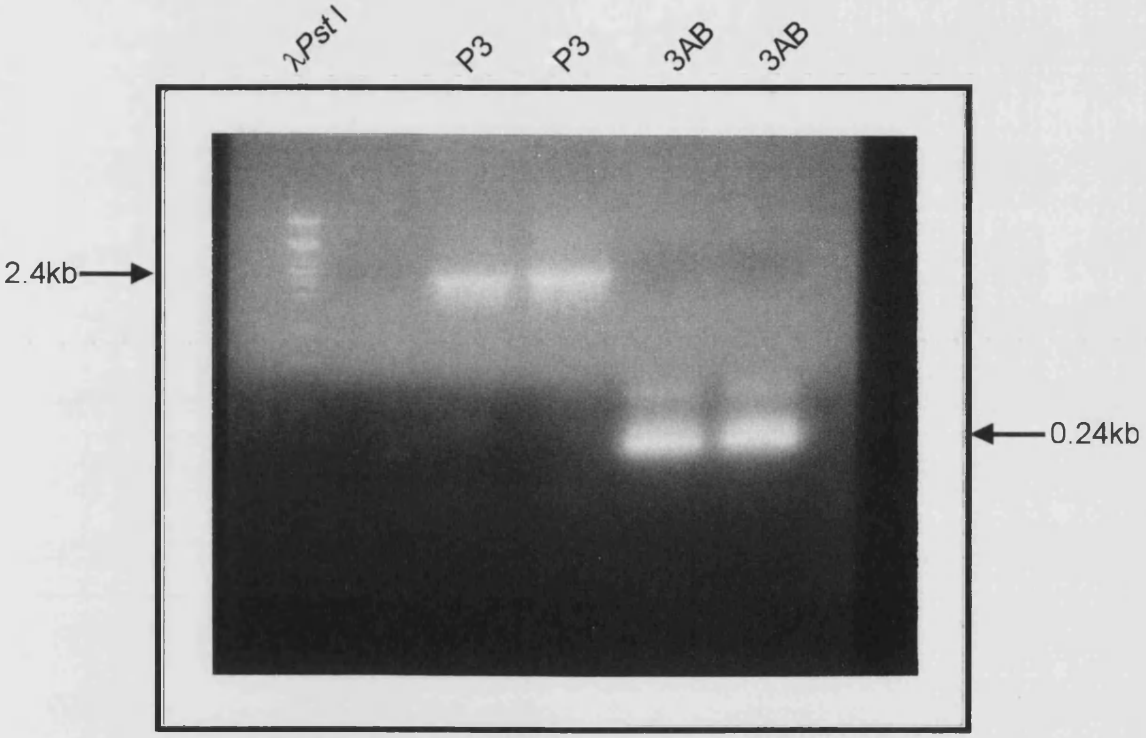

Figure 43: PCR amplification of 3AB and P3

Using Promega *Taq* polymerase and HAV primers. Conditions as described in Chapter 2.

4.2.2.3 Successful amplification of 3AB, 3CD, 3D and P3

With lack of progress in amplifying the remaining regions, reactions employing the Expand PCR kits were undertaken, as per the manufacturer's instructions, using the HAV family of primers (HAV4 and HAV8-12) and products obtained were treated as detailed above.

Immediate improvements were observed when the Expand kits were used, as indicated by the amplification again of P3 and 3AB with bands of 2.4kb and 0.24kb respectively, as well as bands of 2.1kb and 1.46kb corresponding to 3CD and 3D respectively (Figure 45).

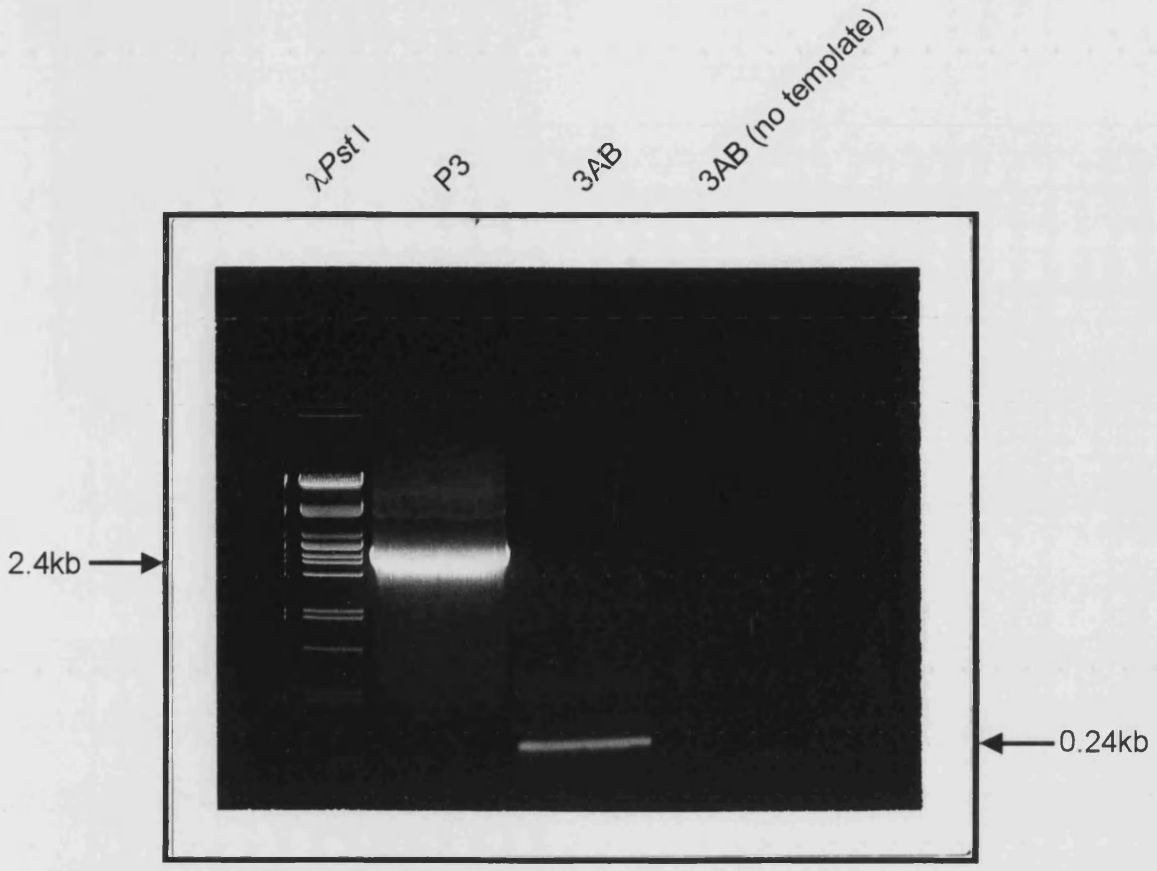

Figure 44: Amplification of 3AB and P3

Using Expand High Fidelity PCR Kit and HAV primers.

1 x	94°C for 2 minutes
30 x	94°C for 30 seconds
	65°C for 30 seconds
	72°C for 2 minutes
1 x	72°C for 5 minutes

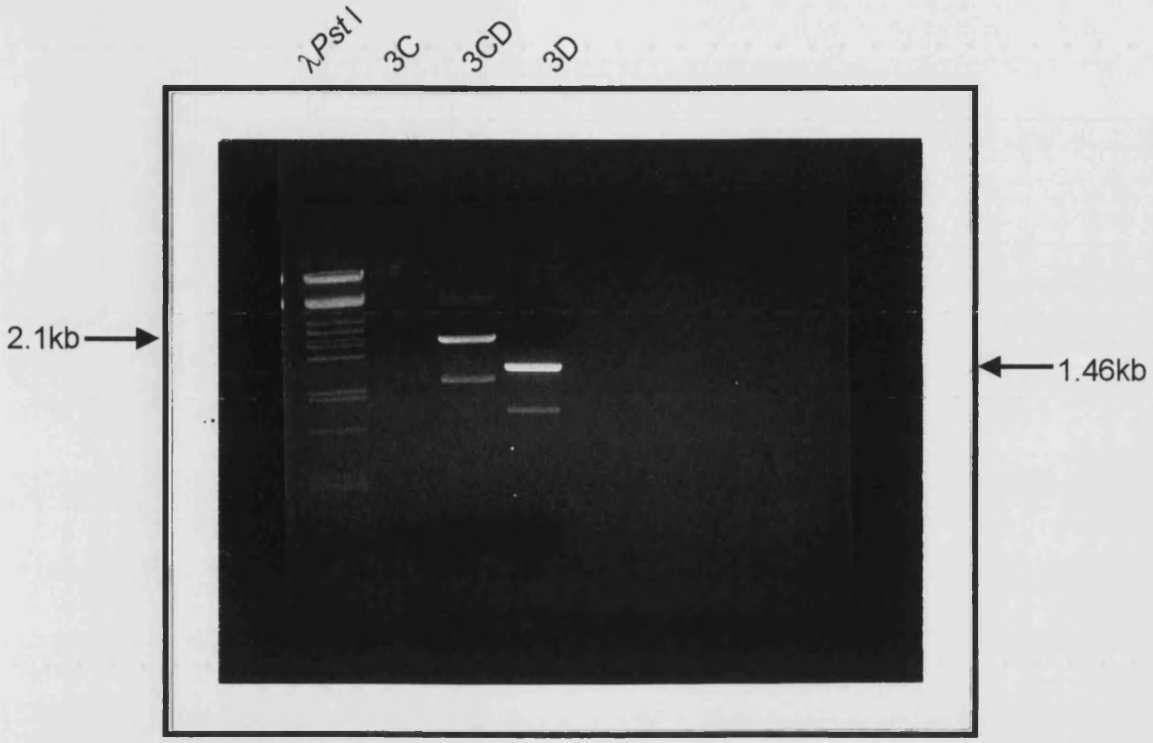

Figure 45: Amplification of 3C, 3CD and 3D

Using Expand High Fidelity PCR Kit and HAV primers.

1 x	94°C for 2 minutes
30 x	94°C for 30 seconds
	50°C for 30 seconds
	72°C for 2 minutes
1 x	72°C for 5 minutes

Unfortunately, shortly after this, PCR reactions became non-reproducible using the cycles and solutions previously successful and, after making checks, it appeared that the HAV primers used had degraded. New ready-pure primers, the LJ family (Figure 46 and Appendix), purchased from Perkin Elmer were used for all subsequent PCR reactions. These reactions also employed the Expand kits already mentioned.

4.2.3 Amplification by the PCR, using LJ primers

The LJ family of primers were used in all subsequent amplification reactions (Figure 46) and their sequences can be found in the Appendix. The position on the genome of the HAV primers used prior to this, and their sequences can also be found in Appendices 1 and 2.

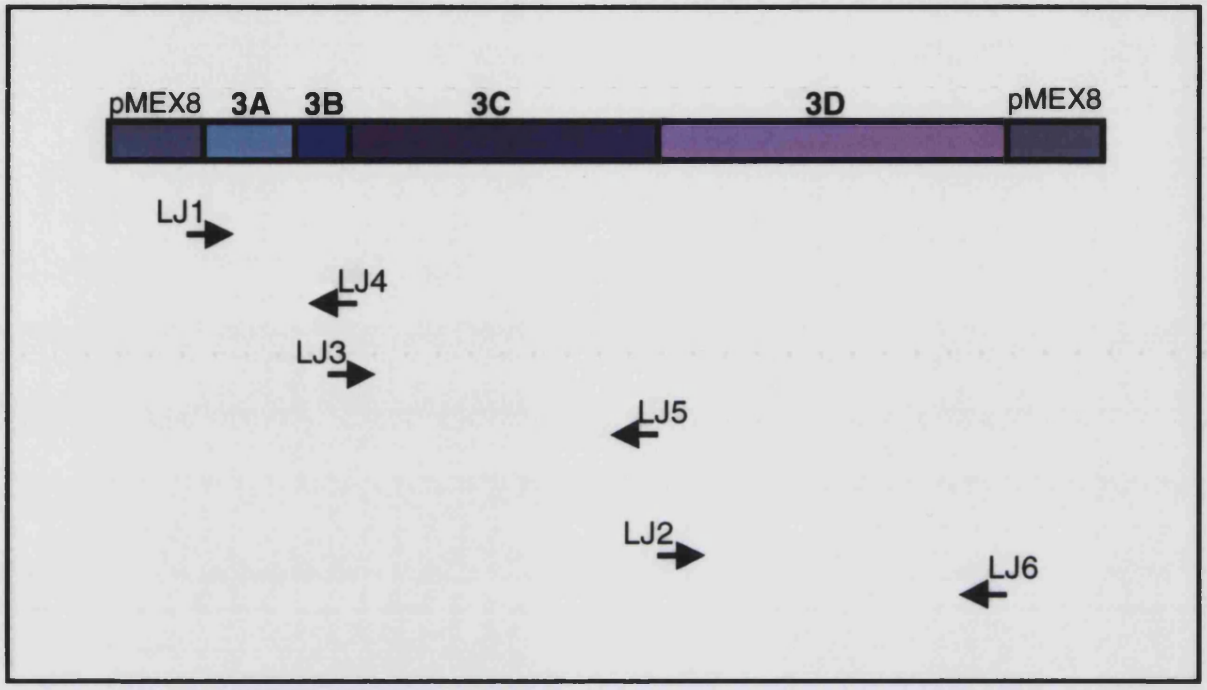

Figure 46: Position on genome of LJ primers

See Appendix 2 for sequences

4.2.3.1 Successful amplification of 3AB, 3C, 3CD, 3D and P3

Successful amplification of all the desired products: 3AB signified by a band at 0.24kb, 3C by a band at 0.66kb, 3CD by a band at 2.1kb, 3D by a band at 1.5kb and P3 by a band at 2.4kb ensued (Figure 47) and these products were gel purified and attempts at cloning these products into the vector pMAL-c2™ were made.

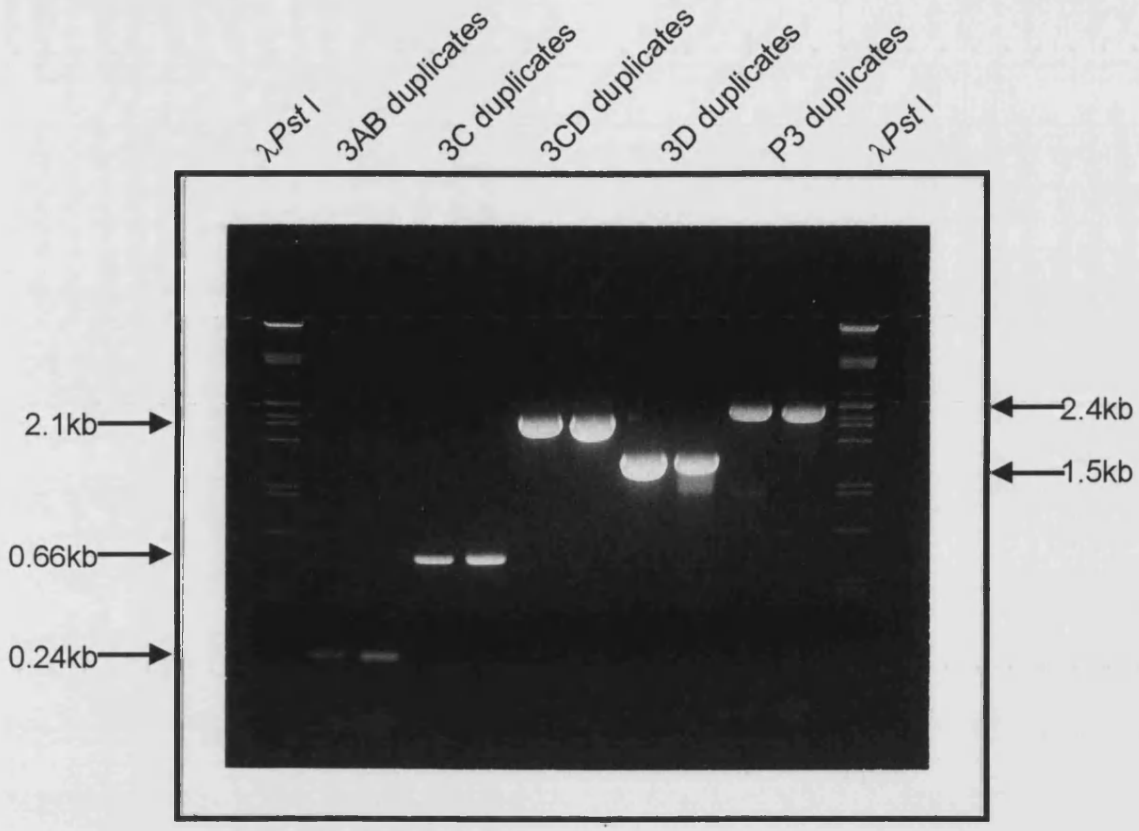

Figure 47: Amplification of 3AB, 3C, 3CD, 3D and P3

Using Expand High Fidelity PCR Kit and LJ primers. Cycles and temperatures as described in Chapter 2.

4.2.4 Cloning of HAV regions P3, 3AB, 3C, 3CD and 3D into pMAL™-c2

Subsequent DNA inserts, amplified using Expand PCR kits, were successfully purified straight from the reaction mixtures using the QIAgen PCR purification kit and ligated into pMAL™-c2, cut with *Xmn*I and *Bam*HI, and verification of the existence of these new constructs has been confirmed by restriction digest (Figure 48 to Figure 50), protein expression (Figure 51 to Figure 54) and sequence analysis (Figure 55 and Figure 56).

4.2.5 Confirmation of successful cloning

Screening for the presence of inserts was undertaken in the following ways:

4.2.5.1 Restriction digestion of putative constructs

Minipreps of the putative constructs 3AB/pMAL, 3C/pMAL, 3D/pMAL, 3CD/pMAL and P3/pMAL were produced and double-digested using the restriction enzymes *Sac*I, found just upstream from the *Xmn*I site used for cloning and *Bam*HI, one of the sites used for cloning, resulting in the removal of the insert from the vector, in positive clones, thus yielding two bands: one the size of the vector alone, approximately 6.6kb and one the size of the respective insert.

In the case of Figure 48 we can see the desired bands of both 2.1kb (3CD) and 1.5kb (3D), visualised by UV light on the agarose gel. Similarly, in Figure 49, where one can clearly see the desired band of 0.66kb representing 3C and in Figure 50, we can see that clones AB2 and AB4 are cloned successfully, as are P3-5 and P3-8 to the right of this figure.

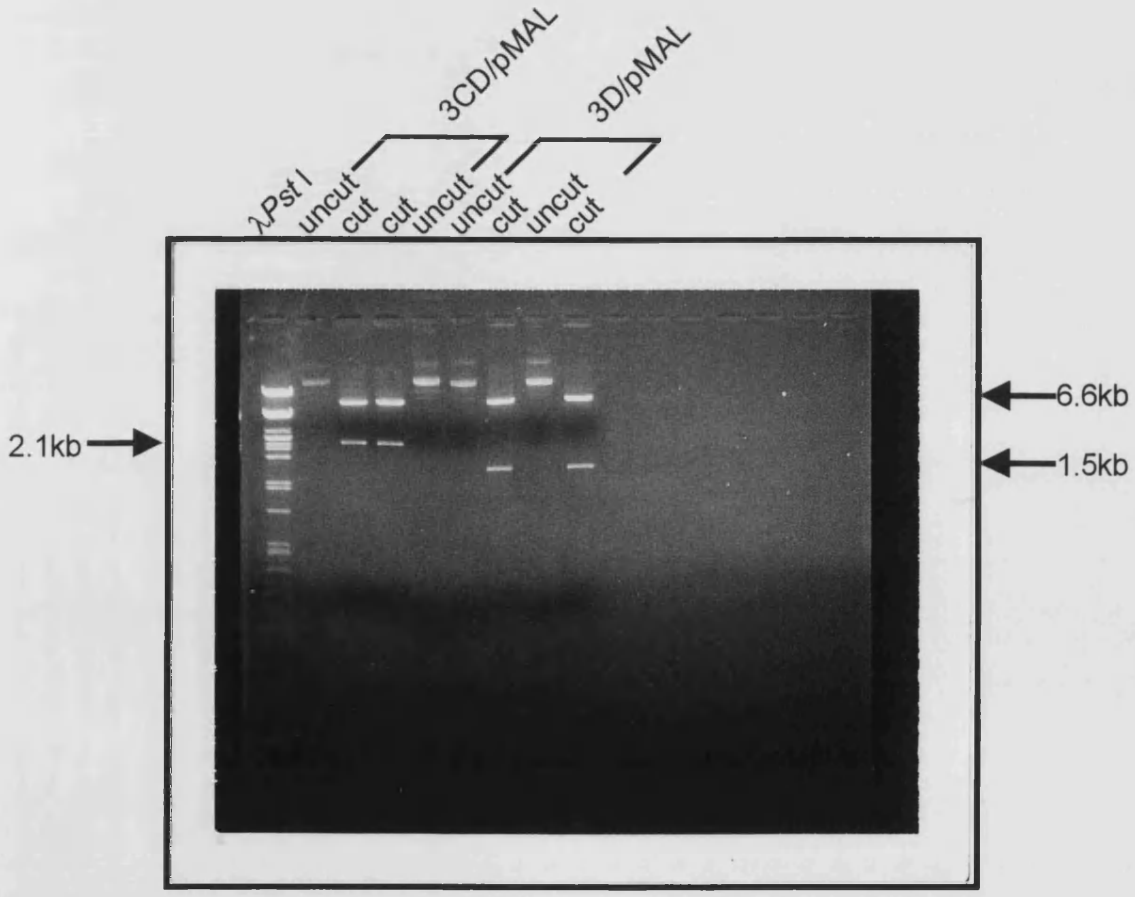

Figure 48: Clone confirmation of 3D/pMAL and 3CD/pMAL by restriction digest

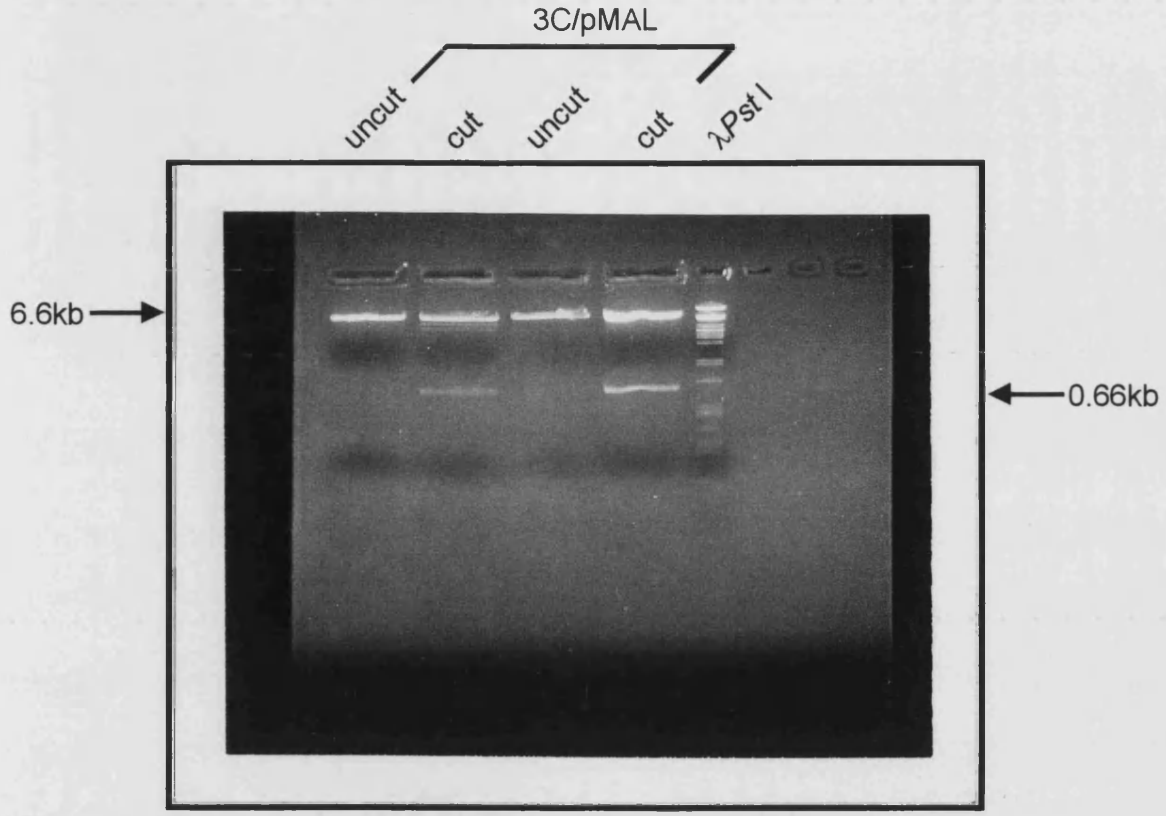

Figure 49: Clone confirmation of 3C/pMAL by restriction digest

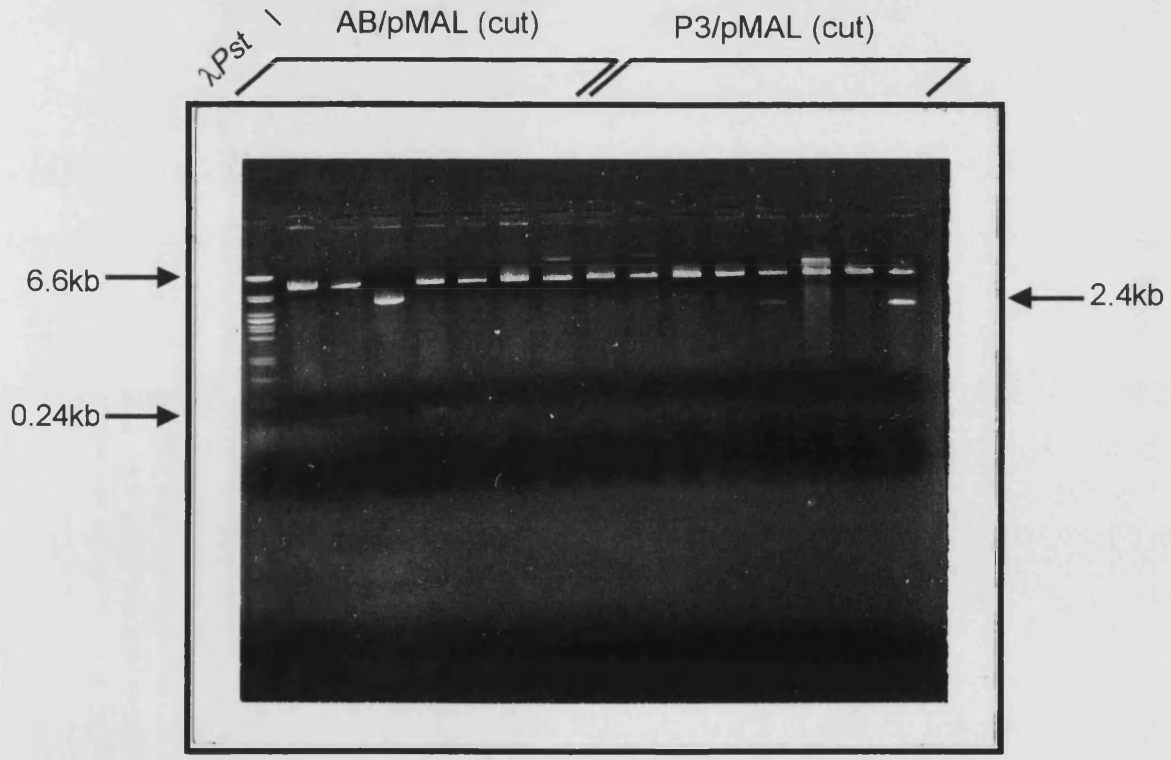

Figure 50: Clone confirmation of 3AB/pMAL and P3/pMAL by restriction digest

4.2.5.2 Protein expression in putative pMAL constructs

A culture of each of the new constructs, 3AB/pMAL, 3C/pMAL, 3CD/pMAL, 3D/pMAL and P3/pMAL was grown in LB, containing the appropriate antibiotics until an OD_{600} of 0.5 was reached. A 1ml aliquot was removed and IPTG was added to the remainder of the culture to a concentration of 0.3mM. This was incubated at 37°C for 2 hours and then the uninduced and induced cultures were centrifuged at 15,000*g*, the pellets resuspended in reducing sample-buffer, boiled for 5 minutes and then subjected to SDS-PAGE on a 10% gel which was subsequently blotted to nitrocellulose. Blots probed with the available anti-3D peptide antibody yielded little in the way of conclusive evidence and hence are not shown.

With the exception of 3AB/pMAL, bands of the size estimated for the respective fusion proteins were observed (Figure 51 to Figure 54). These proteins were expected to have the molecular masses shown in Table 12.

Table 12: Predicted molecular weights of fusion proteins produced

HAV PROTEIN	HAV PROTEIN (kDa)	FUSION PROTEIN	FUSION PROTEIN (kDa)
P3	89	MBP-P3	139.8
3CD	77	MBP-3CD	127.8
3D	53	MBP-3D	103.8
3C	24	MBP-3C	74.8
3AB	~12 (truncated)	MBP-3AB	62.8

4.2.5.2.1 Expression of 3D/pMAL and 3CD/pMAL

As can be clearly seen dramatic differences can be seen in all four possible clones of 3D/pMAL and 3CD/pMAL as compared with the control which shows a band of ~50kDa probably corresponding to the MBP-β-gal-α fusion which has a molecular weight of 50.8kDa (Figure 51 and Figure 52). Bands of ~125kDa and ~100kDa, thought to correspond to MBP-3CD and MBP-3D can be seen. Interestingly, a faint band at about 75kDa can also be seen and is thought represents MBP-3C, which could imply that the protease activity of 3CD is active in this instance.

4.2.5.2.2 Expression of 3AB/pMAL?

Attempts at expressing the MBP-3AB protein resulted in either clearing of the culture or production of what appeared to be MBP alone. Sequencing of clone 4 of 3AB/pMAL revealed 93.8% identity with the complete RNA genome of HAV in a 243bp overlap (Figure 56), however attempts at culturing bacteria containing this construct proved difficult, with clearing of the cultures being observed shortly after induction. Further DNA analysis on this construct revealed that the insert had been expelled from the plasmid. Further attempts at subcloning proved unsuccessful. With hindsight this result should have been expected due to the toxicity to bacteria of expressed 3AB (Beneduce *et al.*, 1995; Pisani *et al.*, 1995).

4.2.5.2.3 Expression of P3/pMAL

A similar effect is seen in Figure 53 and Figure 54 where in clone 8 of MBP-P3, at ~139kDa, MBP-P3 can be seen to be cleaving itself into what appears to be perhaps the nonstructural proteins. If this is the case and it cleaves off 3D and 3C (or 3CD for that matter) from itself, what remains bound to MBP will be 3AB. In a sense this is a negative result as the whole P3 region was not obtained, however, with problems encountered during 3AB/pMAL expression, this construct could still perhaps be of some use. Prolonged induction of P3/pMAL resulted in clearing of cultures similar to that seen in 3AB/pMAL implying that MBP-3AB was the resultant product of the autocatalysis being observed, however time did not permit proper assessment of growth kinetics. This is supported by the presence of a band of approximately 63kDa which could correspond to MBP-3AB and appears on both the Coomassie-stained gel and on the Western blot. Interestingly a band of ~43kDa can be seen upon induction of clone 5 of P3/pMAL indicating either an out of frame fusion or a severe protein degradation problem.

4.2.5.2.4 Expression of 3C/pMAL

Expression of MBP-3C was easily observed with a protein of about 75kDa being produced as can be seen in lanes 9 and 11 of Figure 53 and Figure 54. Using this construct as a positive control for bacterial expression it was apparent that this system was working successfully and was worthy of pursuance.

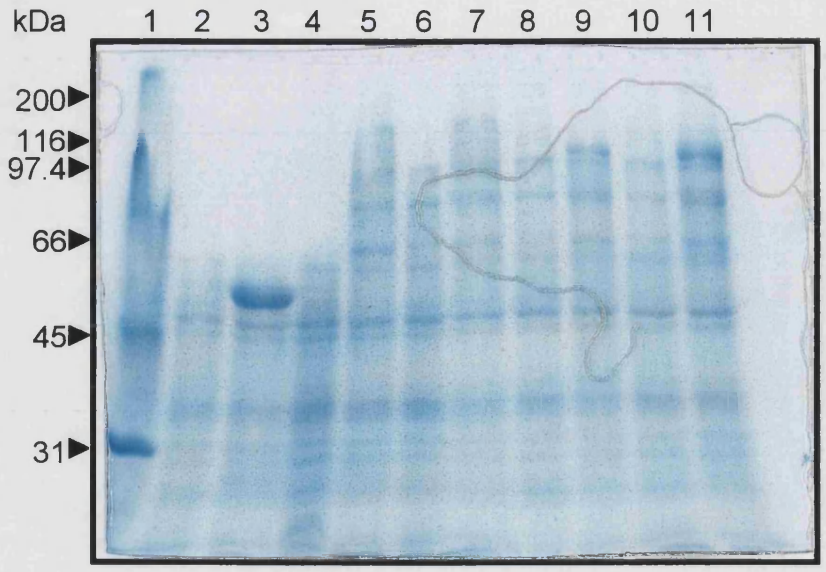

Figure 51: Coomassie-stained 10% SDS-PAGE gel of 3CD/pMAL and 3D/pMAL

Lane 1:	markers	
Lane 2:	uninduced	pMAL (control)
Lane 3:	induced	
Lane 4:	uninduced	3CD (clones 1 and 3)
Lane 5:	induced	
Lane 6:	uninduced	
Lane 7:	induced	
Lane 8:	uninduced	3D (clones 1 and 2)
Lane 9:	induced	
Lane 10:	uninduced	
Lane 11:	induced	

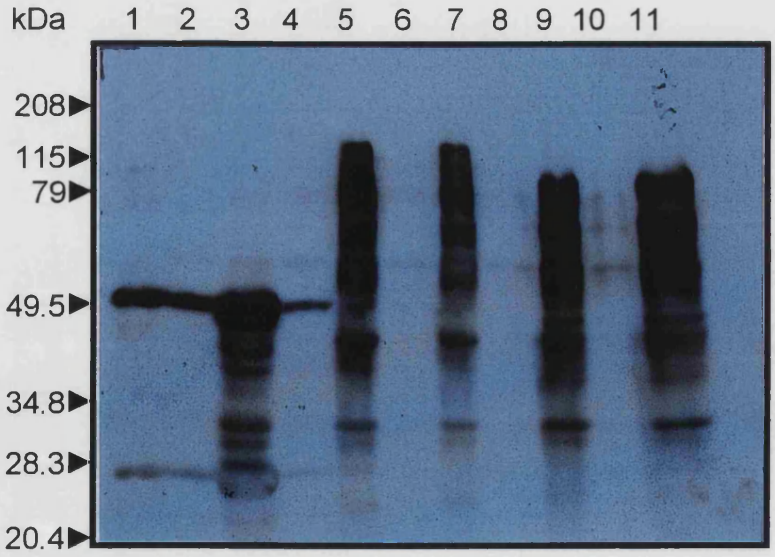

Figure 52: Western blot of gel of 3CD/pMAL and 3D/pMAL

Lane order as above. Exposure of 4 seconds.

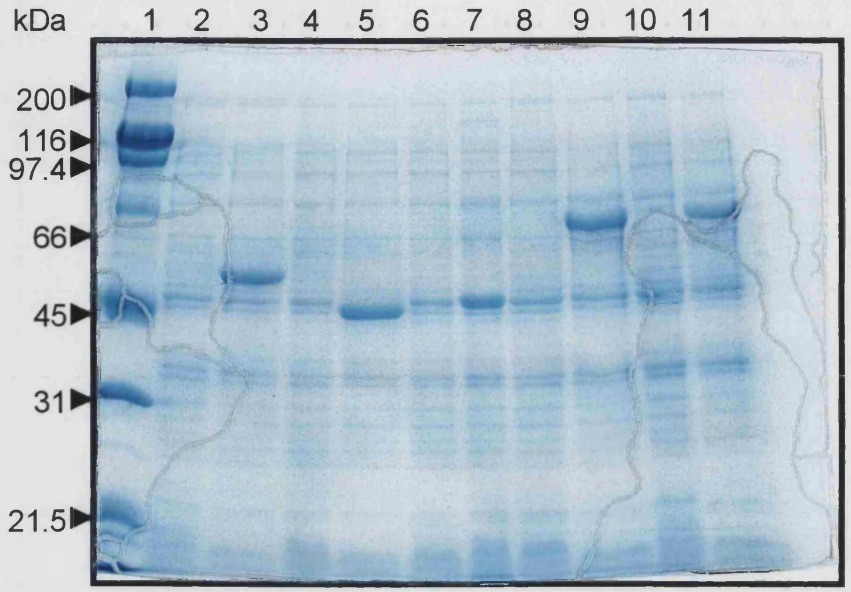

Figure 53: Coomassie-stained 10% SDS-PAGE gel of P3/pMAL and 3C/pMAL

Lane 1:	markers	
Lane 2:	uninduced	pMAL (control)
Lane 3:	induced	
Lane 4:	uninduced	
Lane 5:	induced	P3 (clones 5 and 8)
Lane 6:	uninduced	
Lane 7:	induced	
Lane 8:	uninduced	
Lane 9:	induced	3C (clones 1 and 2)
Lane 10:	uninduced	
Lane 11:	induced	

Figure 54: Western blot of gel of P3/pMAL and 3C/pMAL

Lane order as above. Exposure of 5 seconds.

4.2.5.3 Sequencing of putative constructs

Samples containing approximately 300-500ng of miniprep DNA and 3.2pmol of *malE* primer were sequenced on an automated ABI 377 Prism Sequencer. Sequences were analysed using the GCG suite of programs and this confirmed that the genes had been successfully cloned. The results are shown summarised in Table 13. Typical results are shown in Figure 55 and Figure 56 for P3/pMAL and 3AB/pMAL respectively.

Table 13: Summary of sequencing results for pMAL constructs

	CONSTRUCT	IDENTITY	OVERLAP (bp)
Human HAV RNA, complete genome (hpacg)	3C/pMAL (clone 2)	60.8%	549
hpacg	3CD/pMAL (clone 3)	88.2%	825
hpacg	3D/pMAL (clone 2)	86.1%	648
hpacg	P3/pMAL (clone 8)	96.6%	412
hpacg	3AB/pMAL (clone 4)	93.8%	243

```
Human hepatitis virus type A RNA, complete genome
ACCESSION NUMBER M20273

96.6% identity in 412 bp overlap

               60        70        80        90       100       110
p38.se AACAACAACCTCGGGATCGAGGGAAGGAGCTTTCCATCTGGTGAACCATCNAACTCTAAA
                                    ||||||||||||||||||||:|| || |||
hpacg  GATAGTGCAATGGCAGAGTTTTTTCAGTCTTTTCCATCTGGTGAACCATCGAATTCCAAA
          5020      5030      5040      5050      5060      5070

              120       130       140       150       160       170
p38.se TTATCTGGCTTTTTCCAATCTGTTAGTAATCACAAGTGGGTTGCTGTGGGAGCTGCAGTT
       |||||||||||||||||||||||| ||||||||||||||||||||||||||||||||||
hpacg  TTATCTGGCTTTTTCCAATCTGTTACTAATCACAAGTGGGTTGCTGTGGGAGCTGCAGTT
          5080      5090      5100      5110      5120      5130

              180       190       200       210       220       230
p38.se GGTGTTCTTGGAGTGCTCGTTGGGGGATGGTTTGTGTATTAGCATTTCTCCCGAAAAGAG
       ||| ||||||||||||||||||||||||||||||||| ||||||||||||||||||||
hpacg  GGTATTCTTGGAGTGCTCGTTGGGGGATGGTTTGTGTATAAGCATTTCTCCCGAAAAGAG
          5140      5150      5160      5170      5180      5190

              240       250       260       270       280       290
p38.se GAAGAGCCAATTCCAACTGAAGGGGTATATCATGGTGTAACTAANCCTAAGCAAGTGATT
       |||||||||||||||| ||||||||||||||||||||||||:||||||||||||||||
hpacg  GAAGAGCCAATTCCAGCTGAAGGGGTATATCATGGTGTAACTAAGCCTAAGCAAGTGATT
          5200      5210      5220      5230      5240      5250

              300       310       320       330       340       350
p38.se AAATTAGATGCAGATCCAGTAGAATCTCAGTCAACTTTGGAAATAGCAGGACTGGTTAGG
       ||||||||||||||||||||||||||||||||||||||||||||||||||||||||||||
hpacg  AAATTAGATGCAGATCCAGTAGAATCTCAGTCAACTTTGGAAATAGCAGGACTGGTTAGG
          5260      5270      5280      5290      5300      5310

              360       370       380       390       400       410
p38.se AAGAATTTGGTTCAGTTTGGAGTTGGAGAGAAGAATGGATGTGTGAGATGGGTTATGAAT
       ||||||||||||||||||||||||||||||||||||||||||||||||||||||||||||
hpacg  AAGAATTTGGTTCAGTTTGGAGTTGGAGAGAAGAATGGATGTGTGAGATGGGTTATGAAT
          5320      5330      5340      5350      5360      5370

              420       430       440       450       460       470
p38.se GCCTTANGGGTNAAAGATGATTGGTTGCTTGTACCTTCCCATGCTTACNNATTTGAAGAA
       ||||||:||||:||||||||||||||||||||||||||||||||::|||||| ||||
hpacg  GCCTTAGGGGTGAAAGATGATTGGTTGCTTGTACCTTCCCATGCTTACAAATTTG-AGAA
          5380      5390      5400      5410      5420       5430

              480       490
p38.se AGATTATGAANTGATGGAGTTT
       ||||||||||:||||||||||
hpacg  AGATTATGAAATGATGGAGTTTTATTTTAATAGAGGTGGAACTTACTATTCAATTTCAGC
          5440      5450      5460      5470      5480      5490
```

Figure 55: Alignment of part of putative P3/pMAL with part of the sequence encoding the complete RNA genome of human HAV

This sequence represents the highest nucleotide identities obtained from searching the Genbank and EMBL databases using the GCG programme Fasta (Pearson & Lipman, 1988).

```
Human hepatitis virus type A RNA, complete genome
ACCESSION NUMBER M20273

93.8% identity in 243 bp overlap

              60        70        80        90       100       110
ab4.se AACAACAACCTCGGGATCGAGGGAAGGAGCTTTCCATCTGGTGAACCATCGAACTCTAAA
                                        |||||||||||||||||||||||| || |||
hpacg  GATAGTGCAATGGCAGAGTTTTTTCAGTCTTTTCCATCTGGTGAACCATCGAATTCCAAA
          5020      5030      5040      5050      5060      5070

             120       130       140       150       160       170
ab4.se TTATCTGGCTTTTTCCAATCTGTTAGTAATCACAAGTGGGTTGCTGTGGGAGCTGCAGTT
       |||||||||||||||||||||||| ||||||||||||||||||||||||||||||||||
hpacg  TTATCTGGCTTTTTCCAATCTGTTACTAATCACAAGTGGGTTGCTGTGGGAGCTGCAGTT
          5080      5090      5100      5110      5120      5130

             180       190       200       210       220       230
ab4.se GGTGTTCTTGGAGTGCTCGTTGGGGGATGGTTTGTGTATTANCATTTCTCCCNAAAAGAG
       ||| |||||||||||||||||||||||||||||||||| |:||||||||||:|||||||
hpacg  GGTATTCTTGGAGTGCTCGTTGGGGGATGGTTTGTGTATAAGCATTTCTCCCGAAAAGAG
          5140      5150      5160      5170      5180      5190

             240       250       260       270       280       290
ab4.se GAANAGCCAATTCCAACTGAANGGGTATATCATGGTGTAACTAANCCTAAGCAAGTGATT
       |||:||||||||||| |||||:|||||||||||||||||||||:|||||||||||||||
hpacg  GAAGAGCCAATTCCAGCTGAAGGGGTATATCATGGTGTAACTAAGCCTAAGCAAGTGATT
          5200      5210      5220      5230      5240      5250

             300       310       320       330       340       350
ab4.se AANTTAGATNCAGATCCAGTACAATCTCAGTNATAAGGATCCTCTANAGTCNACCTGCAG
       ||:|||||||:|||||||||||| |||||||||:|
hpacg  AAATTAGATGCAGATCCAGTAGAATCTCAGTCAACTTTGGAAATAGCAGGACTGGTTAGG
          5260      5270      5280      5290      5300      5310

             360       370       380       390       400       410
ab4.se GCAANNTTGGCACTGGCCGTCGTTTTACAACTTCGTNACTGGGAAAAACCCTGGCNTTCC

hpacg  AAGAATTTGGTTCAGTTTGGAGTTGGAGAGAAGAATGGATGTGTGAGATGGGTTATGAAT
          5320      5330      5340      5350      5360      5370
```

Figure 56: Alignment of part of putative 3AB/pMAL with part of the sequence encoding the complete RNA genome of human HAV

This sequence represents the highest nucleotide identities obtained from searching the Genbank and EMBL databases using the GCG programme Fasta (Pearson & Lipman, 1988).

4.2.6 Pilot experiments showing expression and amylose binding capabilities

Initially, pilot experiments were undertaken for each of the successful constructs, in order to find out the conditions for protein expression ideally suited to each construct. The samples

run on the SDS-PAGE gels were initially uninduced, induced for 1 hour, induced for 2 hours, induced for 3 hours, crude cell extract, insoluble matter and protein bound to amylose. Coomassie-stained gels and anti-MBP probed Western blots are shown below for each HAV construct except 3AB/pMAL.

4.2.6.1 Pilot expression of 3C/pMAL

When expression of MBP-3C was satisfactory a distinct band of ~75kDa was observed, (lanes 5 to 10 of Figure 57) which reacted with anti-MBP antibody and yielded a major band of ~75kDa (Figure 58). Crude extract lanes showed that the band of interest was relatively soluble and it appeared also to be the dominant band bound to amylose in lane 10 of these two figures. The lane containing undiluted protein bound to amylose resin in Figure 58 revealed, however a few other proteins which bound to amylose resin. It was clear however that the polypeptide predominantly binding to amylose was that corresponding to the MBP-3C species. Some bands appeared smaller than they actually were on the gel and blot due to slight 'smiling' caused by temperature fluctuations.

4.2.6.2 Pilot expression of 3CD/pMAL

In the case of the pilot experiment with 3CD/pMAL, polypeptides (~125kDa) of about the size expected for MBP-3CD (127.8kDa) were observed. In addition very faint bands of ~90kDa, 75kDa, 66kDa, and 44kDa were observed on the Coomassie-stained gel (Figure 59) of 3CD/pMAL. Only the 75kDa, 66kDa and 44kDa bands were observed to be soluble and either only weakly reacted with the anti-MBP antibody (Figure 60) or were present in very small amounts. Some of these bands present can be accounted for however, with the band of 75kDa possibly corresponding to MBP-3C, if the 3CD has undergone autocatalysis at its natural cleavage site. It is expected that the 43kDa protein would possibly correspond to MBP2* indicating either an out of frame fusion or a severe protein degradation problem. No proteins were observed to bind to amylose resin. Again 'smiling' of the bands has occurred.

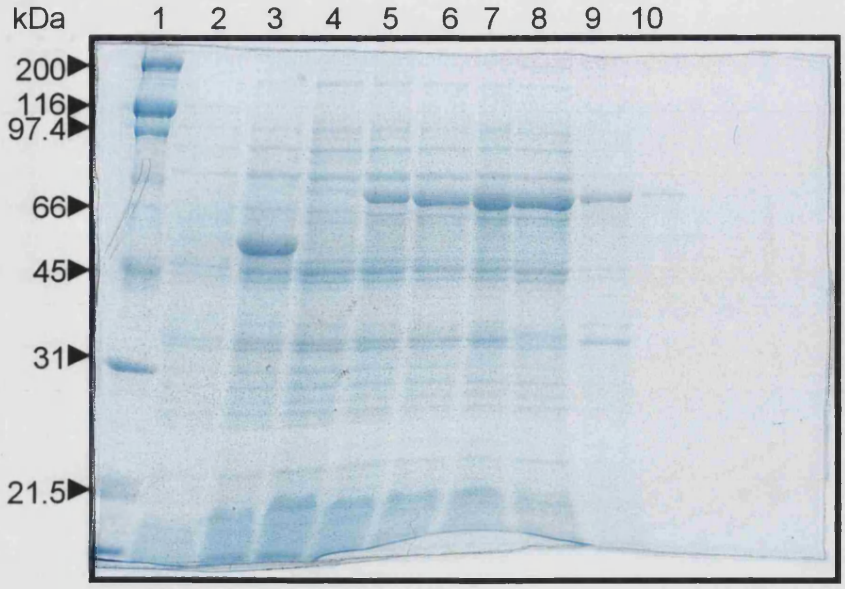

Figure 57: Pilot expression of 3C/pMAL - Coomassie-stained gel

Lane 1: markers
Lane 2: uninduced } pMAL (control)
Lane 3: induced }
Lane 4: uninduced
Lane 5: induced 1 hour
Lane 6: induced 2 hours
Lane 7: induced 3 hours } 3C/pMAL
Lane 8: crude extract
Lane 9: insoluble extract
Lane 10: protein bound to amylose resin

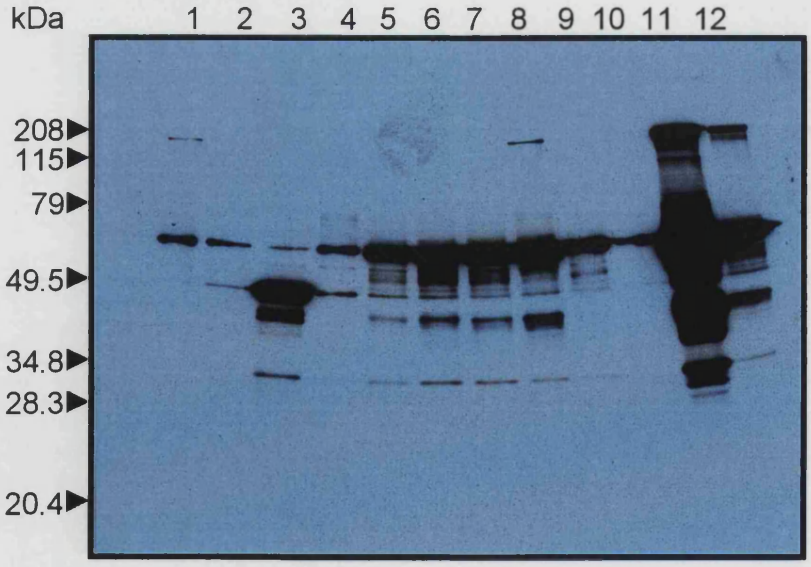

Figure 58: Pilot expression of 3C/pMAL - Western blot

Exposure of 1 minute. Lane order as above with samples diluted 1:10 with the addition of:-
Lane 11: crude extract (neat)
Lane 12: protein bound to amylose resin (neat)

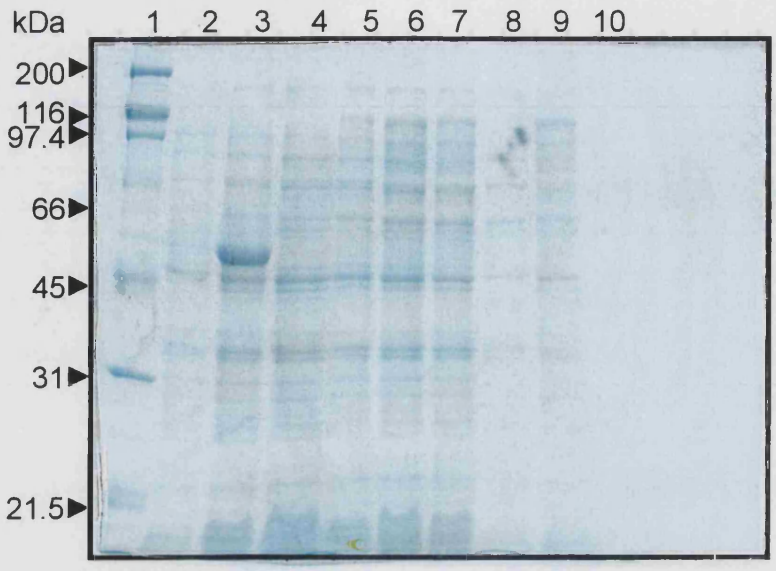

Figure 59: Pilot expression of 3CD/pMAL - Coomassie-stained gel

Lane 1: markers
Lane 2: uninduced } pMAL (control)
Lane 3: induced }
Lane 4: uninduced
Lane 5: induced 1 hour
Lane 6: induced 2 hours
Lane 7: induced 3 hours } 3CD/pMAL
Lane 8: crude extract
Lane 9: insoluble extract
Lane 10: protein bound to amylose resin

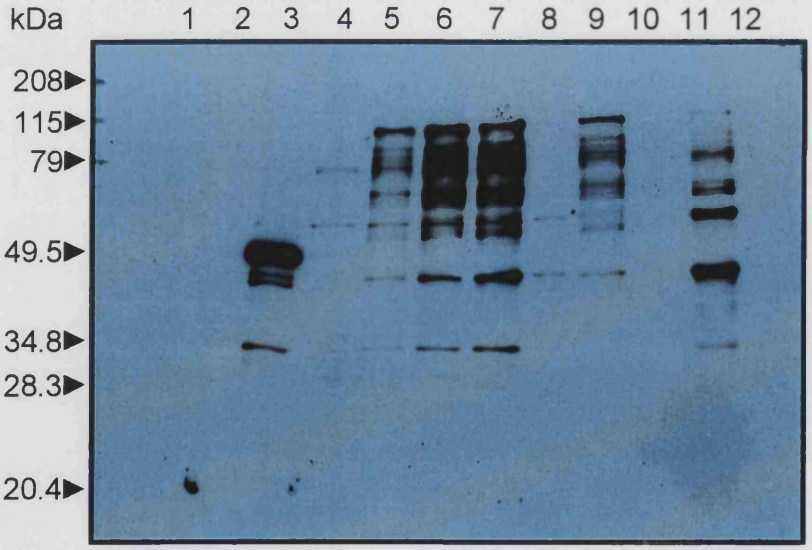

Figure 60: Pilot expression of 3CD/pMAL - Western blot

Exposure of 5 minutes. Lane order as above with samples diluted 1:10 with the addition of:-
Lane 11: crude extract (neat)
Lane 12: protein bound to amylose resin (neat)

4.2.6.3 Pilot expression of 3D/pMAL

Upon induction with IPTG, 3D/pMAL expressed high levels of a dominant protein of ~100kDa proteins, expected to represent MBP-3D (Figure 61). Expression of this protein increased proportionally with induction time. The MBP-3D appeared to be soluble to an extent, however the bulk of it was insoluble and temperature of induction was subsequently altered (reduced to 23°C) in the hope of remedying this. A very faint band was observed by SDS-PAGE to bind to amylose resin, however this was easier to see on the Western blot (Figure 62). A smaller band of ~75kDa appears to bind amylose resin as well, if not better, than the putative MBP-3D protein, however its identity is unknown.

4.2.6.4 Pilot expression of P3/pMAL

The results of the pilot experiment with P3/pMAL were confusing. A novel band of ~139kDa can be seen in lanes 5, 6 and 7 (Figure 63). The lane showing crude extract revealed that the actual MBP-P3 present was insoluble and only proteins of 95kDa, ~83kDa, ~75kDa, 63kDa, and ~43kDa were present in the soluble crude extract. For the mostpart, these proteins, however were also present in varying degrees in the control. The band of 63kDa could correspond to MBP-3AB and appeared to be present in P3/pMAL lanes only. A clear band of ~139kDa could be seen in the insoluble extract lane which shows promise, but autocatalysis, or at least proteolysis, is obviously occurring as the MBP fusion protein binding to amylose resin is only 43kDa long, which could correspond to degraded MBP alone. The 83kDa protein could correspond to MBP-3ABC, however this remains unknown.

Similar results were seen in the Western blot of P3/pMAL (Figure 64) with a band of the predicted size being visible in lanes 5, 6 and 7, but the amylose affinity resin bound either to a much smaller protein or to no protein at all and MBP was present alone. Bands of ~75kDa and ~83kDa were also observed, the latter of which could as already mentioned correspond to MBP-3ABC, but this remains unknown. Analysis of neat crude extract revealed that a minute amount of P3/pMAL was soluble, along with a protein of ~83kDa and one of ~66kDa. Attempts continued at changing conditions to yield more favourable results.

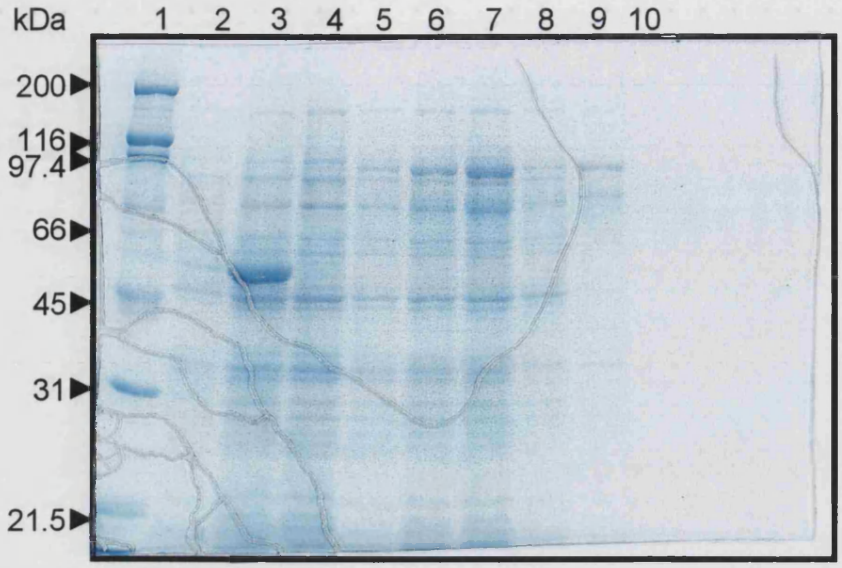

Figure 61: Pilot expression of 3D/pMAL - Coomassie-stained gel

Lane 1: markers
Lane 2: uninduced } pMAL (control)
Lane 3: induced }
Lane 4: uninduced
Lane 5: induced 1 hour
Lane 6: induced 2 hours
Lane 7: induced 3 hours } 3D/pMAL
Lane 8: crude extract
Lane 9: insoluble extract
Lane 10: protein bound to amylose resin

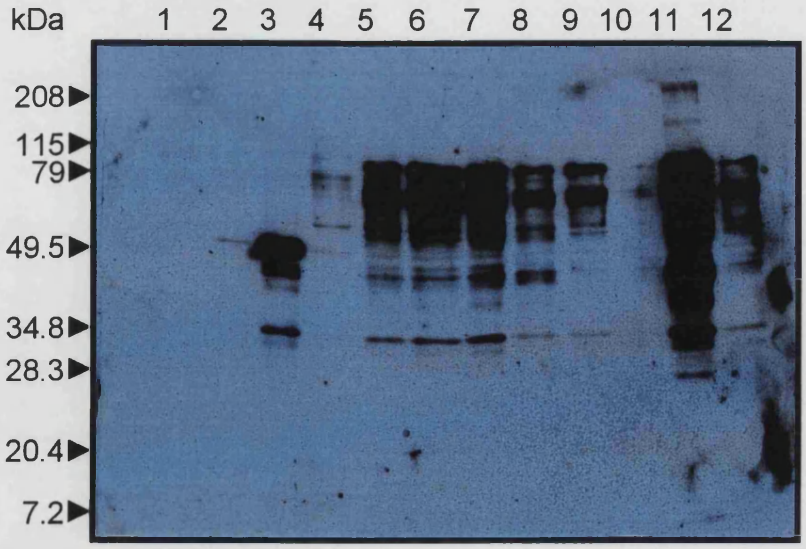

Figure 62: Pilot expression of 3D/pMAL - Western blot

Exposure of 2 minutes. Lane order as above with samples diluted 1:10 with the addition of:-
Lane 11: crude extract (neat)
Lane 12: protein bound to amylose resin (neat)

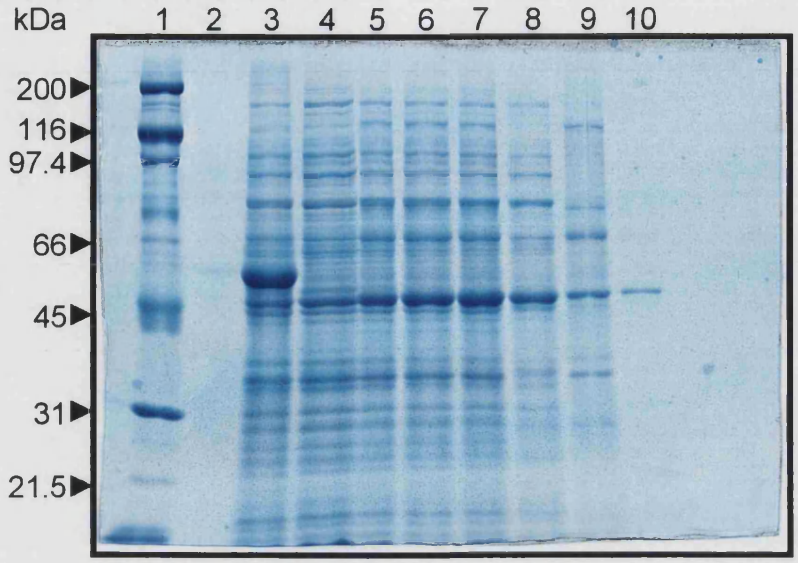

Figure 63: Pilot expression of P3/pMAL - Coomassie-stained gel

Lane 1: markers
Lane 2: uninduced } pMAL (control)
Lane 3: induced }
Lane 4: uninduced
Lane 5: induced 1 hour
Lane 6: induced 2 hours
Lane 7: induced 3 hours } P3/pMAL
Lane 8: crude extract
Lane 9: insoluble extract
Lane 10: protein bound to amylose resin

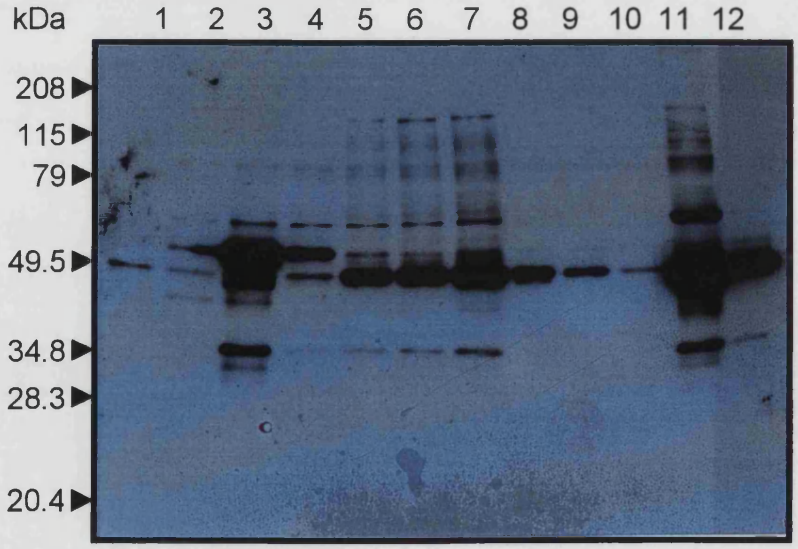

Figure 64: Pilot expression of P3/pMAL - Western blot

Exposure of 1 minute. Lane order as above with samples diluted 1:10 with the addition of:-
Lane 11: crude extract (neat)
Lane 12: protein bound to amylose resin (neat)

Table 14: Expressed proteins demonstrating solubility and amylose binding capabilities

BAND (kDa)	EXPRESSED	SOLUBLE	AMYLOSE BINDING
~139 (MBP-P3?)	✓	✗	✗
~125 (MBP-3CD?)	✓	✗	✗
~100 (MBP-3D?)	✓	✓?	✓?
~75 (MBP-3C?)	✓	✓	✓
~63 (MBP-3AB?)	✓?	?	?

4.2.7 Large-scale purification and factor Xa cleavage

After optimisation of the expression conditions for each construct, large-scale production was launched. Generally 1L cultures of each construct were grown as detailed in 2.2.7.2, however due to poor yield at times, cultures of 4L were used in some cases, by inoculating 4L of Rich Media with 40ml of overnight culture and growing to an A_{600} of ~0.5 or cell density of 2 x 10^8 cells/ml. Essentially, the same protocol was followed but scaled up to accommodate the larger volumes involved. By reducing the temperature of induction (Bishai *et al.*, 1987) to 23°C and inducing for longer (one has to increase the time of induction to compensate for the slower growth at reduced temperature - the rule of thumb used here was 2x for every 7°C below 37°C) solubility was marginally increased for MBP-3D, however degradation or cleavage of the putative processing intermediates, P3 and 3CD was still observed.

Protein-containing fractions eluted from amylose columns were identified by Bradford Assay, pooled and concentrated to approximately 1mg/ml for subsequent factor Xa cleavage as described in 2.2.7.3. Pilot experiments to assess factor Xa cleavage yielded the following results. In each case a band of the size predicted for MBP was seen at ~50kDa, and in some cases uncut fusion protein and the target protein alone at their respective masses were observed. As can be seen, the yields were variable and low.

4.2.7.1 Factor Xa cleavage of MBP-P3

Factor Xa cleavage of a sample hoped to contain MBP-P3 yielded unusual results as shown in Figure 65. The appearance of two bands upon factor Xa cleavage of 'MBP-P3' indicates that it is in fact a fusion protein and not just MBP alone. The obvious bands are ~55kDa,

corresponding to uncut fusion protein and a band of ~50kDa, probably corresponding to MBP. The small second cleavage product is not observed on the gel as the markers indicate that a protein of approximately 21.5kDa is the smallest protein likely to be observed. Perhaps the protein released, and lost, could correspond to 3AB, or 3A. The approximate size of MBP-3AB is 63.8kDa. Perhaps the band of ~55kDa could correspond to MBP-3A, however this is unlikely unless further degradation has occurred or the 3A region is truncated more so than previously thought. It must be borne in mind that a truncated 3A region was used for cloning purposes. Interestingly, prolonged induction times of P3/pMAL also caused clearing of the culture and this could imply that autocatalytic cleavage is occurring releasing toxic MBP-3AB or MBP-3A, resulting in 'leaky' cells as was observed with expression of HAV 3A by both my 3AB/pMAL construct and by Beneduce *et al.* (1995).

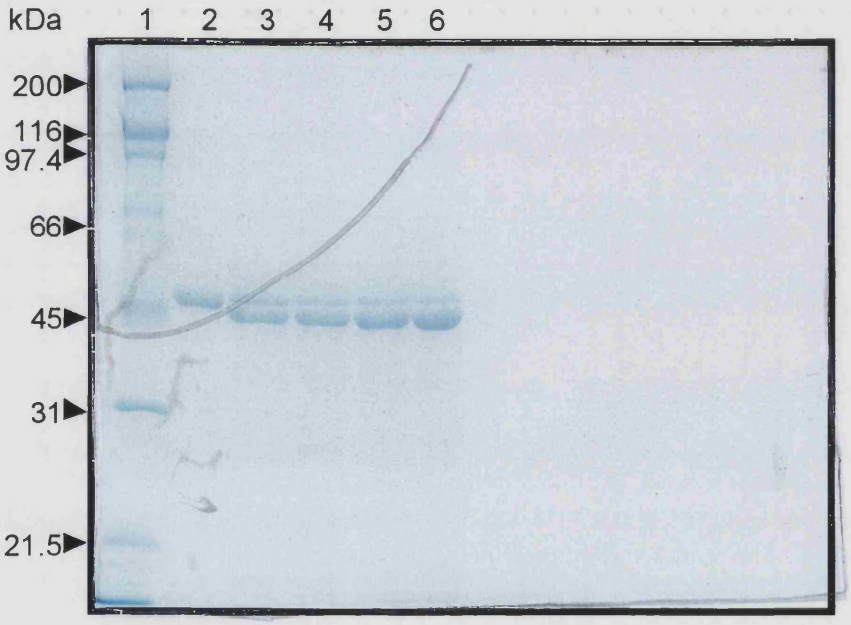

Figure 65: Factor Xa cleavage of MBP-P3

Coomassie-stained 10% SDS-PAGE gel.

Lane 1:	markers	
Lane 2:	uncut	pilot-scale
Lane 3:	2 hour digestion	
Lane 4:	4 hour digestion	
Lane 5:	8 hour digestion	
Lane 6:	24 hour digestion	

4.2.7.2 Factor Xa cleavage of MBP-3C

In the case of 3C/pMAL the band of 75kDa corresponding to MBP-3C was clearly present in all 7 lanes (Figure 66). As expected, and hoped for, digestion with factor Xa produced a further two bands of ~50kDa (expected to be MBP) and one of 24kDa, the size of the target protein, 3C, alone.

4.2.7.3 Factor Xa cleavage of MBP-3D

3D/pMAL eluted from column appeared to be a heterogeneous mixture even before cleavage commenced. The uncut sample originated from pooled concentrated samples eluted from a 15ml amylose column, as was described in Chapter 2. The bands appearing at the very top of the gel of molecular mass ~100kDa may be MBP-3D. Other bands of ~75kDa and ~66kDa were also observed throughout the samples, as well as a band of ~50kDa (MBP) and the target protein appears as a very faint smear at 53kDa as expected. This result is not as 'clean' as that of 3C/pMAL but suggested that it would be possible to purify $3D^{pol}$ from this material. Since I was unable to purify sufficient quantities of MBP-3CD and MBP-P3 due to insolubility and self-cleavage, only MBP-3D and MBP-3C were pursued to this stage.

Figure 66: Factor Xa cleavage of MBP-3C

Coomassie-stained 10% SDS-PAGE gel.

Lane 1:	markers	
Lane 2:	uncut	pilot-scale
Lane 3:	2 hour digestion	
Lane 4:	4 hour digestion	
Lane 5:	8 hour digestion	
Lane 6:	24 hour digestion	
Lane 7:	24 hour digestion	large-scale

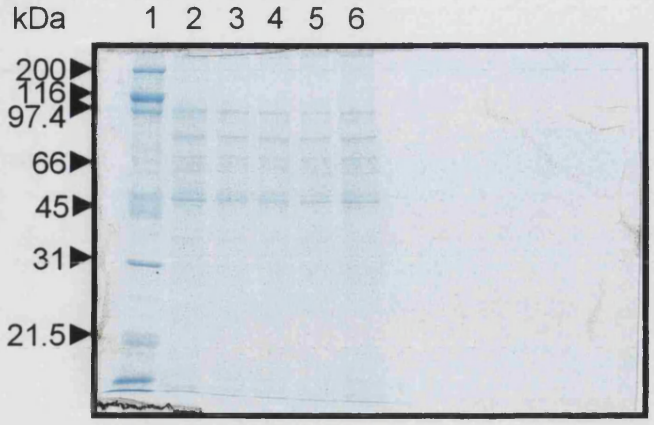

Figure 67: Factor Xa cleavage of MBP-3D

Coomassie-stained 10% SDS-PAGE gel.

Lane 1:	markers	
Lane 2:	uncut	
Lane 3:	2 hour digestion	
Lane 4:	4 hour digestion	pilot-scale
Lane 5:	8 hour digestion	
Lane 6:	24 hour digestion	
Lane 7:	24 hour digestion	large-scale

All three of the fusion proteins containing 3D sequences were analysed further for eventual use in activity assays. Although P3/pMAL offered little hope for eventual purification of the whole P3 region, the observed bacterial lysis was interesting and was worthy of further investigation, unfortunately time for extensive research was unavailable, however attempts at purifying the MBP-P3 protein continued.

4.2.8 FPLC purification of proteins from factor Xa cleavage mixture

As described in Chapter 2, FPLC using anion exchange chromatography with a Mono-Q column was the chosen method for purifying the target protein away from MBP and factor Xa as it provided an additional purification step for removing trace contaminants.

4.2.8.1 FPLC analysis of MBP-3C cleavage mixture

The elution profile for 3C is not shown here, however, SDS-PAGE analysis of the fractions collected are shown in Figure 68 and Figure 69 and indicates that the system continued to work.

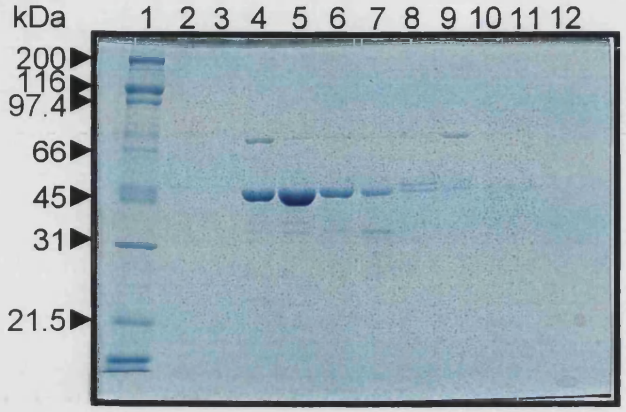

Figure 68: SDS-PAGE analysis of fractions of eluted from Mono-Q column loaded with MBP-3C cleavage mixture- gel 1

Coomassie-stained 10% SDS-PAGE gel

Lane 1:	markers
Lane 2:	aliquot of sample loaded onto column
Lane 3:	aliquot of flow-through during equilibration of column
Lane 4:	fraction 8
Lane 5:	fraction 9
Lane 6:	fraction 10
Lane 7:	fraction 11
Lane 8:	fraction 12
Lane 9:	fraction 13
Lane 10:	fraction 14
Lane 11:	fraction 15
Lane 12:	fraction 16

Protein of ~50kDa, corresponding to MBP was observed along with protein of ~75kDa (uncut MBP-3C?), however no protein bands of 24kDa, corresponding to the target 3C protein were observed. Close inspection of the equilibration flow-through of the Mono-Q column revealed that the 3C target protein had in fact passed straight through the column and predominantly uncleaved or MBP alone was bound to the column. The gels showing this are not shown as the bands were very faint and only visible with the help of a light box. The fractions of flow-through were subsequently concentrated to ~1mg/ml and the resultant solution containing 3C was beaded into liquid nitrogen for storage. It was thought that protease activity assays could be set up if time permitted.

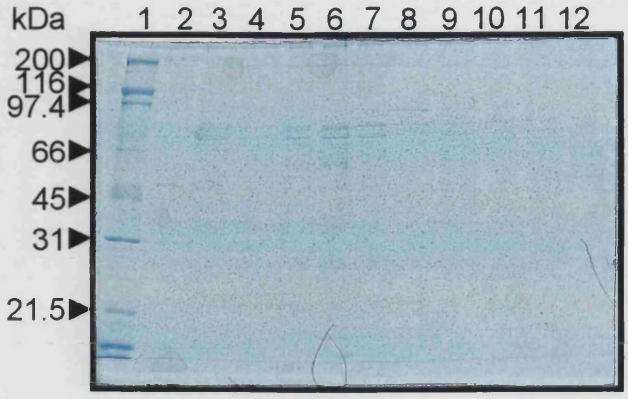

Figure 69: SDS-PAGE analysis of fractions eluted from Mono-Q column loaded with MBP-3C cleavage mixture - gel 2

Coomassie-stained 10% SDS-PAGE gel

Lane 1:	markers
Lane 2:	fraction 17
Lane 3:	fraction 18
Lane 4:	fraction 19
Lane 5:	fraction 20
Lane 6:	fraction 21
Lane 7:	fraction 22
Lane 8:	fraction 23
Lane 9:	fraction 24
Lane 10:	fraction 25
Lane 11:	fraction 26
Lane 12:	fraction 27

4.2.8.2 FPLC analysis of MBP-3D cleavage mixture

The elution profile for MBP-3D cleavage mixture is shown below and revealed the apparent low yield.

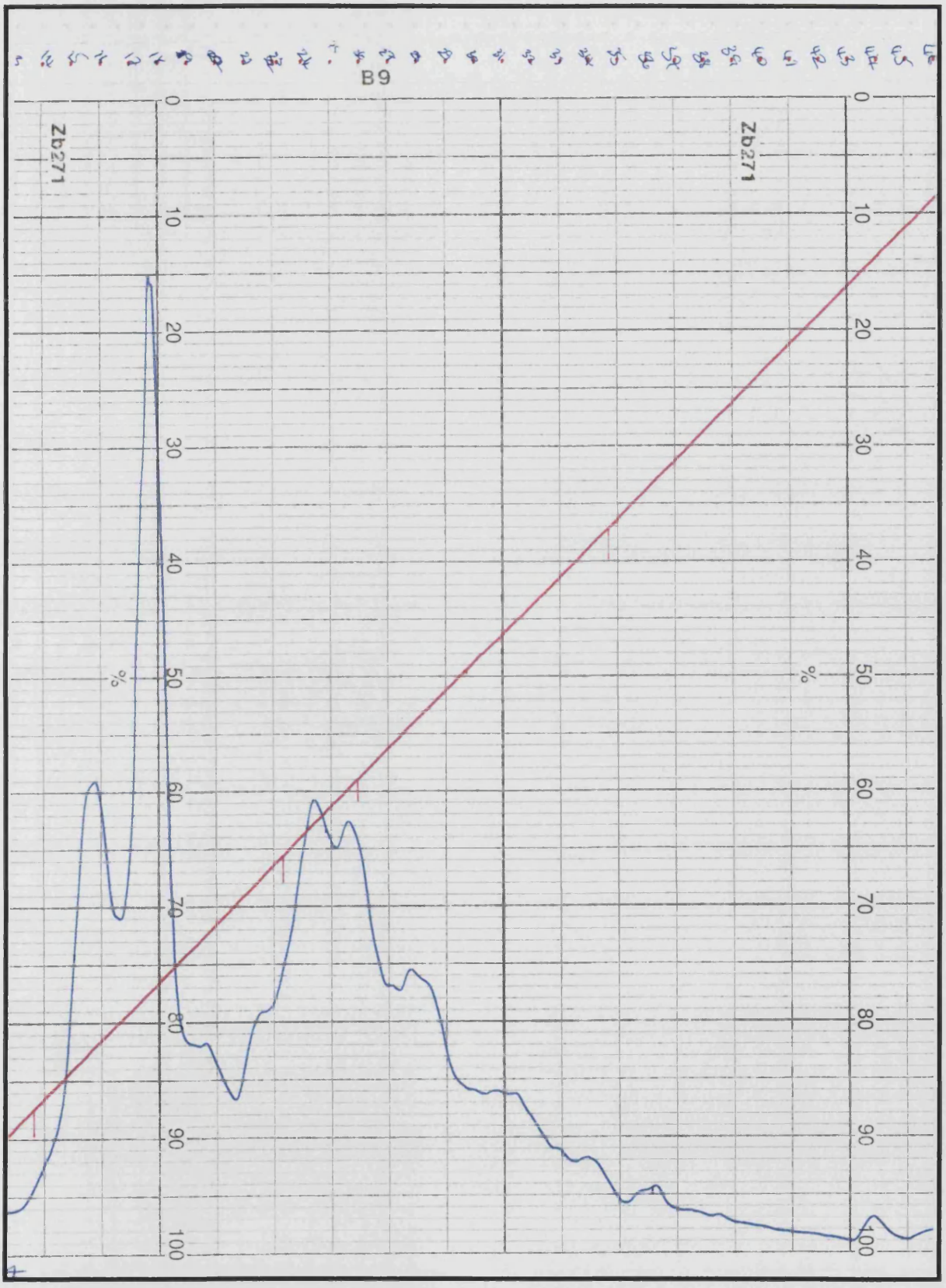

Figure 70: Chart recording of FPLC of 3D-MBP cleavage mixture

6ml fusion protein cleavage mixture (~1mg/ml) was loaded at a rate of 0.5ml/min. Chart recorder running at 0.5cm/ml and 0.5 full scale deflection. Trace represents OD_{260}.

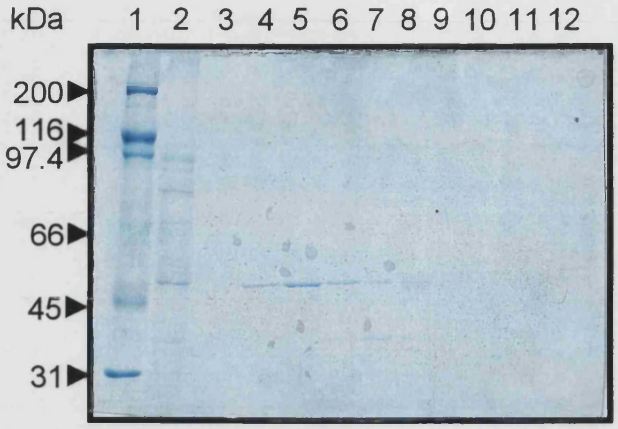

Figure 71: SDS-PAGE analysis of fractions eluted from Mono-Q column loaded with MBP-3D cleavage mixture - gel 1

Coomassie-stained 10% SDS-PAGE gel

Lane 1:	markers
Lane 2:	aliquot of sample loaded onto column
Lane 3:	aliquot of flow-through during equilibration of column
Lane 4:	fraction 17
Lane 5:	fraction 18
Lane 6:	fraction 19
Lane 7:	fraction 20
Lane 8:	fraction 21
Lane 9:	fraction 23
Lane 10:	fraction 24
Lane 11:	fraction 25
Lane 12:	fraction 26

SDS-PAGE analysis of the fractions eluted from a Mono-Q column loaded with cleaved MBP-3D revealed little, with MBP being the protein most easily observed followed by a protein, of ~80kDa. Fractions thought to contain any protein of the desired size were concentrated and the results can be seen in Figure 73.

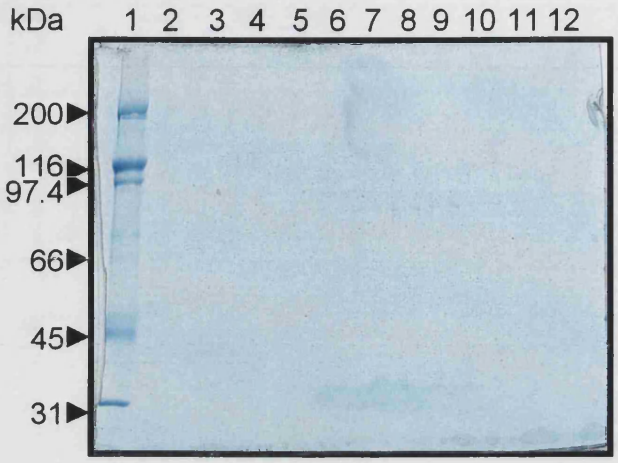

Figure 72: SDS-PAGE analysis of fractions eluted from Mono-Q column loaded with MBP-3D cleavage mixture - gel 2

Coomassie-stained 10% SDS-PAGE gel

Lane 1:	markers
Lane 2:	fraction 27
Lane 3:	fraction 28
Lane 4:	fraction 29
Lane 5:	fraction 30
Lane 6:	fraction 31
Lane 7:	fraction 32
Lane 8:	fraction 33
Lane 9:	fraction 34
Lane 10:	fraction 35
Lane 11:	fraction 36
Lane 12:	fraction 37

Figure 73: Concentration of proteins eluted from Mono-Q column loaded with MBP-3D cleavage mixture

Coomassie-stained 10% SDS-PAGE gel

Lane 1:	markers
Lane 2:	original MBP-3D eluted from amylose column and concentrated
Lane 3:	factor Xa cleavage products loaded onto Mono-Q
Lane 4:	fraction 18 (MBP)
Lane 5:	fraction 27 concentrated (~48kDa?)
Lane 6	fraction 31 and 32 pooled and concentrated (~52kDa?)

Once concentrated the volume of 'purified' protein obtained with 3D in particular, was minute, however the fractions thought to contain protein of, roughly, the desired mass were concentrated to ~0.5mg/ml, beaded into liquid nitrogen and stored for assay purposes. The results indicate that yields of the putative 3D polypeptide were very low (~5μg from 4 litres of culture) and it was not completely pure, however, yields were sufficient to permit assays for RNA polymerase activity to be carried out, on both the MBP-3D fusion protein and the cleaved MBP-3D.

4.3 Discussion

As a first step in the characterisation of the polymerase enzyme, a purified preparation of HAV $3D^{pol}$ was required and having enjoyed limited success with bacterial expression systems, it was thought best to continue down this path. Some problems were encountered with regard to template sequence, primer denaturation etc., however once solved, amplification of the desired regions was successful and allowed subsequent subcloning into pMAL™-c2. Restriction analysis indicated that fragments of the expected size have been cloned into this expression vector and sequencing results show that the inserts have been cloned into pMAL™-c2 in the correct orientation. Expression of the desired proteins was successful to an extent. Some insolubility was initially observed which in some cases was helped to a degree by inducing cultures at lower temperatures for a longer time period as recommended by the manufacturer. Harvesting of the cells had to be undertaken as quickly as possible keeping the cells chilled at all times, which reduced the loss of protein through degradation by proteases released from the bacterial cells during harvesting.

The inserts, P3, 3C, 3CD and 3D, ligated into pMAL-c2, have been over-expressed in *E. coli*, some of the fusion proteins have been affinity purified, cleaved from the MBP by Factor Xa and one, possibly two of these have been separated from the MBP. Overexpression of processing intermediates, such as P3 and 3CD yielded both encouraging and disappointing results: the proteins appeared to be active in their fusion protein form, as autocatalytic cleavage appears to have occurred in the correct positions, resulting in the constituent proteins being seen by SDS-PAGE analysis, however, this proteolysis could be due to indigenous bacterial proteinases recognising the respective cleavage junctures within the expressed proteins of 3CD and P3. Others have experienced such autocatalytic activity when expressing processing intermediates and have had to generate mutants with changes in the cleavage sites to allow purification of the precursor (Harris *et al.*, 1994 and references therein; Kusov & Gauss-Müller, 1997 and references therein). Although active as fusion proteins which was encouraging, the protein linked to the MBP after autocatalysis, important for affinity chromatography, was thought to be 3C, in the case of 3CD, and 3AB, in the case of P3. As such, affinity purification of these intermediates was not ultimately possible.

Protein 3AB of other picornaviruses has been shown to be toxic and the data obtained here suggest that HAV 3AB, as a fusion with MBP, is also active in bacterial cells with the observation that clearing of the cultures upon induction occurred, probably correlating with lysis of cells as described by Beneduce *et al.* (1995) and Pisani *et al.* (1995). Furthermore, as previously mentioned, the truncated 3A region cloned in would result in a 3A protein

lacking the N-terminal amino acids and the data presented in this Chapter supports the observation of Beneduce *et al.* (1995) that such an N-terminal deletion would render this protein toxic to bacteria. Shortly afterwards, results obtained during expression of this construct revealed that there was a problem. Subsequent DNA analysis of the 3AB/pMAL constructs revealed that the plasmid had lost its insert, the 3AB region. Further attempts at cloning this region proved unsuccessful. Similarly, if P3/pMAL was induced for extended periods of time (8 to 16 hours), clearing of the culture was observed which could be due to autocatalysis or degradation causing release of MBP-3AB or MBP-3A, and this product again causing cell lysis. This result could imply that the 3C protease was also active in the system used. While this was a disappointing result, with regard to eventual purification of 3AB, with hindsight, it was a predictable result and indicates that the system is working. So, with good circumstantial evidence that 3C and 3AB were active in this expression system, it was thought worthwhile to attempt purification and activity analysis of the 3D protein.

When concentrating on the polymerase and protease proteins, limited success was realised. Purification of 3C in acceptable amounts was relatively easy (It was at this stage of the project that Bergmann *et al.* (1997) published their results of the refined crystal structure of this protein), however the larger 3D polymerase proved harder to purify with yields being dismally low and solubility presenting a problem as others have found (Palmer, 1994; Tesar *et al.*, 1994). Attempts at improving solubility by reducing induction temperatures (Bishai *et al.*, 1987) proved marginally helpful, but the yield of 'pure protein' obtained from 4 litres of culture remained poor (<5μg of 'pure' 3D compared with >500μg of 'pure' 3C). It could be that the fusion protein produced was just too large for the bacteria to cope with. Very large-scale expression of this construct would be necessary to actually isolate the target $3D^{pol}$ protein, however, the facilities are not available here. Protease assays of the 3C protein purified would have been another aspect for investigation if time permitted.

Essentially though, a variety of products resulted from these expression experiments which could subsequently be used in activity assays. These included soluble cell extract, MBP-fusion proteins and MBP-fusion cleavage mixture. The 'purified' 3D obtained was thought insufficient for activity assay analysis. Assays were undertaken as described in Chapter 5 using the whole cell extract, MBP-fusion protein and the MBP-fusion cleavage mixture samples described above with the hope of observing some incorporation of ^{3}H-UTP signifying the presence of active polymerase enzyme.

5. Assay for poly(A):oligo(U)-dependent poly(U) polymerase activity and the effect of other non-structural P3 proteins on this activity

5.1 Introduction

Previous attempts to express the HAV 3D region in *E.* coli have been unsuccessful, resulting in intracellular accumulation of an insoluble product which showed no activity (Updike *et al.*, 1990) although the 3C proteinase has been successfully expressed in *E. coli* (Gauss-Müller, 1991). Efforts to detect and characterise a biochemical activity of the 3D protein have so far been unsuccessful (Tesar *et al.*, 1994) although a weak poly(U) polymerase activity was detected in the periplasmic space of *E. coli* carrying pRITPOL (Wolstenholme *et al.*, 1993). The poly(U) polymerase described had many of the properties expected for a picornavirus $3D^{pol}$, with a temperature optimum of about 30°C, a requirement for Mg^{2+} and not Mn^{2+}, and a dependence on the presence of an oligonucleotide primer for activity.

Particular problems highlighted previously include the absence of apparent soluble protein in preparations used for activity assays and, perhaps, inappropriate conditions used for assays. In addition, repeated efforts to show RNA polymerase activity in extracts of HAV-infected BS-C-1 cells, either in a template-dependent form or as an enzyme-template complex, have also been negative (Tesar *et al.*, 1994 and references therein). Preliminary data obtained in this laboratory by Palmer (1994) indicated that a poly(A):oligo(U)-dependent poly(U) polymerase activity, representative of RNA polymerase activity, was present in the cytoplasm of *E. coli* transformed with HAV P3/pMEX8 and in the periplasmic space of *E. coli* transformed with Protein A/HAV P3/pMEX8 as well as pRITPOL. For Palmer (1994) reproducibility of initially encouraging results using this assay, however, presented a problem, and a number of strategies were employed by Palmer (1994) in order to improve the protocol:

1. ***E. coli* strain change to JM-105**

   Eliminated the possibility that the reason for poor enzymic activity was due to construct instability in JRR-600. In the current project, the strain used for assay analysis of pMAL constructs was XL-2 and miniprep analysis revealed that the constructs had been faithfully retained in each case.

2. **Reduced induction period**

   Long induction period of 15 hours leading to degradation of the RNA-dependent RNA polymerase? 5 hour induction was believed to be sufficient for good expression of the 3D protein without risking degradation, however both induction periods were employed here.

3. **Addition of RNAse inhibitors**

   Eliminated the possibility that low activity encountered previously was the result of nuclease-destruction of the radiolabelled RNA due either to reagent contamination or endogenous nucleases in the extracts. Then, as in this study, RNA-guard and dithiothreitol (DTT) were added to the reaction.

4. **Poly(A):poly(U) template**

   To exclude the possibility that a lack of observed $3D^{pol}$ activity was due to a defective oligo(U) primer a new template and primer were investigated by Palmer (1994). Poly(A):poly(U) replaced poly(A) as the template and oligo(U) as the primer. This method assumes that there are imperfections in the template in the form of missing uracil and adenine residues. Any breaks along the poly(U) strand would therefore be filled in by the enzyme, utilising the tritiated UTP. The poly(A):poly(U) template was used in the activity assays reported here.

Here, the poly(A):oligo(U)-dependent poly(U) polymerase assay, originally developed for the PV RNA-dependent RNA polymerase, modified by Palmer (1994) as described in Chapter 2 and explained above, was applied in the detection of HAV RNA-dependent RNA polymerase activity in the available purification products from the pMAL protein purification system. It was hoped that improvements to the results already obtained in this laboratory would be made by use of a more 'pure' enzyme preparation in the form of MBP-fusion protein, MBP-3D. In addition, it was expected that the MBP fusion partner would aid the solubility of the 3D protein. Investigation into the effects of other nonstructural proteins on any enzyme activity observed could also be undertaken using similar preparations of fusion proteins representing the 3CD and P3 regions. At commencement, it was hoped that a 'purified' sample of 3AB or its fusion protein would be available at this stage to determine whether this protein exerts the same stimulation on HAV polymerase activity as its PV counterpart does on PV polymerase activity, however, as previously discussed this was not possible.

Using the HAV 'optimised' protocol, the poly(U) polymerase activity of whole cell lysate (induced for 5 and 15 hours), as well as purified MBP-fusion protein and factor Xa cleaved fusion protein was assessed. Unfortunately, the yield of 'purified' proteins 3D obtained was insufficient for assay analysis. Data gleaned from whole cell lysate experiments appeared confusing and predictions as to what was occurring could not be made, however results obtained from assays undertaken using MBP-fusion proteins proved more promising possibly due to the absence of bacterial contamination.

Furthermore, the results obtained appeared to be reproducible.

This Chapter could be regarded as an investigation into the suitability of the 'optimised/modified' poly(U) polymerase assay as well as an assessment of the effectiveness of using purified fusion proteins or their cleavage products in such assays.

5.2 Results

5.2.1 Assays of crude cell extract of pMAL constructs

Poly(U) polymerase assays of soluble cell lysates of pMAL and 3D/pMAL, and the effect of 3CD/pMAL and P3/pMAL lysates induced also for 5 and 15 hours were undertaken as described and the incorporation of ^{3}H-UTP in nmoles/mg protein was plotted against time (Figure 74).

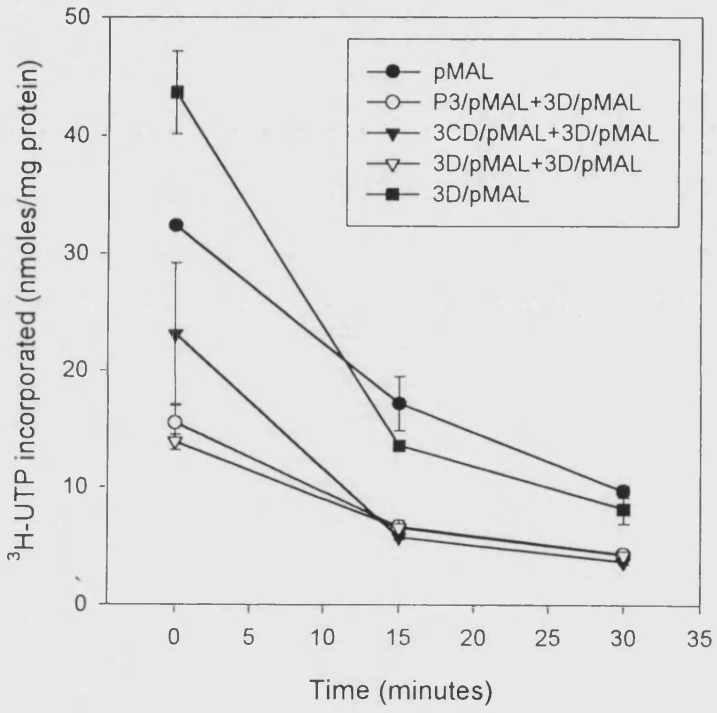

Figure 74: Incorporated ^{3}H-UTP for assays of cell lysates induced for 5 hours

Standard reaction mixture of 125µl containing 50µg protein (25µg single sample assays), 50mM Hepes, 8mM $Mg(CH_3COO)_2$, 1.7µM [5,6-^{3}H] UTP, 20µg/ml poly(A):poly(U) template, 74Units RNA-guard, 4mM DTT, 20µg/ml rifampicin was incubated at 31°C and samples taken at the time points indicated above. All measurements are the average of triplicate samples.

Data from assays undertaken using cell lysates of induced pMAL constructs (5 hour induction) appeared similar to data obtained by Palmer (1994) for the HAV P3/pMEX8, Protein A/HAV P3/pMEX8 and pRITPOL constructs, with high incorporation at time '0'

which decreased to virtually background levels by the next time point. Reaction mixtures were set up simultaneously and incubated on ice until one minute prior to addition of enzyme extract at time '0'. Initial readings were high for all 'enzyme mixtures' tested, but the amount of radiolabelled precipitate measured at '0' minutes decreased as the pre-assay incubation time increased. This suggested that a precipitate incorporating radiolabelled UTP was forming rapidly as the reaction mixture was set up and appeared to partially redissolve before addition of enzyme extract. The precipitate may affect polymerase activity by depriving the enzyme of assay constituents and/or forming an inactive complex with the enzyme. The decrease in detected labelled RNA observed could however be due to the presence of nucleases in the reaction mixture. The conditions described may not therefore be appropriate for assay of the putative HAV RNA polymerase. The 3D/pMAL soluble lysate exhibited the greatest incorporation of ^{3}H-UTP, which was a promising result, however, pMAL alone gave a reading well above background levels. Levels of incorporation for a combination of 3D/pMAL and 3CD/pMAL appear to be above background levels, however, the standard error apparent could indicate no real incorporation. The concentration of protein present could cause interference, with single lysate assays exhibiting greater incorporation throughout the 15 minutes. Strangely, doubling the concentration of 3D/pMAL appeared to reduce incorporation which is not as we would expect if incorporation was really reflecting enzyme activity.

It was hoped that by incorporating more time points poly(U) polymerase activity could be better assessed and as such the assay was repeated with soluble lysates induced for 5 hours and 15 hours (Figure 75 and Figure 76) with sampling taking place at t=0, ½. 2, 5, 10, and 15 minutes.

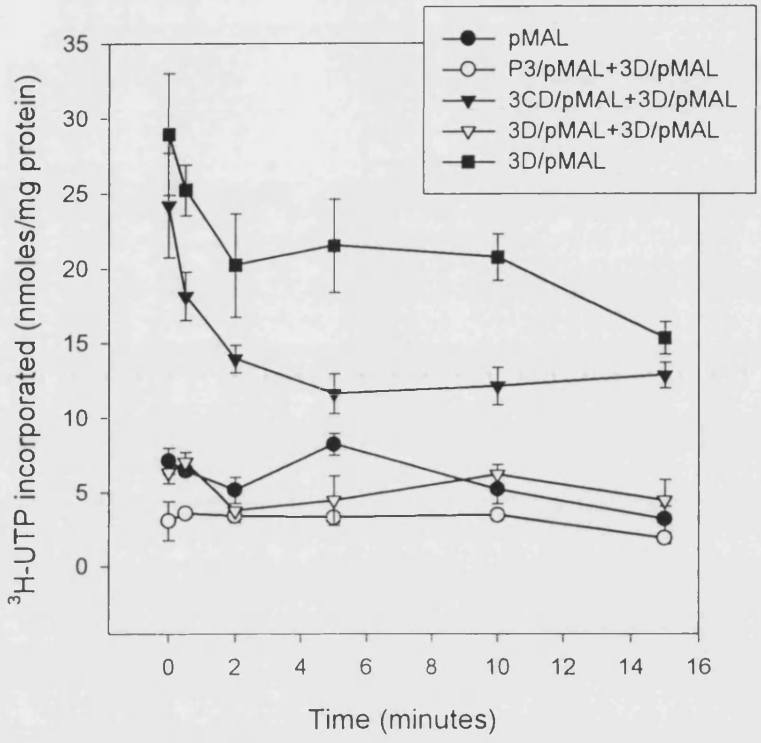

Figure 75: Incorporated ^{3}H-UTP for assays of soluble lysates induced for 5 hours

Standard reaction mixture as before. All measurements are the average of triplicate samples.

Results for 5 hour induced lysates incorporating more time points revealed little more than those using only three time points. A measure of activity, which decayed over time, was observed with 3D/pMAL. When assayed in combination with soluble lysates of3CD/pMALs incorporation of ^{3}H-UTP was also apparent but at a lower level and at a rate which decayed more rapidly than 3D/pMAL alone. This was an encouraging result in that, at least some 'activity' was seen and found to be reproducible (Typical data shown). Lysates of 3D/pMAL mixed with lysates of P3/pMAL and 3D/pMAL were observed to show little activity and in fact exhibited no 'activity' above that observed for pMAL.

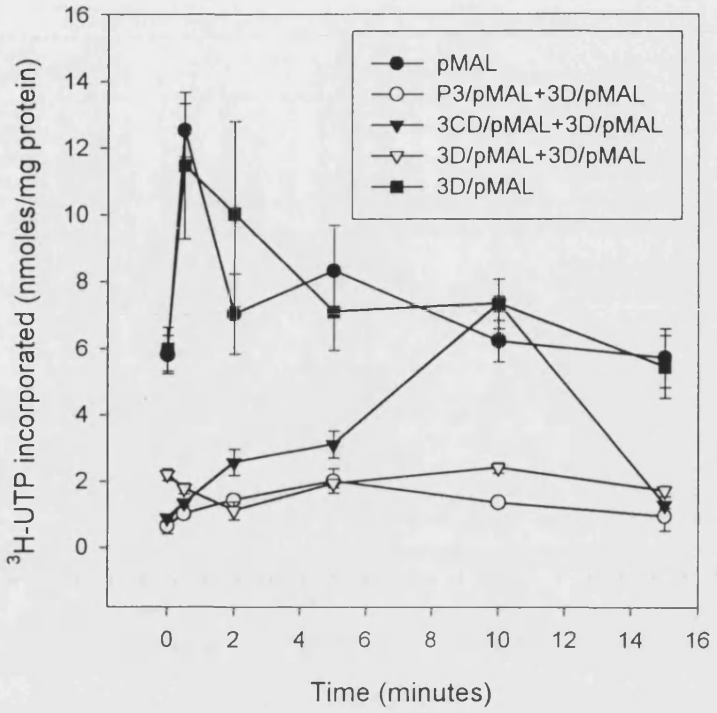

Figure 76: Incorporated ^{3}H-UTP for assays of cell lysates induced for 15 hours
Standard reaction as before. All measurements are the average of triplicate samples.

The incorporation of ^{3}H-UTP observed for 15 hour induced whole cell lysates was dramatically lower than the corresponding figures for 5 hour induced lysates with the highest reading being less than 14nmoles/mg protein compared with more than 30nmoles/mg protein observed for samples induced for 5 hours. Furthermore, data obtained for the lysates of pMAL fusions expressed for 15 hours were confusing to say the least with pMAL alone giving one of the highest readings. If this was really indicative of true enzyme activity, one would expect an increase in activity with an increase in protein concentration, however this was not observed here and the samples containing pMAL or 3D/pMAL alone gave higher readings than those samples containing mixtures of lysates. It could be, yet again, that the sheer amount of protein present in samples induced for such a length of time is causing problems or interfering in some way. Doubling the amount of 3D/pMAL would be expected to give a higher level of incorporation of ^{3}H-UTP as there is more putative enzyme present, however the activity observed for this combination was little more than background suggesting that the precipitation of UTP observed was not due to a true enzyme activity.

The curve representing the 3D/pMAL and 3CD/pMAL lysate mixture displayed an increase in 'activity' which peaked at about 10 minutes then decayed rapidly, however no real conclusions could be drawn from these results. This could be due to RNAse in the lysate being active in spite of the inclusion of inhibitors in the assay buffer. It was hoped that by assaying the purified MBP-fusion proteins, lacking contamination from bacterial proteins, a better picture of the activities of the expressed fusion proteins could be obtained. Furthermore, all subsequent experiments were set up just prior to assaying in order to reduce pre-assay incubation time in the hope of minimising the possible precipitation of assay certain constituents. Moreover, all assays were started with the addition of enzyme as is normal, however radiolabelled UTP became the penultimate solution added to the reaction in the hope of remedying the precipitation problem.

5.2.2 Assays of MBP-fusion proteins

Fusion proteins, eluted from amylose columns, were concentrated to ~1mg/ml and assayed for poly(U) polymerase activity using the 'optimised' protocol employed previously. The fusion proteins assessed, included MBP-3D, MBP-3CD and MBP-P3 and combinations thereof. The results of four separate assays are shown below in Figure 77 and Figure 78.

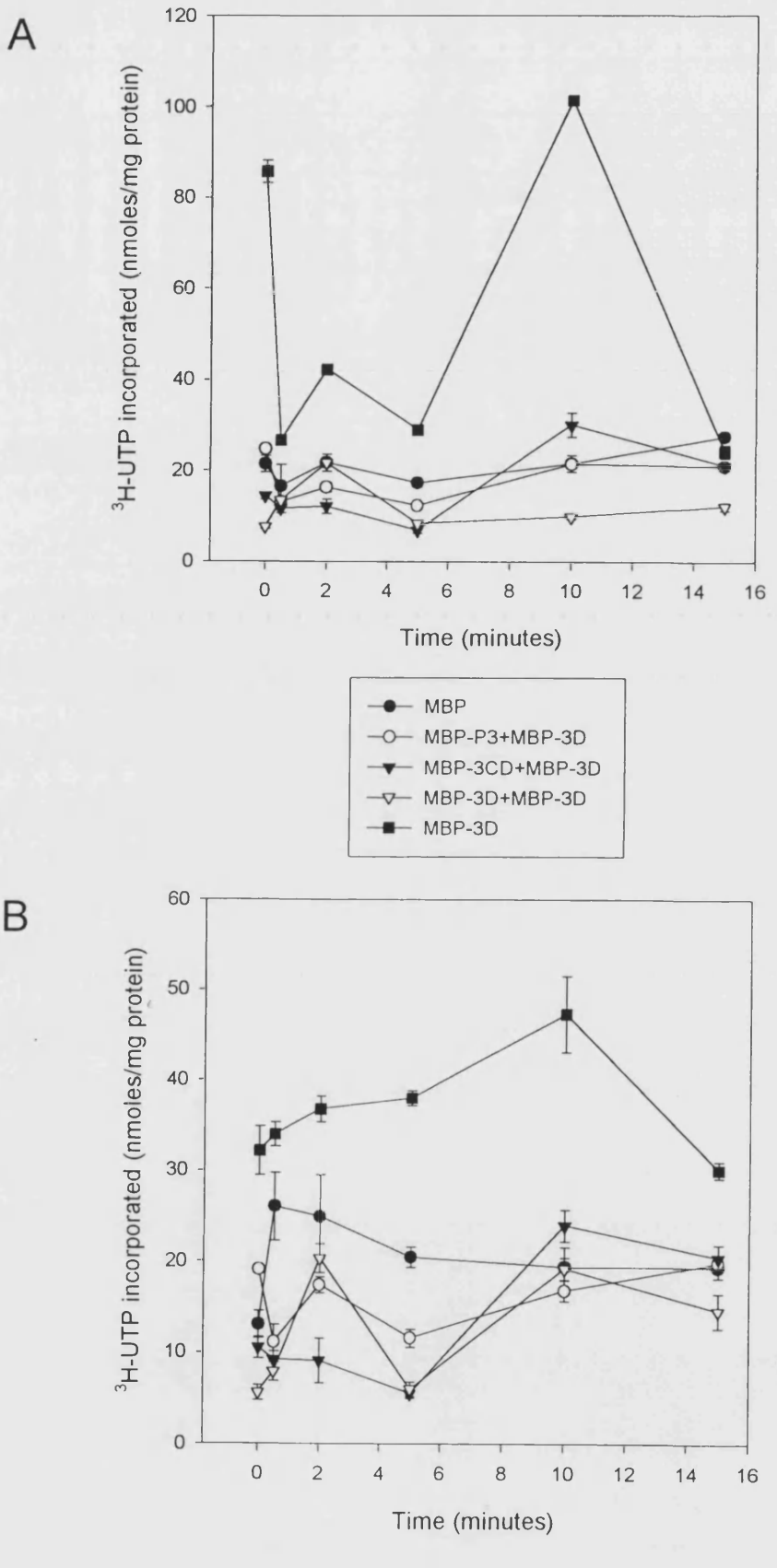

Figure 77: Incorporated ^{3}H-UTP for assay of purified MBP-fusion proteins

Identical assays undertaken, A and B. All measurements are the average of triplicate samples.

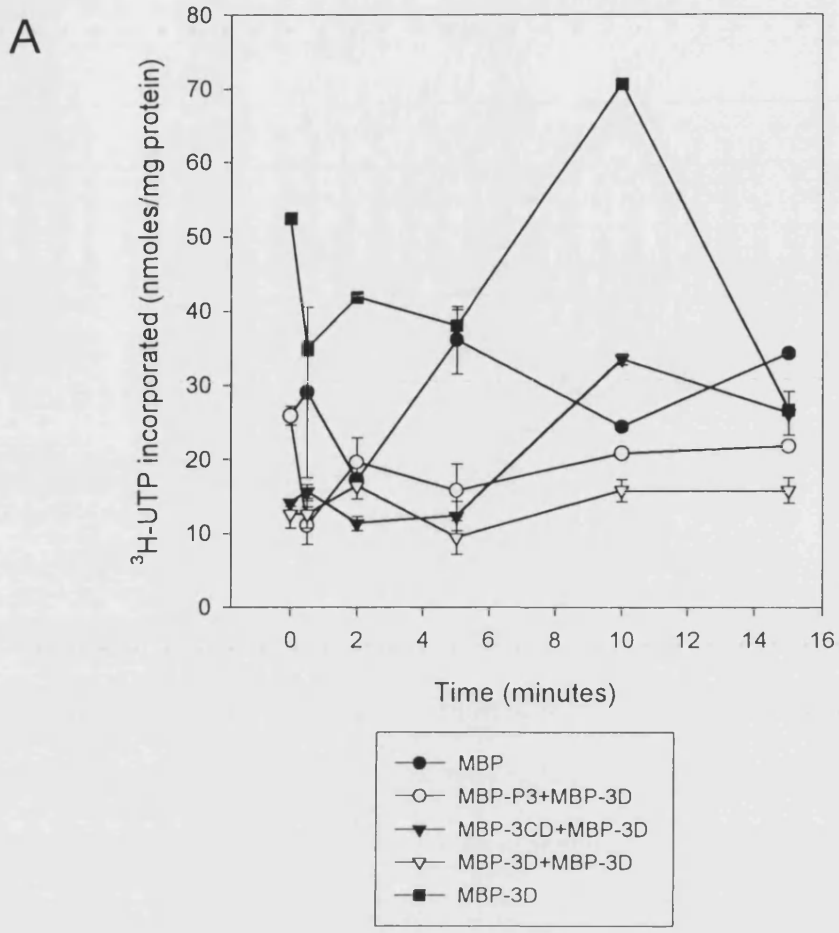

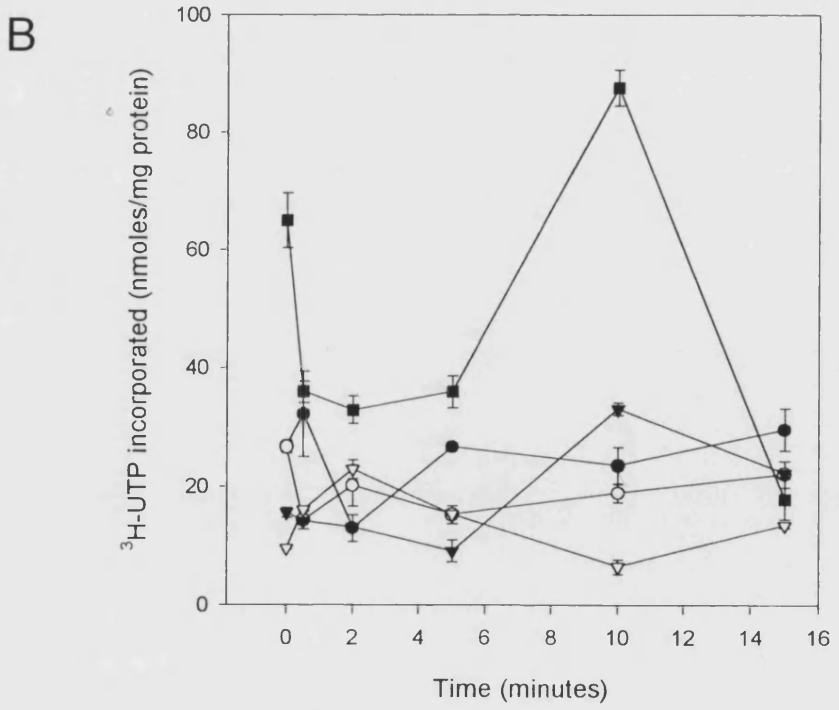

Figure 78: Incorporated ^{3}H-UTP for assay of purified MBP-fusion proteins

Identical assays undertaken, A and B. All measurements are the average of triplicate samples.

Assays of purified MBP-fusion proteins again yielded very confusing results with assays conducted on subsequent days yielding slightly differing results. Four typical results are shown in Figure 77 and Figure 78. Although differences were apparent, a consistent encouraging observation was that a certain degree of incorporation was seen for the MBP-3D protein. Unfortunately, again the sample containing double quantities of MBP-3D revealed very low activity in all assays. In some assays MBP-3D mixed with MBP-P3 showed an increase in the amount of radiolabelled UTP incorporated at about 10 minutes which, although very slight, could be due to the processing of the P3 releasing polypeptides useful or essential for polymerase activity. One would expect in this situation to see a 'lag' phase. This slight 'activity', however decayed toward 15 minutes and in all cases displayed incorporation not much higher than that observed for MBP alone.

5.2.3 Assays of fusion protein cleavage products

Digestion of the MBP-fusion proteins used previously with factor Xa for 24 hours, as described in Chapter 2, yielded cleavage products which although not purified from the MBP, were employed in another set of activity assays. Again, four sets of typical results are shown in Figure 79 and Figure 80.

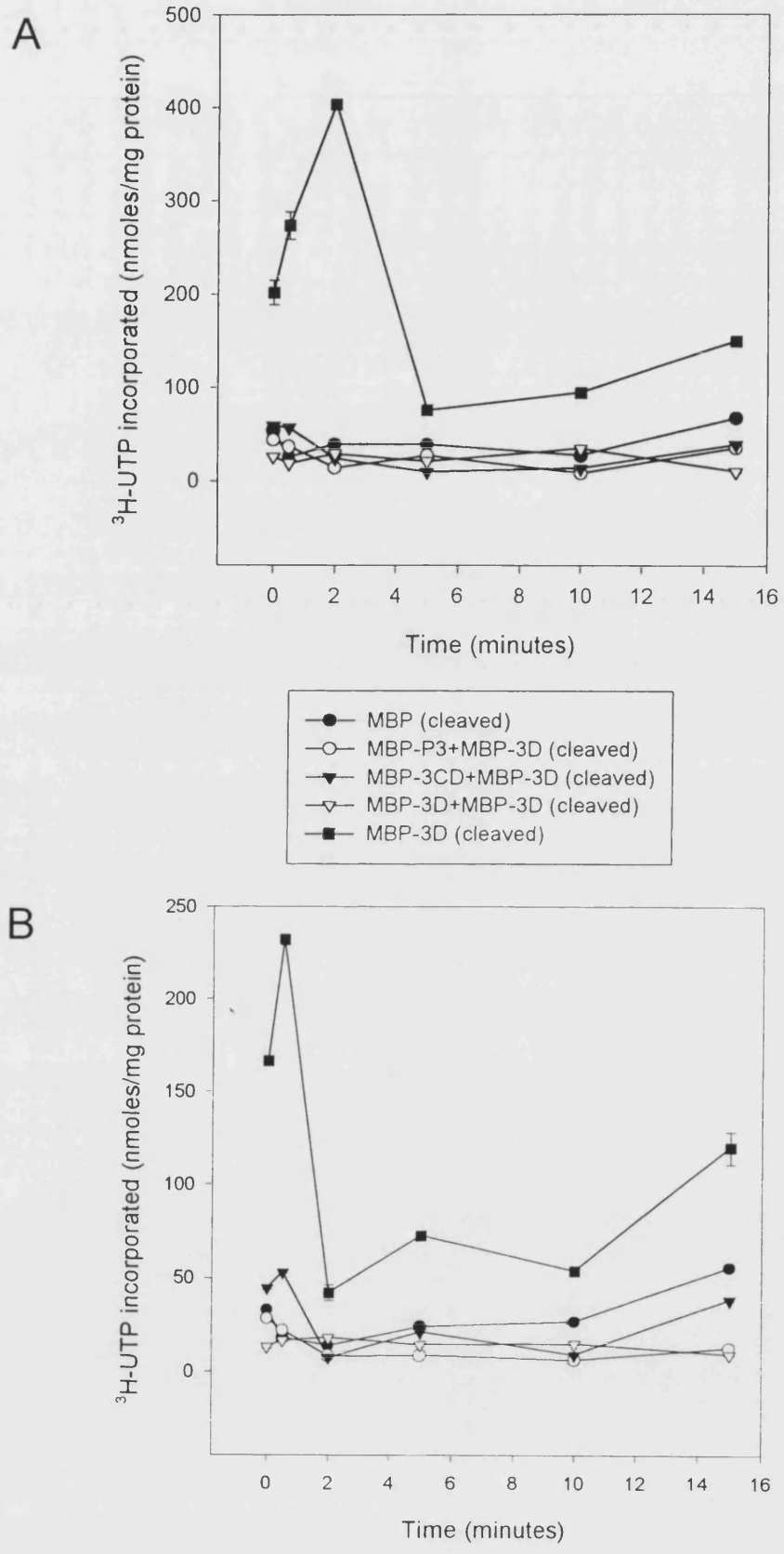

Figure 79: Incorporated ^{3}H-UTP for assays of MBP-fusion cleavage products

Identical assays unertaken, A and B. All measurements are the average of triplicate samples.

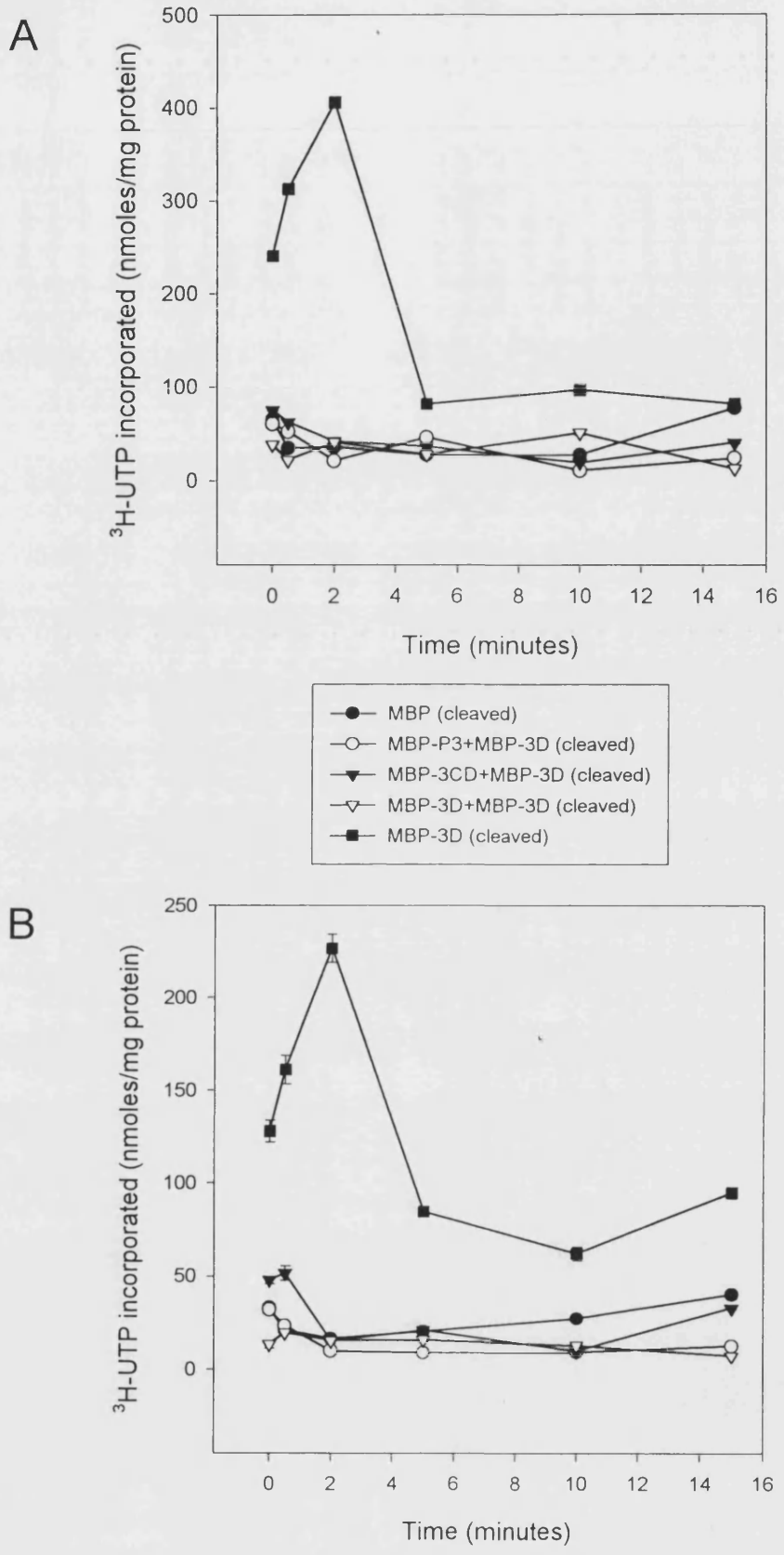

Figure 80: Incorporated H-UTP for assays of MBP-fusion protein cleavage products

Identical assays undertaken, A and B. All measurements are the average of triplicate samples.

In the case of the cleaved fusion proteins, poly(U) activity was apparent for the cleavage products of MBP-3D alone. The activity observed decayed after 2 minutes, almost down to background levels and well below initial levels, indicating degradation of RNA. Interestingly the incorporation of radiolabelled UTP in the case of cleaved MBP-3D occurs rapidly and decay is evident after, at most 5 minutes. This is, in contrast to the incorporation observed for analysis of fusion proteins, where the MBP-3D apparently incorporates ^{3}H-UTP only after at least 5 minutes. Perhaps this is indicative of a 'lag' phase? In some cases, the cleavage products of MBP-3CD mixed with MBP-3D gave a higher than 'background' reading initially which then decayed to background levels. Again, the increased protein present appeared to reduce activity, however cleaved MBP-3CD and cleaved MBP-P3 yielded low results which would not be expected if only protein saturation hampered the enzyme activity. Unfortunately, as before doubling the concentration of cleaved MBP-3D drastically impaired the incorporation of ^{3}H-UTP apparent.

Interestingly, when plotted together (Figure 81), the results for the MBP-fusion proteins and their cleaved products revealed that only the cleaved MBP-3D displayed dramatic poly(U) polymerase activity. When assayed in conjunction with MBP-3CD and MBP-P3, cleaved or uncleaved, all exhibited similar activity profiles, not discernable from the control levels observed for MBP alone. Others have used fusion proteins for successful characterisation of viral polypeptides, however, it was observed here that the 3D protein required cleavage from, but not necessarily separation from, the MBP for activity. The reason for this is not known. In conclusion, however, this was a very encouraging result and implied that the assay, as modified by Palmer (1994), could be suitable for the investigation and characterisation of the HAV 3D^{pol}. The reason why increasing the concentration of MBP-3D cleaved or otherwise reduces the activity observed for MBP-3D alone, remains unknown. It appears though, that the semi-purified 3D protein obtained using the pMAL purification system was both soluble and active and as such, fulfilled some of the aims of this project. Time unfortunately did not permit further investigation of this result.

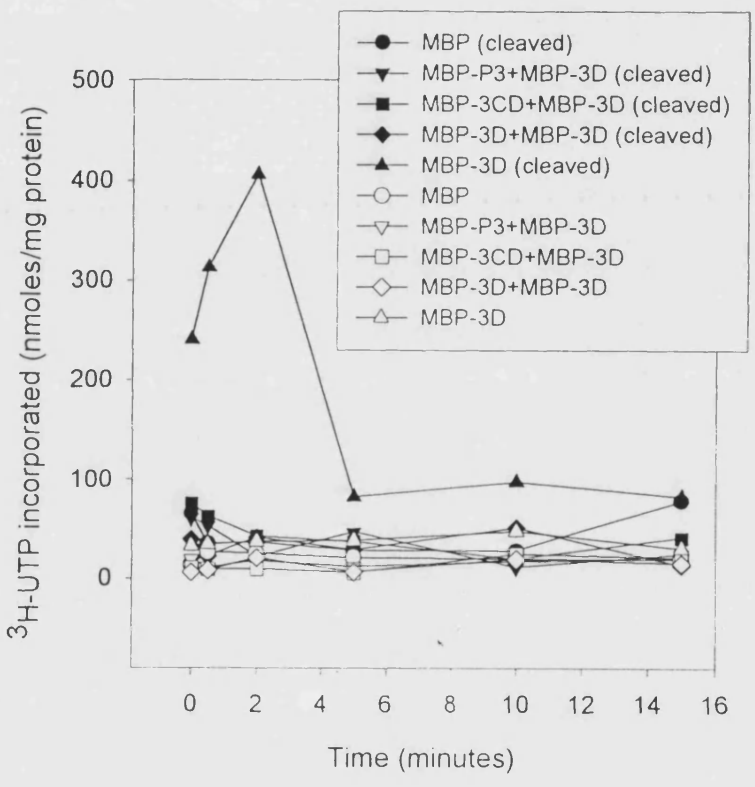

Figure 81: Incorporated ^{3}H-UTP for assays of both MBP-fusions and their cleavage products

Plot of a typical MBP-fusion protein assay result superimposed on a plot of cleaved MBP-fusion protein assay result. All measurements are the average of triplicate samples.

5.3 Discussion

In principle, one of the more easily assayed functions of the polypeptides encoded by the nonstructural regions of picornaviruses is the RNA-and poly(U) polymerising activity of the picornavirus $3D^{pol}$. The $3D^{pol}$ of other picornaviruses have been successfully expressed in bacterial cells and have been shown to have properties similar to the activities detected in infected cells. Generally, bacterially expressed picornavirus RNA polymerases are primer-dependent, usually assayed using a poly(A):oligo(U) template, show a requirement for magnesium ions and are inhibited by manganese, with a temperature optimum of about 30°C (Morrow *et al.*, 1987; Richards *et al.*, 1987; Plotch *et al.*, 1989; Neufeld *et al.*, 1991; Sankar & Porter, 1991). Wolstenholme *et al.*, 1993 detected a novel poly(U) polymerase activity in the periplasmic space of *E. coli* cells transformed with pRITPOL and this activity showed many of the expected properties of a picornavirus $3D^{pol}$.

Preliminary assay data of pMAL constructs (5 hour induced cell lysates) appeared similar to data obtained by Palmer (1994) for the Protein A/HAV P3/pMEX8, HAV P3/pMEX8 and pRITPOL constructs used previously, with initial high counts at time '0' which decreased to background levels by the next time point. These results support the observation that a precipitate incorporating radiolabelled UTP was forming rapidly as the reaction mixture was set up, indicating that perhaps the assay conditions of the putative HAV RNA polymerase may not be appropriate. It is conceivable that the RNA polymerase is being subjected to degradation or precipitation in the assay or the enzyme extract due to an inherent insolubility as observed previously (Tesar *et al.*, 1994). It should be noted that the 'zero' time-points were taken after addition of enzyme and a 2 second vortex, and as such are not true zeros. This could imply that a rapid incorporation is observed in the 2 seconds it takes to vortex the tube.

Palmer (1994) observed that the 'incorporation' did not decay as rapidly for Protein A/HAV P3/pMEX8 or pRITPOL as observed for the HAV P3/pMEX8 construct, possibly due to a lower concentration of endogenous nucleases located in the periplasmic space than in the intracellular extract. Here, only intracellular extracts were used and as such no comparison regarding decay could be made. Decay of the 'activity' was however observed, and in some cases was very rapid, often decaying to background levels after only 2 to 5 minutes.

Fears of degradation of the RNA-dependent RNA polymerase due to a long induction

period of 15 hours appeared unfounded; however, the vast quantities of protein present in some samples appeared to interfere with the putative polymerase activity although the mechanisms of this interference are not known. It could be, however, that degradation is occurring, hence the low activity observed. If this was the case, however, it would be unlikely that the 3D/pMAL and pMAL lysates would show the degree of activity, albeit low, displayed. Furthermore, the 3′ NTR may be required which is known in EMCV to be involved in binding of the polymerase prior to replication, poly(A) alone being unable to bind the enzyme (Cui *et al.*, 1993), and it is conceivable that a lack of both poly(A) tail and the 3′ NTR in this case prevents binding of HAV $3D^{pol}$ to the poly(A):poly(U) template.

Several explanations could be forwarded for the lack of activity observed in cell lysate experiments, including phosphatase contamination of the reaction mixture which may cause UTP degradation such that little UTP can participate in chain elongation. This could be remedied by addition of phosphatase inhibitors to the reaction mixture. The primer or template may be defective or inappropriate thereby inhibiting elongation of the poly(U) chain. It has been shown that when assaying purified picornaviral RNA polymerase, activity becomes absolutely dependent on addition of exogenous template and primer. 50% of normal enzyme activity, however, has been observed in experiments lacking oligo(U), possibly due to the presence of a host factor which normally acts as a primer *in vivo* (Wolstenholme *et al.*, 1993). This could also be explained by the presence of RNase which is not inhibited by the inhibitors used; moreover, perhaps the 3D could have RNase activity itself. The latter could be especially true in the case of purified fusion proteins free from bacterial contamination, unless of course the enzyme has either co-purified with an RNase or perhaps been contaminated during column chromatography with an RNase.

The much sought-after observation of 'activity' of a bacterially-expressed $3D^{pol}$ demonstrated that the assay described could be suitable for the investigation and perhaps eventual characterisation of the HAV $3D^{pol}$. The effect of other nonstructural proteins on this 'activity' could not definitively be investigated, with little in the way of conclusive evidence from addition of MBP-3CD or MBP-P3 (possibly MBP-3AB, MBP-3A, or MBP?) in their variously 'purified' forms to polymerase assays. The observation that the addition of 3CD/pMAL to 3D/pMAL yielded 'activity' above background in some cases was interesting; however, upon addition of more purified forms of these proteins this augmentation was not apparent, implying an artefactual nature of this result. As

described, purification of 3AB was not realised and as such, addition of this protein to standard polymerase assays was not effected which is unfortunate in light of the stimulation afforded by its PV counterpart of PV $3D^{pol}$ which amounts to nearly 100-fold (Lama *et al.*, 1994).

Although not shown, 3C/pMAL, 3CD/pMAL and P3/pMAL, and their respective purified fusion proteins and cleavage products, assayed alone yielded no incorporation above background levels. The lack of activity observed in assays of the two processing intermediates could be due to incorrect cleavages due to processing interference caused by bacterial proteases, although this seems unlikely in view of the SDS-PAGE and Western analysis results demonstrating, what appears to be, correct cleavage, be it autocatalytically or by bacterial intervention. Even more unlikely is the presence of bacterial proteases in purified fusion protein samples implying that this lack of activity is due to another unknown effect. In the case of the putative MBP-P3 or P3/pMAL, lack of activity could purely be due to the fact that no real HAV-specific polypeptides were present and only MBP or a degradation product was present in the reaction. Obviously, the apparent insolubility of MBP-P3 and MBP-3CD would compound the matter, resulting in the absence of the desired protein in the reaction mixture, with only constituent proteins present.

Assuming that the incorporation observed when assaying MBP-3D (and its Factor Xa cleavage product) alone is not artefactual, it is apparent that addition of MBP-3C, MBP-3CD, MBP-3D, MBP-P3, or MBP (and their respective cleavage products) reduces the incorporation observed with MBP-3D (or its cleavage product) alone. This could be due to interference or competition from excess protein by an unknown mechanism. With regard to this phenomenon in the assays where doubling the amount of MBP-3D in the reaction also reduces the apparent incorporation, it is possible that by assaying a more dilute sample would dilute out an inhibitor present in the sample, thus allowing more incorporation to occur. After an initial increase in incorporation with time a reduction is observed in most of the graphs showing MBP-3D or MBP-3D cleavage products and it would be beneficial to investigate the cause of this, whether it be due to RNases or some other mechanism of degradation.

The weak poly(U) polymerase activity observed previously by Wolstenholme and colleagues (1993) could arise in one of three possible ways, listed overleaf:

1. **Protein 3CD is active as a polymerase**
   If this is the case, one would expect the activity to decline rapidly as cleavage would result in production of 3C and 3D, both lacking activity.

2. **Polymerase becomes active when cleavage of 3CD releases 3D**
   If this is the case, one would expect to see a lag phase and sigmoid curve, as with time an increase in the enzyme concentration would be seen resulting in an increase in activity.

3. **Both of the above occur**
   If both 1 and 2 are true, one would expect an intermediate result. It is unlikely that both would have the same activity, one would be more active than the other.

The basis for the slow growth properties of HAV likely resides in the activities and functions of its nonstructural proteins or RNA sequences. The absence of virus-induced interference with host cell macromolecular synthesis and the failure to accumulate nonstructural proteins during infection (Updike *et al.*, 1991) have impeded the characterisation of viral proteins by standard analyses of infected cell cultures. Some progress has been made, however by expression of subgenomic HAV cDNAs in recombinant systems (Gauss-Müller *et al.*, 1991; Jia *et al.*, 1991a; Harmon *et al.*, 1992). It has been suggested that the slow replication of HAV in cell culture may be due to inefficient replication of viral RNA (Anderson *et al.*, 1988) although this also could be explained by an inefficient viral RNA polymerase however expression of the HAV 3D in *E. coli* remains elusive, with prior attempts resulting in intracellular accumulation of an insoluble product which showed no activity (Updike *et al.*, 1990). Overall, therefore, the lack of activity observed is not a new phenomenon. A similar lack of polymerase activity has been routinely observed when attempting to assay HAV 3D protein from other expression systems. Repeated efforts to show RNA polymerase activity in extracts of HAV-infected BS-C-1 cells, either in a template-dependent form or as an enzyme-template complex, have also been negative (Tesar *et al.*, 1994 and references therein).

+0

To conclude, however, two observations were made from the work undertaken here. Firstly, the addition of large quantities of protein appeared to inhibit activity. Secondly, the cleavage products of the purified MBP-fusion protein 3D did appear to have some poly(U) polymerase activity albeit at a low level. With hindsight, the use of, perhaps PV $3D^{pol}$, as a positive control would have been useful to assess the performance of the

6. Conclusions

Hepatitis A virus has been classified as a separate genus in the picornavirus family on the basis of relatively low sequence relatedness between its RNA or protein sequences and those of members of the other picornavirus genera (Francki *et al.*, 1991). Moreover, HAV undergoes a slow, relatively prolonged, nonlytic growth cycle resulting in persistent infection of cultured cells, in contrast to the rapid, lytic cycles of other picornaviruses in most host cells (Wheeler *et al.*, 1986a; De Chastonay & Siegl, 1987; Harmon *et al.*, 1989; Cho & Ehrenfeld, 1991).

The main aim of this project was to characterise the non-structural P3 proteins of the HAV in order to elucidate the reason for its slow proliferation in cell culture which is causing practical and economic difficulties in vaccine production. Although not wholly successful in achieving the ultimate aim of characterisation of the $3D^{pol}$ enzyme of HAV, certain advances towards this aim were attained throughout this project. These include:

1. **Successful expression of a polypeptide of the same size as the $3D^{pol}$ enzyme and its partial purification from the periplasm using a GTP-agarose affinity protocol.**

   The GTP-agarose purification protocol was successful in partially purifying the putative 53kDa RNA polymerase from the periplasmic space extract, however a second protein of 36kDa, presumed to be Protein A-3A, was copurified. The fact that the Protein A sequence encodes an IgG binding domain indicates its inadequacies as a fusion partner especially in this case. If this result were reproducible a further purification step, ammonium sulphate fractionation or ion-exchange chromatography, would be necessary before the 53kDa protein is sufficiently pure for use in an assay system free from bacterial proteins. It is interesting to note that the failure of 3CD to bind to GTP supports the observation that the precursor of PV $3D^{pol}$, $3CD^{pro}$, has no RNA polymerase activity (Harris *et al.*, 1992). However, it remains possible that the HAV CD may be a component of the RNA polymerase.

2. **Successful amplification and cloning of P3 regions, 3AB, 3C, 3CD, 3D and the whole of P3, into the pMAL™-c2 expression vector.**

   Amplification of the constituent regions was successful only after problems with template had been solved. Cloning of all of the aforementioned recombinant plasmids regions and transformation of bacteria with these recombinants proved successful with bands of the desired size being observed upon restriction digest. This success was further supported by the presence of bands, in all but one case, of the predicted sizes of the respective fusion proteins as well as sequencing evidence.

3. **Expression of apparently active polypeptides MBP-3C and MBP-3AB as well as expression of MBP-3CD, MBP-3D and MBP-P3.**

Several points can be raised regarding the expression of the MBP-fusion proteins in terms of their activity, solubility and yield. Expression of MBP-3AB resulted in lysis of bacteria supporting the observations of Beneduce *et al.* (1995) and Pisani *et al.* (1995) that protein 3A or 3AB is toxic to bacteria. The 3AB region cloned into pMAL™-c2 actually codes for a protein lacking the first 14 amino acids, thereby lacking the N-terminal negatively charged amino acids thought to be essential for formation of an α-helix with amphipathic properties (Pisani *et al.*, 1995). Furthermore, the data of Beneduce *et al.* (1997) indicate that both the formation of a putative amphipathic helix and the presence of negative charges at N-terminus are crucial for the cytotoxic feature of 3A. This is in contrast with the observations made here, where, upon induction, cell lysis occurred. Unable to purify this protein, the effect of this polypeptide on polymerase activity could not be investigated with regard to the 100-fold stimulation of $3D^{pol}$ as observed in PV upon addition of purified PV 3AB (Lama *et al.*, 1994). The plasmid lost the insert and further attempts at cloning were unsuccessful.

Expression of the P3 and 3CD intermediates revealed that autocatalysis was occurring indicating that either the 3C protease was active or that indigenous bacterial proteinases were effecting cleavage at the correct cleavage sites. Although, again this showed a degree of activity of the MBP-3C protease expressed in this system, it meant that purification of the intermediates was not possible and generation of inserts containing a mutation at the respective cleavage site would be necessary. Solubility of fusion proteins varied with 3C being very easily expressed and purified, 3D, 3CD and P3 were invariably insoluble but by inducing at reduced temperatures, often at 21-23°C, for longer periods, solubility and thereby purification were somewhat improved.

Another interesting observation worthy of a mention is the probable cleavage of MBP-P3 to MBP-3A or MBP-3AB which was evident by virtue of the fact that prolonged induction of P3/pMAL resulted in lysis of bacteria similar to that seen for 3AB/pMAL. A band of the size predicted for MBP-P3 was observed in these cells but was found to be almost wholly insoluble. Cleavage with factor Xa revealed that only a very small protein could be fused to MBP, possibly 3A, but more likely to be a component of the induced MBP protein. This suggests that only very low concentrations of 3AB are

required to lyse the bacterial cells.

Acceptable yields were obtained for few of the fusion proteins, with large cultures being required for each. Losses at each step of purification meant that the eventual yield of purified protein (3C and 3D only) was minimal. Even at this stage the purity of 3D was questionable, with contaminating proteins of other molecular weights.

4. **Assessment of the poly(U) polymerase activity of pMAL constructs by assaying soluble cell lysates, MBP-fusion proteins and their factor Xa cleavage products.**

   Two observations in particular can be highlighted from the series of activity assays undertaken. Firstly, the addition of more protein to the assay appeared to interfere with the incorporation of radiolabelled UTP. Moreover, on doubling the concentration of putative polymerase 'enzyme' a drastic diminution of incorporation was observed. This poses a problem when analysing enzyme activity as one would expect an augmentation of incorporation when increasing the concentration of enzyme. Secondly, reproducible incorporation of large amounts of ^{3}H-UTP was observed consistently when assaying MBP-3D, and in particular its factor Xa cleavage products. Comparison of all the collected data revealed that only the cleaved MBP-3D incorporated radiolabelled UTP at levels above background, however the 'enzyme' did not exhibit classic 'enzyme activity' which was unfortunate. Apparent contamination of the protein with RNase would possibly account for the decay in incorporation observed with time, however, samples free from bacterial contamination also exhibited such decay, which could be due to copurification with an RNase, contamination of the fusion protein with an RNase possibly from the column, or perhaps the MBP-3D protein possesses some RNase activity itself. Increasing enzyme concentration would increase the RNase concentration which could contribute to the diminished incorporation observed when doubling the concentration of the putative polymerase enzyme.

If further investigation into the HAV RNA-dependent RNA polymerase is successful in the long-term, then it will go some way to explaining the slow and non-cytopathic growth of this virus in tissue culture, and eventually lead to the development of a more appropriate and less expensive vaccine against hepatitis A.

7. Appendices

7.1 Appendix 1

7.1.1 Primer location on genome

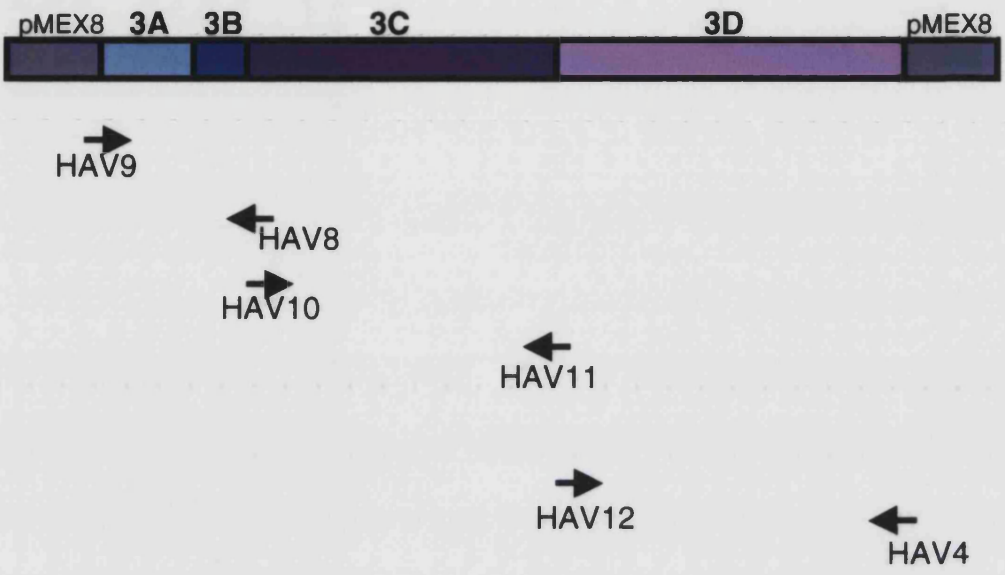

Figure 82: Schematic of HAV P3/pMEX8 showing approximate location of HAV primers

Numbering consistent with text. Not to scale.

7.1.2 Calculation of annealing temperature of primer

Predicted melting temperatures (T_m) of HAV primers estimated using the equation:

$$T_m = 61.8+((41(G+C)-675)/\text{number of nucleotides})$$

7.2 Appendix 2

7.2.1 Primer sequences and location on genome

```
                  <3A
4981 TTGTGGTCTCAGGGAATTTCAGATGATGATAATGATAGTGCAATGGCAGAGTTTTTTCAG 5040
      L  W  S  Q  G  I  S  D  D  D  N  D  S  A  M  A  E  F  F  Q

5041 TCTTTTCCATCTGGTGAACCATCGAATTCCAAATTATCTGGCTTTTTCCAATCTGTTACT 5100
      S  F  P  S  G  E  P  S  N  S  K  L  S  G  F  F  Q  S  V  T

5101 AATCACAAGTGGGTTGCTGTGGGAGCTGCAGTTGGTATTCTTGGAGTGCTCGTTGGGGGA 5160
      N  H  K  W  V  A  V  G  A  A  V  G  I  L  G  V  L  V  G  G
                                                      3A><3B
5161 TGGTTTGTGTATAAGCATTTCTCCCGAAAAGAGGAAGAGCCAATTCCAGCTGAAGGGGTA 5220
      W  F  V  Y  K  H  F  S  R  K  E  E  E  P  I  P  A  E  G  V

5221 TATCATGGTGTAACTAAGCCTAAGCAAGTGATTAAATTAGATGCAGATCCAGTAGAATCT 5280
      Y  H  G  V  T  K  P  K  Q  V  I  K  L  D  A  D  P  V  E  S
     3B><3C
5281 CAGTCAACTTTGGAAATAGCAGGACTGGTTAGGAAGAATTTGGTTCAGTTTGGAGTTGGA 5340
      Q  S  T  L  E  I  A  G  L  V  R  K  N  L  V  Q  F  G  V  G

5341 GAGAAGAATGGATGTGTGAGATGGGTTATGAATGCCTTAGGGGTGAAAGATGATTGGTTG 5400
      E  K  N  G  C  V  R  W  V  M  N  A  L  G  V  K  D  D  W  L

5401 CTTGTACCTTCCCATGCTTACAAATTTGAGAAAGATTATGAAATGATGGAGTTTTATTTT 5460
      L  V  P  S  H  A  Y  K  F  E  K  D  Y  E  M  M  E  F  Y  F

5461 AATAGAGGTGGAACTTACTATTCAATTTCAGCTGGTAATGTTGTCATTCAATCTTTGGAT 5520
      N  R  G  G  T  Y  Y  S  I  S  A  G  N  V  V  I  Q  S  L  D

5521 GTGGGATTTCAGGATGTTGTTCTGATGAAGGTTCCTACAATTCCTAAGTTTAGAGATATT 5580
      V  G  F  Q  D  V  V  L  M  K  V  P  T  I  P  K  F  R  D  I

5581 ACCCAACATTTTATTAAGAAGGGAGATGTGCCTAGAGCTTTGAATCGTCTGGCAACATTA 5640
      T  Q  H  F  I  K  K  G  D  V  P  R  A  L  N  R  L  A  T  L

5641 GTGACAACTGTGAATGGAACTCCTATGTTAATTTCTGAGGGGCCATTAAAGATGGAAGAG 5700
      V  T  T  V  N  G  T  P  M  L  I  S  E  G  P  L  K  M  E  E

5701 AAAGCTACTTATGTTCATAAGAAAAATGATGGTACAACAGTTGATTTAACTGTGGACCAG 5760
      K  A  T  Y  V  H  K  K  N  D  G  T  T  V  D  L  T  V  D  Q

5761 GCATGGAGAGGAAAAGGCGAGGGTCTTCCTGGAATGTGTGGTGGGGCCTTGGTTTCATCA 5820
      A  W  R  G  K  G  E  G  L  P  G  M  C  G  G  A  L  V  S  S

5821 AATCAGTCTATACAGAATGCAATTTTGGGTATTCATGTTGCTGGAGGAAATTCAATTCTT 5880
      N  Q  S  I  Q  N  A  I  L  G  I  H  V  A  G  G  N  S  I  L
                                                              3C>
5881 GTTGCAAAATTGGTTACTCAAGAAATGTTCCAAAATATTGATAAGAAAATTGAAAGTCAG 5940
      V  A  K  L  V  T  Q  E  M  F  Q  N  I  D  K  K  I  E  S  Q
     <3D
5941 AGAATCATGAAAGTGGAATTTACTCAGTGTTCAATGAATGTAGTCTCCAAAACGCTTTTT 6000
      R  I  M  K  V  E  F  T  Q  C  S  M  N  V  V  S  K  T  L  F

6001 AGAAAGAGTCCCATTCATCATCACATTGATAAAACCATGATCAATTTTCCTGCAGCTATG 6060
      R  K  S  P  I  H  H  H  I  D  K  T  M  I  N  F  P  A  A  M
```

```
6061 CCTTTTTCTAAAGCCGAAATTGATCCAATGGCTATGATGTTATCTAAGTATTCATTACCC 6120
      P  F  S  K  A  E  I  D  P  M  A  M  M  L  S  K  Y  S  L  P

6121 ATTGTAGAAGAGCCAGAGGATTATAAAGAAGCTTCAATTTTTTATCAAAATAAAATAGTA 6180
      I  V  E  E  P  E  D  Y  K  E  A  S  I  F  Y  Q  N  K  I  V

6181 GGCAAGACTCAGCTAGTTGATGATTTTCTAGATCTTGATATGGCCATTACAGGGGCCCCA 6240
      G  K  T  Q  L  V  D  D  F  L  D  L  D  M  A  I  T  G  A  P

6241 GGAATTGATGCTATTAATATGGATTCATCTCCTGGATTTCCTTATGTTCAAGAGAGGTTG 6300
      G  I  D  A  I  N  M  D  S  S  P  G  F  P  Y  V  Q  E  R  L

6301 ACCAAAAGAGATTTAATTTGGTTGGATGAGAATGGTTTATTGCTGGGAGTTCATCCAAGA 6360
      T  K  R  D  L  I  W  L  D  E  N  G  L  L  L  G  V  H  P  R

6361 TTGGCTCAGAGAATTTTGTTCAATACTGTCATGATGGAAAATTGTTCTGATTTGGATGTT 6420
      L  A  Q  R  I  L  F  N  T  V  M  M  E  N  C  S  D  L  D  V

6421 GTTTTTACTACTTGCCCAAAAGATGAATTGAGACCATTGGAGAAGGTGTTGGAATCAAAA 6480
      V  F  T  T  C  P  K  D  E  L  R  P  L  E  K  V  L  E  S  K

6481 ACAAGAGCTATTGATGCTTGTCCTCTGGATTACACAATTTTGTGTCGAATGTACTGGGGT 6540
      T  R  A  I  D  A  C  P  L  D  Y  T  I  L  C  R  M  Y  W  G

6541 CCAGCTATTAGTTATTTTCATTTGAATCCAGGGTTCCATACAGGTGTTGCTATTGGCATA 6600
      P  A  I  S  Y  F  H  L  N  P  G  F  H  T  G  V  A  I  G  I

6601 GATCCTGACTGTCAGTGGGATGAATTATTTAAAACAATGATAAGATTTGGAGATGTCGGT 6660
      D  P  D  C  Q  W  D  E  L  F  K  T  M  I  R  F  G  D  V  G

6661 CTTGATTTAGATTTTTCTGCTTTTGATGCTAGTCTTAGTCCATTTATGATTAGGGAAGCA 6720
      L  D  L  D  F  S  A  F  D  A  S  L  S  P  F  M  I  R  E  A

6721 GGTAGAATTATGAGTGAATTGTCTGGAACTCCATCCCATTTTGGAACAGCTCTCATGAAT 6780
      G  R  I  M  S  E  L  S  G  T  P  S  H  F  G  T  A  L  M  N

6781 ACTATCATTTATTCTAAGCATTTGCTGTACAACTGTTGTTATCATGTTTGTGGTTCAATG 6840
      T  I  I  Y  S  K  H  L  L  Y  N  C  C  Y  H  V  C  G  S  M

6841 CCTTCTGGGTCTCCTTGCACAGCTTTGCTGAATTCAATTATCAATAATGTCAATTTGTAT 6900
      P  S  G  S  P  C  T  A  L  L  N  S  I  I  N  N  V  N  L  Y

6901 TATGTGTTTTCCAAGATATTTGGAAAGTCTCCAGTTTTCTTTTGTCAGGCTTTGAAGATT 6960
      Y  V  F  S  K  I  F  G  K  S  P  V  F  F  C  Q  A  L  K  I

6961 CTCTGTTATGGAGATGATGTTCTTATAGTTTTTTCCCGAGATGTTCAGATTGATAATCTT 7020
      L  C  Y  G  D  D  V  L  I  V  F  S  R  D  V  Q  I  D  N  L

7021 GATTTGATTGGACAAAAAATTGTAGATGAGTTTAAGAAACTTGGCATGACAGCTACTTCT 7080
      D  L  I  G  Q  K  I  V  D  E  F  K  K  L  G  M  T  A  T  S

7081 GCTGACAAAAATGTACCTCAGCTGAAGCCAGTTTCAGAATTGACTTTTCTCAAGAGATCT 7140
      A  D  K  N  V  P  Q  L  K  P  V  S  E  L  T  F  L  K  R  S

7141 TTCAATTTGGTAGAAGATAGGATCAGACCTGCAATTTCGGAAAAAACCATTTGGTCTTTG 7200
      F  N  L  V  E  D  R  I  R  P  A  I  S  E  K  T  I  W  S  L

7201 ATAGCATGGCAGAGAAGTAACGCTGAGTTTGAGCAGAATTTGGAAAATGCTCAGTGGTTT 7260
      I  A  W  Q  R  S  N  A  E  F  E  Q  N  L  E  N  A  Q  W  F
```

```
7261 GCTTTTATGCATGGCTATGAGTTTTATCAGAAATTTTATTATTTCGTTCAGTCTTGTTTG 7320
      A  F  M  H  G  Y  E  F  Y  Q  K  F  Y  Y  F  V  Q  S  C  L

7321 GAGAAAGAGATGATAGAATACAGACTAAAATCATATGATTGGTGGAGAATGAGATTCTAT 7380
      E  K  E  M  I  E  Y  R  L  K  S  Y  D  W  W  R  M  R  F  Y
                                 3D>
7381 GACCAGTGCTTCATTTGTGACCTTTCATAA 7411
      D  Q  C  F  I  C  D  L  S  *
```

7.2.2 Primer sequences

PRIMER	SEQUENCE	T_m
LJ1 (sense)	*Cac* 8I 5′TCG GCAAGC TTT CCA TCT GGT GAA CCA TCA AAT TCT AAA TTA TCT AGT TTT TTC CAA TCT$_{3'}$	70.7°C
LJ2 (sense)	*Cac* 8I 5′TCG GCAAGC AGA ATA ATG AAA GTG GAA TTT AGT$_{3'}$	63.2°C
LJ3 (sense)	*Cac* 8I 5′TCG GCAAGC ACT TTG GAA ATA GCA AGT$_{3'}$	59.6°C
LJ4 (anti-sense)	*Bam* HI 5′TCT ACT GGATCC TTA TCA CTG AGA TTC TAC TGG$_{3'}$	61.8°C
LJ5 (anti-sense)	*Bam* HI 5′TCT ACT GGATCC TTA AAC AAA TCA CTG ACT TTC AAT TTT CT$_{3'}$	61.4°C
LJ6 (anti-sense)	*Bam* HI 5′TCT ACT GGATCC TTA AAC AAA TCA TGA AAG GTC ACA A$_{3'}$	61.0°C

PRIMER	SEQUENCE	ESTIMATED T_m
HAV4 (anti-sense)	*Sal* I $^{5'}$TCC GTCGAC TTA AAC AAA TCA TGA AAG GTC ACA $A_{3'}$	57.6°C
HAV8 (anti-sense)	*Kpn* I *Nsi* I $^{5'}$A GCC GGTACC ATGCAT TTA TCA CTG AGA TTC TAC TGG$_{3'}$	62.4°C
HAV9 (sense)	*Kpn* I $^{5'}$T CGG GGTACC ATG TCT TTT CCA TCT GGT GAA CAA TCG AAT TCC AAA TTA TCT GGC TTT TTC CAA $TCT_{3'}$	68.2°C
HAV10 (sense)	*Xmn* I $^{5'}$T CGG GAAGGATTTC ATG AAC TTT GGA AAT AGC AGG $A_{3'}$	60.1°C
HAV11 (anti-sense)	*Sal* I $^{5'}$TCC GTCGAC TTA AAC AAA TCA CTG ACT TTC AAT TTT $C_{3'}$	57.8°C
HAV12 (sense)	*Xmn* I $^{5'}$T CGG GAAGGATTTC ATG AAT TAT GAA AGT GGA GTT TAC TCA $G_{3'}$	61.3°C

7.2.3 Sequence of peptide for antibody production

M I E Y R L K S Y D W W R M F Y D Q C

7.3 Appendix 3

7.3.1 *Escherichia coli* genetic markers

MARKER	DESCRIPTION
Amy	Amylase
Ara	Mutation destroys ability to use arabinose
Cam^r	Chloramphenicol resistance
EndA1	DNA specific endonuclease 1, mutation improves quality and quantity of miniprep
F	Contains the F plasmid
GyrA46	DNA gyrase subunit A
HsdR($r_k^-m_k^+$)	Ablates type I restriction but not methylation of *E. coli* strain K
Lac	Unable to utilise lactose
LacIq	Overproduces the *lac* repressor protein
LacZ	β-Galactosidase
LacZM15	Specific N-terminal deletion permitting α-complementation
ProAB	Requires proline for growth
RecA1	Recombination deficient
RelA1	Permits RNA synthesis in absence of protein synthesis
RpsL	30S ribosomal subunit S12: mutation confers streptomycin resistance
SupE44	Suppressor of amber (UAG) mutations
Thi	Requires thiamin (vitamin B1) for growth
Tn10(tetR)	Contains the TN10 transposon, conferring tetracycline resistance

8. References

Acharya, R., Fry, E., Stuart, D., Fox, G., Rowlands, D., and Brown F. (1989) The three-dimensional structure of foot-and-mouth-disease virus at 2.9Å resolution. *Nature* **337**:709-716.

Agol, V. I. (1997) Recombination and other genomic rearrangements in picornaviruses. *Seminars in Virology* **8**:77-84.

Ahlquist, P., and Kaesberg, P. (1979) Determination of the length distribution of poly(A) at the 3′ terminus of the virion RNAs of EMC virus, poliovirus, rhinovirus, RAV-61 and CPMV and of mouse globin mRNA. *Nucleic Acids Research* **7**:1195-1204.

Aldabe, R., and Carrasco, L. (1995) Induction of membrane proliferation by poliovirus proteins 2C and 2BC. *Biochemical and Biophysical Research Communications* **206**:64-76.

Aldabe, R., Irurzun, A., and Carrasco, L. (1997) Poliovirus protein 2BC increases cytosolic free calcium concentrations. *Journal of Virology* **71**:6214-6217.

Allaire, M., Chernala, M. M., Malcolm, B. A., and James, M. N. G. (1994) Picornaviral 3C cysteine proteinases have a fold similar to chymotrypsin-like serine proteinases. *Nature* **369**:72-76.

Ambros, V., and Baltimore, D. (1978) Protein is linked to the 5′ end of poliovirus by a phosphodiester linkage to tyrosine. *The Journal of Biological Chemistry* **253**:5263-5266.

Ambros, V., and Baltimore, D. (1980) Purification and properties of a HeLa cell enzyme able to remove the 5′ terminal protein from polioviral RNA. *The Journal of Biological Chemistry* **255**:6739-6744.

Ambros, V., Pettersson, R. F., Baltimore, D. (1978) An enzymatic activity in uninfected cells that cleaves the linkage between poliovirion RNA and the 5′ terminal protein. *Cell* **5**:1439-1446.

Anderson, D. A., and Ross, B. C. (1990) Morphogenesis of hepatitis A virus: isolation and characterization of subviral particles. *Journal of Virology* **64**:5284-5289.

Anderson, D. A., Ross, B. C., and Locarnini, S. A. (1988) Restricted replication of hepatitis A virus in cell culture: encapsidation of viral RNA depletes the pool of RNA available for replication. *Journal of Virology* **62**:4201-4206.

Andino, R., Rieckhof, G. E., Achacoso, P. L., and Baltimore, D. (1993) Poliovirus RNA synthesis utilises an RNP complex formed around the 5′-end of viral RNA. *The EMBO Journal* **12**:3587-3598.

Andino, R., Rieckhof, G. E., and Baltimore, D. (1990) A functional ribonucleoprotein complex forms around the 5′ end of poliovirus RNA. *Cell* **63**:369-380.

André, F. E. (1995) Approaches to a vaccine against hepatitis A: development and manufacture of an inactivated vaccine. *The Journal of Infectious Diseases* **171**:S33-S39.

Ansardi, D. C., Porter, D. C., and Morrow, C. D. (1992) Myristylation of poliovirus capsid precursor P1 is required for assembly of subviral particles. *Journal of Virology* **66**:4556-4563.

Ashida, M., Hara, H., Kojima, H., Kamimura, T., Ichida, F., and Hamada, C. (1989) Propagation of hepatitis A virus in hybrid cell lines derived from marmoset liver and Vero cells. *Journal of General Virology* **70**:2487-2494.

Bae, Y. -S., Eun, H. -M., and Yoon, J. -W. (1989) Genomic differences between the diabetogenic and nondiabetogenic variants of encephalomyocarditis virus. *Virology* **170**:282-287.

Baker, S., Richards, O. C., and Ehrenfeld, E. (1995) Elongation activity of poliovirus RNA polymerase derived from Sabin type 1 sequence is not temperature sensitive. *Journal of General Virology* **76**:2081-2084.

Baltimore, D., Girard, M., and Darnell, J. E. (1966) Aspects of the synthesis of poliovirus RNA and the formation of virus particles. *Virology* **29**:179-189.

Banerjee, R., Echeverri, A., and Dasgupta, A. (1997) Poliovirus-encoded 2C polypeptide specifically binds to the 3′-terminal sequences of viral negative-strand RNA. *Journal of Virology* **71**:9570-9578.

Baroudy, B. M., Ticehurst, J. R., Miele, T. A., Maizel Jr., J. V., Purcell, R. H., and Feinstone, S. M. (1985) Sequence analysis of hepatitis A virus cDNA coding for capsid proteins and RNA polymerase. *Proceedings of the National Academy of Science USA* **82**:2143-2147.

Belsham, G. J., and Sonenberg, N. (1996) RNA-protein interactions in regulation of picornavirus RNA translation. *Microbiological Reviews* **60**:499-511.

Beneduce, F., Ciervo, A., and Morace, G. (1997) Site-directed mutagenesis of hepatitis A virus protein 3A: effects on membrane interaction. *Biochimica et Biophysica Acta* **1326**:157-165.

Beneduce, F., Pisani, G., Divizia, M., Panà, A., and Morace, G. (1995) Complete nucleotide sequence of a cytopathic hepatitis A virus strain isolated in Italy. *Virus Research* **36**:299-309.

Bergmann, E. M., Mosimann, S. C., Chernaia, M. M., Malcolm, B. A., and James, M. N. G. (1997) The refined crystal structure of the 3C gene product from hepatitis A virus: specific proteinase activity and RNA recognition. *Journal of Virology* **71**:2436-2448.

Bibb, J. A., Witherell, G., Bernhardt, G., and Wimmer, E. (1994) Interaction of poliovirus with its cell surface binding site. *Virology* **201**:107-115.

Birnboim, H. C., and Doly, J. (1979) A rapid alkaline extraction procedure for screening recombinant plasmid DNA. *Nucleic Acids Research* **7**:1513.

Bishai, W. R., Rappuoli, R., and Murphy, J. R. (1987) High-level expression of a proteolytically sensitive diphtheria-toxin fragment in *Escherichia coli*. *Journal of Bacteriology* **169**:5140-5151.

Bishop, N. E., and Anderson, D. A. (1993) RNA-dependent cleavage of VP0 capsid protein in provirions of hepatitis A virus. *Virology* **197**:616-623.

Bishop, N. E., and Anderson, D. A. (1997) Early interactions of hepatitis A virus with cultured cells: viral elution and the effect of pH and calcium ions. *Archives of Virology* **142**:2161-2178.

Blair, W. S., Nguyen, J. H. C., Parsley, T. B., and Semler, B. L. (1996) Mutations in the poliovirus 3CD proteinase S1-specificity pocket affect substrate recognition and RNA binding. *Virology* **218**:1-13.

Blyn, L. B., Swiderek, K. M., Richards, O. C., Stahl, D. C., Semler, B. L., and Ehrenfeld, E. (1996) Poly (rC) binding protein 2 binds to stem loop IV of the poliovirus RNA 5′-noncoding region - identification by automated liquid chromatography tandem mass spectrometry. *Proceedings of the National Academy of Science USA* **93**:11115-11120.

Blyn, L. B., Towner, J. S., Semler, B. L., and Ehrenfeld, E. (1997) Requirement of poly (rC) binding protein 2 for translation of poliovirus RNA. *Journal of Virology* **71**:6243-6246.

Borman, A. M., and Kean, K. M. (1997) Intact eukaryotic initiation factor 4G is required for hepatitis A virus internal initiation of translation. *Virology* **237**:129-136.

Borman, A. M., Deliat, F. G., and Kean, K. M. (1994) Sequences within the poliovirus internal ribosome entry segment control viral RNA synthesis. *The EMBO Journal* **13**:3149-3157.

Borman, A. M., Le Mercier, P., Girard, M., and Kean, K. M. (1997) Comparison of picornaviral IRES-driven internal initiation of translation in cultured cells of different origins. *Nucleic Acids Research* **25**:925-932.

Borovec, S. V., and Anderson, D. A. (1993) Synthesis and assembly of hepatitis A virus-specific proteins in BS-C-1 cells. *Journal of Virology* **67**:3095-3102.

Brack, K., Frings, W., Dotzauer, A., and Vallbracht, A. (1998) A cytopathogenic, apoptosis-inducing variant of hepatitis A virus. *Journal of Virology* **72**:3370-3376.

Bradford, M. M. (1976) A rapid and sensitive method for the quantitation of microgram quantities of protein utilising the principle of protein-dye binding. *Analytical Biochemistry* **72**:248-254.

Brown, E. A., Day, S. P., Jansen, R. W., and Lemon, S. M. (1991) The 5′ nontranslated region of hepatitis A virus RNA: secondary structure and elements required for translation *in vitro*. *Journal of Virology* **65**:5828-5838.

Burns, C. C., Richards, O. C., and Ehrenfeld, E. (1992) Temperature-sensitive polioviruses containing mutations in RNA polymerase. *Virology* **189**:568-582.

Carneiro, J. S., Equestre, M., Pagnotti, P., Gradi, A., Sonenberg, N., and Bercoff, R. P. (1995) 5′ UTR of hepatitis A virus RNA: mutations in the 5′-most pyrimidine-rich tract reduce its ability to direct internal initiation of translation. *Journal of General Virology* **76**:1189-1196.

Charini, W. A., Todd, S., Gutman, G. A., and Semler, B. L. (1994) Transduction of a human RNA sequence by poliovirus. *Journal of Virology* **68**:6547-6552.

Chemaia, M. M., Malcolm, B. A., Allaire, M., and James, M. (1993) Hepatitis A virus 3C protease: some properties, crystallisation and preliminary crystallographic characterisation. *Journal of Molecular Biology* **234**:890-893.

Cho, M. W., and Ehrenfeld, E. (1991) Rapid completion of the replication cycle of hepatitis A virus subsequent to reversal of guanidine inhibition. *Virology* **180**:770-780.

Cho, M. W., Richards, O. C., Dmitrieva, T. M., Agol, V., and Ehrenfeld, E. (1993) RNA duplex unwinding activity of poliovirus RNA-dependent RNA polymerase $3D^{pol}$. *Journal of Virology* **67**:3010-3018.

Cho, M. W., Teterina, N., Egger, D., Bienz, K., and Ehrenfeld, E. (1994) Membrane rearrangement and vesicle induction by recombinant poliovirus 2C and 2BC in human cells. *Virology* **202**:129-145.

Chow, M., Newman, J. F. E., Filman, D., Hogle, J. M., Rowlands, D. J., and Brown, F. (1987) Myristylation of picornavirus capsid protein VP4 and its structural significance. *Nature* **327**:482-486.

Cohen, J. I., Rosenblum, B., Ticehurst, J. R., Daemer, R. J., Feinstone, S. M., and Purcell, R. H. (1987a) Complete nucleotide sequence of an attenuated hepatitis A virus: comparison with wild-type virus. *Proceedings of the National Academy of Science USA* **84**:2497-2501.

Cohen, J. I., Ticehurst, J. R., Feinstone, S. M., Rosenblum, B., and Purcell, R. H. (1987b) Hepatitis A virus cDNA and its transcripts are infectious in cell culture. *Journal of Virology* **61**:3035-3039.

Cohen, J. I., Ticehurst, J. R., Purcell, R. H., Buckler-White, A., and Baroudy, B. M. (1987c) Complete nucleotide sequence of wild-type hepatitis A virus: comparison with different strains of hepatitis A virus and other picornaviruses. *Journal of Virology* **61**:50-59.

Couch, R. B. (1996) Chapter 23, Rhinoviruses. In *Fields Virology* 3rd edition. Fields, B. N., Knipe, D. M., and Howley, P.M. *et al.* eds. Lippincott - Raven Publishers, Philadelphia. pp713-734.

Coulepis, A. G., Tannock, J. A., Locarnini, S. A., and Gust, I. D. (1981) Evidence that the genome of hepatitis A virus consists of single-stranded RNA. *Journal of Virology* **37**:473-477.

Cowan, R. U., and Anderson, D. A. (1997) Response from Cowan and Anderson. *Trends in Microbiology* **5**:47-48.

Cui, T., Sankar, S., and Porter, A. G. (1993) Binding of encephalomyocarditis virus RNA polymerase to the 3′-noncoding region of the viral RNA is specific and requires the 3′-poly(A) tail. *The Journal of Biological Chemistry* **268**:26093-26098.

Curry, S., Chow, M., and Hogle, J. M. (1996) The poliovirus 135S particle is infectious. *Journal of Virology* **70**:7125-7131.

Curry, S., Fry, E., Blakemore, W., Abu-Ghazaleh, R., Jackson, T., King, A., Lea, S., Newman, J., and Stuart, D. (1997) Dissecting the roles of VP0 cleavage and RNA packaging in picornavirus capsid stabilization: the structure of empty capsids of foot-and-mouth disease virus. *Journal of Virology* **71**:9743-9752.

Das, S., Coward, P., and Dasgupta, A. (1994) A small yeast RNA selectively inhibits internal initiation of translation programmed by poliovirus RNA: specific interaction with cellular proteins that bind to the viral 5′-untranslated region. *Journal of Virology* **68**:7200-7211.

Datta, U., and Dasgupta, A. (1994) Expression and subcellular localization of poliovirus VPg-precursor protein 3AB in eukaryotic cells: evidence for glycosylation *in vitro*. *Journal of Virology* **68**:4468-4477.

Davies, M. V., Pelletier, J., Meerovitch, K., Sonenberg, N., and Kaufman, R.J. (1991) The effect of poliovirus proteinase $2A^{pro}$ expression on cellular metabolism. *The Journal of Biological Chemistry* **266**:14714-14720.

Davis, G. J., Wang, Q. M., Cox, G. A., Johnson, R. B., Wakulchik, M., Dotson, C. A., and Villarreal, E. C. (1997) Expression and purification of recombinant rhinovirus 14 3CD proteinase and its comparison to the 3C proteinase. *Archives of Biochemistry and Biophysics.* **346**:125-130.

de Chastonay, J., and Siegl, G. (1987) Replicative events in hepatitis A virus-infected MRC-5 cells. *Virology* **157**:268-275.

de Prat-Gay, G. (1997) Conformational preferences of a peptide corresponding to the major antigenic determinant of foot-and-mouth disease virus: implications for peptide-vaccine approaches. *Archives of Biochemistry and Biophysics* **341**:360-369.

de Quinto, S. L., and Martínez-Salas, E. (1997) Conserved structural motifs located in distal loops of aphthovirus internal ribosome entry site domain 3 are required for internal initiation of translation. *Journal of Virology* **71**:4171-4175.

de Sena, J, and Mandel, B. (1977) Studies on the *in vitro* uncoating of poliovirus II. Characteristics of the membrane-modified particle. *Virology* **78**:554-566.

Deka, N., Sharma, M. D., and Mukerjee, R. (1994) Isolation of the novel agent from human stool samples that is associated with sporadic non-A, non-B hepatitis. *Journal of Virology* **68**:7810-7815.

del Angel, R. M., Papavassiliou, A. G., Fernández-Tomás, C., Silverstein, S. J., and Racaniello V. R. (1989) Cell proteins bind to multiple sites within the 5′ untranslated region of poliovirus RNA. *Proceedings of the National Academy of Science USA* **86**:8299-8303.

Devereux, J., Haeberli, P., and Smithies, O. (1984) Comprehensive set of sequence-analysis programs for the vax. *Nucleic Acids Research* **12**:387-395.

Diamond, D. C., Wimmer, E., von der Helm, K., and Deinhardt, F. (1986) The genomic map of hepatitis A virus: an alternate analysis. *Microbial Pathogenesis* **1**:217-219.

Doedens, J. R., and Kirkegaard, K. (1995) Inhibition of cellular protein secretion by poliovirus proteins 2B and 3A. *The EMBO Journal* **14**:894-907.

Domingo, E., Díez, J., Martínez, M. A., Hernández, J., Holguín, A., Borrego, B., and Mateu, M. G. (1993) New observations on antigenic diversification of RNA viruses. Antigenic variation is not dependent on immune selection. *Journal of General Virology* **74**:2039-2045.

Dotzauer, A., Feinstone, F. M., and Kaplan, G. (1994) Susceptibility of nonprimate cell lines to hepatitis A virus infection. *Journal of Virology* **68**:6064-6068.

Dotzauer, A., Vallbracht, A., and Keil, G. M. (1995) The proposed gene for VP1 of HAV encodes for a larger protein than that observed in HAV-infected cells and virions. *Virology* **213**:671-675.

Duff, B., and Duff, P. (1998) Hepatitis A vaccine: ready for prime time. *Obstetrics and Gynecology* **91**:468-471.

Duke, G. M., Osorio, J. E., and Palmenberg, A. C. (1990) Attenuation of mengovirus through genetic engineering of the 5′ noncoding poly(C) tract. *Nature* **343**:474-476.

Duplay, P., Bedouelle, H., Fowler, A., Zabin, I., Saurin, W., and Hofnung, M. (1984) Sequences of the malE gene and its product, the maltose-binding protein of *E. coli* K12. *The Journal of Biological Chemistry* **259**:10606-10613.

Echeverri, A. C., and Dasgupta, A. (1995) Amino terminal regions of poliovirus 2C protein mediate membrane binding. *Virology* **208**:540-553.

Egger, D., Pasamontes, L., Bolten, R., Boyko, V., and Bienz, K. (1996) Reversible dissociation of the poliovirus replication complex: functions and interactions of its components in viral RNA synthesis. *Journal of Virology* **70**:8675-8683.

Elroy-Stein, O., Fuerst, T.R., and Moss, B. (1989) Cap-independent translation of mRNA conferred by encephalomyocarditis virus 5′ sequence improves the performance of the vaccinia virus/bacteriophage T7 hybrid expression system. *Proceedings of the National Academy of Science USA* **86**:6126-6130.

Elroy-Stein, O., and Moss, B. (1990) Cytoplasmic expression system based on constitutive synthesis of bacteriophage T7 RNA polymerase in mammalian cells. *Proceedings of the National Academy of Science USA* **87**:6743-6747.

Emerson, S. U., Huang, Y. K., and Purcell, R. H. (1993) 2B and 2C mutations are essential but mutations throughout the genome of HAV contribute to adaptation to cell culture. *Virology* **194**:475-480.

Emini, E. A., Berger, J., and Hughes, J. V. (1985) Priming of an anti-hepatitis-A virus antibody response by poliovirus-specific synthetic peptides: localization of potential antigenic sites of hepatitis-A virus neutralization. *Vaccines 85??*:217-220.

Feinstone, S. M., Kapikian, A. Z., and Purcell, R. H. (1973) Hepatitis A: detection by immune electron microscopy of a viruslike antigen associated with acute illness. *Science* **182**:1026-1028.

Flanegan, J. B., and Baltimore, D. (1977) Poliovirus-specific primer-dependent RNA polymerase able to copy poly(A). *Proceedings of the National Academy of Science USA* **74**:3677-3680.

Frankel, A. D., Mattaj, I. W., and Rio, D. C. (1991) RNA-protein interactions. *Cell* **67**:1041-1046.

Fu, J., Stein, S., Rosenstein, L., Bodwell, T., Routbort, M., Semler, B. L., and Roos, R. P. (1990) Neurovirulence determinants of genetically engineered Theiler viruses. *Proceedings of the National Academy of Science USA* **87**:4125-4129.

Funkhouser, A. W., Raychaudhuri, G., Purcell, R. H., Govindarajan, S., Elkins, R., and Emerson, S. U. (1996) Progress toward the development of a genetically engineered attenuated hepatitis A virus vaccine. *Journal of Virology* **70**:7948-7957.

Gauss-Müller, V., Jürgensen, D., and Deutzman, R. (1991) Autoproteolytic cleavage of recombinant 3C proteinase of hepatitis A virus. *Virology* **182**:861-864.

Gauss-Müller, V., Mingquan, Z., von der Helm, K., and Deinhardt, F. (1990) Recombinant proteins VP1 and VP3 of hepatitis A virus prime for neutralising response. *Journal of Medical Virology* **31**:277-283.

Georgescu, M. M., Balanant, J., Macadam, A., Otelea, D., Combiescu, M., Combiescu, A. A., Crainic, R., and Delpeyroux, F. (1997) Evolution of the Sabin type 1 poliovirus in humans: characterization of strains isolated from patients with vaccine-associated paralytic poliomyelitis. *Journal of Virology* **71**:7758-7768.

Glass, M. J., and Summers, D. F. (1993) Identification of a *trans*-acting activity from liver that stimulates hepatitis A virus translation *in vitro*. *Virology* **193**:1047-1050.

Glass, M. J., Jia, X. -Y., and Summers, D. F. (1993) Identification of the hepatitis A virus internal ribosome entry site: *in vivo* and *in vitro* analysis of bicistronic RNAs containing the HAV 5′ noncoding region. *Virology* **193**:842-852.

Gorbalenya, A. E., Donchenko, A. P., Blinov, V. M., and Koonin, E. V. (1989) Cysteine proteases of positive strand RNA viruses and chymotrypsin-like serine proteases. A distinct protein superfamily with a common structural fold. *FEBS Letters* **243**:103-114.

Gorbalenya, A. E., Koonin, A. P., and Wolf, Y. I. (1990) A new superfamily of putative NTP-binding domains encoded by genomes of small DNA and RNA viruses. *FEBS Letters* **262**:145-148.

Gosert, R., Cassinotti, P., Siegl, G., and Weitz, M. (1996) Identification of hepatitis A virus non-structural protein 2B and its release by the major virus protease 3C. *Journal of General Virology* **77**:247-255.

Gosert, R., Dollenmaier, G., and Weitz, M. (1997) Identification of active-site residues in protease 3C of hepatitis A virus by site-directed mutagenesis. *Journal of Virology* **71**:3062-3068.

Graff, J., and Ehrenfeld, E. (1998) Coding sequences enhance internal initiation of translation by hepatitis A virus RNA *in vitro*. *Journal of Virology* **72**:3571-3577.

Graff, J., Kasang, C., Normann, A., Pfisterer-Hunt, M., Feinstone, S. M., and Flehmig, B. (1994) Mutational events in consecutive passages of hepatitis A virus strain GBM during cell culture adaptation. *Virology* **204**:60-68.

Grubman, M. J., Zellner, M., Bablanian, G., Mason, P. W., and Piccone, M. E. (1995) Identification of the active-site residues of the 3C proteinase of foot-and-mouth disease virus. *Virology* **213**:581-589.

Gutiérrez, A. L., Denova-Ocampo, M., Racaniello, V. R., and del Angel, R. M. (1997) Attenuating mutations in the poliovirus 5′ untranslated region alter its interaction with polypyrimidine tract-binding protein. *Journal of Virology* **71**:3826-3833.

Gutiérrez, A. L., Martínez-Salas, E., Pintado, B., and Sobrino, F. (1994) Specific inhibition of aphthovirus infection by RNAs transcribed from both the 5′ and the 3′ noncoding regions. *Journal of Virology* **68**:7426-7432.

Haghighat, A., Svitkin, Y., Novoa, I., Kuechler, E., Skern, T., and Sonenberg, N. (1996) The eIF4G-eIF4E complex is the target for direct cleavage by the rhinovirus 2A proteinase. *Journal of Virology* **70**:8444-8450.

Hahn, H., and Palmenberg, A. C. (1996) Mutational analysis of the encephalomyocarditis virus primary cleavage. *Journal of Virology* **70**:6870-6875.

Hall, D. J., and Palmenberg, A. C. (1996) Cleavage site mutations in the encephalomyocarditis virus P3 region lethally abrogate the normal processing cascade. *Journal of Virology* **70**:5954-5961.

Hämmerle, T., Hellen, C. U. T., and Wimmer, E. (1991) Site-directed mutagenesis of the putative catalytic triad of poliovirus 3C proteinase. *The Journal of Biological Chemistry* **266**:5412-5416.

Hämmerle, T., Molla, A., and Wimmer, E. (1992) Mutational analysis of the proposed FG loop of poliovirus proteinase 3C identifies amino acids that are necessary for PV-3CD cleavage and might be determinants of a function distinct from proteolytic activity. *Journal of Virology* **66**:6026-6034.

Harmon, S. A., Richards, O. C., Summers, D. F., and Ehrenfeld, E. (1991) The 5′-terminal nucleotides of hepatitis A virus RNA, but not poliovirus RNA, are required for infectivity. *Journal of Virology* **65**:2757-2760.

Harmon, S. A., Updike, W., Jia, X. -Y., Summers, D. F., Ehrenfeld, E. (1992) Polyprotein processing in *cis* and *trans* by hepatitis A virus 3C protease cloned and expressed in *Escherichia coli*. *Journal of Virology* **66**:5242-5247.

Harris, K. S., Reddigari, S. R, Nicklin, M. J. H., Hämmerle, T., and Wimmer, E. (1992) Purification and characterization of poliovirus polypeptide 3CD, a proteinase and a precursor for RNA polymerase. *Journal of Virology* **66**:7481-7489.

Harris, K. S., Xiang, W., Alexander, L., Lane, W. S., Paul, A. V., and Wimmer, E. (1994) Interaction of poliovirus polypeptide $3CD^{pro}$ with the 5′ and 3′ termini of the poliovirus genome. Identification of viral and cellular cofactors needed for efficient binding. *The Journal of Biological Chemistry* **269**:27004-27014.

Hellen, C. U. T., Witherell, G. W., Schmid, M., Shin, S. H., Pestova, T. V., Gil, A., and Wimmer, E. (1993) A cytoplasmic 57-kDa protein that is required for translation of picornavirus RNA by internal ribosomal entry is identical to the nuclear pyrimidine tract-binding protein. *Proceedings of the National Academy of Science USA* **90**:7642-7646.

Hewat, E. A., Verdaguer, N., Fita, I., Blakemore, W., Brookes, S., King, A, Newman, J., Domingo, E., Mateu, M. G., and Stuart, D. I. (1997) Structure of the complex of an Fab fragment of a neutralising antibody with foot-and-mouth disease virus: positioning of a highly mobile antigenic loop. *The EMBO Journal* **16**:1492-1500.

Hogle, J. M., Chow, M., and Filman, D. J. (1985) Three-dimensional structure of poliovirus at 2.9Å resolution. *Science* **229**:1358-1367.

Hollinger, F. B., and Ticehurst, J. R. (1996) Chapter 24, Hepatitis A Virus. In *Fields Virology* 3rd edition. Fields, B. N., Knipe, D. M., and Howley, P.M. *et al.* eds. Lippincott - Raven Publishers, Philadelphia. pp735-782.

Hope, D. A., Diamond, S. E., and Kirkegaard, K. (1997) Genetic dissection of interaction between poliovirus 3D polymerase and viral protein 3AB. *Journal of Virology* **71**:9490-9498.

Jackson, T., Ellard, F. M., Abu-Ghazaleh, R., Brookes, S. M., Blakemore, W. E., Corteyn, A. H., Stuart, D. I., Newman, J. W. I., and King, A. M. Q. (1996) Efficient infection of cells in culture by type O foot-and-mouth disease virus requires binding to cell surface heparan sulfate. *Journal of Virology* **70**:5282-5287.

Jacobson, S. J., Konings, D. A. M., and Sarnow, P. (1993) Biochemical and genetic evidence for a pseudoknot structure at the 3′ terminus of the poliovirus RNA genome and its role in viral RNA amplification. *Journal of Virology* **67**:2961-2971.

Jansen, R. W., Newbold, J. E., and Lemon, S. M. (1988) Complete nucleotide sequence of a cell culture-adapted variant of hepatitis A virus: comparison with wild-type virus with restricted capacity for *in vitro* replication. *Virology* **163**:299-307.

Jarousse, N., Martinat, C., Syan, S., Brahic, M., and McAllister, A. (1996) Role of VP2 amino acid 141 in tropism of Theiler's virus within the central nervous system. *Journal of Virology* **70**:8213-8217.

Jia, X. -Y., Ehrenfeld, E., Summers, D. F. (1991a) Proteolytic activity of hepatitis A virus 3C protein. *Journal of Virology* **65**:2595-2600.

Jia, X. -Y., Scheper, G., Brown, D., Updike, W., Harmon, S., Richards, O., Summers, D., and Ehrenfeld, E. (1991b) Translation of hepatitis A virus RNA *in vitro*: aberrant internal initiations influenced by 5′ noncoding region. *Virology* **182**:712-722.

Jia, X., -Y., Summers, D. F., and Ehrenfeld, E. (1992) Host antibody response to viral structural and nonstructural proteins after hepatitis A virus infection. *The Journal of Infectious Diseases* **165**:273-280.

Jia, X. -Y., Summers, D. F., and Ehrenfeld, E. (1993) Primary cleavage of the HAV capsid protein precursor in the middle of the proposed 2A coding region. *Virology* **193**:515-519.

Jia, X. -Y., Tesar, M., Summers, D. F., Ehrenfeld, E. (1996) Replication of hepatitis A viruses with chimeric 5′ nontranslated regions. *Journal of Virology* **70**:2861-2868.

Jin, Y. -M., Pardoe, I. U., Burness, A. T. H., and Michalak, T. I. (1994) Identification and characterisation of the cell surface 70-kilodalton sialoglycoprotein(s) as a candidate receptor for encephalomyocarditis virus on human nucleated cells. *Journal of Virology* **68**:7308-7319.

Joachims, M., Harris, K. S., and Etchison, D. (1995) Poliovirus protease 3C mediates cleavage of microtubule-associated protein 4. *Virology* **211**:451-461.

Johnson, V. H., and Semler, B. L. (1988) Defined recombinants of poliovirus and Coxsackievirus: sequence-specific deletions and functional substitutions in the 5′-noncoding regions of viral regions of viral RNAs. *Virology* **162**:47-57.

Jürgensen, D., Kusov, Y. Y., Fäcke, M., Kräusslich, H. -G.,, and Gauss-Müller, V. (1993) Cell-free translation and proteolytic processing of the hepatitis A virus polyprotein. *Journal of General Virology* **74**:677-683.

Kaplan, G., Totsuka, A., Thompson, P., Akatsuka, T., Moritsugu, Y., and Feinstone, S. M. (1996) Identification of a surface glycoprotein on African-Green monkey kidney-cells as a receptor for hepatitis A virus. *The EMBO Journal* **15**:4282-4296.

Karnauchow, T. M., Tolson, D. L., Harrison, B. A., Altman, E., Lublin, D. M., and Dimock, K. (1996) The HeLa receptor for enterovirus 70 is decay-accelerating factor (CD55). *Journal of Virology* **70**:5143-5152.

Kaufman, R. J., Davies, M. V., Wasley, L. C., and Michnik, D. (1991) Improved vectors for stable expression of foreign genes in mammalian cells by use of the untranslated leader sequence from EMC virus. *Nucleic Acids Research* **16**:4485-4490.

Kean, K. M., Teterina, N. L., Marc, D., and Girard, M. (1991) Analysis of putative active site residues of the poliovirus 3C protease. *Virology* **181**:609-619.

Kim, S., Smith, T. J., Chapman, M. S., Rossman, M. G., Pevear, D. C., Dutko, F. J., Felock, P. J., Diana, G. D., McKinlay, M. A. (1989) The crystal structure of human rhinovirus serotype 1A (HRV 1A). *Journal of Molecular Biology* **210**:91-112.

Kitamura, N., Semler, B., Rothberg, P. G., Larsen, G. R., Adler, C. J., Dorner, A. J., Emini, E. A., Hanecak, R., Lee, J. J., van der Werf, S., Anderson, C. W., and Wimmer, E. (1981) Primary structure, gene organisation and polypeptide expression of poliovirus RNA. *Nature* **291**:547-553.

Knowlton, K. U., Jeon, E. -S, Berkley, N., Wessely, R., and Huber, S. (1996) A mutation in the puff region of VP2 attenuates the myocarditic phenotype of an infectious cDNA of the Woodruff variant of Coxsackievirus B3. *Journal of Virology* **70**:7811-7818.

Kusov, Y. Y., and Gauss-Müller, V. (1997) *In vitro* RNA binding of the hepatitis A virus proteinase 3C (HAV $3C^{pro}$) to secondary structure elements within the 5′ terminus of the HAV genome. *RNA* **3**:291-302.

Kusov, Y. Y., Morace, G., Probst, C., and Gauss-Müller, V. (1997) Interaction of hepatitis A virus (HAV) precursor proteins 3AB and 3ABC with the 5′ and 3′ termini of the HAV RNA. *Virus Research* **51**:151-157.

Kusov, Y., Weitz, M., Dollenmeier, G., Gauss-Müller, V., and Siegl, G. (1996) RNA-protein interactions at the 3′ end of the hepatitis A virus RNA. *Journal of Virology* **70**:1890-1897.

Laemmli, U. K. (1970) Cleavage of structural proteins during the assembly of the head of bacteriophage T4. *Nature* **227**:680-685.

Lama, J., and Carrasco, L. (1992) Expression of poliovirus nonstructural proteins in *Escherichia coli* cells. *The Journal of Biological Chemistry* **267**:15932-15937.

Lama, J., and Carrasco, L. (1996) Screening for membrane-permeabilizing mutants of the poliovirus protein 3AB. *Journal of General Virology* **77**:2109-2119.

Lama, J., Guinea, R., Martinez-Abarca, F., and Carrasco, L. (1992) Cloning and inducible synthesis of poliovirus nonstructural proteins. *Gene* **117**:185-192.

Lama, J., Paul, A. V., Harris, K. S., and Wimmer, E. (1994) Properties of purified recombinant poliovirus protein 3AB as substrate for viral proteinases and as co-factor for RNA polymerase $3D^{pol}$. *The Journal of Biological Chemistry* **269**:66-70.

Lama, J., Sanz, M. A., and Rodríguez, P. L. (1995) A role for 3AB protein in poliovirus genome replication. *The Journal of Biological Chemistry* **270**:14430-14438.

Lawson, M. A., and Semler, B. L. (1991) Poliovirus thiol proteinase 3C can utilise a serine nucleophile within the putative catalytic triad. *Proceedings of the National Academy of Science USA* **88**:9919-9923.

le Guyader, F., Apaire-Marchais, V., Brillet, J., and Billaudal, S. (1993) Use of genomic probes to detect hepatitis A virus and enterovirus RNAs in wild shellfish and relationship of viral contamination to bacterial contamination. *Applied and Environmental Microbiology* **59**:3963-3968.

Le, S. -Y., Chen, J. -H., Sonenberg, N., and Maizel Jr., J. V. (1993) Conserved tertiary structural elements in the 5′ nontranslated region of cardiovirus, aphthovirus and hepatitis A virus RNAs. *Nucleic Acids Research* **21**:2445-2451.

Lemon, S. M. (1985) Type A viral hepatitis: new developments in an old disease. *The New England Journal of Medicine* **313**:1059-1067.

Lemon, S. M. (1994) Hepatitis A virus. In *Encyclopedia of Virology - Volume 2.* Webster, R. G. and Granoff, A. eds. Academic Press Ltd, London. pp546-554.

Lemon, S. M., and Robertson, B. H. (1993) Current perspectives in the virology and molecular biology of hepatitis A virus. *Seminars in Virology* **4**:285-295.

Lemon, S. M., and Thomas, D. L. (1997) Vaccines to prevent viral hepatitis. *New England Journal of Medicine* **336**:196-204.

Lemon, S. M., Barclay, W., Ferguson, M., Murphy, P., Jing, L., Burke, K., Wood, D., Katrak, K., Sangar, D., Minor, P. D., and Almond, J. W. (1992) Immunogenicity and antigenicity of chimeric picornaviruses which express hepatitis A virus (HAV) peptide sequences: evidence for a neutralization domain near the amino terminus of VP1 of HAV. *Virology* **188**:285-295.

Lemon, S. M., Binn, L. N., and Marchwicki, R. H. (1983) Radioimmunofocus assay for quantitation of hepatitis A virus in cell cultures. *Journal of Clinical Microbiology* **17**:834-839.

Lemon, S. M., Murphy, P. C., Schields, P.A., Ping, L. -H., Feinstone, S. M., Cromeans, S. T., and Jansen, R. W. (1991) Antigenic and genetic variants arising during persistent infection: evidence for genetic recombination. *Journal of Virology* **64**:2056-2065.

Lemon, S. M., Whetter, L., Chang, K. H., and Brown, E. A. (1992) Why do human hepatitis viruses replicate so poorly in cell cultures? *FEMS Microbiology Letters* **100**:455-460.

Leong, L. E. C., Walker, P. A., and Porter, A. G. (1993) Human rhinovirus-14 protease 3C ($3C^{pro}$) binds specifically to the 5′-noncoding region of the viral RNA. *The Journal of Biological Chemistry* **268**:25735-25739.

Linnen, J., Wages Jr., J., Zhang-Keck, Z. -Y., Fry, K. E., Krawczynski, K. Z., Alter, H., Koonin, E., Gallagher, M., Alter, M., Hadziyannis, S., Karayiannis, P., Fung, K., Nakasuji, Y., Shih, J. W. K., Young, L., Piatak, M., Hoover, C., Fernandez, J., Chen, S., Zou, J. C., Morris, T., Hyams, K. C., Ismay, S., Lifson, J. D., Hess, G., Foung, S. K. H., Thomas, H., Bradley, D., Margolis, H., Kim, J. P. (1996) Molecular cloning and disease association of hepatitis G virus: a transfusion-transmissable agent. *Science* **271**:505-508.

Locarnini, S. (1997) The attachment receptor for hepatitis A virus. *Trends in Microbiology* **5**:45-47.

Logan, J. D., Abu-Ghazaleh, R., Blakemore, W., Curry, S., Jackson, T., King, A., Lea, S., Lewis, R., Newman, J., Parry, N., Rowlands, D., Stuart, D., and Fry, E. (1993) Structure of a major immunogenic site on foot-and-mouth-disease virus. *Nature* **362**:566-568.

Lu, H. -H, Li, X., Cuconati, A., and Wimmer, E. (1995) Analysis of picornavirus $2A^{pro}$ proteins: separation of proteinase from translation and replication functions. *Journal of Virology* **69**:7445-7452.

Lu, H. -H., Yang, C. -F., Murdin, A. D., Klein, M. H., Harber, J. J., Kew, O. M., and Wimmer, E. (1994) Mouse neurovirulence determinants of poliovirus type 1 strain LS-a map to the coding regions of capsid protein VP1 and proteinase $2A^{pro}$. *Journal of Virology* **68**:7507-7515.

Lucioni, C., Cipriani, V., Mazzi, S., and Panunzio, M. (1998) Cost of an outbreak of hepatitis A in Puglia, Italy. *Pharmacoeconomics* **13**:257-266.

Luo, M., Vriend, G., Kamer, G., Minor, I., Arnold, E., Rossmann, M. G., Boege, U., Scraba, D. G., Duke, G. M., and Palmenberg A. C. (1987) The atomic structure of Mengo virus at 3.0 Å resolution. *Science* **235**:182-191.

Macadam, A. J., Ferguson, G., Burlison, J., Stone, D., Skuce, R., Almond, J. W., and Minor, P. D. (1992) Correlation of RNA secondary structure and attenuation of Sabin vaccine strains of poliovirus in tissue culture. *Virology* **189**:415-422.

Macadam, A. J., Ferguson, G., Fleming, T., Stone, D. M., Almond, J. W., and Minor, P. D. (1994) Role for poliovirus protease 2A in cap independent translation. *The EMBO Journal* **13**:924-927.

Macadam, A. J., Pollard, S. R., Ferguson, G., Dunn, G., Skuce, R., Almond, J. W., and Minor, P. D. (1991) The 5′ noncoding region of the type 2 poliovirus vaccine strain contains determinants of attenuation and temperature sensitivity. *Virology* **181**:451-458.

MacCallum, F. O. (1947) Homologous serum jaundice. *Lancet* **2**:691-692.

Malcolm, B. A., Chin, S. M., Jewell, D. A., Stratton-Thomas, J. R., Thudium, K. B., Ralston, R., and Rosenberg, S. (1992) Expression and characterisation of recombinant hepatitis A virus 3C proteinase. *Biochemistry* **31**:3358-3363.

Malcolm, B. A., Lowe, C., Shechosky, S., McKay, R. T., Yang, C. C., Shah, V. J., Simon, R. J., Vederas, J. C., and Santi, D. V. (1995) Peptide aldehyde inhibitors of hepatitis A virus 3C proteinase. *Biochemistry* **34**:8172-8179.

Mandel, M., and Higa, A. (1970) Clacium-dependent bacteriophage DNA infection. *Journal of Molecular Biology* **53**:154.

Martin, A., Escriou, N., Chao, S. -F., Girard, M., Lemon, S. M., and Wychowski, C. (1995) Identification and site-directed mutagenesis of the primary (2A/2B) cleavage site of the hepatitis A virus polyprotein: functional impact on the infectivity of HAV RNA transcripts. *Virology* **213**:213-222.

Mateu, M. G. (1995) Antibody recognition of picornaviruses and escape from neutralisation - a structural view. *Virus Research* **38**:1-24.

Matthews, D. A., Smith, W. W., Ferre, R. A., Condon, B., Budahazi, G., Sisson, W., Villafranca, J. E., Janson, C. A., McElroy, H. E., Gribskov, C. L., and Worland, S. (1994) Structure of human rhinovirus 3C protease reveals a trypsin-like polypeptide fold, RNA-binding site, and means for cleaving precursor polyprotein. *Cell* **77**:761-771.

Mattion. N. M., Harnish, E. C., Crowley. J. C., and Reilly, P. A. (1996) Foot-and-mouth disease virus 2A protease mediates cleavage in attenuated Sabin 3 poliovirus vectors engineered for delivery of foreign antigens. *Journal of Virology* **70**:8124-8127.

McBride, A. E., Schlegel, A., and Kirkegaard, K. (1996) Human protein Sam68 relocalization and interaction with poliovirus RNA polymerase in infected cells. *Proceedings of the National Academy of Science USA* **93**:2296-2301.

Melchers, W. J. G., Hoenderop, J. G. J., Bruins Slot, H. J., Pleij, C. W. A., Pilipenko, E. V., Agol, V. I., and Galama, J. M. D. (1997) Kissing of the two predominant hairpin loops in the Coxsackie B virus 3′ untranslated region is the essential structural feature of the origin of replication required for negative-strand RNA synthesis. *Journal of Virology* **71**:686-696.

Melnick, J. L. (1996) Chapter 22, Enteroviruses: polioviruses, Coxsackieviruses, Echoviruses, and newer enteroviruses. In *Fields Virology* 3rd edition. Fields, B. N., Knipe, D. M., and Howley, P.M. *et al.* eds. Lippincott - Raven Publishers, Philadelphia. pp655-712.

Michiels, T., Dejong, V., Rodrigus, R., and Shaw-Jackson, C. (1997) Protein 2A is not required for Theiler's virus replication. *Journal of Virology* **71**:9549-9556.

Mirzayan, C., and Wimmer, E. (1994) Biochemical studies on poliovirus polypeptide 2C: evidence for ATPase activity. *Virology* **199**:176-187.

Molla, A., Harris, K. S., Paul, A. V., Shin, S. H., Mugavero, J., and Wimmer, E. (1994) Stimulation of poliovirus proteinase $3C^{pro}$-related proteolysis by the genome-linked protein VPg and its precursor 3AB. *The Journal of Biological Chemistry* **269**:27015-27020.

Molla, A., Paul, A. V., and Wimmer, E. (1993a) Effects of temperature and lipophilic agents on poliovirus formation and RNA synthesis in a cell free system. *Journal of Virology* **67**:5932-5938.

Molla, A., Paul, A. V., Schmid, M., Jang, S. K., and Wimmer, E. (1993b) Studies on dicistronic polioviruses implicate viral proteinase $2A^{pro}$ in RNA replication. *Virology* **196**:739-747.

Morrow, C. D., Warren, B., and Lentz, M. R. (1987) Expression of enzymatically active poliovirus RNA-dependent RNA polymerase in *Escherichia coli*. *Proceedings of the National Academy of Science USA* **84**:6050-6054.

Moscufu, N., and Chow, M. (1992) Myristate-protein interactions in poliovirus: interactions of VP4 threonine 28 contribute to the structural conformation of assembly intermediates and the stability of assembled virions. *Journal of Virology* **66**:6849-6857.

Mosimann, S. C., Cherney, M. M., Sia, S., Plotch., S., and James, M. N. G. (1997) Refined X-ray crystallographic structure of poliovirus 3C gene product. *Journal of Molecular Biology* **273**:1032-1047.

Moss, E. G., and Racaniello, V. R. (1991) Host range determinants located on the interior of the poliovirus capsid. *The EMBO Journal* **10**:1067-1074.

Murray, M. G., Bradley, J., Yang, X. -F., Wimmer, E., Moss, E. G., and Racaniello, V. R. (1988) Poliovirus host range is determined by a short amino acid sequence in neutralization antigenic site I. *Science* **241**:213-215.

Nainan, O. V., Brinton, M. A., and Margolis, H. S. (1992) Identification of amino acids located in the antibody binding sites of human hepatitis A virus. *Virology* **191**:984-987.

Najarian, R., Caput, D., Gee, W., Potter, S. J., Renard, A., Merryweather, J., van Nest, G., and Dina, D. (1985) Primary structure and gene organisation of human hepatitis A virus. *Proceedings of the National Academy of Science USA* **82**:2627-2631.

Najita, L., and Sarnow, P. (1990) Oxidation-reduction sensitive interaction of a cellular 50kD protein with an RNA hairpin in the 5′ noncoding region of the poliovirus genome. *Proceedings of the National Academy of Science USA* **87**:5846-5850.

Neufeld, K. L., Galarza, J. M., Richards, O. C., Summers, D. F., and Ehrenfeld, E. (1994) Identification of terminal adenylyl transferase activity of the poliovirus polymerase $3D^{pol}$. *Journal of Virology* **68**:5811-5818.

Neufeld, K. L., Richards, O. C., and Ehrenfeld, E. (1991) Purification, characterisation, and comparison of poliovirus RNA polymerase from native and recombinant sources. *The Journal of Biological Chemistry* **266**:24212-24219.

Newman, J. F. E., and Brown, F. (1997) Foot-and-mouth disease virus and poliovirus particles contain proteins of the replication complex. *Journal of Virology* **71**:7657-7662.

Newman, J. F. E., Piatti, P. G., Gorman, B. M., Burrage, T. G., Ryan, M. D., Flint, M., and Brown, F. (1994) Foot-and-mouth disease virus particles contain replicase protein 3D. *Proceedings of the National Academy of Science USA* **91**:733-737.

Nomoto, A., Lee, Y. F., and Wimmer, E. (1976) The 5′-end of poliovirus mRNA is not capped with $m^7G(5')ppp(5')Np$. *Proceedings of the National Academy of Science USA* **73**:375-80.

Nüesch, J. P. F., Weitz, M., and Siegl, G. (1993) Proteins specifically binding to the 3′ untranslated region of hepatitis A virus RNA in persistently infected cells. *Archives of Virology* **128**:65-79.

Nutter, E. L. (1993) First year report. Expression of hepatitis A RNA polymerase in the baculovirus expression system. *Department of Biochemistry, University of Bath.*

Oberste, M. S., and Flanegan, J. B. (1988) Measurement of poliovirus RNA polymerase binding to poliovirion and nonviral RNAs using a filter-binding assay.

Oliveira, M. A., Zhao, R., Lee, W. M., Kremer, M. J., Minor, I., Rueckert, R. R., Diana, G. D., Pevear, D. C., Dutko, F. J., McKinlay, M. A., and Rossmann, M. G. (1993) The structure of human rhinovirus 16. *Structure* **1**:51-68.

Palmenburg, A. C. (1989) Sequence alignments of picornaviral capsid proteins. In *Molecular Aspects of Picornavirus Infection and Detection.* Semler, B. L. and Ehrenfeld, E. eds. American Society for Microbiology, Washington, D.C. pp211-241.

Palmenberg, A. C. (1990) Proteolytic processing of picornaviral polyprotein. *Annual Review of Microbiology* **44**:603-623.

Palmenberg, A. C., and Rueckert, R. R. (1982) Evidence for intramolecular self-cleavage of picornaviral replicase precursors. *Journal of Virology* **41**:244-249.

Palmer, D. G. (1994) Final year project report no. **573**. *School of Biological Sciences, University of Bath.*

Pata, J. D., Schultz, S. C., and Kirkegaard, K. (1995) Functional oligomerisation of poliovirus RNA-dependent RNA polymerase. *RNA* **1**:466-477.

Paul, A. V., Cao, X., Harris, K. S., Lama, J., and Wimmer, E. (1994) Stimulation of poly(U) synthesis by purified poliovirus protein 3AB. *The Journal of Biological Chemistry* **269**:29173-29181.

Paul, A. V., Tada, H., Von der Helm, K., Wissel, T., Kiehn, R., Wimmer, E., and Deinhardt, F. (1987) The entire nucleotide sequence of the genome of human hepatitis A virus (isolate MBB). *Virus Research* **8**:153-157.

Pearson, W. R., and Lipman, D. J. (1988) Improved tools for biological sequence comparison. *Proceedings of the National Academy of Science USA* **85**:2444-2448.

Pfister, T., Egger, D., and Bienz, K. (1995) Poliovirus subviral particles associated with progeny RNA in the replication complex. *Journal of General Virology* **76**:63-71.

Pilipenko, E. V., Gmyl, A. P., Maslova, S. V., Svitkin, Y. V., Sinyakov, A. N., and Agol, V. I. (1992) Prokaryotic-like *cis* elements in the cap-independent internal initiation of translation on picornavirus RNA. *Cell* **68**:119-131.

Ping, L. -H., Jansen, R. W., Stapleton, J. T., Cohen, J. I., and Lemon, S. M. (1988) Identification of an immunodominant antigenic site involving the capsid protein VP3 of hepatitis A virus. *Proceedings of the National Academy of Science USA* **85**:8281-8285.

Pisani, G., Beneduce, F., Gauss-Müller, V., and Morace, G. (1995) Recombinant expression of hepatitis A virus protein 3A: interaction with membranes. *Biochemical and Biophysical Research Communications* **211**:627-638.

Plotch, S. J., and Palant, O. (1995) Poliovirus protein 3AB forms a complex with and stimulates the activity of the viral RNA polymerase, $3D^{pol}$. *Journal of Virology* **69**:7169-7179.

Plotch, S. J., Palant, O., and Gluzman, Y. (1989) Purification and properties of poliovirus RNA polymerase expressed in *Escherichia coli*. *Journal of Virology* **63**:216-225.

Porter, A. G. (1993) Picornavirus nonstructural proteins: emerging roles in virus replication and inhibition of host cell functions. *Journal of Virology* **67**:6917-6921.

Probst, C., Jecht, M., and Gauss-Müller, V. (1997) Proteinase 3C-mediated processing of VP1-2A of two hepatitis A virus strains: *in vivo* evidence for cleavage at amino acid position 273/274 of VP1. *Journal of Virology* **71**:3288-3292.

Provost, P. J., and Hilleman, M. R. (1979) Propagation of human hepatitis A virus in cell culture *in vitro*. *Proceedings of the Society for Experimental Biology and Medicine* **160**:213-221.

Purcell, R. H. (1994) Hepatitis viruses: changing patterns of human disease. *Proceedings of the National Academy of Science USA* **91**:2401-2406.

Racaniello, V. R., and Baltimore, D. (1981) Molecular cloning of poliovirus cDNA and determination of the complete nucleotide sequence of the viral genome. *Proceedings of the National Academy of Science USA* **78**:4887-4891.

Richards, O. C., Baker, S., and Ehrenfeld, E. (1996) Mutation of lysine residues in the nucleotide binding segments of the poliovirus RNA-dependent RNA polymerase. *Journal of Virology* **70**:8564-8570.

Richards, O. C., Hansen, J. L., Schultz, S., and Ehrenfeld, E. (1995) Identification of nucleotide binding sites in the poliovirus RNA polymerase. *Biochemistry* **34**:6288-6295.

Richards, O. C., Ivanoff, L. A., Bienkowska-Szewczyk, K., Butt, B., Petteway Jr., S. R., Rothstein, M. A., and Ehrenfeld, E. (1987) Formation of poliovirus RNA polymerase 3D in *Escherichia coli* by cleavage of fusion proteins expressed from cloned viral cDNA. *Virology* **161**:348-356.

Richards, O. C., Yu, P., Neufeld, K. L., and Ehrenfeld, E. (1992) Nucleotide binding by the poliovirus RNA polymerase. *The Journal of Biological Chemistry* **267**:17141-17146.

Rinehart, J. E., Gómez, R. M., and Roos, R. P. (1997) Molecular determinants for virulence in Coxsackievirus B1 infection. *Journal of Virology* **71**:3986-3991.

Rivera, V. M., Welsh, J. D., and Maizel Jr., J. V. (1988) Comparative sequence analysis of the 5′ noncoding region of the enteroviruses and rhinoviruses. *Virology* **165**:42-50.

Roberts, L. O., and Belsham, G. J. (1997) Complementation of detective picornavirus internal ribosome entry site (IRES) elements by the coexpression of fragments of the IRES. *Virology* **227**:53-62.

Robertson, B. H., Brown, V. K., and Bradley, D. W. (1987) Nucleic acid sequence of the VP1 region of attenuated MS-1 hepatitis A virus. *Virus Research* **8**:309-316.

Rodríguez, P. L., and Carrasco, L. (1993) Poliovirus protein 2C has ATPase and GTPase activities. *The Journal of Biological Chemistry* **268**:8105-8110.

Rodríguez, P. L., and Carrasco, L. (1995)Poliovirus 2C contains two regions involved in RNA binding activity. *The Journal of Biological Chemistry* **270**:10105-10112.

Roehl, H. H., Parsley, T. B., Ho, T. V., and Semler, B. L. (1997) processing of a cellular polypeptide by 3CD proteinase is required for poliovirus ribonucleoprotein complex formation. *Journal of Virology* **71**:578-585.

Rohll, J. B., Moon, D. H., Evans, D. J., and Almond, J. W. (1995) The 3′ untranslated region of picornavirus RNA: features required for efficient genome replication. *Journal of Virology* **69**:7835-7844.

Ross, B. C., and Anderson, D. A. (1991) Characterization of hepatitis A virus capsid proteins with antisera raised to recombinant antigens. *Journal of Virological Methods* **32**:213-220.

Ross, B. C., Anderson, D. A., and Gust, I. D. (1991) Hepatitis A virus and hepatitis A infection. *Advances in Virus Research* **39**:209-253.

Rossmann, M. G., Arnold, E., Erickson, J. W., Frankenberger, E. A., Griffith, J. P., Hecht, H. -J., Johnson, J. E., Kamer, G., Luo, M., Mosser, A. G., Rueckert, R. R., Sherry, B., and Vriend, G. (1985) Structure of a human common cold virus and functional relationship to other picornaviruses. *Nature* **317**:145-153.

Rothberg, P. G., Harris, T. J. R., Nomoto, A., and Wimmer, E. (1978) O^4-(5′-uridylyl) tyrosine is the bond between the genome-linked protein and the RNA of poliovirus. *Proceedings of the National Academy of Science USA* **75**:4868-4872.

Rueckert, R. R. (1996) Chapter 21, *Picornaviridae*: the viruses and their replication. In *Fields Virology* 3rd edition. Fields, B. N., Knipe, D. M., and Howley, P.M. *et al.* eds. Lippincott - Raven Publishers, Philadelphia. pp609-654.

Rueckert, R. R., and Wimmer, E. (1984) Systematic nomenclature of picornavirus proteins. *Journal of Virology* **50**:957-959.

Rueckert, R. R., Dunker, A. K., and Stoltzfus, C. M. (1969) The structure of Maus-Elberfeld virus: a model. *Proceedings of the National Academy of Science USA* **62**:912-919.

Ryan, M. D., and Drew, J. (1994) Foot-and-mouth disease virus 2A oligopeptide mediated cleavage of an artificial polyprotein. *The EMBO Journal* **13**:928-933.

Ryan, M. D., King, A. M. Q., and Thomas, G. P. (1991) Cleavage of foot-and-mouth-disease virus polyprotein is mediated by residues located within a 19 amino acid sequence. *Journal of General Virology* **72**:2727-2732.

Sambrook, J., Fritch, E. F., and Maniatis, T. (1989) Molecular cloning. A laboratory manual. Cold Spring Harbour Laboratory Press, USA.

Sandoval, I. V., and Carrasco, L. (1997) Poliovirus infection and expression of the poliovirus protein 2B provoke the disassembly of the golgi complex, the organelle target for the antipoliovirus drug Ro-090179. *Journal of Virology* **71**:4679-4693.

Sanger, F., Nicklen, S., and Coulson, A. R. (1977) DNA sequencing with chain terminating inhibitors. *Proceedings of the National Academy of Science USA* **74**:5463-5467.

Sankar, S., and Porter, A. G. (1991) Expression, purification and properties of recombinant encephalomyocarditis virus RNA-dependent RNA polymerase. *Journal of Virology* **65**:2993-3000.

Sankar, S., and Porter, A. G. (1992) Point mutations which drastically affect the polymerization activity of encephalomyocarditis virus RNA-dependent RNA polymerase correspond to the active site of *Escherichia coli* DNA polymerase I. *The Journal of Biological Chemistry* **267**:10168-10176.

Schlegel, A., Giddings Jr, T. H., Ladinsky, M. S., and Kirkegaard, K. (1996) Cellular origin and ultrastructure of membranes induced during poliovirus infection. *Journal of Virology* **70**:6576-6588.

Schober, D., Kronenberger, P., Prchla, E., Blaas, D., and Fuchs, R. (1998) Major and minor receptor group human rhinoviruses penetrate from endosomes by different mechanisms. *Journal of Virology* **72**:1354-1364.

Scholtz, E., Heinricy, U., and Flehmig, B. (1989) Acid stability of hepatitis A virus. *Journal of General Virology* **70**:2481-2485.

Schultheiß, T., Kusov, Y. Y., and Gauss-Müller, V. (1994) Proteinase 3C of hepatitis A virus (HAV) cleaves the HAV polyprotein P2-P3 at all sites including VP1/2A and 2A/2B. *Virology* **198**:275-281.

Schultz, D. E., Honda, M., Whetter, L. E., McKnight, K. L., and Lemon, S. M. (1996) Mutations within the 5′ nontranslated RNA of cell culture-adapted hepatitis A virus which enhance cap-independent translation in cultured African green monkey kidney cells. *Journal of Virology* **70**:1041-1049.

Shaffer, D. R., Brown, E. A., and Lemon, S. A. (1994) Large deletion mutations involving the first pyrimidine rich tract of the 5′ nontranslated RNA of human hepatitis A virus define two adjacent domains associated with distinct replication phenotypes. *Journal of Virology* **68**:5568-5578.

Shapiro, C. N. (1994) Transmission of hepatitis viruses. *Annals of Internal Medicine* **120**:82-84.

Shaw, F. (1997) Epidemiology of hepatitis A in the United States. *Viral Hepatitis* **6**:14-15.

Shen, Y., Igo, M., Yalamanchili, P., Berk, A. J., and Dasgupta, A. (1996) DNA binding domain and subunit interactions of transcription factor IIIC revealed by dissection with poliovirus 3C protease. *Molecular Cell Biology* **16**:4163-4171.

Shiroki, K., Ishii, T., Aoki, T., Kobashi, M., Ohka, S., and Nomoto, A. (1995) A new *cis*-acting element for RNA replication within the 5′ noncoding region of poliovirus type 1 RNA. *Journal of Virology* **69**:6825-6832.

Shiroki, K., Ishii, T., Aoki, T., Ota, Y., Yang, W. -X., Komatsu, T., Ami, Y., Arita, M., Abe, S., Hashizume, S., and Nomoto, A. (1997) Host range phenotype induced by mutations in the internal ribosomal entry site of poliovirus RNA. *Journal of Virology* **71**:1-8.

Siegl, G., Weitz, M., and Kronauer, G. (1984) Stability of hepatitis A virus. *Intervirology* **22**:218-226.

Skinner, M. A., Racaniello, V. R., Dunn, G., Cooper, J., Minor, P. D., and Almond, J. W. (1989) New model for the secondary structure of the 5′ non-coding RNA of poliovirus is supported by biochemical and genetic data that also show that RNA secondary structure is important in neurovirulence. *Journal of Molecular Biology* **207**:379-392.

Sommergruber, W., Zorn, M., Blaas, D., Fessl, F., Volkmann, P., Maurer-Fogy, I., Pallai, P., Merluzzi, V., Matteo, M., Skern, T., and Kuechler, E. (1989) Polypeptide 2A of human rhinovirus type 2: identification as a protease and characterization by mutational analysis. *Virology* **169**:68-77.

Stanway, G. (1990) Structure, function and evolution of picornaviruses. *Journal of General Virology* **71**:2483-2501.

Stapleton, J. T., and Lemon, S. M. (1987) Neutralization escape mutants define a dominant immunogenic neutralisation site on hepatitis A virus. *Journal of Virology* **61**:491-498.

Stapleton, J. T., Frederick, J., and Meyer, B. (1991) Hepatitis A virus attachment to cultured cell lines. *The Journal of Infectious Diseases* **164**:1098-1103.

Stewart, S. R., and Semler, B. L. (1997) RNA determinants of picornavirus cap-independent translation initiation. *Seminars in Virology* **8**:242-255.

Strebel, K., and Beck, E. (1986) A second protease of foot-and-mouth-disease virus. *Journal of Virology* **58**:893-899.

Takahara, Y., Ando, N., Kohara, M., Hagino-Yamagishi, K., Nomoto, A., Itoh, H., Numao, N., and Kondo, K. (1989) Purification of enzymatically active poliovirus proteinase 3C produced in *Escherichia coli*. *Gene* **79**:249-258.

Takeda, N., Yang, C. -F., Kuhn, R. J., and Wimmer, E. (1987) Uridylylation of the genome-linked protein of poliovirus *in vitro* is dependent upon an endogenous RNA template. *Virus Research* **8**:193-204.

Takegami, T., Kuhn, R. J., Anderson, C. W., and Wimmer, E. (1983) Membrane-dependent uridylylation of the genome-linked protein VPg of poliovirus. *Proceedings of the National Academy of Science USA* **80**:7447-7451.

Taylor, G. M., Goldin, R. D., Karayiannis, P., and Thomas, H. C. (1992) *In situ* hybridization studies in hepatitis A infection. *Hepatology* **16**:642-648.

Tedeschi, V., Purcell, R. H., and Emerson, S. U. (1993) Partial characterization of hepatitis A viruses from three intermediate passage levels of a series resulting in adaptation to growth in cell culture and attenuation of virulence. *Journal of Medical Virology* **39**:16-22.

Tesar, M., Harmon, S. A., Summers, D. F., and Ehrenfeld, E. (1992) Hepatitis A virus polyprotein synthesis initiates from two alternative AUG codons. *Virology* **186**:609-618.

Tesar, M., Jia, X. -Y., Summers, D. R., and Ehrenfeld, E. (1993) Analysis of a potential myristylation site in hepatitis A virus capsid protein VP4. *Virology* **194**:616-626.

Tesar, M., Pak, I., Jia, X. -Y., Richards, O. C., Summers, D. F., and Ehrenfeld, E. (1994) Expression of hepatitis A virus precursor protein P3 *in vivo* and *in vitro*: polyprotein processing of the 3CD cleavage site. *Virology* **198**:524-533.

Teterina, N. L., Bienz, K., Egger, D., Gorbalenya, A. E., and Ehrenfeld, E. (1997a) Induction of intracellular membrane rearrangements by HAV proteins 2C and 2BC. *Virology* **237**:66-77.

Teterina, N. L., Gorbalenya, A. E., Egger, D., Bienz, K., and Ehrenfeld, E. (1997b) Poliovirus 2C protein determinants of membrane binding and rearrangements in mammalian cells. *Journal of Virology* **71**:8962-8972.

Thompson, P., Lu, J., and Kaplan, G. G. (1998) The Cys-rich region of hepatitis A virus cellular receptor 1 is required for binding of hepatitis A virus and protective monoclonal antibody 190/4. *Journal of Virology* **72**:3751-3761.

Ticehurst, J. R., Racaniello, V. R., Baroudy, B. M., Baltimore, D., Purcell, R. H., and Feinstone, S. M. (1983) Molecular cloning and characterization of hepatitis A virus cDNA. *Proceedings of the National Academy of Science USA* **80**:5885-5889.

Tobin, G. J., Young, D. C., and Flanegan, J. B. (1989) Self-catalyzed linkage of poliovirus terminal protein VPg to poliovirus RNA. *Cell* **59**:511-519.

Todd, S., Nguyen, J. H., and Semler, B. L. (1995) RNA-protein interactions directed by the 3′ end of human rhinovirus genomic RNA. *Journal of Virology* **69**:3605-3614.

Todd, S., Towner, J. S., and Semler, B. L. (1997a) Translation and replication properties of the human rhinovirus genome *in vivo* and *in vitro*. *Virology* **229**:90-97.

Todd, S., Towner, J. S., Brown, D. M., and Semler, B. L. (1997b) Replication-competent picornaviruses with complete genomic RNA 3′ noncoding region deletions. *Journal of Virology* **71**:8868-8874.

Tolskaya, E. A., Romanova, L. I., Kolesnikova, M. S., Gmyl, A. P., Gorbalenya, A. E., and Agol, V. I. (1994) Genetic studies on the poliovirus 2C protein, an NTPase. *Journal of Molecular Biology* **236**:1310-1323.

Towbin, H., Staehelin, T., and Gordon, J. (1979) Electrophoretic transfer of proteins from polyacrylamide gels to nitrocellulose sheets: procedures and some applications. *Proceedings of the National Academy of Science USA* **76**:4350-4354.

Troxler, M., Egger, D., Pfister, T., and Bienz, K. (1992) Intracellular localization of poliovirus RNA by *in situ* hybridization at the ultrastructural level using single-stranded riboprobes. *Virology* **191**:687-697.

Uncapher, C. R., DeWitt, C. M., and Colonno, R. J. (1991) The major and minor group receptor families contain all but one human rhinovirus serotype. *Virology* **180**:814-817.

Updike, W. S., Tesar, M., and Ehrenfeld, E. (1991) Detection of hepatitis A virus polyproteins in infected BS-C-1 cells. *Virology* **185**:411-418.

van Kuppeveld, F. J. M., Galama, J. M. D., Zoll, J., and Melchers, W. J. G. (1995) Genetic analysis of a hydrophobic domain of Coxsackie B3 virus protein 2B: a moderate degree of hydrophobicity is required for a *cis*-acting function in viral RNA synthesis. *Journal of Virology* **69**:7782-7790.

van Kuppeveld, F. J. M., Melchers, W. J. G., Kirkegaard, K., and Doedens, J. R. (1997) Structure-function analysis of Coxsackie B3 virus protein 2B. *Virology* **227**:111-118.

van Kuppeveld, F. J. M., van den Hurk, P. J. J. C., Zoll, J., Galama, J. M. D., and Melchers, W. J. G. (1996) Mutagenesis of the Coxsackie B3 virus 2B/2C cleavage site: determinants of processing efficiency and effects on viral replication. *Journal of Virology* **70**:7632-7640.

Vance, L. M., Moscufo, N., Chow, M., and Heinz, B. A. (1997) Poliovirus 2C region functions during encapsidation of viral RNA. *Journal of Virology* **71**:8759-8765.

Verdaguer, N., Mateu, M. G., Bravo, J., Domingo, E., and Fita, I. (1996) Induced pocket to accommodate the cell attachment arg-gly-asp motif in a neutralising antibody against foot-and-mouth disease virus. *Journal of Molecular Biology* **256**:364-376.

Wang, Q. M., Sommergruber, W., and Johnson, R. B. (1997) Cleavage specificity of human rhinovirus-2 2A protease for peptide substrates. *Biochemical and Biophysical Research Communications* **235**:562-566.

Ward, G., Rieder, E., and Mason, P. W. (1997) Plasmid DNA encoding replicating foot-and-mouth disease virus genome induces antiviral immune responses in swine. *Journal of Virology* **71**:7442-7447.

Weitz, M., Baroudy, B. M., Maloy, W. L., Ticehurst, J. R., and Purcell, R. H. (1986) Detection of a genome-linked protein (VPg) of hepatitis A virus and its comparison with other picornaviral VPgs. *Journal of Virology* **60**:124-130.

Westrop, G. D., Wareham, K. A., Evans, D. M. A., Dunn, G., Minor, P. D., Magrath, D. I., Taffs, F., Marsden, S., Skinner, M. A., Schild, G. C., and Almond, J. W. (1989) Genetic basis of attenuation of the Sabin type 3 oral poliovirus vaccine. *Journal of Virology* **63**:1338-1344.

Wheeler, C. M., Fields, H. A., Schable, C. A., Meinke, W. J., and Maynard, J. E. (1986a) Adsorption, purification, and growth characteristics of hepatitis A virus strain HAS-15 propagated in fetal rhesus monkey kidney cells. *Journal of Clinical Microbiology* **23**:434-440.

Wheeler, C. M., Robertson, B. H., Van Nest, G., Dina, D., Bradley, D. W., and Fields, H. A. (1986b) Structure of the hepatitis A virion: peptide mapping of the capsid region. *Journal of Virology* **58**:307-313.

Whetter, L. E., Day, S. P., Elroy-Stein, O., Brown, E. A., and Lemon, S. M. (1994) Low efficiency of the 5′ nontranslated region of hepatitis A virus RNA in directing cap-independent translation in permissive monkey kidney cells. *Journal of Virology* **68**:5253-5263.

Wimmer, E., Hellen, C. U. T., and Cao, X. (1993) Genetics of poliovirus. *Annual Review of Genetics* **27**:353-436.

Witherell, G. W., and Wimmer, E. (1994) Encephalomyocarditis virus internal ribosomal entry site RNA-protein interactions. *Journal of Virology* **68**:3183-3192.

Wolstenholme, A. J., Coates, J. P., and Douglass, W. (1993) Expression of hepatitis A virus poly(U) polymerase in the periplasmic space of *Escherichia coli. Journal of General Virology* **74**:531-534.

Wood, D. J., and Macadam, A. J. (1997) Laboratory tests for live attenuated poliovirus vaccines. *Biologicals* **25**:3-15.

Wyckoff, E. E., Hershey, J. W. B., and Ehrenfeld, E. (1990) Eukaryotic initiation factor 3 is required for poliovirus 2A protease-induced cleavage of the p220 component of eukaryotic initiation factor 4F. *Proceedings of the National Academy of Science USA* **87**:9529-9533.

Xiang, W., Cuconati, A., Paul, A. V., Cao., X., and Wimmer, E. (1995a) Molecular dissection of the multifunctional poliovirus RNA-binding protein 3AB. *RNA* **1**:892-904.

Xiang, W., Harris, K. S., Alexander, L., and Wimmer, E. (1995b) Interaction between the 5′-terminal cloverleaf and 3AB/3CD^{pro} of poliovirus is essential for RNA replication. *Journal of Virology* **69**:3658-3667.

Xiang, W., Paul, A. V., and Wimmer, E. (1997) RNA signals in entero- and rhinovirus genome replication. *Seminars in Virology* **8**:256-273.

Yalamanchili, P., Banerjee, R., and Dasgupta, A. (1997a) Poliovirus-encoded protease 2A^{pro} cleaves the TATA-binding protein but does not inhibit host cell RNA polymerase II transcription *in vitro*. *Journal of Virology* **71**:6881-6886.

Yalamanchili, P., Datta, U., and Dasgupta, A. (1997b) Inhibition of host cell transcription by poliovirus: cleavage of transcription factor CREB by poliovirus-encoded protease 3C^{pro}. *Journal of Virology* **71**:1220-1226.

Yalamanchili, P., Harris, K., Wimmer, E., and Dasgupta, A. (1996) Inhibition of basal transcription by poliovirus: a virus-encoded protease (3C^{pro}) inhibits formation of TBP-TATA box complex *in vitro*. *Journal of Virology* **70**:2922-2929.

Yalamanchili, P., Weidman, K., and Dasgupta, A. (1997c) Cleavage of transcriptional activator Oct-1 by poliovirus encoded protease 3C^{pro}. *Virology* **239**:176-185.

Yotsuyanagi, H., Iino, S., Koike, K., Yasuda, K., Hino, K., and Kurokawa, K. (1993) Duration of viraemia in human hepatitis A viral infection as determined by polymerase chain reaction. *Journal of Medical Virology* **40**:35-38.

Yotsuyanagi, H., Koike, K., Yasuda, K., Moriya, K., Shintani, Y., Fujie, H., Kurokawa, K., and Iino, S. (1996) Prolonged faecal excretion of hepatitis A virus in adult patients with hepatitis A as determined by polymerase chain reaction. *Hepatology* **24**:10-13.

Ypma-Wong, M. F., and Semler, B. L. (1987) *In vitro* molecular genetics as a tool for determining the differential cleavage specificities of the poliovirus 3C proteinase. *Nucleic Acids Research* **15**:2069-2088.

Ypma-Wong, M. F., Dewalt, P. G., Johnson, V. H., Lamb, J. G., Semler, B. L. (1988) Protein 3CD is the major poliovirus proteinase responsible for cleavage of the P1 capsid precursor. *Virology* **166**:265-270.

Zajac, A. J., Amphlett, E. M., Rowlands, D. J., and Sangar, D. V. (1991) Parameters influencing the attachment of hepatitis A virus to a variety of continuous cell lines. *Journal of General Virology* **72**:1667-1675.

Zhang, H., Chao, S. -F., Ping, L. -H., Grace, K., Clarke, B., and Lemon, S. M. (1995) An infectious cDNA clone of a cytopathic hepatitis A virus: genomic regions associated with rapid replication and cytopathic effect. *Virology* **212**:686-697.

Zhang, S., and Racaniello, V. R. (1997) Expression of the poliovirus receptor in intestinal epithelial cells is not sufficient to permit poliovirus replication in the mouse gut. *Journal of Virology* **71**:4915-4920.

Zhao, R., Hadfield, A. T., Kremer, M. J., and Rossmann, M. G. (1997) Cations in human rhinoviruses. *Virology* **227**:13-23.

Zhao, R., Pevear, D. C., Kremer, M. J., Giranda, V. L., Kofron, J., Rossmann, M. G., and Kuhn, R. J. (1996) The structure of human rhinovirus 3 at 3.0 Å resolution. *Structure* **4**:1205-1220.

Ziegler, E., Borman, A. M., Deliat, F. G., Liebig, H. -D., Jugovic, D., Kean, K. M., Skern, T., and Kuechler, E. (1995) Picornavirus 2A proteinase-mediated stimulation of internal initiation of translation is dependent on enzymatic activity and the cleavage products of cellular proteins. *Virology* **213**:549-557.